

THE IRIIDIUM CATALYZED ORTHO BORYLATION OF AROMATICS

By

Donald Plattner

A THESIS

Submitted to  
Michigan State University  
in partial fulfillment of the requirements  
for the degree of

Chemistry – Master of Science

2014

## ABSTRACT

### THE IRIIDIUM CATALYZED ORTHO BORYLATION OF AROMATICS

By

Donald Plattner

The ability to functionalize arenes is one of the quintessential features of modern chemistry. As such, being able to catalytically modify an arene substrate with perfect regioselectivity is a worthwhile goal. To this end, two methods for functionalizing substrates with precise ortho selectivity have been achieved, using the borylating reagent pinacolborane (HBPin), and bis(pinacolato)borane ( $B_2Pin_2$ ).

The first method involves the ortho borylation of aniline substrates using BPin as an easily removable traceless directing group. By forming an N-BPin bond in situ, the nitrogen's remaining hydrogen is able to act as an outer sphere directing group, coordinating to the oxygen bonds on a BPin group attached to the iridium catalyst. In this way, the ortho borylation of aniline substrates was performed with great success and with even higher yields than were obtained with the similar Boc protected method.

The second method involves the use of a new ligand, SiPBz, which enables the ortho borylation of methyl benzoate substrates via a chelate driven mechanism. The full substrate scope of the ligand shows high yields and very good selectivity. Subtle ligand modifications were also tested in order to determine the optimum ligand for different types of substrates.

Copyright by  
DONALD PLATTNER  
2014

## ACKNOWLEDGEMENTS

First and foremost I would like to thank my advisor, Mitch Smith for his enormous help and patience. Not only was his insight utterly invaluable, he also taught me how to think like a chemist, a skill which will carry with me throughout my professional life. I feel indebted to him for everything that I have learned, not just in regards to chemistry.

I would also like to thank everyone involved in the Boron Group, especially Rob Maleczka for his acute attention to detail. I could not have asked for better lab mates than Kristin, Behnaz, Yu-Ling, Buddha, Dmitrijs, Tim, and Olivia. A special thanks also goes to one-time graduate student and full time friend, Sean, who was always encouraging and always helpful.

Dan Holmes and Kermit also deserve a great deal of thanks for their willingness to help regardless of the time or their workload. Also I don't know what I would have done without Richard's help in deciphering x-ray structures.

I would also like to thank my family, Shari, Virginia, and Don (Uno), for never failing to give me encouragement throughout my graduate studies. They have supported me through thick and thin.



# TABLE OF CONTENTS

LIST OF TABLES .....	vii
LIST OF FIGURES .....	viii
KEY TO SYMBOLS .....	xv
CHAPTER 1 .....	1
Introduction to Iridium Catalyzed C-H Borylation.....	1
Arene Functionalization.....	1
C-H Activation.....	3
Boronic Acids .....	5
Ir-Catalyzed C-H Borylation .....	7
Optimization of Ir-Catalyzed C-H Borylation .....	9
Mechanism.....	11
REFERENCES .....	18
CHAPTER 2 .....	20
Outer Sphere Directed Borylation .....	20
Introduction.....	20
Replication of Hydrogen Bonding Effect .....	21
BPin as a Traceless Directing Group .....	23
Substrate Scope.....	25
Borylation of Aniline .....	28
Application Towards the Borylation of Drugs.....	30
REFERENCES .....	33
CHAPTER 3 .....	34
Chelate Directed C-H Borylation.....	34
Silica-SMAP .....	34
PAr <sup>F</sup> <sub>3</sub> Ligand and Derivatives.....	36
Silyl Directed Borylation .....	39
Development of SiPBz Ligand .....	40
Substrate Scope.....	41
Optimization of SiPBz Ligand.....	48
REFERENCES .....	54
CHAPTER 4 .....	56
Conclusion .....	56
CHAPTER 5 .....	57
Experimental Information.....	57

Spectra.....	90
REFERENCES .....	174

## LIST OF TABLES

Table 3.1. Variations of the SiPBz Ligand .....	49
Table 3.2 Optimization of the SiPBz Ligand Comparing Results of 33 and 34 .....	50
Table 3.3 Optimization of the SiPBz Ligand Comparing Results of 35 and 36 .....	51
Table 3.4 Optimization of the SiPBz Ligand Comparing Results of 37 and 38 .....	52

## LIST OF FIGURES

Figure 1.1. Outcomes of Electrophilic Aromatic Substitution .....	2
Figure 1.2. Method for Ortho Functionalization.....	3
Figure 1.3. First Example of C-H Activation .....	4
Figure 1.4. First Sterically Driven C-H Activation.....	4
Figure 1.5. First Catalytically Driven Intermolecular Functionalization.....	5
Figure 1.6. BPin Conversion.....	6
Figure 1.7. Traditional Methods for Borylation of Arenes .....	7
Figure 1.8. Thermodynamics for the Borylation of Hydrocarbons .....	7
Figure 1.9. First Trace Borylation.....	8
Figure 1.10. Photochemical Borylation of Toluene.....	8
Figure 1.11. Rhenium Photocatalyzed Borylation of Alkanes .....	9
Figure 1.12. First Thermodynamically Driven Iridium Catalyzed Aromatic C-H Borylation .....	9
Figure 1.13. Contrast Between Iridium and Rhodium System in the Borylation of Benzylic Bonds .....	10
Figure 1.14. Six Coordinate Complexes .....	12
Figure 1.15. Isolated 5-Coordinate Complex.....	12
Figure 1.16. Proposed Catalytic Cycle .....	13
Figure 1.17. Effect of Charge on the Energies of intermediates.....	15
Figure 2.1. Transition State For Iridium Catalyzed Borylation of Pyrrole.....	21
Figure 2.2. General Procedure for the Boc Protection of Anilines Followed by Ortho Borylation .....	22
Figure 2.3. The Outer Sphere Transition State .....	23

Figure 2.4 Traceless Borylation of Aniline Substrates .....	25
Figure 2.5. The Failed Ortho Borylation of 2-Chloroaniline.....	27
Figure 2.6. Transition State for the Ortho Borylated Products .....	27
Figure 2.7. The Diborylation of Monoborylated Anilines.....	29
Figure 2.8 Borylated Aniline Isomers.....	30
Figure 2.9. The Borylation of 7-amino-4-methylcoumarin, and Bupropion HCl.....	31
Figure 3.1. Silica-SMAP Ligand .....	34
Figure 3.2. Reactions Involving Silica-SMAP .....	35
Figure 3.3. Reactions using the $\text{PAr}^{\text{F}}_3$ ligand.....	36
Figure 3.4. $\text{PAr}^{\text{F}}_3$ Transition State Leading to Ortho Borylation.....	37
Figure 3.5. Functionalization Using $\text{AsPh}_3$ Ligand.....	38
Figure 3.6. Mechanism for the Silyl Directed Borylation of Phenols .....	39
Figure 3.7. Synthesis of the SiPBz ligand .....	40
Figure 3.8. SiPBz Substrate Scope .....	42
Figure 3.9. SiPBz Substrate Scope Continued.....	43
Figure 3.10. Borylation of Carbamates.....	45
Figure 3.11. Proposed Mechanism for the SiPBz Ligand.....	46
Figure 3.12. Carbamate Intermediate.....	47
Figure 3.13 Failed Cyano Substrate Reactions .....	48
Figure 4.1 methyl 2,3-dimethoxy-6-(4,4,5,5-tetramethyl-1,3,2-dioxaborolan-2-yl)benzoate (21).....	72
Figure 4.2 methyl 2,3-dichloro-6-(4,4,5,5-tetramethyl-1,3,2-dioxaborolan-2-yl)(benzoate) (32).....	80

Figure 5.1. $^1\text{H}$ NMR (500 MHz, $\text{CDCl}_3$ ) (1).....	90
Figure 5.2. $^{13}\text{C}$ NMR (125 MHz, $\text{CDCl}_3$ ) (1) .....	91
Figure 5.3. $^1\text{H}$ NMR (500 MHz, $\text{CDCl}_3$ ) (2).....	92
Figure 5.4. $^{13}\text{C}$ NMR (125 MHz, $\text{CDCl}_3$ ) (2) .....	93
Figure 5.5. $^1\text{H}$ NMR (500 MHz, $\text{C}_6\text{D}_6$ ) (3).....	94
Figure 5.6. $^{13}\text{C}$ NMR (125 MHz, $\text{C}_6\text{D}_6$ ) (3) .....	95
Figure 5.7. $^1\text{H}$ NMR (500 MHz, $\text{CDCl}_3$ ) (4).....	96
Figure 5.8. $^{13}\text{C}$ NMR (125 MHz, $\text{CDCl}_3$ ) (4) .....	97
Figure 5.9. $^1\text{H}$ NMR (500 MHz, $\text{CDCl}_3$ ) (5).....	98
Figure 5.10. $^{13}\text{C}$ NMR (125 MHz, $\text{CDCl}_3$ ) (5) .....	99
Figure 5.11. $^1\text{H}$ NMR (500 MHz, $\text{CDCl}_3$ ) (6a).....	100
Figure 5.12. $^{13}\text{C}$ NMR (125 MHz, $\text{CDCl}_3$ ) (6a) .....	101
Figure 5.13. $^1\text{H}$ NMR (500 MHz, $\text{CD}_3\text{CN}$ ) (6b).....	102
Figure 5.14. $^{13}\text{C}$ NMR (125 MHz, $\text{CDCl}_3$ ) (6b) .....	103
Figure 5.15. $^1\text{H}$ NMR (500 MHz, $\text{CDCl}_3$ ) (7).....	104
Figure 5.16. $^{13}\text{C}$ NMR (125 MHz, $\text{CDCl}_3$ ) (7) .....	105
Figure 5.17. $^1\text{H}$ NMR (500 MHz, $\text{CDCl}_3$ ) (8).....	106
Figure 5.18. $^{13}\text{C}$ NMR (125 MHz, $\text{CDCl}_3$ ) (8) .....	107
Figure 5.19. $^1\text{H}$ NMR (500 MHz, $\text{CDCl}_3$ ) (9).....	108
Figure 5.20. $^{13}\text{C}$ NMR (125 MHz, $\text{CDCl}_3$ ) (9) .....	109

Figure 5.21.	$^1\text{H}$ NMR (500 MHz, DMSO- $\text{d}_6$ ) (10)	110
Figure 5.22.	$^{13}\text{C}$ NMR (125 MHz, DMSO- $\text{d}_6$ ) (10)	111
Figure 5.23.	$^1\text{H}$ NMR (500 MHz, $\text{CDCl}_3$ ) (11)	112
Figure 5.24.	$^{13}\text{C}$ NMR (125 MHz, $\text{CDCl}_3$ ) (11)	113
Figure 5.25.	$^1\text{H}$ NMR (500 MHz, DMSO- $\text{d}_6$ ) (12)	114
Figure 5.26.	$^{13}\text{C}$ NMR (125 MHz, $\text{CDCl}_3$ ) (12)	115
Figure 5.27.	$^1\text{H}$ NMR (500 MHz, $\text{CDCl}_3$ ) (13)	116
Figure 5.28.	$^{13}\text{C}$ NMR (125 MHz, $\text{CDCl}_3$ ) (13)	117
Figure 5.29.	$^1\text{H}$ NMR (500 MHz, $\text{CDCl}_3$ ) (14)	118
Figure 5.30.	$^{13}\text{C}$ NMR (125 MHz, $\text{CDCl}_3$ ) (14)	119
Figure 5.31.	$^1\text{H}$ NMR (500 MHz, $\text{CDCl}_3$ ) (15)	120
Figure 5.32.	$^{13}\text{C}$ NMR (125 MHz, $\text{CDCl}_3$ ) (15)	121
Figure 5.33.	$^1\text{H}$ NMR (500 MHz, $\text{CDCl}_3$ ) (16)	122
Figure 5.34.	$^{13}\text{C}$ NMR (125 MHz, $\text{CDCl}_3$ ) (16)	123
Figure 5.34.	$^1\text{H}$ NMR (500 MHz, $\text{CDCl}_3$ ) (17)	124
Figure 5.35.	$^{13}\text{C}$ NMR (125 MHz, $\text{CDCl}_3$ ) (17)	125
Figure 5.36.	$^1\text{H}$ NMR (500 MHz, $\text{CDCl}_3$ ) (18)	126
Figure 5.37.	$^{13}\text{C}$ NMR (125 MHz, $\text{CDCl}_3$ ) (18)	127
Figure 5.38.	$^1\text{H}$ NMR (500 MHz, $\text{CDCl}_3$ ) (19)	128
Figure 5.39.	$^{13}\text{C}$ NMR (125 MHz, $\text{CDCl}_3$ ) (19)	129

Figure 5.40.	$^1\text{H}$ NMR (500 MHz, $\text{CDCl}_3$ ) (20a)	130
Figure 5.41.	$^{13}\text{C}$ NMR (125 MHz, $\text{CDCl}_3$ ) (20a)	131
Figure 5.42.	$^1\text{H}$ NMR (500 MHz, $\text{CDCl}_3$ ) (20b)	132
Figure 5.43.	$^{13}\text{C}$ NMR (125 MHz, $\text{CDCl}_3$ ) (20b)	133
Figure 5.44.	$^1\text{H}$ NMR (500 MHz, $\text{CDCl}_3$ ) (21)	134
Figure 5.45.	$^{13}\text{C}$ NMR (125 MHz, $\text{CDCl}_3$ ) (21)	135
Figure 5.46.	$^1\text{H}$ NMR (500 MHz, $\text{CDCl}_3$ ) (22)	136
Figure 5.47.	$^{13}\text{C}$ NMR (125 MHz, $\text{CDCl}_3$ ) (22)	137
Figure 5.48.	$^1\text{H}$ NMR (500 MHz, $\text{CDCl}_3$ ) (23)	138
Figure 5.49.	$^{13}\text{C}$ NMR (125 MHz, $\text{CDCl}_3$ ) (23)	139
Figure 5.50.	$^1\text{H}$ NMR (500 MHz, $\text{CDCl}_3$ ) (24a)	140
Figure 5.51.	$^{13}\text{C}$ NMR (125 MHz, $\text{CDCl}_3$ ) (24a)	141
Figure 5.52.	$^1\text{H}$ NMR (500 MHz, $\text{CDCl}_3$ ) (24b)	142
Figure 5.53.	$^{13}\text{C}$ NMR (125 MHz, $\text{CDCl}_3$ ) (24b)	143
Figure 5.54.	$^1\text{H}$ NMR (500 MHz, $\text{CDCl}_3$ ) (25)	144
Figure 5.55.	$^{13}\text{C}$ NMR (125 MHz, $\text{CDCl}_3$ ) (25)	145
Figure 5.56.	$^1\text{H}$ NMR (500 MHz, $\text{CDCl}_3$ ) (26a)	146
Figure 5.57.	$^{13}\text{C}$ NMR (125 MHz, $\text{CDCl}_3$ ) (26a)	147
Figure 5.58.	$^1\text{H}$ NMR (500 MHz, $\text{CDCl}_3$ ) (26b)	148
Figure 5.59.	$^{13}\text{C}$ NMR (125 MHz, $\text{CDCl}_3$ ) (26b)	149



Figure 5.60.	$^1\text{H}$ NMR (500 MHz, $\text{CDCl}_3$ ) (27).....	150
Figure 5.61.	$^{13}\text{C}$ NMR (125 MHz, $\text{DMSO-d}_6$ ) (27).....	151
Figure 5.62.	$^1\text{H}$ NMR (500 MHz, $\text{CDCl}_3$ ) (28).....	152
Figure 5.63.	$^{13}\text{C}$ NMR (125 MHz, $\text{CDCl}_3$ ) (28) .....	153
Figure 5.64.	$^1\text{H}$ NMR (500 MHz, $\text{CDCl}_3$ ) (29).....	154
Figure 5.65.	$^{13}\text{C}$ NMR (125 MHz, $\text{CDCl}_3$ ) (28) .....	155
Figure 5.66.	$^1\text{H}$ NMR (500 MHz, $\text{CDCl}_3$ ) (30).....	156
Figure 5.67.	$^{13}\text{C}$ NMR (125 MHz, $\text{CDCl}_3$ ) (30) .....	157
Figure 5.68.	$^1\text{H}$ NMR (500 MHz, $\text{CDCl}_3$ ) (31).....	158
Figure 5.69.	$^{13}\text{C}$ NMR (125 MHz, $\text{CDCl}_3$ ) (32) .....	159
Figure 5.70.	$^1\text{H}$ NMR (500 MHz, $\text{CDCl}_3$ ) (32).....	160
Figure 5.71.	$^1\text{H}$ NMR (500 MHz, $\text{C}_6\text{D}_6$ ) (33).....	161
Figure 5.72.	$^{13}\text{C}$ NMR (125 MHz, $\text{CDCl}_3$ ) (33) .....	162
Figure 5.73.	$^1\text{H}$ NMR (500 MHz, $\text{C}_6\text{D}_6$ ) (34).....	163
Figure 5.74.	$^{13}\text{C}$ NMR (125 MHz, $\text{CDCl}_3$ ) (34) .....	164
Figure 5.75.	$^1\text{H}$ NMR (500 MHz, $\text{C}_6\text{D}_6$ ) (35).....	165
Figure 5.76.	$^{13}\text{C}$ NMR (125 MHz, $\text{CDCl}_3$ ) (35) .....	166
Figure 5.77.	$^1\text{H}$ NMR (500 MHz, $\text{C}_6\text{D}_6$ ) (36).....	167
Figure 5.78.	$^{13}\text{C}$ NMR (125 MHz, $\text{CDCl}_3$ ) (36) .....	168
Figure 5.79.	$^1\text{H}$ NMR (500 MHz, $\text{CD}_2\text{Cl}_2$ ) (37).....	169

Figure 5.80. $^{13}\text{C}$ NMR (125 MHz, $\text{CDCl}_3$ ) (37) .....	170
Figure 5.81. $^1\text{H}$ NMR (500 MHz, $\text{CD}_3\text{OD}$ ) (38).....	171
Figure 5.82. $^{13}\text{C}$ NMR (125 MHz, $\text{CDCl}_3$ ) (38) .....	172

## KEY TO SYMBOLS

Ac	acyl
BCat	catecholborane
BDE	bond dissociation energy
Boc	tert-butoxycarbonyl
B <sub>2</sub> Pin <sub>2</sub>	bis(pinacolato)borane
COD	1,5-cyclooctadiene
COE	cis-cyclooctene
Cp	cyclopentadienyl
Cp*	pentamethylcyclopentadienyl
$\eta$	eta, hapticity
$\Delta E^\ddagger$	activation energy
$\Delta E$	energy difference between the ground states
DoM	directed ortho metallation
dmabpy	4,4'-Bis(N,N-diethylamino)-2,2'-bipyridine
dmpe	1,2-bis(dimethylphosphino)ethane
dppe	1,2-bis(diphenylphosphino)ethane
dtbpy	4,4'-di-tert-butyl-2,2'-dipyridyl
HBPIn	pinacolborane
<i>m</i>	meta
MTBE	methyl <i>tert</i> -butyl ether
<i>n</i>	normal (straight chain hydrocarbon)

NPA	natural population analysis
<i>o</i>	ortho
<i>p</i>	para
PAr <sup>F</sup> <sub>3</sub>	P(3,5)-bis(CF <sub>3</sub> ) <sub>2</sub> -C <sub>6</sub> H <sub>3</sub> ) <sub>3</sub>
SiPBz	(2-(diisopropylsilyl)phenyl)di- <i>p</i> -tolylphosphane
TEA	triethylamine
tmphen	3,4,7,8-tetramethyl-1,10-phenanthroline

## CHAPTER 1

### Introduction to Iridium Catalyzed C-H Borylation

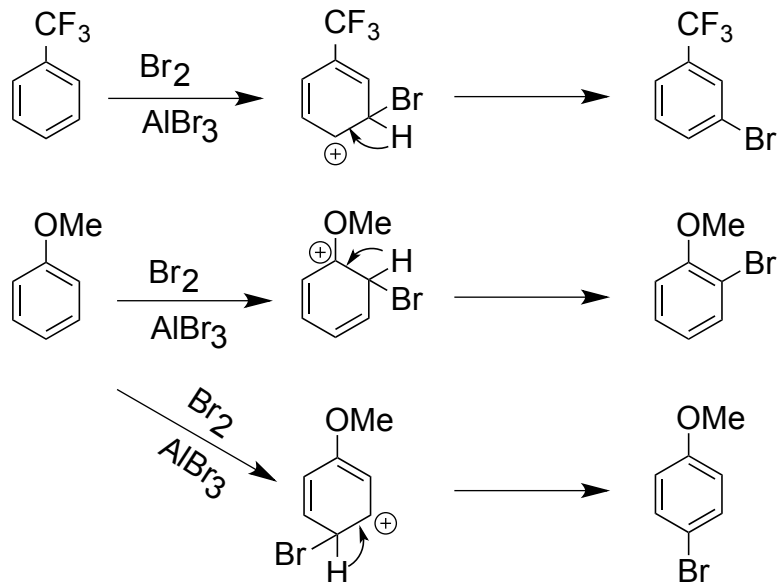
#### Arene Functionalization

Arenes are one of the most fundamental and important substances in all of chemistry. They provide the backbone for millions of different types of chemicals, and are the very foundation for many industrial syntheses and pharmaceuticals. Their utility simply cannot be overstated.

Benzene itself was originally discovered in 1825 by Michael Faraday in what was the first case of describing it as a unique chemical.<sup>1</sup> A mere 24 years later, the first industrial scale synthesis was described and implemented.<sup>2</sup> Finally, benzene was accurately described in the same way it is in modern textbooks; as a six member carbon ring with six hydrogen's and three alternating double bonds.<sup>3</sup>

Of course, being able to further functionalize benzene substrate is essential, and especially difficult due to general low reactivity. To these ends, numerous methods have been developed. The most common method, and the one that most chemists remember learning first, is the electrophilic aromatic substitution reactions, as shown in Figure 1.1.

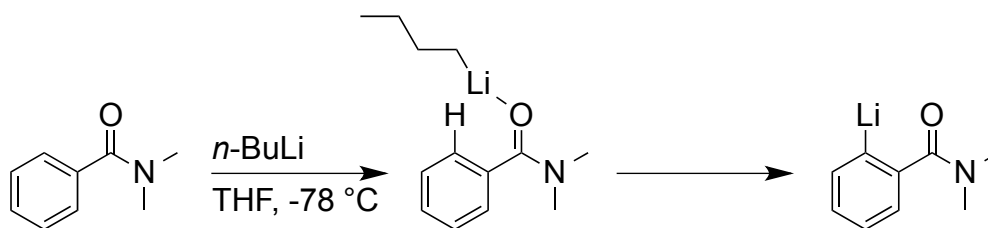
**Figure 1.1. Outcomes of Electrophilic Aromatic Substitution**



As shown above, the regioselectivity of the reactions are governed almost entirely by electronic factors, with electron donating groups causing substitution at the para and ortho positions, and electron withdrawing groups causing substitution at the meta positions. Unfortunately, this regioselectivity can cause a number of problems in the design of variously substituted aromatic rings. For instance, creating an all meta-substituted arene with only ortho/para directing groups is incredibly difficult,<sup>4,5</sup> as is functionalizing an aromatic ring with more than one deactivating group, and obtaining only ortho functionalized products with no para isomers.

The latter of these problems is solved, at least in part, by directed ortho metallation, DoM. In such reactions, exclusive ortho functionalization is achieved using a directing metallation group, which can act as a Lewis base in order to coordinate with the alkyl lithium metal and guide it towards deprotonating the ortho position and replacing it with a lithium metal, as seen in Figure 1.2.<sup>6,7</sup>

**Figure 1.2 Method for Ortho Functionalization**



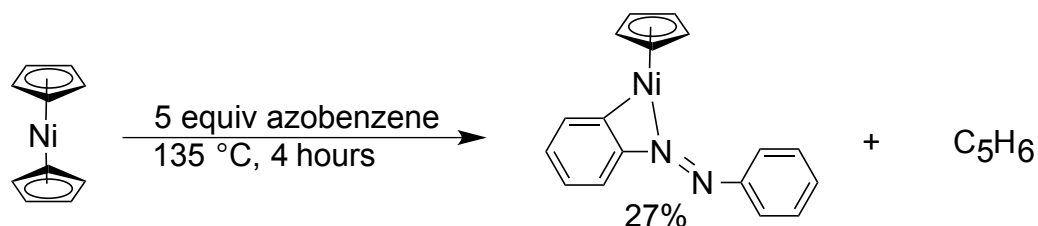
From there, the lithium metal can be replaced with a wide range of functional groups. However, this method has multiple drawbacks inherent to the process, the most obvious being the requirement of energy intensive low temperatures, and the necessity of stoichiometric quantities of *n*-BuLi which is not present in the final product.

### C-H Activation

Despite the utility of the above-mentioned functionalization methods, they and others have their stated drawbacks. In order to find a way around many of the problems, catalytic systems were designed in which the transition metal could be regenerated in order to improve atom economy and in such a way that the reaction could be performed with a different type of selectivity.

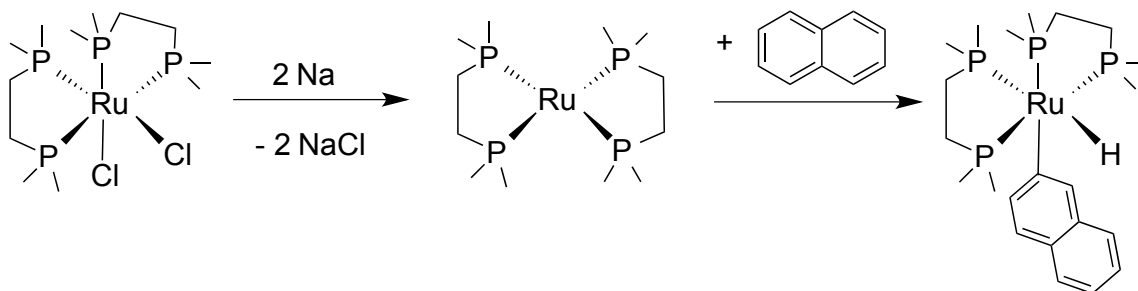
The first example of C-H activation was discovered in a reaction of between azobenzene and a nickel catalyst.<sup>8</sup> Figure 1.3.

**Figure 1.3. First Example of C-H Activation**



Further progress was made in the category of transition metal catalyzed arene functionalization when a ruthenium compound  $Ru(dmpe)_2Cl_2$  ( $dmpe = 1,2$ -bis(dimethylphosphino)ethane), was shown to undergo oxidative addition with the naphthalene solvent, as shown in Figure 1.4.<sup>9</sup> Interestingly, this reaction was shown to selectively activate only the least hindered C-H bonds of the naphthalene substrate.

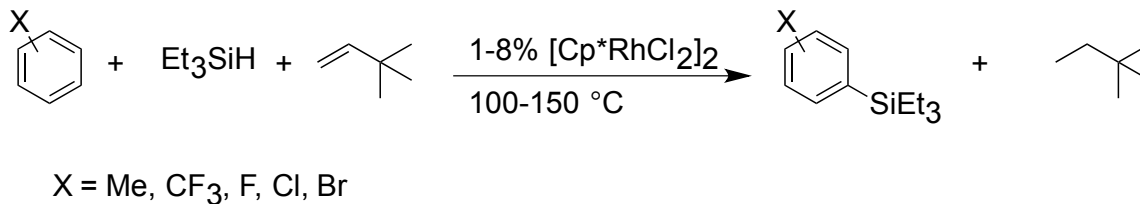
**Figure 1.4. First Sterically Driven C-H Activation**



Although this was a large step in the right direction, in order for a catalytic cycle to work, it of course has to have some component with which to undergo reductive elimination and yield a functionalized product. To this end, the first transition metal catalyzed intermolecular functionalization of an arene ring was designed, as depicted in Figure 1.5.<sup>10</sup>



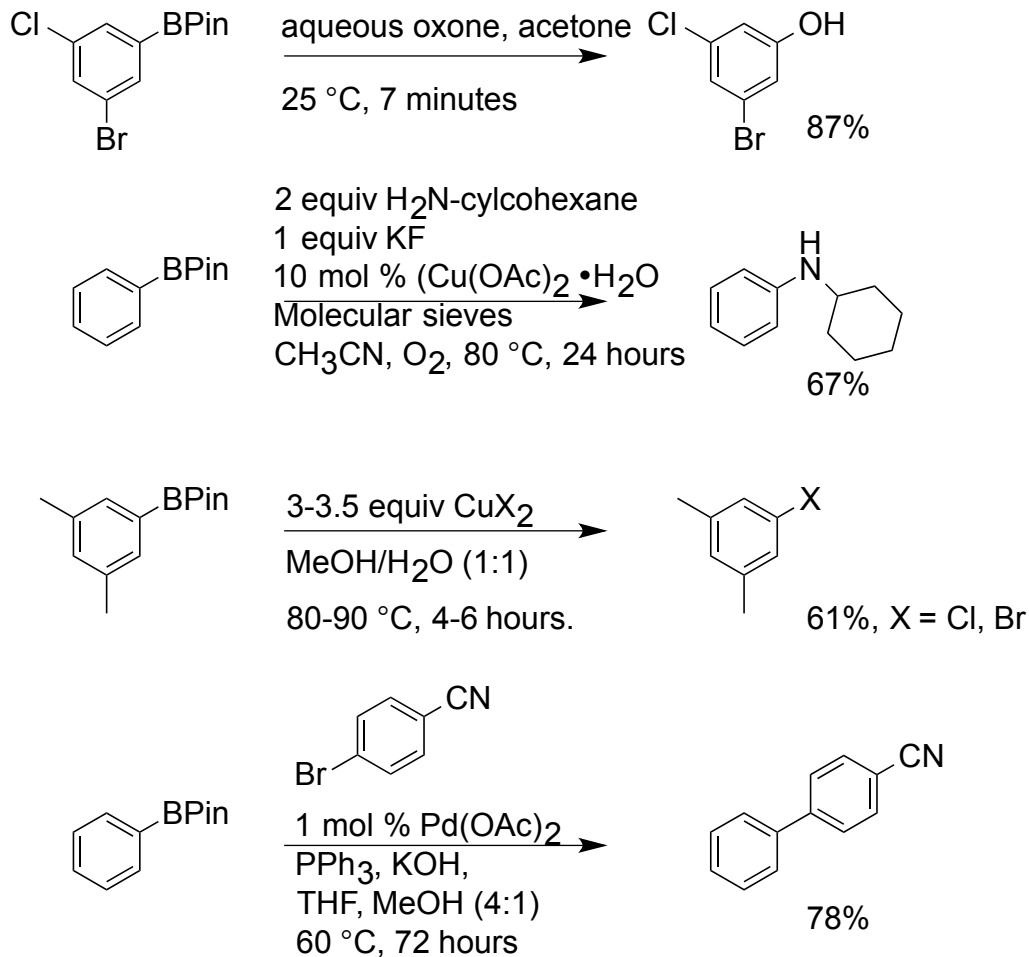
**Figure 1.5. First Catalytically Driven Intermolecular Functionalization**



### Boronic Acids

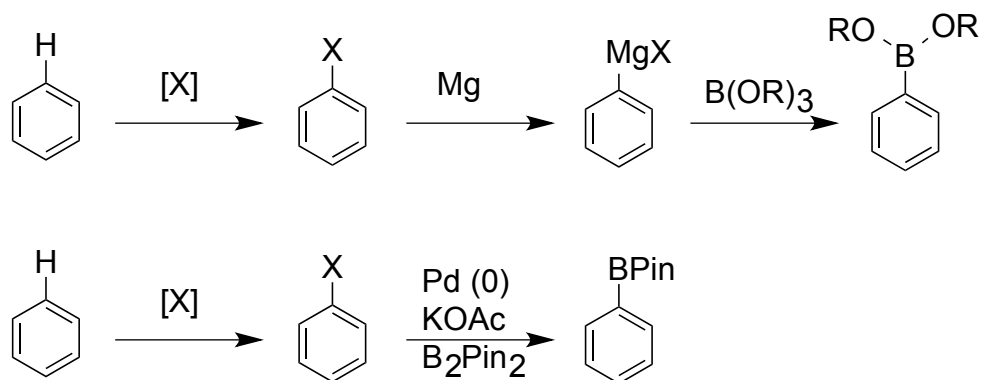
Being able to functionalize an aromatic ring with a functional group that can be further modified is also a very useful tool. To this end, boronic acids are a particularly useful functional group, as they have been shown not to be air sensitive, and can be further converted to a number of functional groups<sup>11</sup> including phenols,<sup>12</sup> anilines,<sup>13</sup> halogens,<sup>14,15</sup> and are used in coupling reactions.<sup>16</sup> (Figure 1.6)

**Figure 1.6. BPin Conversion**



The useful organoboranes tend to come in the form of boronic acids and boronic esters. However, putting a boron reagent on an aromatic ring is less trivial than it might seem. Traditional methods for preparing boronic esters are shown below in Figure 1.7.

**Figure 1.7. Traditional Methods for Borylation of Arenes**

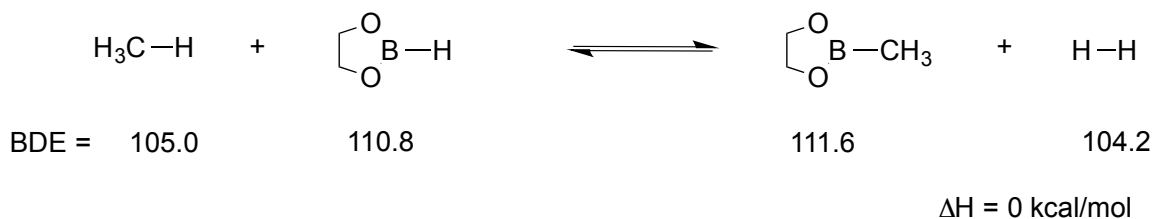


In both the Grignard<sup>17</sup> and the palladium catalyzed method<sup>18</sup>, a halogen, [X], is required to be present in order for it to be further modified in the borylation process. This is wasteful in terms of both atom economy and it can be nontrivial to install halogens on various substrates. It can also be difficult to achieve selectivity when multiple halogens are present.

### Ir-Catalyzed C-H Borylation

The most efficient route to borylation would be performed directly and without the necessary assistance of other functional groups. The thermodynamics of such a conversion for methane are shown below in Figure 1.8 and are very encouraging.<sup>19,20</sup>

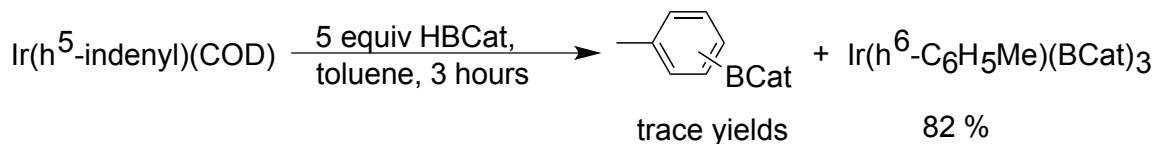
**Figure 1.8. Thermodynamics for the Borylation of Hydrocarbons**



Because such a reaction is effectively thermoneutral, it supports the concept that an unsubstituted hydrocarbon could be borylated directly.

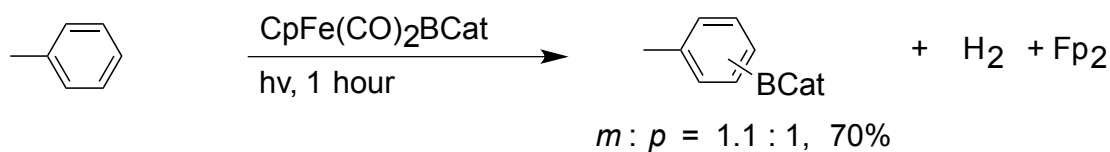
The first ever direct aromatic borylation using an iridium catalyst resulted as a byproduct of a reaction involving  $\text{Ir}(\eta^6\text{-C}_6\text{H}_5\text{Me})(\text{BCat})_3$  (BCat = catecholboryl) and a toluene solvent.<sup>21</sup> However, the borylated product only occurred in trace amounts as detected by GCMS. Figure 1.9.

**Figure 1.9. First Trace Borylation**



A much more successful aromatic borylation was obtained using  $\text{CpFe}(\text{CO})_2\text{BCat}$ , to photochemically borylate toluene.<sup>22</sup> Curiously, borylation of the substrate occurred only at the least sterically hindered locations (meta : para = 1.1 : 1). Unfortunately, these reactions did not occur catalytically. Figure 1.10.

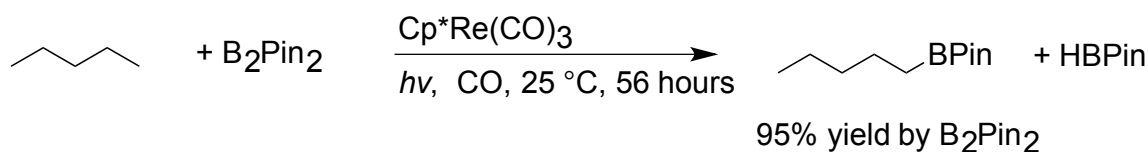
**Figure 1.10. Photochemical Borylation of Toluene**



Four years later, a method for photocatalytically borylating alkanes at the least sterically hindered terminal methyl group was determined, using a rhenium catalyst.

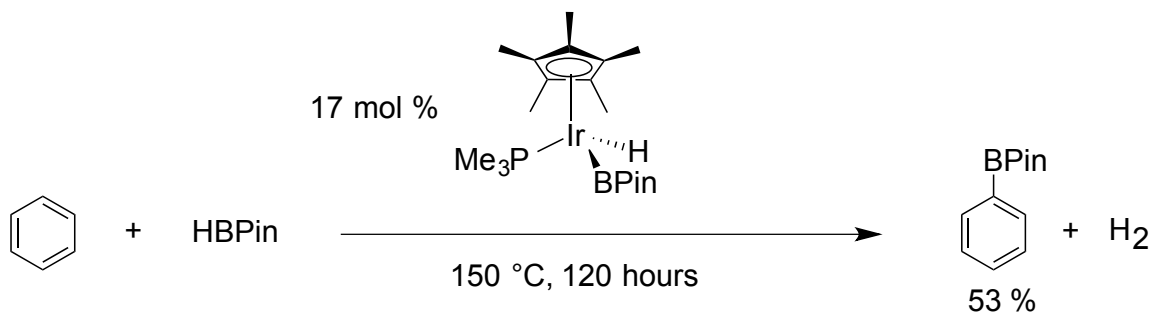
(Figure 1.11)<sup>23</sup>

**Figure 1.11. Rhenium Photocatalyzed Borylation of Alkanes**



That same year, the first thermodynamically driven iridium catalyzed aromatic C-H borylation was observed, as shown in Figure 1.12.<sup>24</sup>

**Figure 1.12. First Thermodynamically Driven Iridium Catalyzed Aromatic C-H Borylation**

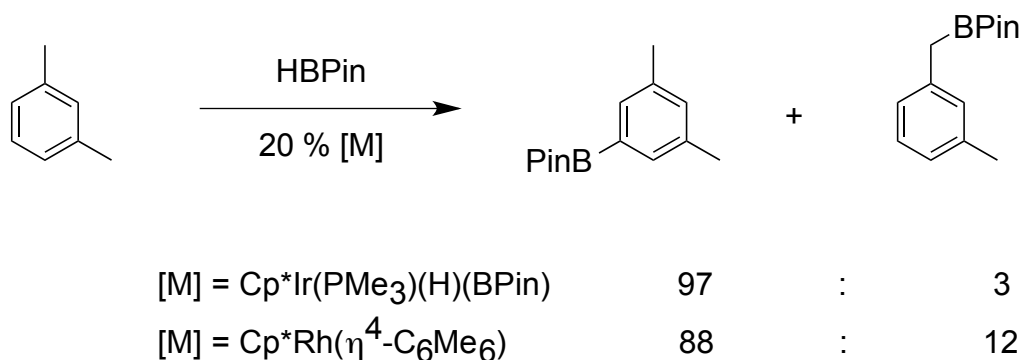


### Optimizing of Ir-Catalyzed C-H Borylation

Since that primitive era referred to as the “late 90’s,” many improvements have been made to the overall catalytic system and much insight has been gained into how the

reaction proceeds. To begin with, following the development of the catalyst, the scope of the catalytic reactions was found to be quite extensive. By generating the  $\text{Cp}^*\text{Ir}(\text{PMe}_3)(\text{H})(\text{BPin})$  catalyst in situ from  $\text{Cp}^*\text{Ir}(\text{PMe}_3)(\text{H})_2$  and then reacting it with multiple substrates, it was observed that the catalytic system was almost totally sterically driven, giving borylated products in the least hindered locations of the a variety of arene rings.<sup>25</sup> The selectivity of the reactions was also much better than the reported  $\text{Cp}^*\text{Rh}(\eta^4\text{-C}_6\text{Me}_6)$  catalyst which had been shown to also be capable of sterically directed C-H activation of alkanes.<sup>26</sup> In the case of the rhodium catalyst, not only did the system cause defluorination of fluorinated aromatics, but it also caused borylation of benzylic bonds as shown in Figure 1.13.

**Figure 1.13. Contrast Between Iridium and Rhodium System in the Borylation of Benzylic Bonds**



However, even though the selectivity of the iridium system was superior to the rhodium system, the reaction yields were still hampered by low turnover numbers. In an effort to improve the yield, a catalytically active Ir (III) species,  $\text{Ir}(\text{dppe})(\text{BPin})_3$  (dppe =

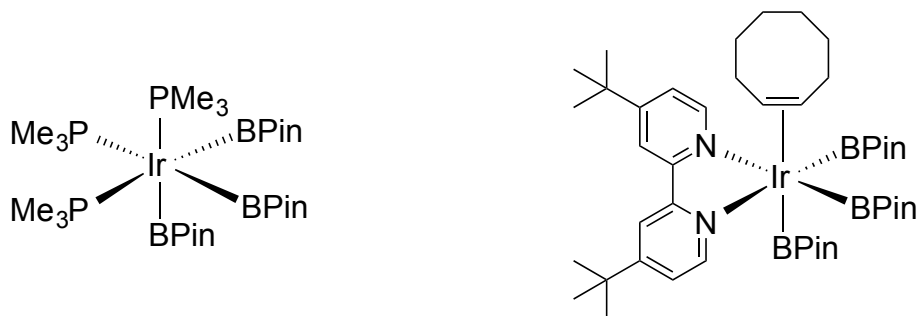
1,2-bis(diphenylphosphino)ethane) was proposed to be generated from ( $\eta^6$ -mesitylene)Ir(BPin)<sub>3</sub> and dppe.<sup>27</sup> This chelating ligand, dppe, was found to greatly improve the turnover numbers of the catalyst. Furthermore, this species was able to successfully borylate substrates containing iodine substituents, which contrasted with tested Iridium (I) species, [Ir(BPin)(PMe<sub>3</sub>)<sub>4</sub>].

Around that time, a similar system was developed using the Iridium (I) source, [Ir(COD)(OMe)]<sub>2</sub> and a different electron donating ligand, 4,4'-di-tert-butyl-2,2'-dipyridyl (dtbpy). This ligand catalyst setup would form the basic framework for many future iridium catalyzed borylations.<sup>28</sup>

## Mechanism

In order to determine how the actual catalytic cycle worked, as well as the type of intermediates formed during the cycle, a variety of calculations and experiments were performed. To begin with, it was widely believed that a five-coordinate complex was the intermediate which performed the C-H functionalization of the arene substrates, but the difficulty of isolating reactive intermediates is well known.<sup>29</sup> Because of this, pre-catalyst complexes could only be isolated as six-coordinate complexes shown in Figure 1.14.

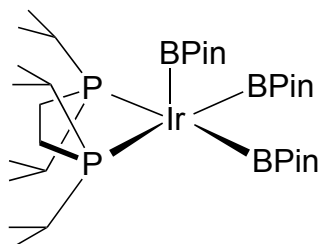
**Figure 1.14. Six Coordinate Complexes**



In these cases, it was believed to be necessary for the phosphorus ligand and COE ligand, respectively, to dissociate in order to obtain the active catalyst that would then undergo C-H activation of the substrate.

In order to obtain an actual five-coordinate iridium trisboryl complex that reacts in the same way that other as the ligands, the mesitylene trisboryl complex was reacted with a 1,2-bis(di-*i*-propyl-phosphino)ethane to yield the complex in Figure 1.15.<sup>30</sup>

**Figure 1.15. Isolated 5-Coordinate Complex**

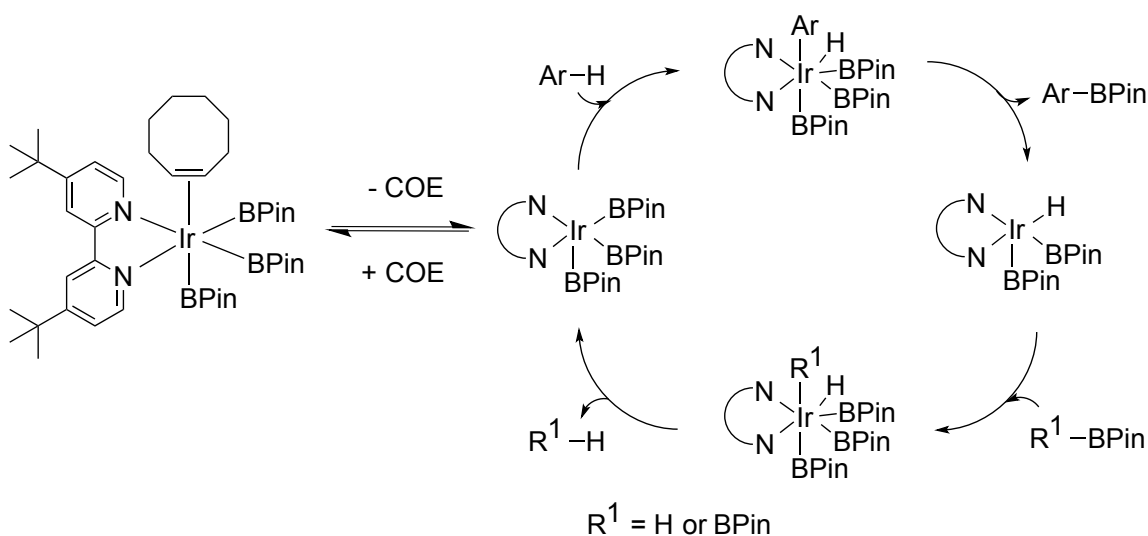


Reactions using this complex not only occurred with the same selectivity as other Ir (III) complexes, but also occurred faster than them because ligand predissociation isn't necessary. The presence of such a complex lent credence to previous kinetic experiments which had determined the complex in Figure 1.9 underwent dissociation of



the COE to obtain an active Ir-dtbpy complex.<sup>31</sup> The proposed mechanism for the overall catalytic cycle is shown below in Figure 1.16.

**Figure 1.16. Proposed Catalytic Cycle**



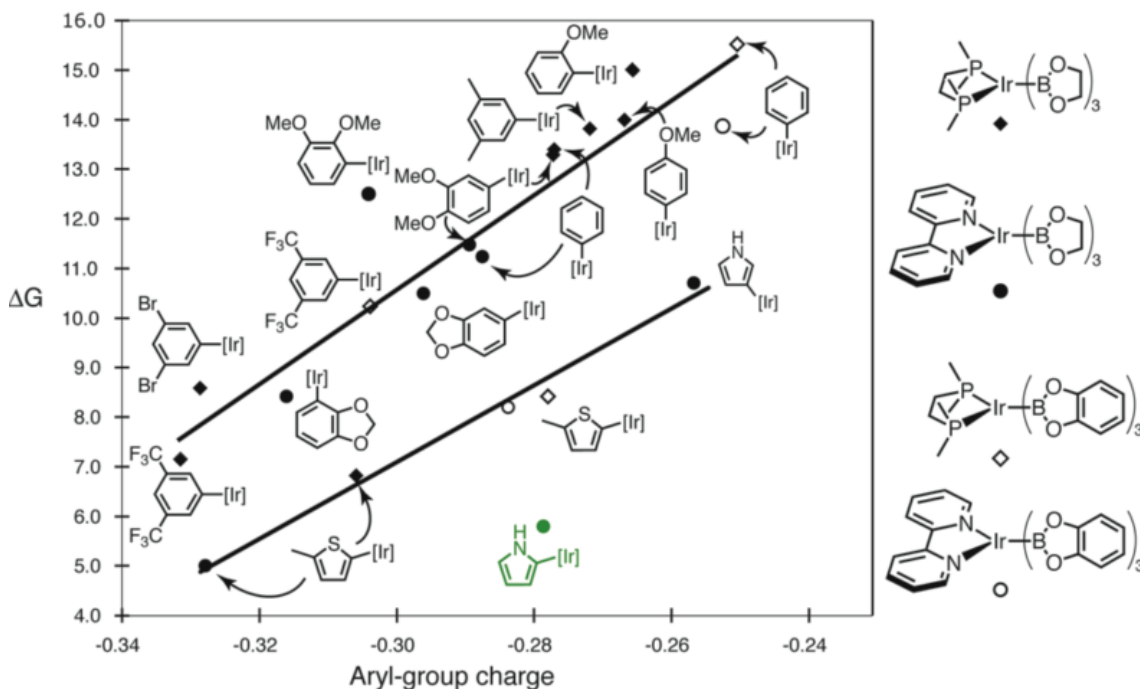
To begin with, the reaction occurs after an iridium (I) source, such as  $[\text{Ir}(\text{COD})(\text{OMe})_2]_2$ , undergoes reaction with a ligand, such as dtbpy, and a boron source, such as  $\text{B}_2\text{Pin}_2$  or  $\text{HBPin}$ . The resulting product can then undergo reversible dissociation of COE to yield a five-coordinate complex that undergoes oxidative addition with the substrate to form an  $18\text{ e}^-$  Ir (V) complex. Once reductive elimination occurs to yield a borylated substrate ( $\text{Ar-BPin}$ ), the catalyst is regenerated by undergoing oxidative addition with a boron source,  $\text{R}^1\text{-BPin}$  ( $\text{R}^1 = \text{BPin or H}$ ), followed by reductive elimination of  $\text{R}^1\text{-H}$ .

Although the iridium catalyzed borylations are sterically driven, certain pieces of information suggest that electronics do play a factor. Even early publications showed that aromatics containing electron withdrawing substituents tended to give higher yields than their electron donating counterparts. One particularly interesting example was the borylation of methoxy benzene, which yielded borylation,  $m : p = 4 : 1$ , and even contained some ortho borylation, which contrasts with the expected ratio of  $m : p = 2 : 1$ .<sup>25</sup> Furthermore, the borylation of aromatic heterocycles has been shown to be determined primarily by the position of the heteroatom.<sup>32</sup>

In order to determine what role electronic factors were playing, the energies of various transition states and intermediates were calculated for a group of reactions which involved iridium complex.<sup>33</sup> Because there was a high correlation between the activation energy for the transition state of the various substrates,  $\Delta E^\ddagger$ , and the reliably calculated energy difference between the ground states,  $\Delta E$ , it was concluded that the products will result from the  $\Delta E^\ddagger$  transition state.

With this in mind, Vanchura et al compared the  $\Delta E$  of various substrates to the natural population analysis, NPA, charge on the aromatic ring during the transition state and obtained a linear fit, as shown in Figure 1.17.

**Figure 1.17. Effect of Charge on the Energies of intermediates**



Their interpretation of the data was that the best-fit line correlated to the effect that charge had on the energies of the intermediates, and as a result the transition state, and that based on what they knew from how various substrates like veratrole, anisole, and benzodioxole reacted, that any intermediate below the line reacts favorably due to factors that are irrespective of the electronic effects.

They also concluded that anything which promotes the transfer of negative charge from the iridium catalyst to the arene substrate encourages product formation, as does any substrate functional group which promotes proton transfer to the iridium catalyst.

The optimal boron source was also determined experimentally to be a pinacolate derivative as opposed the catecholate.<sup>34</sup> The reason for this being that the electron density of the pinacolate derivatives are much greater than that of the catecholate types,

which improves the ability of the catalytic system to undergo oxidative addition with a substrate.

With these conditions, the optimal setup and mechanism behind iridium catalyzed sterically driven C-H borylation had been determined.

## REFERENCES

## REFERENCES

- 1) Kaiser, R. *Angew. Chem. Int. Ed.* **1968**, 7, 345.
- 2) Mansfield, C. For Fractal Distillation of Coal Tar. Patent no 11,960. **1848**.
- 3) Kekulé, A. *Liebigs Ann. Chem.* **1872**, 162, 77.
- 4) Hodgson, H. H.; Wignall, J. S. J. *Chem. Soc.* 1926, 2077-2079. (b) Kohn, M.; Zandman, A. *Monatsh. Chem.* 1926, 47, 357-377.
- 5) Maleczka, R. E.; Shi, F.; Holmes, D.; Smith, M. R. *J. Am. Chem. Soc.* **2003**, 125, 7792.
- 6) Snieckus, V. *Chem. Rev.* **1990**, 90, 879.
- 7) Whisler, M. C.; MacNeil, S.; Snieckus, V.; Beak, P. *Angew. Chem. Int. Ed.* **2004**, 43, 2206.
- 8) Kleiman, J. P.; Dubeck, M. *J. Am. Chem. Soc.* **1963**, 85, 1544.
- 9) Chatt, J.; Davidson, J. M. *J. Chem Soc.* **1965**, 843.
- 10) Ezbiansky, K.; Djurovich, P. I.; LaForest, M.; Sinning, D. J.; Zayes, Roberto, Berry, D. H. *Organometallics*. **1998**, 17, 1455.
- 11) Mkhallid, I. A. I.; Barnard, J. H.; Barder, T. B.; Murphy, M. J.; Hartwig, J. F. *Chem. Rev.* **2010**, 110, 890.
- 12) (a) Webb, K. S.; Levy, D. *Tetrahedron Lett.* **1995**, 36, 5117. (b) Maleczka, R. E.; Shi, F.; Holmes, D.; Smith, M. R. *J. Am. Chem. Soc.* **2003**, 125, 7792.
- 13) Tzschucke, C. C.; Murphy, J. M.; Hartwig, J. F. *Org. Lett.* **2007**, 9, 761.
- 14) Murphy, M. M.; Liao, X.; Hartwig, J. F. *J. Am. Chem. Soc.* **2007**, 129, 15434.
- 15) Fier, P. S.; Luo, J.; Hartwig, J. F. *J. Am. Chem. Soc.* **2013**, 135, 2552.
- 16) Myslinska, M.; Heise, G. L.; Walsh, D. J. *Tetrahedron Lett.* **2012**, 53, 2937.
- 17) Clary, J. W.; Rettenmaier, T. J.; Snelling, R.; Bryks, W.; Banwell, J.; Wipke, T. W. *J. Org. Chem.* **2011**, 76, 9602.
- 18) Ishiyama, T.; Murata, M.; Miyaura, N. *J. Org. Chem.* **1995**, 60, 7508

- 19) Rablen, P. R.; Hartwig, J. F. *J. Am. Chem. Soc.* **1994**, *116*, 4121.
- 20) Blanksby, S. J.; Ellison, G. B. *Acc. Chem. Res.* **2003**, *36*, 255
- 21) Henk, P. N.; Blom, H. P.; Westcott, S. A.; Taylor, N. T.; Marder, T. B. *J. Am. Chem. Soc.* **1993**, *115*, 9329.
- 22) Waltz, K. M.; He, X.; Muhoro, C.; Hartwig, J. F. *J. Am. Chem. Soc.* **1995**, *117*, 11357.
- 23) Chen, H.; Hartwig, J. F. *Angew. Chem. Int. Ed.* **1999**, *38*, 3391.
- 24) Iverson, C. N.; Smith, M. R. *J. Am. Chem. Soc.* **1999**, *121*, 7696.
- 25) Cho, J.; Iverson, C. N.; Smith, M. R. *J. Am. Chem. Soc.* **2000**, *122*, 12868.
- 26) Chen, H.; Schlecht, S.; Semple, T. C.; Hartwig, J. F. *Science*, **2000**, *287*, 1995.
- 27) Cho, J.; Tse, M. K.; Holmes, D.; Maleczka, R. E.; Smith, M. R. *Science*, **2002**, *295*, 305.
- 28) Ishiyama, T.; Takagi, J.; Hartwig, J. F.; Miyaura, N. *Angew. Chem. Int. Ed.* **2002**, *41*, 3056.
- 29) Halpern, J. *Science*, **1982**, *217*, 401.
- 30) Chotana, G. A.; Vanchura, B. A.; Tse, M. K.; Staples, R. J.; Maleczka, R. E.; Smith, M. R. *Chem. Commun.* **2009**, 5731.
- 31) Boller, T. M.; Murphy, J. M.; Hapke, M.; Ishiyama, T.; Miyaura, N.; Hartwig, J. F. *J. Am. Chem. Soc.* **2005**, *127*, 14263.
- 32) (a) Cho, J.; Tse, M. K.; Holmes, D.; Maleczka, R. E.; Smith, M. R. *Science*, **2002**, *295*, 305. (b) Sulagna, P.; Chotana, G. A.; Holmes, D.; Reichle, R. C.; Maleczka, R. E.; Smith, M. R. *J. Am. Chem. Soc.* **2006**, *128*, 15552. (c) Kallepalli, V. A.; Shi, F.; Sulagna, P.; Onyeozili, E. N.; Maleczka, R. E.; Smith, M. R. *J. Org. Chem.* **2009**, *74*, 9119.
- 33) Mkhaliid, I. A. I.; Barnard, J. H.; Marder, T. B.; Murphy, J. M.; Hartwig, J. F. *Chem. Rev.* **2010**, *110*, 890.
- 34) Liskey, C. W.; Wei, C. S.; Pahls, D. R.; Hartwig, J. F. *Chem. Commun.* **2009**, 5603.

## CHAPTER 2

### Outer Sphere Directed Borylation

#### Introduction

Although sterics tend to be the dominant controlling factor when it comes to the C-H borylation of arene rings,<sup>1</sup> recent findings have shown a situation where it is possible to control regioselectivity through an outer sphere mechanism<sup>2</sup> as well as a chelate directed mechanism<sup>3,4</sup> and a relay directed mechanism<sup>5</sup>. In the case of the outer sphere mechanism, the regioselectivity of the reaction is caused by interactions between the ligand on the catalyst and a functional group on a substrate.<sup>6</sup>

While this type of mechanism has been seen before in previous work,<sup>7</sup> its novelty with regards to C-H borylation provides a unique alternative to the sterically driven standard methods.

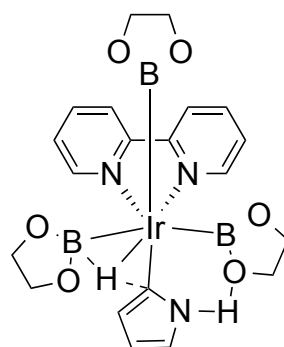
The clue that lead to the development of an iridium catalyzed outer sphere borylation was found during the quest to elucidate how electronic effects play a role in the iridium catalyzed borylation of aromatic substrates.<sup>8</sup>

The key and clear outlier in the comparison of natural population analysis, NPA, to the energy difference between the ground states was the borylation of pyrrole at the 2 position, which was calculated to be 2.3 kcal/mol more favorable than would have otherwise been expected.<sup>9</sup> Even though the regioselectivity of the reaction isn't altered from the expected borylation at the 2 position, it was curious that the reaction was so



much more favorable than borylation at the 3 position despite sterics not being a factor. Subsequent analysis of the bond angles and bond distances in the transition state suggested that hydrogen bonding interactions were taking place between the boryl oxygen and the hydrogen on the nitrogen, which resulted in the stabilized the transition state for borylation at the 2 position. Figure 2.1.

**Figure 2.1. Transition State For Iridium Catalyzed Borylation of Pyrrole**



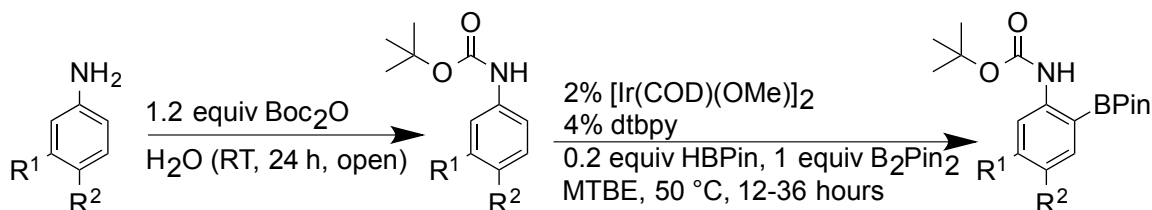
With this in mind, a way to replicate the hydrogen bonding effect was sought in order to alter the selectivity of a reaction to favor ortho borylation where it usually would not be favored.

### **Replication of Hydrogen Bonding Effect**

Further analysis determined that the tert-butoxycarbonyl (Boc) group, when bonded to the nitrogen of an aniline substrate as a protecting group, was capable of causing the hydrogen attached to the nitrogen to mimic the hydrogen bonding effect seen in the pyrrole. In doing so, Boc protection of aniline substrates is able to alter the

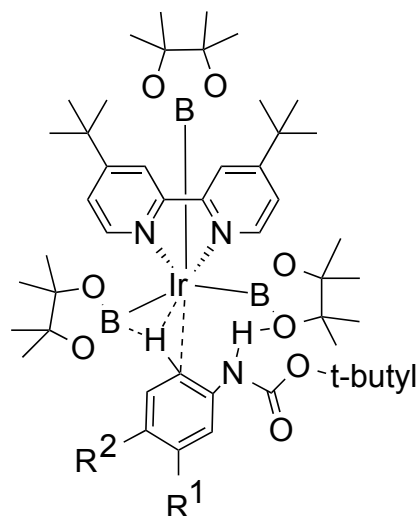
regioselectivity of iridium catalyzed borylation to favor ortho substitution. The general procedure is shown in Figure 2.2.

**Figure 2.2. General Procedure for the Boc Protection of Anilines Followed by Ortho Borylation**



The most supportive piece of evidence that the route by which this was accomplished was indeed an outer sphere mechanism came from experiments involving various dipyridyl ligands. By altering the functional groups on a multitude of dipyridyl ligands, they were able to observe the ligand's electronic effect on the regioselectivity of the Boc protected anilines. What they observed was that functional groups that increased the basicity of the dipyridyl ligands enhanced ortho selectivity of the reaction. It was proposed that in a catalyst/ligand complex where the functional groups on the dipyridyl ligand were electron donating, the basicity of the pinacolate oxygen's was also increased. This hypothesis is supported by the results, where reactions using ligands with electron donating groups favored the ortho borylated product. Thus, outer sphere borylation was the route by which ortho borylation occurred. (Figure 2.3.)

**Figure 2.3. The Outer Sphere Transition State.**



Even though many of the Boc protected aniline substrates showed high selectivity, the overall process had its drawbacks. The most obvious issue was that separate steps were required to add and remove the Boc protecting group before and after borylation. This introduces extra steps and purifications that potentially decreased the overall yield of the reaction.

### **BPin as a Traceless Directing Group**

In order to provide a methodology wherein anilines could be protected in-situ, a strategy involving pinacolborane (HBPin) was devised.<sup>9</sup> N-BPin proved to be quite advantageous as an outer sphere directing group. The fact that the N-BPin bonds could be easily hydrolyzed with the addition of methanol at the end of the reaction allowed us to overcome the drawbacks seen in the borylation of Boc protected anilines. In this way, the HBPin could be used as a traceless directing group, which is highly advantageous when compared to Boc protection.

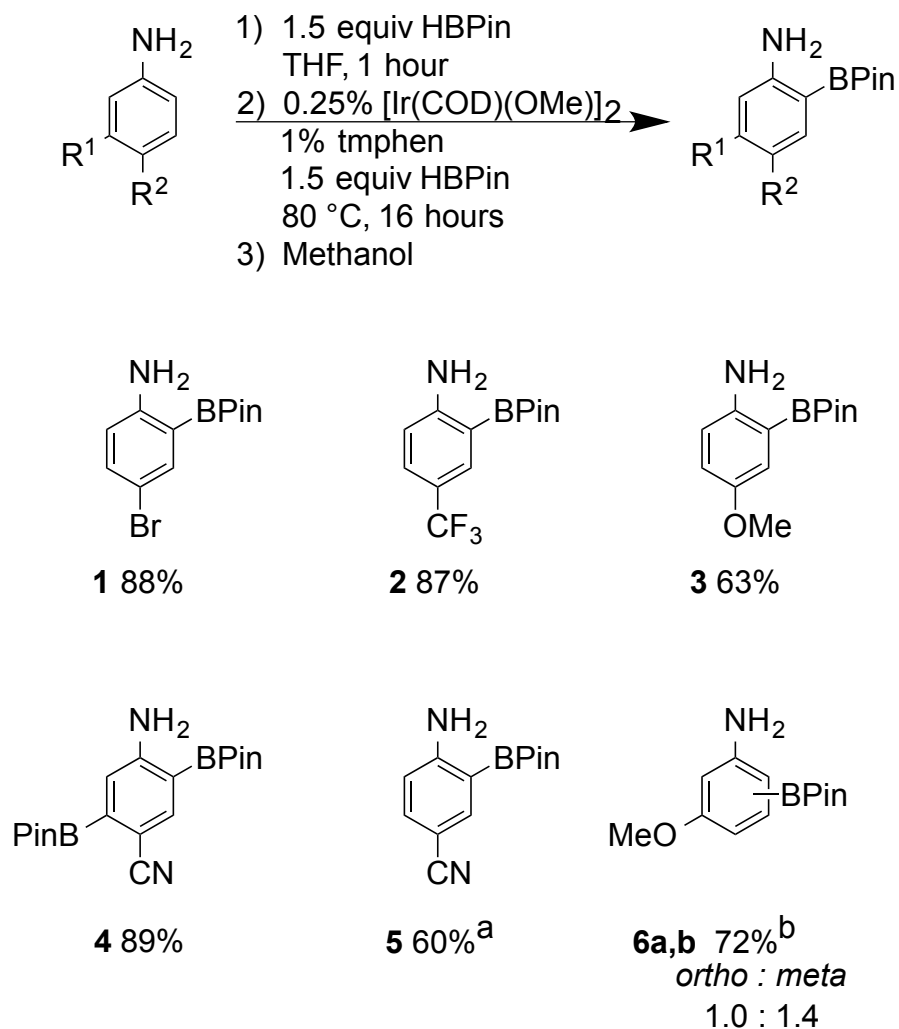
It should be noted that in order for the HBPin to be effective in the outer sphere

borylation of anilines, an incubation period was required wherein the aniline substrate and 1.5 equivalents of HBPIn and were stirred together for an hour.

After full N-BPin conversion was achieved, an iridium catalyst was added, a 3,4,7,8-tetramethyl-1,10-phenanthroline (tmphen) ligand, as opposed to the 4,4'-di-tert-butyl-2,2'-bipyridyl (dtbpy) ligand used for Boc protection, was added in order to mimic the increased ortho selectivity seen with more electron donating ligands in Boc protected ortho borylation, and extra HBPIn was added so that it could be used as the borylating reagent. In this way, outer sphere ortho borylation of aniline substrates was achieved. Figure 2.4. shows the substrate scope for this reaction.

## Substrate Scope

**Figure 2.4. Traceless Borylation of Aniline Substrates**



<sup>a</sup> Conditions: 1.5 mol% [Ir(OMe)COD]<sub>2</sub>, 3.0 mol% dmabpy with 2.0 equivalents HBPIn in *n*-hexane as reaction solvent.

<sup>b</sup> Conditions: 2.5 mol% [Ir(OMe)COD]<sub>2</sub>, 5.0 mol% tmphen.

Immediately, we find that the 4-bromoaniline substrate **1** gives almost exactly the same yield as it did in the Boc protected borylation, even before taking into account the extra steps necessary to add and remove the Boc group. The reaction works well on both

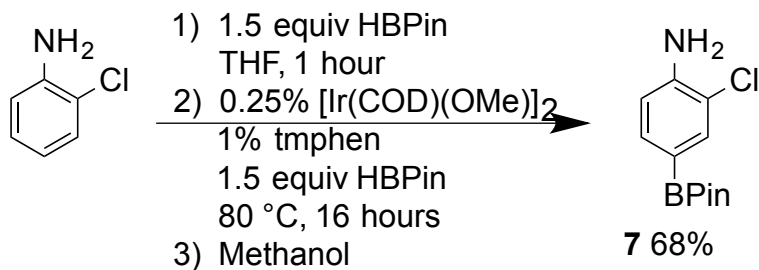
electron withdrawing groups and electron donating groups, although the electron donating methoxy group doesn't seem to be quite as effective. This result can be explained through virtue of the fact that for general iridium catalyzed borylation, proton transfer character is the key electronic contributor to the transition state.<sup>8</sup>

The diborylation of the 4-aminobenzonitrile **4** occurred under standard borylation conditions, probably because the nitrile group does not provide much steric hindrance. In order to obtain pure monoborylated product **5**, a more highly electron donating ligand, 4,4'-Bis(N,N-diethylamino)-2,2'-bipyridine (dmabpy), was used, as was fewer equivalents of HBPIn.

When it came to the borylation of 3-methoxyaniline, the meta product **6b** was surprisingly the major isomer. This differs from what was seen in the borylation of other meta anilines.<sup>9</sup> as well as in the borylation of meta substituted Boc protected anilines. In both of those cases, the meta borylated product was still observed, but only as the minor product. The reason for the large amount of meta product, **6b**, could be that the proton transfer character of the meta transition state is simply much greater than in the ortho, due to the presence of the electron donating methoxy group.

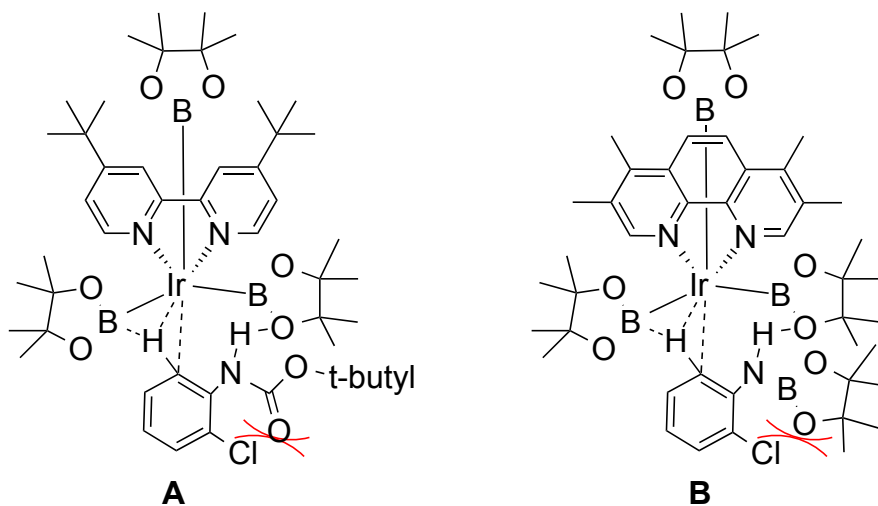
One of the drawbacks with this traceless directing method, as well as the Boc protection method, is that 2-substituted anilines fail to give ortho regioselectivity, as seen in Figure 2.5.

**Figure 2.5. The Failed Ortho Borylation of 2-Chloroaniline**



The reason for this failure becomes apparent when the transition state for the Boc protected aniline is taken into account, as seen in Figure 2.6.

**Figure 2.6. Transition State for the Ortho Borylated Products**



Based on the structure of the Boc protected aniline transition state **A**, there is a large steric clash that occurs between the functional group ortho to the aniline nitrogen, and the Boc group attached to the aniline nitrogen. If this is applied to the analogous N-BPin transition state **B**, the same steric clash is observed.

It is worth noting that while ortho borylation didn't occur, the reaction borylated only the meta position, which is interesting considering that *N,N*-dimethyl aniline

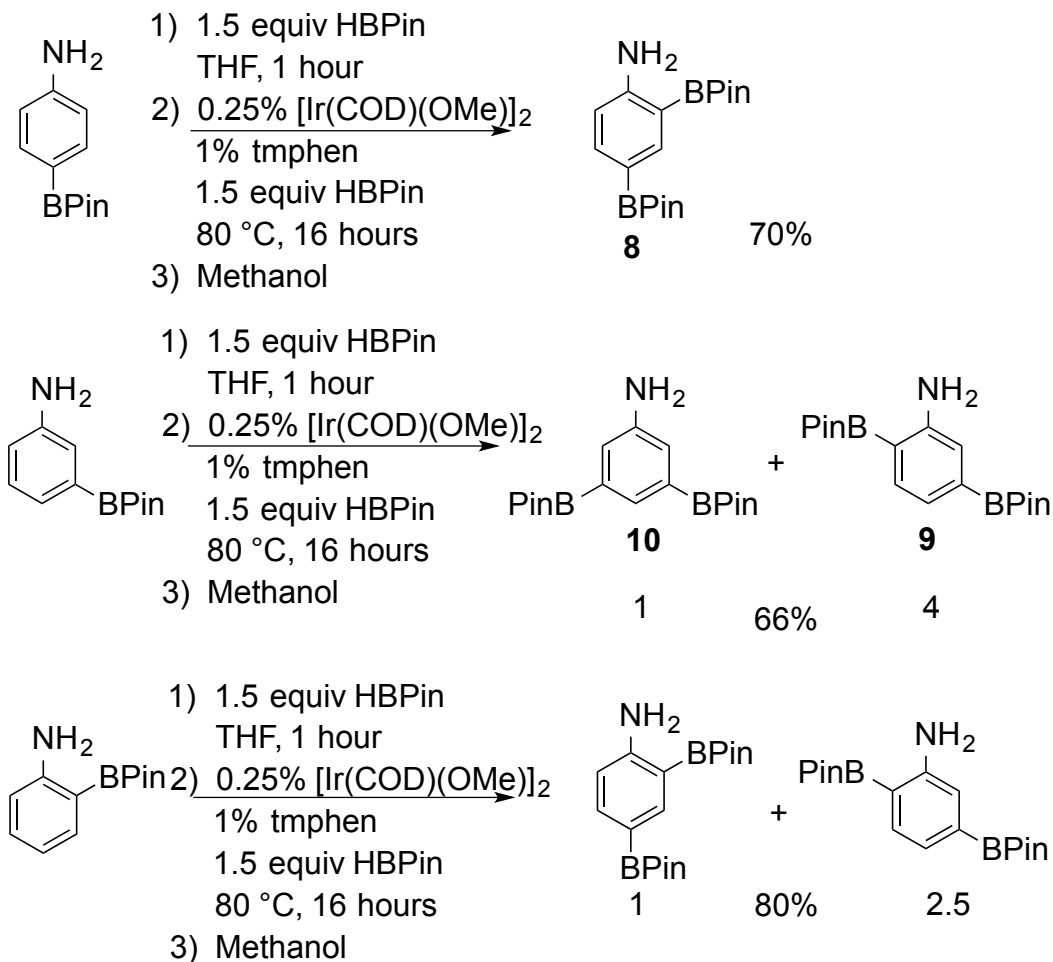
borylation favors the meta position, while still resulting in some para borylation (meta : para = 79:21).<sup>10</sup> Although the source of this meta selectivity is almost certainly electronic, the exact reason behind it is unknown.

### **Borylation of Aniline**

The borylation of aniline proved much more complex and interesting than originally expected. While the borylation of Boc protected aniline yielded the ortho product almost entirely (*o* : *m* : *p* = 90 : 5 : 5), the NMR of the crude reaction mixture of BPin protected aniline was too complex to have only three products in it. A mass spec of the mixture showed that not only was unborylated starting aniline present, but diborylation had also occurred. Initial efforts to separate all seven compounds via TLC were unsuccessful. Therefore, in order to determine the ratio of products, monoborylated anilines were borylated under standard conditions to yield their diborylated counterparts, as seen in Figure 2.7.

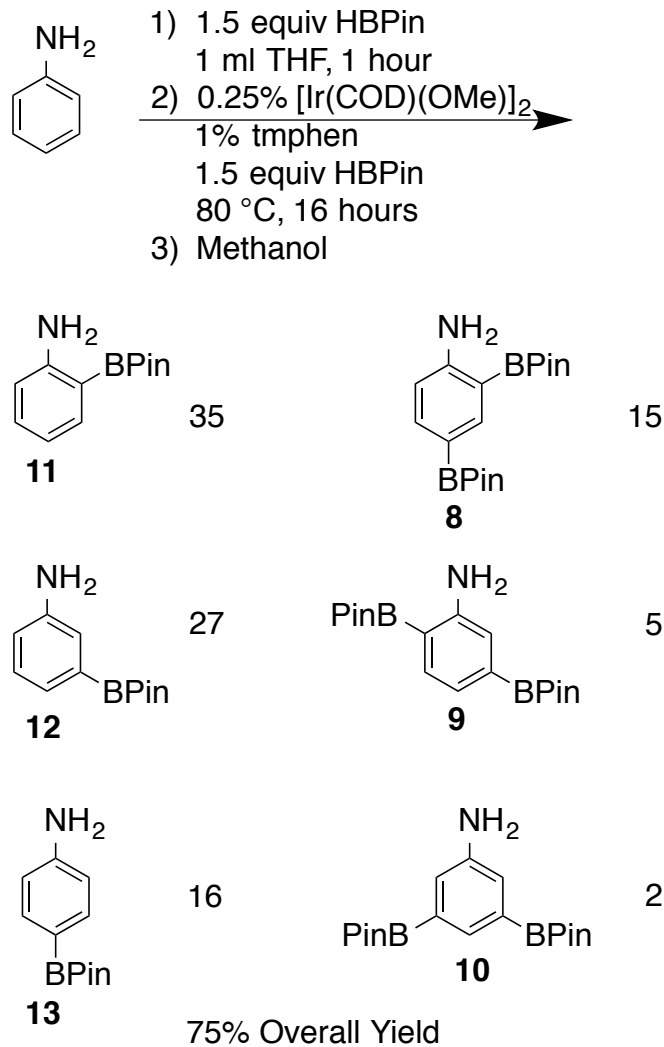


**Figure 2.7. The Diborylation of Monoborylated Anilines**



Using the data collected above, the precise quantities of borylated products were determined. It should be noted that there was no 2,6-diborylated aniline, probably due to steric hindrance. While the most common product was the ortho borylated product, there were a large quantity of other isomers, as seen in Figure 2.8.

**Figure 2.8. Borylated Aniline Isomers.**



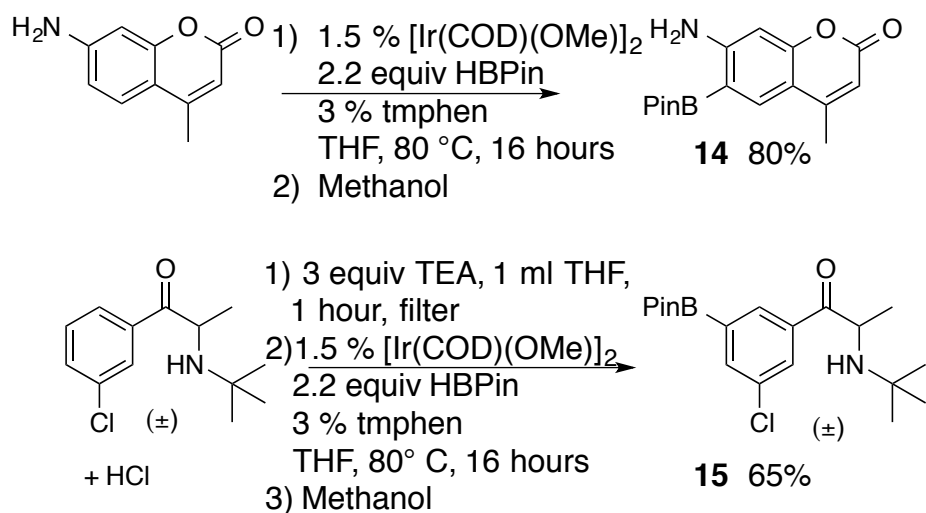
However when the total quantity of HBPIn used was decreased to 1.5 equivalents, a majority of the diborylated products were eliminated, yielding isomers **11** : **12** : **13** : **8** in a ratio of 10 : 6.5 : 4.1 : 1, but with lower overall conversion.

### Application Towards the Borylation of Drugs

Of course, being able to show the practical, real world applications of the traceless protection technique is a worthwhile endeavor. To this ends, 7-amino-4-methylcoumarin, a substrate chromophore, and bupropion HCl, also known as

Wellbutrin®, an antidepressant used as a smoking cessation aid,<sup>11</sup> were borylated, as seen in Figure 2.9.

**Figure 2.9. The Borylation of 7-amino-4-methylcoumarin, and Bupropion HCl**



Although in both cases the least sterically hindered location is likely the one borylated, the drugs do provide examples of the traceless protection effect.

## REFERENCES

## REFERENCES

- 1) Mkhallid, I. A. I.; Barnard, J. H.; Marder, T. B.; Murphy, J. M.; Hartwig, J. F. *Chem. Rev.* **2010**, *110*, 890.
- 2) Roosen, P. C.; Kallepalli, V. A.; Chattopadhyay, B.; Singleton, D. A.; Maleczka, R. E., Jr.; Smith, M. R. *J. Am. Chem. Soc.* **2012**, *134*, 11350.
- 3) Kawamorita, S.; Ohmiya, H.; Hara, K.; Fukuoka, A.; Sawamura, M. *J. Am. Chem. Soc.* **2009**, *131*, 5058
- 4) Ishiyama, T.; Isou, H.; Kikuchi, T.; Miyaura, N. *Chem. Commun.* **2010**, *46*, 159.
- 5) Boebel, A. T.; Hartwig, J. F. *J. Am. Chem. Soc.* **2008**, *130*, 7534
- 6) Samec, J. S. M.; Backvall, J. E.; Andersson, P. G.; Brandt, P. *Chem. Soc. Rev.* **2006**, *35*, 237.
- 7) Das, S.; Incarvito, C. D.; Crabtree, R. H.; Brudvig, G. W. *Science*, **2006**, *212*, 1941.
- 8) Vanchura, B. A., II; Preshlock, S. M.; Roosen, P. C.; Kallepalli, V. A.; Staples, R. J.; Maleczka, R. E., Jr; Smith, M. R. *Chem. Commun.* **2010**, *46*, 7724.
- 9) Paper Pending: Preshlock, S. M.; Plattner, D. L.; Maligres, P. E.; Krska, S. W.; Maleczka, R. E.; Smith, M. R. *Agnew. Chem. Int. Ed.* **2013**.
- 10) Tajuddin, H.; Harrison, P.; Bitterlich, B.; Collings, J. C.; Sim, N.; Batsanov, A. S.; Cheung, S. M.; Kawamorita, S.; Maxwell, A. C.; Shukla, L.; Morris, J.; Lin, Z.; Marder, T. B.; Steel, P. G. *Chem. Sci.*, **2012**, *3*, 3505
- 11) Jorenby, D. E.; Hays, J. T.; Rigotti, N. A.; Azoulay, S.; Watsky, E. J.; Williams, K. E.; Billing, C. B.; Gong, J.; Reebes, K. R. *J. Am. Med. Assoc.*, **2006**, *296*, 53.

## CHAPTER 3

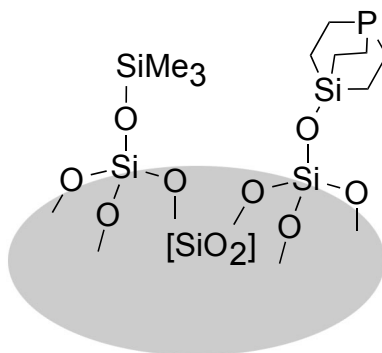
### Chelate Directed C-H Borylation

In recent years there has been a growing interest in iridium catalyzed ortho borylation of methyl benzoates and other aryl ketones,<sup>1,2</sup> with reactions involving silica-constrained monodentate trialkyl phosphine, silica-SMAP<sup>3</sup> and the P(3,5-bis(CF<sub>3</sub>)<sub>2</sub>-C<sub>6</sub>H<sub>3</sub>)<sub>3</sub>, PAr<sup>F</sup><sub>3</sub> ligand<sup>4</sup>, being particularly noteworthy.

#### Silica-SMAP

At the surface, borylations of methyl benzoate using the heterogeneous ligand silica-SMAP (Figure 3.1.) were shown to give high yields with high selectivity and few drawbacks.

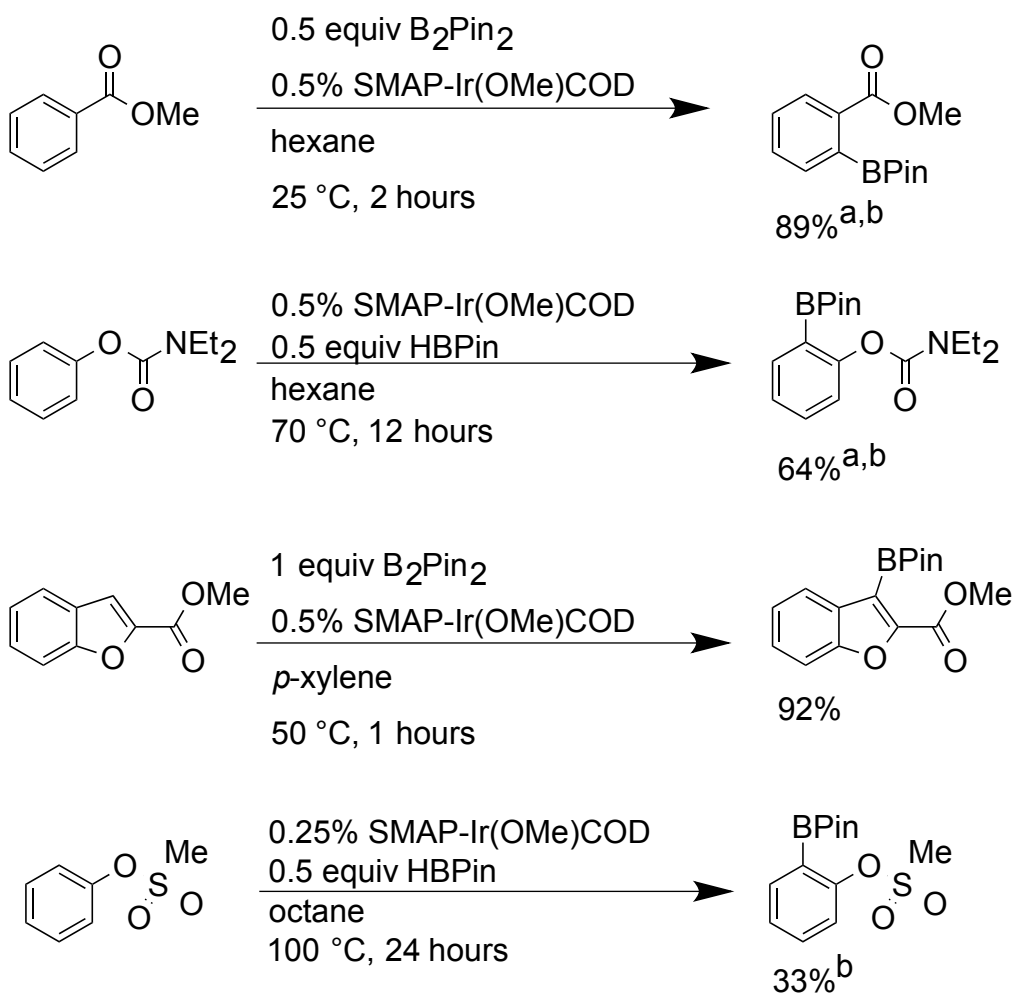
**Figure 3.1. Silica-SMAP Ligand**



Other silica-SMAP reactions using functional groups such carbamates<sup>5</sup>,

heteroatoms bearing methylbenzoate functional groups, and even phenylmethyl sulfonate<sup>6</sup>, to a lesser degree, were also shown to have high selectivity and yields under relatively mild conditions, as seen in Figure 3.2.

**Figure 3.2. Reactions Involving Silica-SMAP**



<sup>a</sup> plus additional minor diborylated products

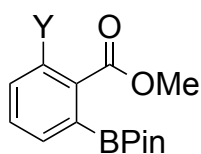
<sup>b</sup> yields based on B<sub>2</sub>Pin<sub>2</sub>/HBPIn

Unfortunately, the largest weakness of silica-SMAP comes in the ligand's preparation which can only be obtained through an arduous process with a 24 percent yield.<sup>7,8</sup> This means that silica-SMAP's viability for large scale reactions, is minimal.

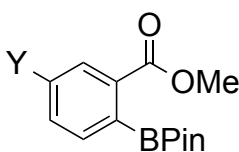
### **PAr<sup>F</sup><sub>3</sub> Ligand and Derivatives**

The PAr<sup>F</sup><sub>3</sub> ligand, on the other hand, can be purchased from chemical retailers. But while reactions with the PAr<sup>F</sup><sub>3</sub> ligand yielded borylated products in with high selectivity's and yields, (Figure 3.3), there were some drawbacks.

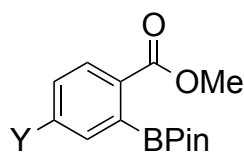
**Figure 3.3. Reactions using the PAr<sup>F</sup><sub>3</sub> ligand.**



Y = Me <sub>2</sub> N	97%
Y = Me	92%
Y = Br	60%
Y = CF <sub>3</sub>	98%



Y = Me <sub>2</sub> N	99%
Y = Me	98%
Y = Br	64%
Y = CF <sub>3</sub>	94%



Y = Me <sub>2</sub> N	93%
Y = Me	99%
Y = Br	57% <sup>a</sup>
Y = CF <sub>3</sub>	98%

Reactions were carried out at 80 °C for 16 hours using 5.0 mmol nonborylated substrate, 1.0 mmol B<sub>2</sub>Pin<sub>2</sub>, 0.015 mmol [Ir(OMe)(COD)]<sub>2</sub>, 0.06 mmol PAr<sup>F</sup><sub>3</sub>, 6 ml octane. Yields were obtained through GC and based on B<sub>2</sub>Pin<sub>2</sub>.

<sup>a</sup> reaction carried out in a mixture of octane and mesitylene (1:1)

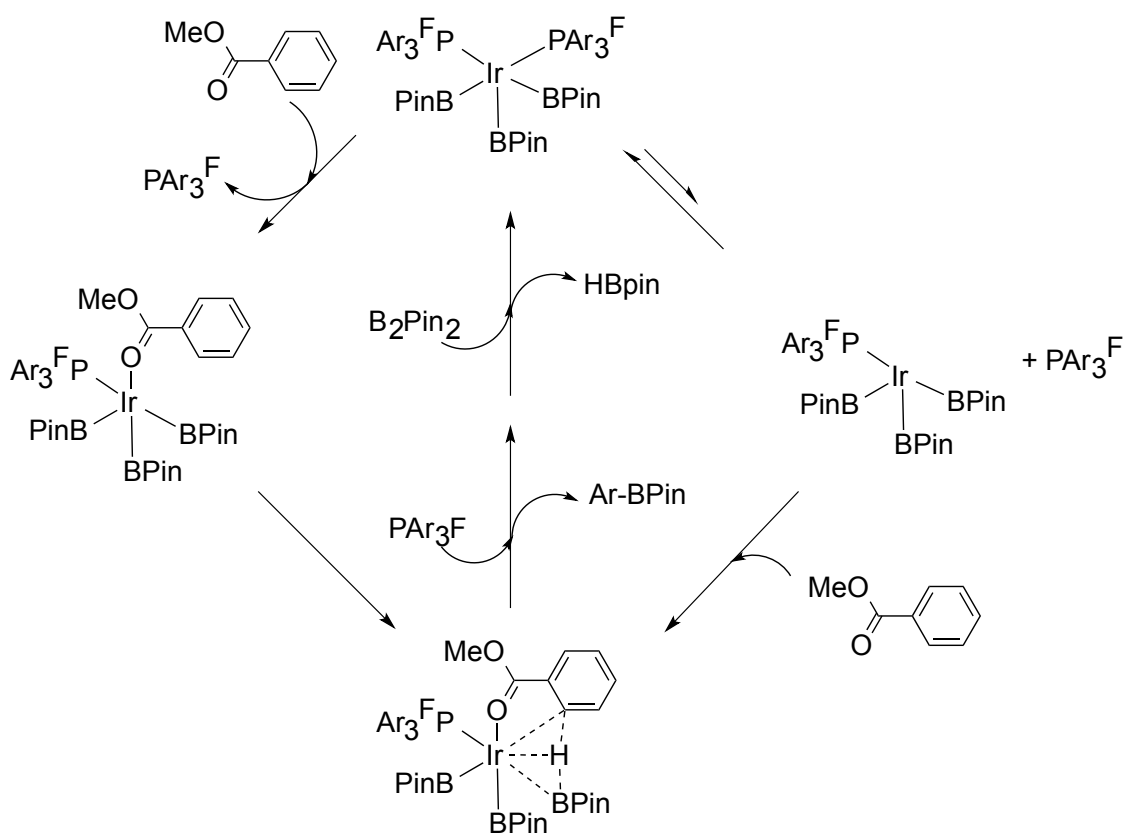
The main issue with the PAr<sup>F</sup><sub>3</sub> ligand is the requirement of a large excess of substrate. This is most likely because the HBPin formed in during reactions acts as an



inhibitor to the catalyst.<sup>9</sup>

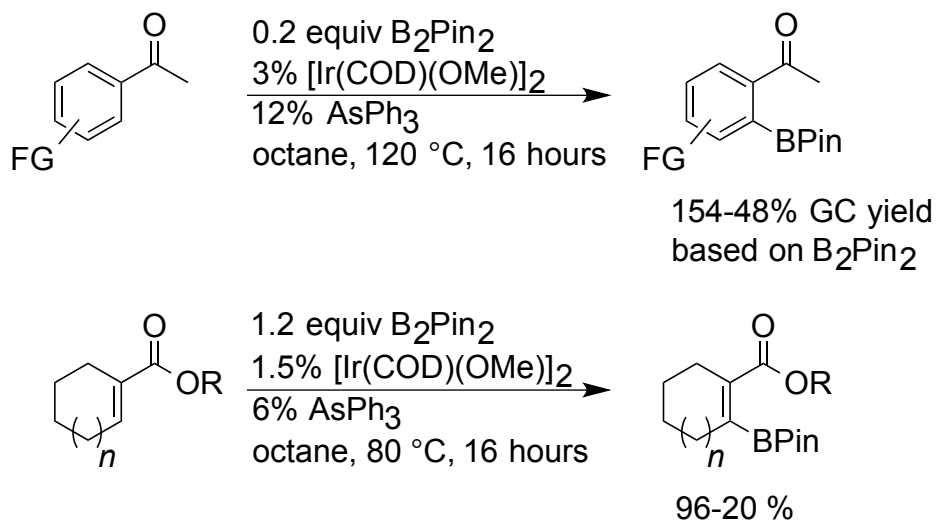
The actual mechanism behind the  $\text{PAr}^{\text{F}}_3$  ligand provides insight into how better, more efficient ligands could be made. Based on the proposed mechanism shown in Figure 3.4, the catalyst thus required either coordination by the ester of the methyl benzoate followed by dissociation of one of the  $\text{PAr}^{\text{F}}_3$  ligands, or dissociation of the  $\text{PAr}^{\text{F}}_3$  ligand followed by coordination of the ester of the methyl benzoate, in order to form the active catalyst. Regardless of which route it takes, one  $\text{PAr}^{\text{F}}_3$  ligand must dissociate in order for the reaction to occur.

**Figure 3.4.  $\text{PAr}^{\text{F}}_3$  Transition State Leading to Ortho Borylation.**



In this same vein of chelate directed mechanisms, the ligand AsPh<sub>3</sub> was shown to borylate a number of different substrate types, and was not limited to methyl benzoates. Whereas the PAr<sup>F</sup><sub>3</sub> ligand was only able to borylate ketones with a 56% yield, the new AsPh<sub>3</sub> ligand obtained yields of over 100% for a number of ketone substrates, based on B<sub>2</sub>Pin<sub>2</sub>.<sup>10</sup> Furthermore, the ligand was shown to effectively borylate α,β-unsaturated esters, although it should be noted that the substrates were limited to ones where the double bond was part of a ring.<sup>11</sup> (Figure 3.5) Unlike the PAr<sup>F</sup><sub>3</sub> ligand, HBPIn was shown to not to have as adverse an effect on reaction yields.

**Figure 3.5. Functionalization Using AsPh<sub>3</sub> Ligand**

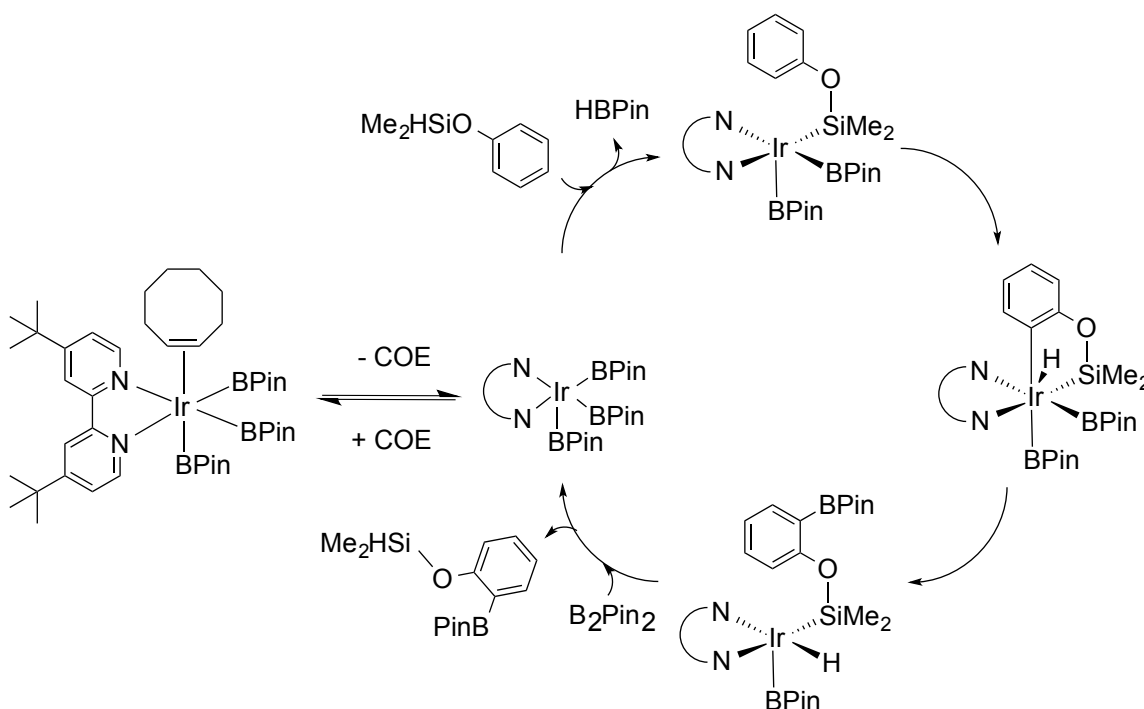


where FG = OMe, Me, Cl, CF<sub>3</sub>  
And R = alkyl groups

## Silyl Directed Borylation

Indirectly related to ortho borylation of methyl benzoates, was the development of a technique which allowed for the ortho borylation of silylated phenols, benzylic hydrosilanes,<sup>12</sup> secondary benzylic C-H bonds,<sup>13</sup> and nitrogen containing heterocycles.<sup>14</sup> The quintessential aspect of this reaction was that it occurred through a relay directed mechanism, wherein the silyl group binds to the iridium catalyst in order to direct C-H borylation, as seen in Figure 3.6.

**Figure 3.6. Mechanism for the Silyl Directed Borylation of Phenols**

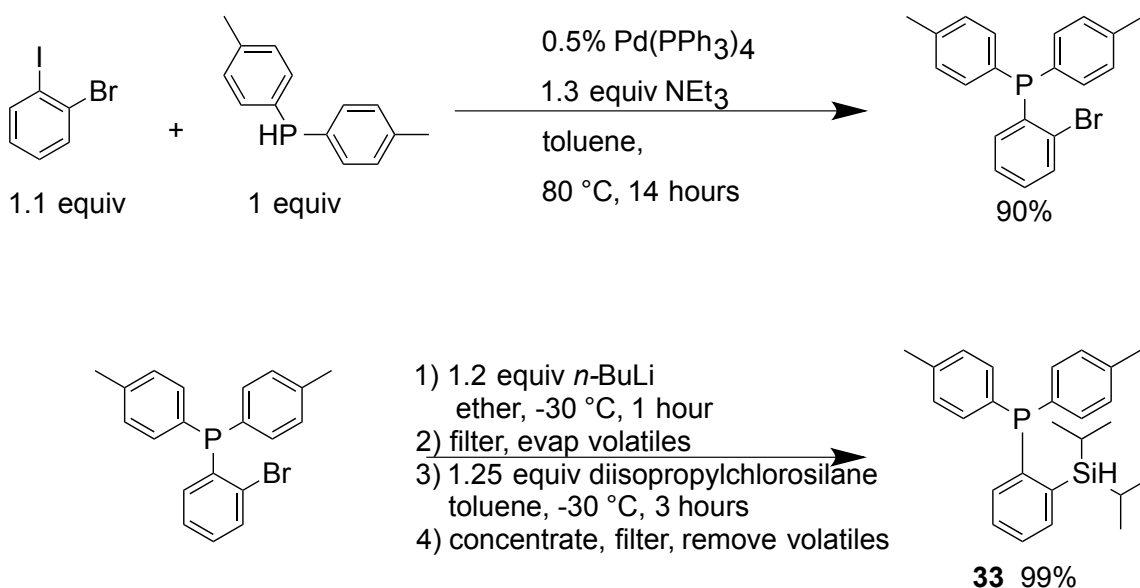


Following the borylation of the substrate, reductive elimination of the ArMe<sub>2</sub>Si-H bond from the iridium occurred, releasing the substrate and allowing the catalyst cycle to continue.

## Development of the SiPBz Ligand

Using the knowledge gained from work done on the  $\text{PAr}^{\text{F}}_3$  ligand mechanism and the insight gained from relay directed borylation of silylated substrates, a new ligand capable of ortho borylation of methyl benzoates was designed. The ligand's synthesis is shown in Figure 3.7.

**Figure 3.7. Synthesis of the SiPBz ligand.**



The SiPBz ligand was developed with three key features in mind. The first feature was that the presence of steric bulk around the silicon part of the ligand, and the second was the presence of a strong backbone, in this case a benzene ring. The reason for these two features was that the work on a previous ligand prototype, as well as work done to isolate the active 5 coordinate  $\text{Ir}^{\text{III}}$  catalyst used for C-H borylation,<sup>15</sup> proved that without the necessary steric bulk, you can get multiple ligands binding to the catalyst, or

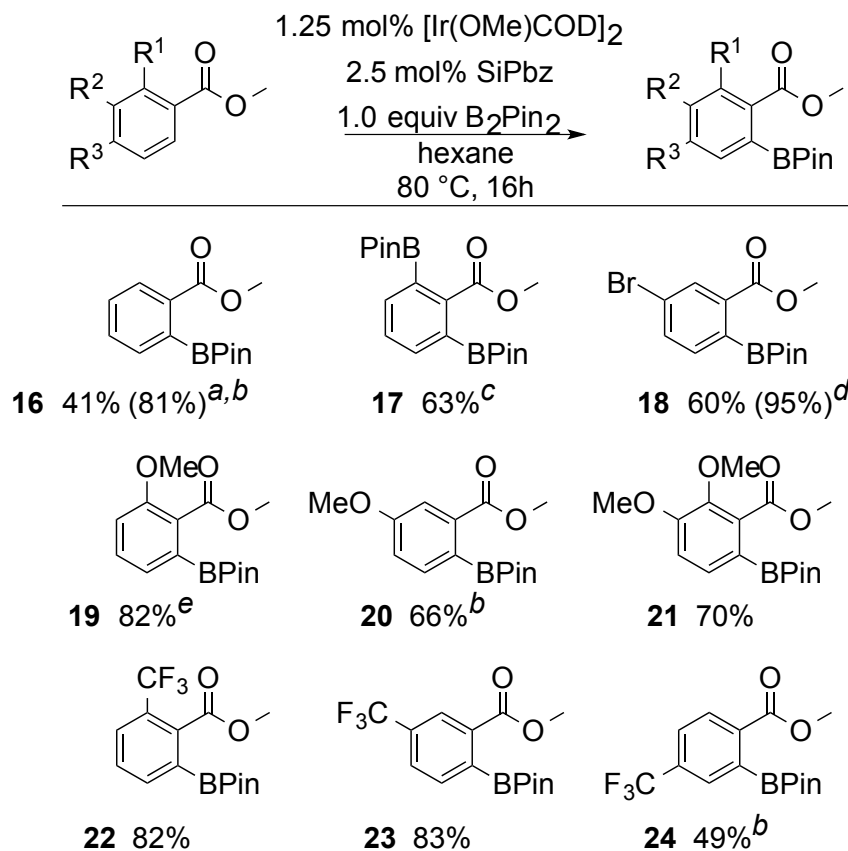
you can get ligands which bind to two metal centers. The third part of the ligand, the phosphorus part, was designed to be electron donating enough that C-H activation could occur. Furthermore, the phosphorus tethers the ligand to the iridium metal, which is useful because ability of the *Arip*r<sub>2</sub>Si-H to reductively eliminate from the iridium.

Because of the presence of a silicon group which binds to the iridium metal, a stable Ir(III) transition state can be obtained when only two other boryl ligands are bound to it. This leaves two coordination sites vacant on the 14 electron catalyst, which allows for a chelate directed mechanism.

### **Substrate Scope**

This ligand, SiPBz, is easy to synthesize, which was the major problem with the silica-SMAP ligands, and is able to react in the presence of HBPin, and therefore reactions do not require an excess of substrate, which was one of the major issues with the PAr<sup>F</sup><sub>3</sub> ligand. The full substrate scope is shown below in Figure 3.8. and Figure 3.9.

**Figure 3.8. SiPBz Substrate Scope**



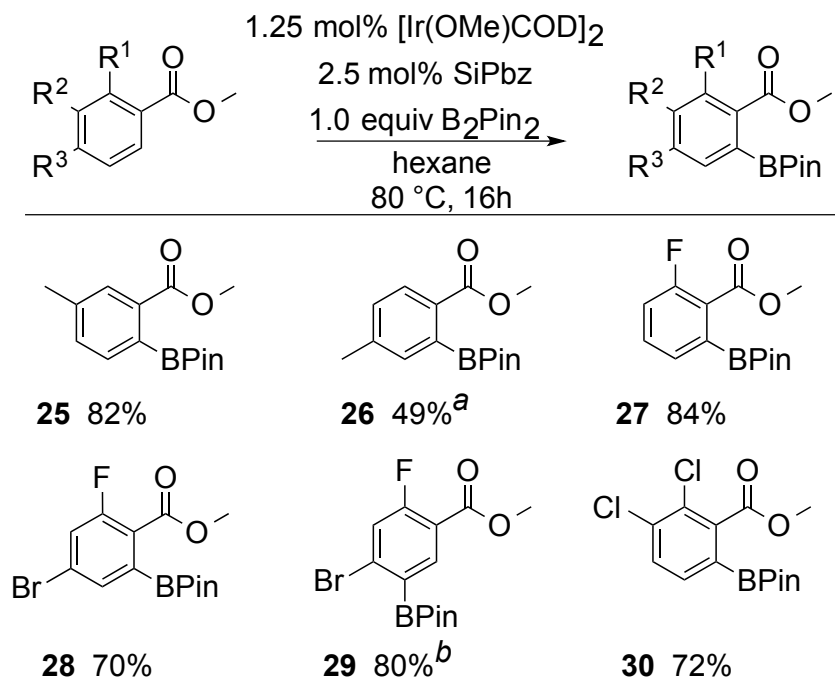
<sup>a</sup> used 0.5 equiv B<sub>2</sub>Pin<sub>2</sub>. <sup>b</sup> resulted in di borylated byproducts. <sup>c</sup> used 2.0 equiv B<sub>2</sub>Pin<sub>2</sub>. <sup>d</sup> used half the amount of substrate, but kept other reagent quantities the same. <sup>e</sup> used 1.25 equiv B<sub>2</sub>Pin<sub>2</sub>.

Initial tests on methyl benzoate using one equivalent of B<sub>2</sub>Pin<sub>2</sub>, yielded a mixture of mono and diborylated product with yields high enough to imply that both HBPIn and B<sub>2</sub>Pin<sub>2</sub> can be used as reagents for the reaction. Indeed, when one equivalent of HBPIn was used, monoborylation does occur, albeit with meta and para borylated products as well (*o* : *m* : *p* = 40 : 14 : 13). However, when 0.5 equivalents of B<sub>2</sub>Pin<sub>2</sub> were used, products were mostly monoborylated, and the yield was high relative to B<sub>2</sub>Pin<sub>2</sub>.

In the case of the  $\text{PAr}^{\text{F}}_3$  ligand, one of the drawbacks was the low yields obtained when using brominated methyl benzoate substrates. Even with the SiPBz ligand, the conversion to **18** using standard conditions was only 33%. However, by halving the amount of substrate and then doubling the quantity of  $\text{B}_2\text{Pin}_2$  while keeping all other factors the same, **18** was obtained with 95% assay yield using DHT standard, and 60% overall yield, with the low yields relative to conversion being attributed to difficulty recrystallizing due to the excess  $\text{B}_2\text{Pin}_2$ .

Substrates containing an electron donating methoxy group, **19**, **20**, **21**, gave borylation with high selectivity as did the borylation substrates with the electron withdrawing trifluoromethyl groups, **22**, **23**, **24**.

**Figure 3.9. SiPBz Substrate Scope Continued**



<sup>a</sup> resulted in di borylated byproducts <sup>b</sup> used 2.5% dtbpy as a ligand instead of SiPBz

It is worth pointing out that the para substituted methyl benzoates, **24** and **26**, both gave diborylation, which was to be expected considering the results of **16**. Attempts to curb diborylation of the substrates by using 0.5 equivalents B<sub>2</sub>Pin<sub>2</sub> merely lowered the overall borylation.

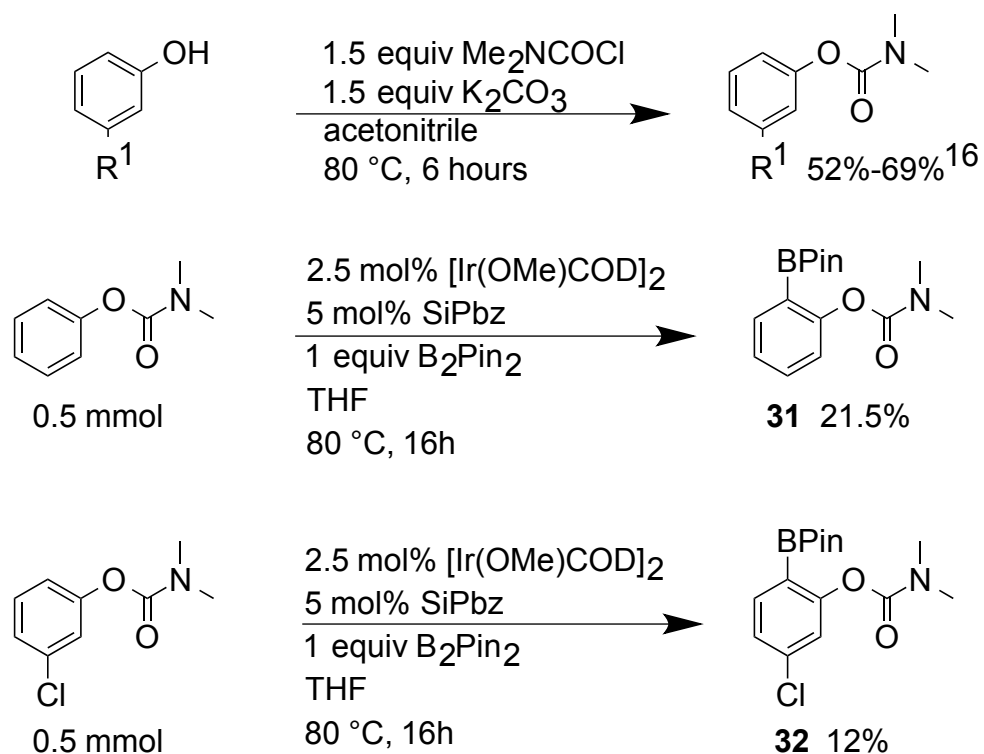
The borylation of **28** occurred with a much higher yield than was expected when compared to **18**. The presence of the fluorine substituent obviously improved yield of **28** compared to **18**, while the presence of the bromine decreased the yield when compared to **27**. The source of the different yields most likely has electronic origins, though non-obvious ones.

Similarly, it is curious that borylation of **30** performed under standard conditions resulted in a modest yield, showing that other halogens like chlorine didn't decrease the reactivity.

Following the borylation of methyl benzoates, it was decided to expand the scope of the reactions to include carbamates, a substrate which had been effectively borylated using silica-SMAP (Figure 3.10).

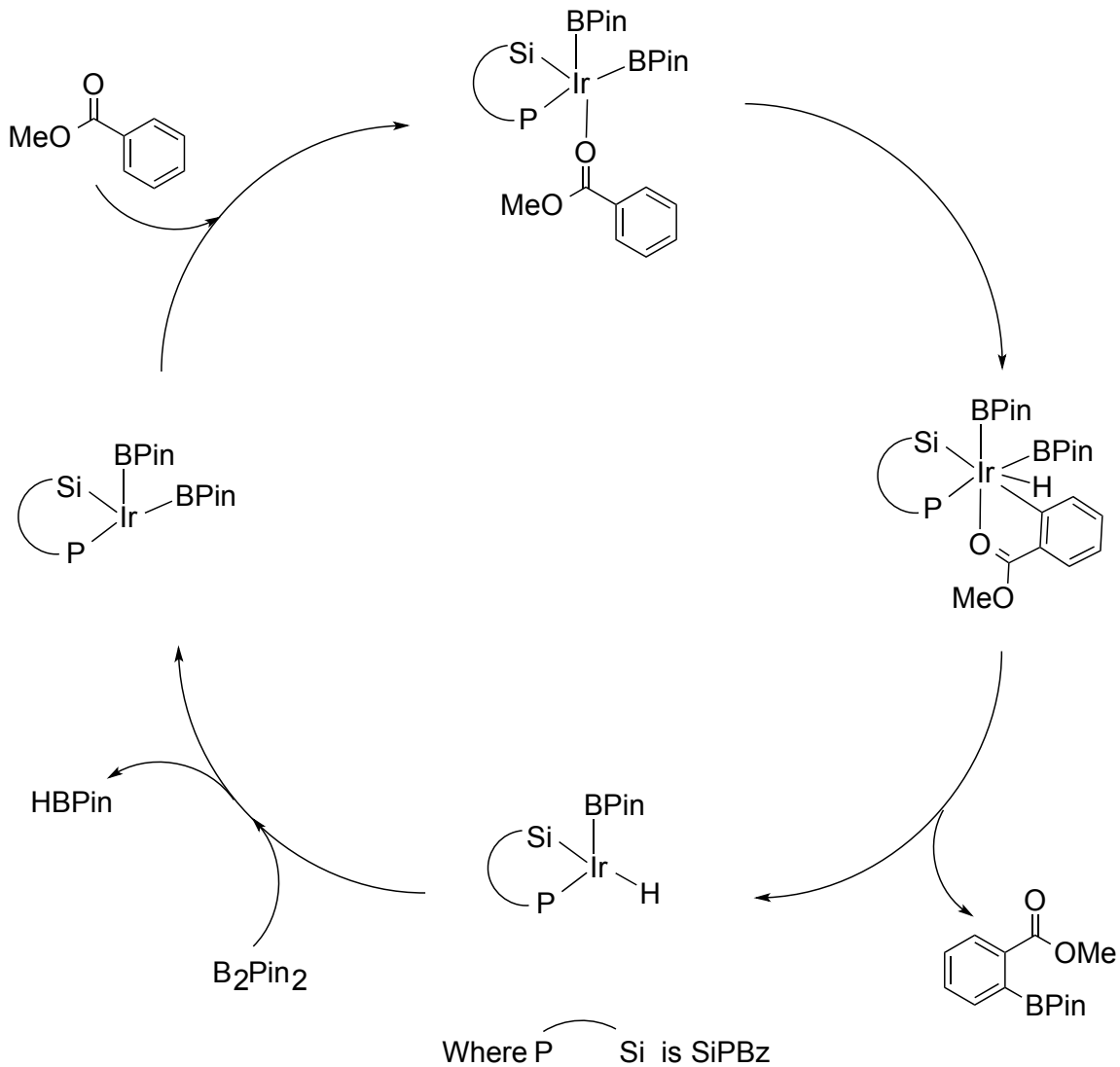


**Figure 3.10. Borylation of Carbamates**



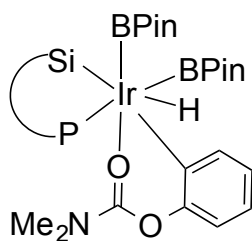
Low yields for these reactions could be traced to two factors. The first came from the theorized transition state. The SiPBz mechanism was designed to perform via a chelate directed mechanism, much like the  $\text{PAr}^{\text{F}}_3$  ligand, as seen in Figure 3.11.

**Figure 3.11. Proposed Mechanism for the SiPBz Ligand**



The key transition state in the mechanism comes in the form of a five-membered intermediate. The borylation of carbamates, however, would require a six-membered ring intermediate, and the resulting ring strain, could cause both to lower yields. (Figure 3.12)

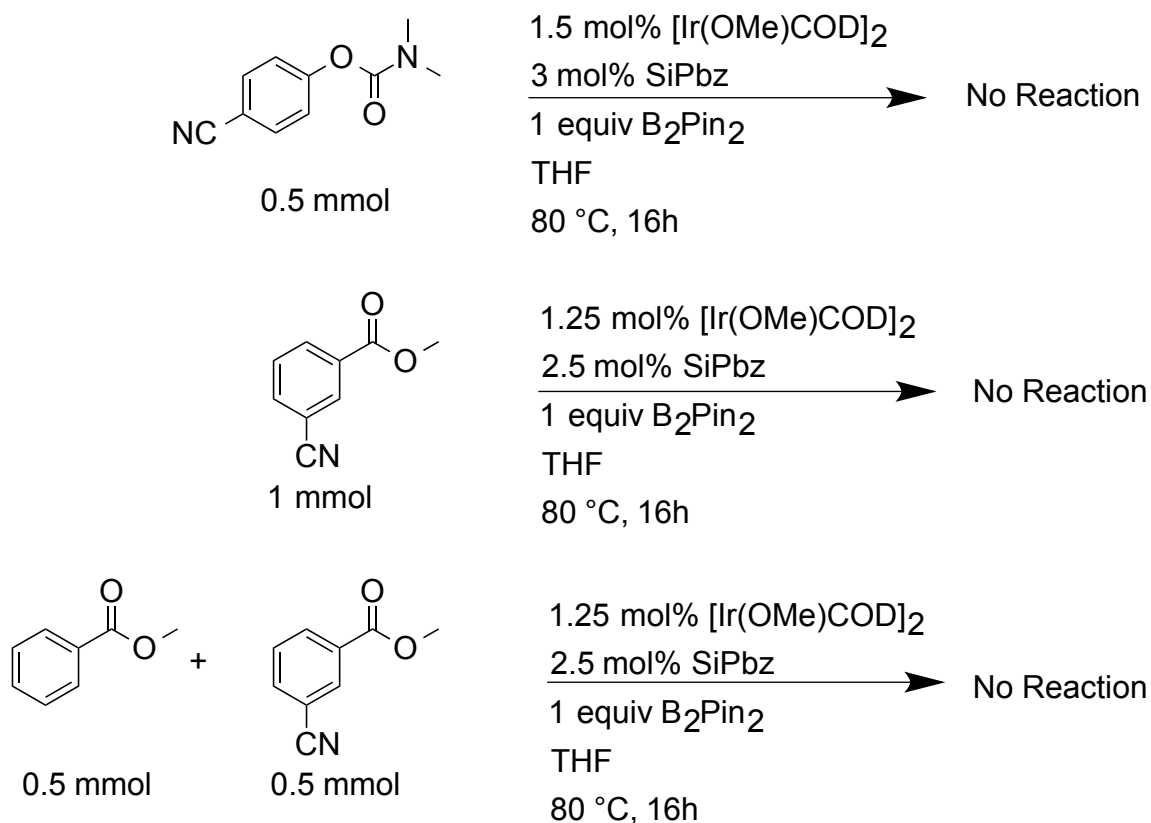
**Figure 3.12. Carbamate Intermediate**



The second factor that caused low yields resulted from difficulty purifying the product and separating it from starting material, due to a lack of carbamate fluorescence. Previous work on the borylation of carbamates using silica-SMAP must have had similar problems, and were therefore forced to use gel permeation chromatography, GPC, to isolate the products. Fortunately, a TLC indicator Alizarin was found to be adequate, although streaking of the products was observed, which resulted in low isolated yields. Worth noting is the fact that no diborylation of **31** was observed. However, this could simply be attributed to the low overall conversion.

Some of the reactions that failed were just as curious as those that worked, and are shown in Fig 3.14. Initial tests on a cyano carbamate revealed no conversion. However, seeing as how low the conversion of other carbamate substrates was, the cause of the failed reaction might of have been simply due to the transition state. Yet when a cyano methyl benzoate substrate was used, no reaction occurred. From here there were two possibilities. The first was that the substrates with a cyano functional group were simply incompatible with the reaction, and the second was that the cyano group was somehow interfering with the catalytic process. The latter looks to be the answer, seeing as how a mixture of cyano methyl benzoate and pure methyl benzoate yield no conversion at all.

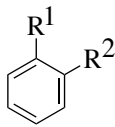
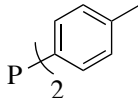
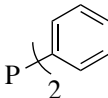
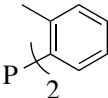
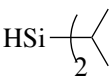
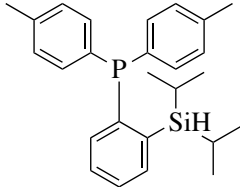
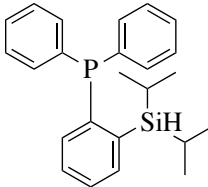
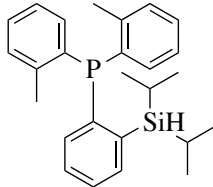
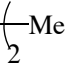
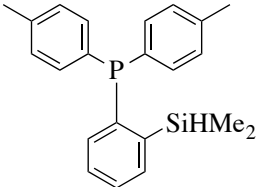
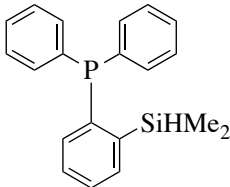
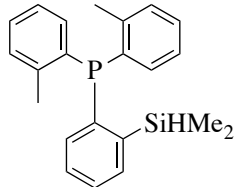
**Figure 3.13 Failed Cyano Substrate Reactions.**



### Optimization of the SiPBz Ligand

One of the greatest attributes of the SiPBz ligand is the ease with which it can be modified in order to optimize selectivity. Phosphorus groups, silicon groups, and even the benzene backbone can easily be changed in order to tweak the reaction selectivity. In order to determine how such alterations might affect the selectivity and conversion of the catalyst, six variations of the catalyst were synthesized and tested on four different substrates, as shown below in Table 3.1, 3.2, 3.3, and 3.4.

**Table 3.1. Variations of the SiPBz Ligand**

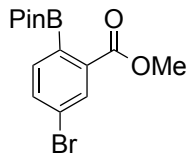
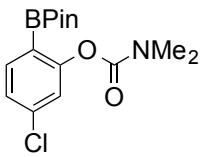
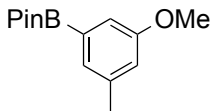
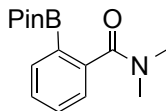
	$R^1 =$ 	$R^1 =$ 	$R^1 =$ 
$R^2 =$ 	 <p><b>33</b> 99%</p>	 <p><b>35</b> 50%</p>	 <p><b>37</b> 73%</p>
$R^2 =$ 	 <p><b>34</b> 85%</p>	 <p><b>36</b> 65%</p>	 <p><b>38</b> 92%</p>

The two minor variations on the phosphorus part of the standard SiPBz ligand, **33**, were chosen in order to determine how a less electron donating ligand, **35**, and how a more constrained ligand, **37**, would affect the conversion.<sup>17</sup>

Less sterically hindered methyl groups on the silicon groups had been shown increase the NMR yield for the borylation of plain carbamate by 5%, and were therefore also tested, **34**, **36**, **38**.

In general, the original SiPBz ligand, **33**, was shown to be the most efficient catalyst of the bunch as seen in the table below.

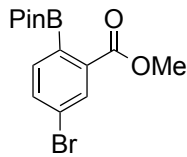
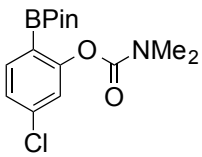
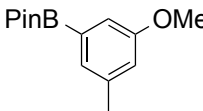
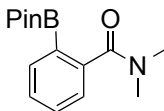
**Table 3.2 Optimization of the SiPBz Ligand Comparing Results of **33** and **34**.**

Ligands				
<b>33</b>	37 %	45 %	8.5 %	43 %
<b>34</b>	17 %	43 %	0.6 %	45 %

Reaction were conducted on a 0.1 mmol scale. Conditions are as follows: 1.25 mol% [Ir(OMe)COD]<sub>2</sub>, 1.0 equiv B<sub>2</sub>Pin<sub>2</sub>, 2.5 mol% ligand, 0.1 mmol unborylated substrate, THF, 80 °C, 16 hours. Yields are NMR yields based on a DHT standard.

The less electron donating ligands, **35** and **36**, didn't seem to have much affect on the conversion of starting material when compared to **33** and **34**, as shown in table 3.3.

**Table 3.3 Optimization of the SiPBz Ligand Comparing Results of **35** and **36**.**

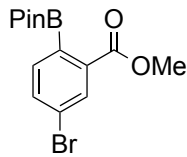
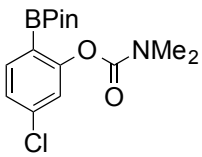
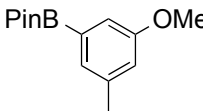
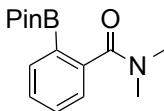
Ligands				
<b>35</b>	47 %	37 %	7.0 %	43 %
<b>36</b>	14 %	33 %	0.6 %	44 %

Reaction were conducted on a 0.1 mmol scale. Conditions are as follows: 1.25 mol% [Ir(OMe)COD]<sub>2</sub>, 1.0 equiv B<sub>2</sub>Pin<sub>2</sub>, 2.5 mol% ligand, 0.1 mmol unborylated substrate, THF, 80 °C, 16 hours. Yields are NMR yields based on a DHT standard.

The exception to this being with the conversion of the brominated methyl benzoate, where **35** gave a 10 % higher conversion than **33**, and with chlorinated carbamate, where **35** gave a 7 % lower conversion than **33**.

The sterically altered ligands, **37** and **38**, almost always gave much lower yields than the rest of the ligands as shown in Table 3.4. This is most likely because the steric bulk prevents coordination to the iridium metal.

**Table 3.4 Optimization of the SiPBz Ligand Comparing Results of 37 and 38.**

Ligands				
37	0.0 %	4.0 %	0.0 %	19 %
38	3.0 %	0.0 %	7.0 %	36 %

Reaction were conducted on a 0.1 mmol scale. Conditions are as follows: 1.25 mol% [Ir(OMe)COD]<sub>2</sub>, 1.0 equiv B<sub>2</sub>Pin<sub>2</sub>, 2.5 mol% ligand, 0.1 mmol unborylated substrate, THF, 80 °C, 16 hours. Yields are NMR yields based on a DHT standard.

Those ligands where the silica groups had been made less hindered, **34**, **36**, **38**, tended to show a mild decrease in conversion compared to their isopropyl counterparts, which was contrary to what was seen with the borylation of pure carbamate by **34**, but followed the line of thinking that a decrease in steric bulk around the silica groups could cause a decrease in conversion.



## REFERENCES

## REFERENCES

- 1) Miyaura, N. *Bull. Chem. Soc. Jpn.* **2008**, *81*, 1535
- 2) Itoh, H.; Kikuchi, T.; Ishiyama, T.; Miyaura, N. *Chem Lett.* **2011**, *40*, 1007
- 3) Kawamorita, S.; Ohmiya, H.; Hara, K.; Fukuoka, A.; Sawamura, M. *J. Am. Chem. Soc.* **2009**, *131*, 5058
- 4) Ishiyama, T.; Isou, H.; Kikuchi, T.; Miyaura, N. *Chem. Commun.* **2010**, *46*, 159.
- 5) Yamazaki, K.; Kawamorita, S.; Ohmiya, H.; Sawamura, M. *Org. Lett.* **2010**, *12*, 3978
- 6) Kawamorita, S.; Ohmiya, H.; Sawamura, M. *J. Org. Chem.* **2010**, *75*, 3855
- 7) Hamasaka, G.; Kawamorita, S.; Ochida, A.; Akiyama, R.; Hara, K.; Fukuoka, A.; Asakura, K.; Chun, W. J.; Ohmiya, H.; Sawamura, M. *Organometallics*. **2008**, *27*, 6495.
- 8) Ochida, A.; Hamasaka, G.; Yamauchi, Y.; Kawamorita, S.; Oshima, N.; Hara, K.; Ohmiya, H.; Sawamura, M. *Organometallics*. **2008**, *27*, 5494.
- 9) Preshlock, S. M. *Ph. D. Thesis. Mich. State. University.* **2013**
- 10) Itoh, H.; Kikuchi, T.; Ishiyama, T.; Miyaura, N. *Chem Lett.* **2011**, *40*, 1007.
- 11) Sasaki, I.; Doi, H.; Hashimoto, T.; Kikuchi, T.; Ito, H.; Ishiyama, T. *Chem Commun.* **2013**, *49*, 7546.
- 12) Boebel, A. T.; Hartwig, J. F. *J. Am. Chem. Soc.* **2008**, *130*, 7534
- 13) Cho, S. H.; Hartwig, J. F. *J. Am. Chem. Soc.* **2013**, *135*, 8157.
- 14) Robbins, D. W.; Boebel, T. A.; Hartwig, J. F. *J. Am. Chem. Soc.* **2010**, *132*, 4068
- 15) Vanchura, B. A., II; Preshlock, S. M.; Roosen, P. C.; Kallepalli, V. A.; Staples, R. J.; Maleczka, R. E., Jr; Smith, M. R., III *Chem. Commun.* **2010**, *46*, 7724.
- 16) John, A.; Nicholas, K. M. *J. Org. Chem.* **2012**, *77*, 5600

- 17) (a) Broggi, J.; Urbina-Blanco, C.; Clavier, H.; Leitgeb, A.; Slugovc, C.; Slawin, A. M. Z.; Nolan, S. P. *Chem. Eur. J.* **2010**, *16*, 9125. (b) Oyetnuji, O. A.; Ramokongwa, G.; Ogunlusi, G. O.; Becker, C. A.L. *Transition. Met. Chem.* **2013**, *38*, 235. (c) Sun, X.; Kryatov, S. V.; Rybak-Akimova, E. V. *Dalton Trans.* **2013**, *42*, 4427.

## CHAPTER 4

### Conclusion

In summary, ortho directed borylation was achieved using HBPin as a traceless directing group for aniline substrates via an outer sphere mechanism. Although the regioselectivity was best for para-substituted anilines, the reactions still displayed relatively good regioselectivity for meta substituted anilines as well. However, the borylation of ortho substituted anilines gave no ortho borylation, although the reaction did yield a single borylated product. The borylation of aniline occurred with a surprisingly diverse quantity of isomers, and the borylation of monoborylated anilines was required in order to determine their ratios. In the end it was concluded that the monoborylated ortho product was the most common product. Furthermore, the borylation of both bupropion HCl and 7-amino-4-methylcoumarin was performed using HBPin as a traceless protecting group.

A new SiPBz ligand was also developed and used for the ortho borylation of methyl benzoate substrates and methyl benzoate derivatives. Such reactions occurred through an inner sphere mechanism and generally gave high yields. Exceptions include substrates which had a bromine group, which gave much lower yields, and those with a nitrile group which gave no yield at all, probably due to interaction of the cyano group with the open coordination site in the iridium catalyst complex. Slight alterations were also made to the SiPBz ligand in order to determine how minor variations in steric bulk and electronics affected the borylation of difficult substrates, like carbamates. In the end it was determined that the original SiPBz ligand was the best of the variations tested.

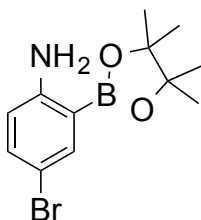
## CHAPTER 5

### Experimental Information

**General Methods.** All reactions were conducted in a nitrogen filled glove-box. THF was distilled from sodium benzophenone solutions. All other solvents were used as received from Sigma-Aldrich (Sure/Seal<sup>TM</sup>) and were stored in the glove-box. All other commercially available materials were used as received. <sup>1</sup>H and <sup>13</sup>C NMR spectra were recorded on a Varian Inova-300 (300.11 and 75.47 MHz respectively), Varian VXR-500 or Varian Unity-500-Plus spectrometer (499.74 and 125.67 MHz respectively) and referenced to residual solvent signals. <sup>11</sup>B spectra were recorded on Varian VXR-500 or Varian Inova-300 operating at 160.41 and 96.29 MHz respectively, and were referenced to neat BF<sub>3</sub>·Et<sub>2</sub>O as the external standard. Melting points were measured on a MEL-TEMP® capillary melting apparatus and are uncorrected.

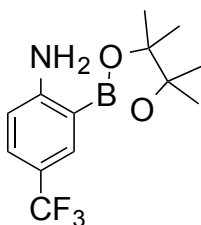
**General Procedure for *ortho*-directed Borylation of Anilines.** In a nitrogen filled glovebox, 1 mmol aniline substrate was dissolved in 1 mL THF in a 15 mL pressure tube containing a magnetic stir bar. 1.5 equiv HBpin (218  $\mu$ L) was added and the reaction vessel was sealed and stirred at room temperature for 1h. 0.25  $\mu$ mol [Ir(OMe)COD]<sub>2</sub> (0.25 mol%) and 1.0  $\mu$ mol 3,4,7,8-tetramethyl-1,10-phenanthroline (1.0 mol%) were added followed by an additional 1.5 equiv HBpin (218  $\mu$ L) and the reaction vessel was sealed and heated at 80 °C for 16h. The reaction mixture was allowed to return to room temperature and the reaction mixture was exposed to air and diluted with 5 mL MeOH. The volatiles were then removed under reduced pressure and the product was purified by passing it through a short plug of SiO<sub>2</sub> in MTBE. and recrystallization from MeOH/H<sub>2</sub>O.

**4-bromo-2-(4,4,5,5-tetramethyl-1,3,2-dioxaborolan-2-yl)-benzenamine (1)**



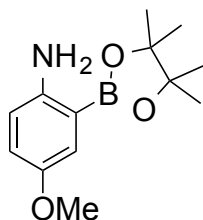
White solid (246 mg, 88% isolated yield); mp: 101-102 °C;  $^1\text{H}$  NMR (500 MHz,  $\text{CDCl}_3$ )  $\delta$  7.27 (d,  $J = 2.4$  Hz, 1H), 7.30 (dd,  $J = 8.8, 2.9$  Hz, 1H), 6.54 (d,  $J = 8.8$  Hz, 1H), 5.05 (br s, 2H), 1.34 (s, 12H);  $^{13}\text{C}$  NMR (125 MHz,  $\text{CDCl}_3$ )  $\delta$  151.7, 138.7, 135.2, 116.9, 109.2, 83.9, 24.9;  $^{11}\text{B}$  NMR (160 MHz,  $\text{CD}_2\text{Cl}_2$ )  $\delta$  30 (br s); HRMS (ESI)  $m/z$  calcd for  $\text{C}_{12}\text{H}_{17}\text{BBBrNO}_2$  [ $\text{M} + \text{H}$ ] $^+$  298.0614, found 298.0609.

**2-(4,4,5,5-tetramethyl-1,3,2-dioxaborolan-2-yl)-4-(trifluoromethyl)-benzenamine (2)**



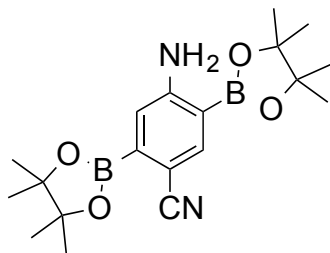
White solid (250 mg, 87% isolated yield); mp: 110-113 °C;  $^1\text{H}$  NMR (500 MHz,  $\text{CDCl}_3$ )  $\delta$  7.27 (d,  $J = 2.4$  Hz, 1H), 7.30 (dd,  $J = 8.8, 2.9$  Hz, 1H), 6.54 (d,  $J = 8.8$  Hz, 1H), 5.05 (br s, 2H), 1.34 (s, 12H);  $^{13}\text{C}$  NMR (125 MHz,  $\text{DMSO}-d_6$ )  $\delta$  151.2, 129.5, 124.7, 120.2 (q, 270.8), 113.9 (q, 32.5), 109.4, 79.2, 20.1;  $^{19}\text{F}$  NMR (470 MHz,  $\text{CDCl}_3$ )  $\delta$  -65.9;  $^{11}\text{B}$  NMR (160 MHz,  $\text{CDCl}_3$ )  $\delta$  30 (br s); HRMS (ESI)  $m/z$  calcd for  $\text{C}_{13}\text{H}_{17}\text{BF}_3\text{NO}_2$  [ $\text{M} + \text{H}$ ] $^+$  288.1385, found 288.1389.

**4-methoxy-2-(4,4,5,5-tetramethyl-1,3,2-dioxaborolan-2-yl)-benzenamine (3)**



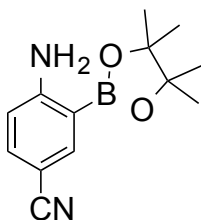
Pale red solid (157 mg, 63% isolated yield); mp: 73-74 °C;  $^1\text{H}$  NMR (500 MHz,  $\text{C}_6\text{D}_6$ )  $\delta$  7.16 (d,  $J = 2.9$  Hz, 1H), 7.60 (d,  $J = 2.9$  Hz, 1H), 6.94 (dd,  $J = 8.3, 2.9$  Hz, 1H), 6.53 (d,  $J = 8.8$  Hz, 1H), 4.31 (br s, 2H), 3.37 (s, 3H), 1.03 (s, 12H);  $^{13}\text{C}$  NMR (125 MHz,  $\text{CDCl}_3$ )  $\delta$  147.9, 133.9, 120.6, 119.6, 116.5, 83.8, 56.0, 24.9;  $^{11}\text{B}$  NMR (160 MHz,  $\text{C}_6\text{D}_6$ )  $\delta$  31 (br s); HRMS (ESI)  $m/z$  calcd for  $\text{C}_{13}\text{H}_{20}\text{BNO}_3$   $[\text{M} + \text{H}]^+$  250.1617, found 250.1616.

**4-amino-2,5-bis(4,4,5,5-tetramethyl-1,3,2-dioxaborolan-2-yl)-benzonitrile (4)**



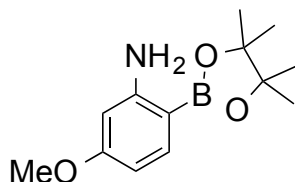
White solid (329 mg, 89% isolated yield); mp: 175-180 °C;  $^1\text{H}$  NMR (500 MHz,  $\text{CDCl}_3$ )  $\delta$  7.26 (s, 1H), 7.93 (s, 1H), 6.97 (s, 1H), 5.15 (br s, 2H), 1.36 (s, 12H), 1.33 (s, 12H);  $^{13}\text{C}$  NMR (125 MHz,  $\text{CDCl}_3$ )  $\delta$  155.3, 143.0, 121.3, 120.2, 103.5, 84.6, 84.1, 24.8;  $^{11}\text{B}$  NMR (160 MHz,  $\text{CDCl}_3$ )  $\delta$  29.7 (br s), 22.3 (s); HRMS (ESI)  $m/z$  calcd for  $\text{C}_{19}\text{H}_{28}\text{B}_2\text{N}_2\text{O}_4$   $[\text{M} + \text{H}]^+$  371.2313, found 371.2314.

#### 4-amino-3-(4,4,5,5-tetramethyl-1,3,2-dioxaborolan-2-yl)benzonitrile (5)



The reaction solvent was hexanes. The reaction was performed using 2.0 equiv HBpin (290  $\mu$ L). The reaction was performed using 1.5  $\mu$ mol [Ir(OMe)COD]<sub>2</sub> (1.5 mol%) and 3.0  $\mu$ mol N<sup>4</sup>,N<sup>4</sup>,N<sup>4'</sup>,N<sup>4'</sup>-tetramethyl-[2,2'-bipyridine]-4,4'-diamine (3.0 mol%). White solid (146 mg, 60% isolated yield, (83% assay yield by <sup>1</sup>H NMR); mp: 96-97 °C; <sup>1</sup>H NMR (500 MHz, CDCl<sub>3</sub>, 7.27)  $\delta$  7.92 (d, *J* = 2.0 Hz, 1H), 7.43 (dd, *J* = 8.8, 2.0 Hz, 1H), 6.57 (d, *J* = 8.8 Hz, 1H), 5.27 (br s, 2H), 1.37 (s, 12H); <sup>13</sup>C NMR (125 MHz, CDCl<sub>3</sub>)  $\delta$  156.5, 141.9, 135.9, 120.2, 114.5, 99.0, 84.2, 24.9; <sup>11</sup>B NMR (160 MHz, CDCl<sub>3</sub>)  $\delta$  30 (br s); HRMS (ESI) *m/z* calcd for C<sub>13</sub>H<sub>17</sub>BN<sub>2</sub>O<sub>2</sub> [M + H]<sup>+</sup> 245.1464, found 245.1467.

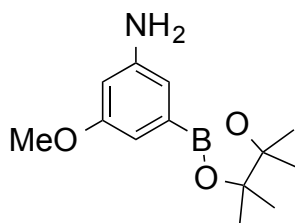
#### 5-methoxy-2-(4,4,5-trimethyl-1,3,2-dioxaborolan-2-yl)aniline (6a)



The reaction was performed using 2.5  $\mu$ mol [Ir(OMe)COD]<sub>2</sub> (2.5 mol%) and 5.0  $\mu$ mol 3,4,7,8-tetramethyl-1,10-phenanthroline (5.0 mol%). Purified by column chromatography; hexanes: EtOAc (70: 30). Red gel (91.0 mg, 26%); <sup>1</sup>H NMR (500 MHz, CDCl<sub>3</sub>, 7.26)  $\delta$  7.54 (d, *J* = 8.3 Hz, 1H), 6.27 (dd, *J* = 8.3, 2.4 Hz, 1H), 6.11 (d, *J* = 2.4 Hz, 1H), 4.76 (br s, 2H), 3.76 (s, 3H), 1.32 (s, 12H); <sup>13</sup>C NMR (125 MHz, CDCl<sub>3</sub>)  $\delta$  163.6, 155.4, 138.4, 103.7, 99.4, 83.2, 54.9, 24.8; <sup>11</sup>B NMR (160 MHz, CDCl<sub>3</sub>)  $\delta$  30 (br s); HRMS (ESI) *m/z* calcd for C<sub>13</sub>H<sub>20</sub>BNO<sub>3</sub> [M + H]<sup>+</sup> 250.1617, found 250.1626

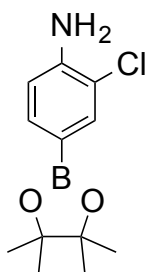


**3-methoxy-5-(4,4,5,5-tetramethyl-1,3,2-dioxaborolan-2-yl)aniline (6b)**



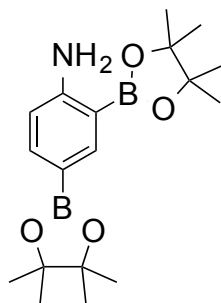
The reaction was performed using 2.5  $\mu\text{mol}$   $[\text{Ir}(\text{OMe})\text{COD}]_2$  (2.5 mol%) and 5.0  $\mu\text{mol}$  3,4,7,8-tetramethyl-1,10-phenanthroline (5.0 mol%). Purified by column chromatography; hexanes: EtOAc (70: 30). Red crystal solid (163.8 mg, 47%); mp: 90-93  $^{\circ}\text{C}$ ;  $^1\text{H}$  NMR (500 MHz,  $\text{CD}_3\text{CN}$ , 1.94)  $\delta$  6.61 (d,  $J$  = 1.4 Hz, 1H), 6.54 (d,  $J$  = 1.9 Hz, 1H), 6.39 (t,  $J$  = 2.6, 1.9 Hz, 1H), 4.15 (br s, 2H), 3.73 (s, 3H), 1.32 (s, 12H);  $^{13}\text{C}$  NMR (125 MHz,  $\text{CDCl}_3$ )  $\delta$  163.3, 146.7, 114.5, 109.1, 104.9, 83.7, 55.2, 24.8;  $^{11}\text{B}$  NMR (160 MHz,  $\text{CD}_3\text{CN}$ )  $\delta$  31 (br s); HRMS (ESI)  $m/z$  calcd for  $\text{C}_{13}\text{H}_{20}\text{BNO}_3$   $[\text{M} + \text{H}]^+$  250.1617, found 250.1620.

**2-chloro-4-(4,4,5,5-tetramethyl-1,3,2-dioxaborolan-2-yl)aniline (7)**



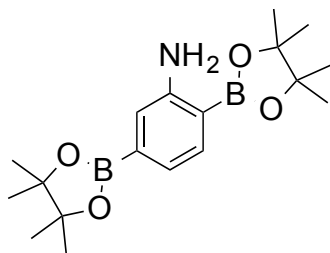
Brown solid (170 mg, 68% isolated yield); mp: 78  $^{\circ}\text{C}$ ;  $^1\text{H}$  NMR (500 MHz,  $\text{CDCl}_3$ , 7.26)  $\delta$  7.69 (s, 1H), 7.49 (d,  $J$  = 7.8 Hz, 1H), 6.74 (d,  $J$  = 7.9 Hz, 1H), 4.25 (br s, 2H), 1.31 (s, 12H);  $^{13}\text{C}$  NMR (125 MHz,  $\text{CDCl}_3$ )  $\delta$  145.4, 136.0, 134.3, 118.7, 114.9, 83.6, 24.8;  $^{11}\text{B}$  NMR (160 MHz,  $\text{CDCl}_3$ )  $\delta$  30 (br s); HRMS (ESI)  $m/z$  calcd for  $\text{C}_{12}\text{H}_{17}\text{BClNO}_2$   $[\text{M} + \text{H}]^+$  254.1121, found 254.1126.

**2,4-bis(4,4,5,5-tetramethyl-1,3,2-dioxaborolan-2-yl)aniline (8)**



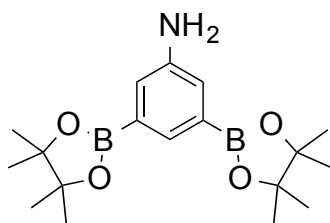
Red solid (242 mg, 70% isolated yield); mp: 152-157 °C;  $^1\text{H}$  NMR (500 MHz,  $\text{CDCl}_3$ , 7.26)  $\delta$  8.11 (s,  $J = 1.4$  Hz, 1H), 7.67 (dd,  $J = 15, 8.3$  Hz, 1H), 6.62 (d,  $J = 7.8$  Hz, 1H), 5.30 (br, s, 2H), 1.33 (s, 24H);  $^{13}\text{C}$  NMR (125 MHz,  $\text{CDCl}_3$ )  $\delta$  156.1, 144.4, 139.4, 113.8, 83.4, 83.1, 24.9, 24.8;  $^{11}\text{B}$  NMR (160 MHz,  $\text{CDCl}_3$ )  $\delta$  31 (br s); HRMS (ESI)  $m/z$  calcd for  $\text{C}_{18}\text{H}_{29}\text{B}_2\text{NO}_4$   $[\text{M} + \text{H}]^+$  346.2368, found 346.2366.

**2,5-bis(4,4,5,5-tetramethyl-1,3,2-dioxaborolan-2-yl)aniline (9)**



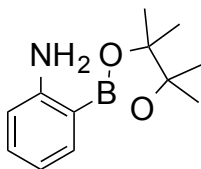
White crystal powder (200 mg, 57% yield); mp: 270-272 °C;  $^1\text{H}$  NMR (500 MHz,  $\text{CDCl}_3$ , 7.26)  $\delta$  7.61 (d,  $J = 7.3$  Hz, 1H), 7.09 (d,  $J = 7.4$  Hz, 1H), 7.04 (s, 1H), 4.70 (br, s, 2H), 1.33 (s, 24H);  $^{13}\text{C}$  NMR (125 MHz,  $\text{CDCl}_3$ )  $\delta$  152.8, 135.9, 122.8 (d,  $J = 22.8$ ), 121.0 (d,  $J = 22.9$ ), 83.7, 83.5, 24.9, 24.7;  $^{11}\text{B}$  NMR (160 MHz,  $\text{CDCl}_3$ )  $\delta$  31 (br, s); HRMS (ESI)  $m/z$  calcd for  $\text{C}_{18}\text{H}_{29}\text{B}_2\text{NO}_4$   $[\text{M} + \text{H}]^+$  346.2368 found 346.2367.

**3,5-bis(4,4,5,5-tetramethyl-1,3,2-dioxaborolan-2-yl)aniline (10)**



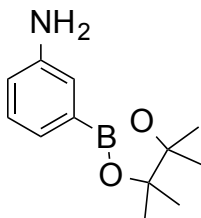
Clear gel (37 mg, 18% yield);  $^1\text{H}$  NMR (500 MHz, DMSO- $d_6$ , 2.48)  $\delta$  7.21 (s, 1H), 7.00 (s, 2H), 5.01 (br, s, 2H), 1.25 (s, 24H);  $^{13}\text{C}$  NMR (125 MHz, DMSO- $d_6$ )  $\delta$  147.9, 129.3, 123.2, 83.7, 25.1;  $^{11}\text{B}$  NMR (160 MHz, DMSO- $d_6$ )  $\delta$  31 (br, s); HRMS (ESI)  $m/z$  calcd for  $\text{C}_{18}\text{H}_{29}\text{B}_2\text{NO}_4$   $[\text{M} + \text{H}]^+$  346.2368 found 346.2365.

**2-(4,4,5,5-tetramethyl-1,3,2-dioxaborolan-2-yl)aniline (11)**



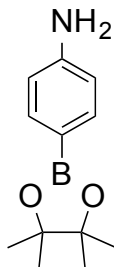
Brown solid (58 mg, 26% NMR yield); mp: 60-62  $^{\circ}\text{C}$ ;  $^1\text{H}$  NMR (500 MHz,  $\text{CDCl}_3$ , 7.27)  $\delta$  7.63 (dd,  $J = 7.3, 1.5$  Hz, 1H), 7.24 (td,  $J = 8.3, 2.0$  Hz, 1H), 6.68 (td,  $J = 8.3, 1.0$  Hz, 1H), 6.61 (d,  $J = 8.3$  Hz, 1H), 4.73 (br, s, 2H), 1.35 (s, 12H);  $^{13}\text{C}$  NMR (125 MHz,  $\text{CDCl}_3$ )  $\delta$  153.6, 135.7, 132.7, 116.8, 114.7, 83.4, 24.9;  $^{11}\text{B}$  NMR (160 MHz,  $\text{CDCl}_3$ )  $\delta$  31 (br, s); HRMS (ESI)  $m/z$  calcd for  $\text{C}_{12}\text{H}_{18}\text{BNO}_2$   $[\text{M} + \text{H}]^+$  220.1511, found 220.1511

**3-(4,4,5,5-tetramethyl-1,3,2-dioxaborolan-2-yl)aniline (12)**



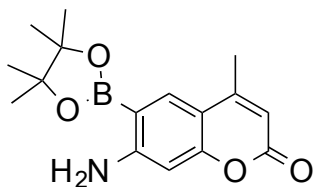
Brown crystal powder (45 mg, 20% NMR yield); mp: 80-82 °C;  $^1\text{H}$  NMR (500 MHz, DMSO- $d_6$ , 2.49)  $\delta$  7.01 (t,  $J$  = 7.3 Hz, 1H), 6.98 (d,  $J$  = 1.5 Hz, 1H), 6.81 (d,  $J$  = 7.3 Hz, 1H), 6.65 (dd,  $J$  = 8.3, 1.5 Hz, 1H), 5.07 (br, s, 2H), 1.25 (s, 12H);  $^{13}\text{C}$  NMR (125 MHz,  $\text{CDCl}_3$ )  $\delta$  145.7, 128.7, 124.9, 121.1, 117.9, 83.6, 24.8;  $^{11}\text{B}$  NMR (160 MHz,  $\text{CDCl}_3$ )  $\delta$  31 (br, s); HRMS (ESI)  $m/z$  calcd for  $\text{C}_{12}\text{H}_{18}\text{BNO}_2$   $[\text{M} + \text{H}]^+$  220.1511, found 220.1514.

**4-(4,4,5,5-tetramethyl-1,3,2-dioxaborolan-2-yl)aniline (13)**



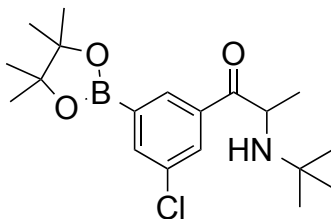
Brown crystal powder (26 mg, 12.6% NMR yield); mp: 140-148 °C;  $^1\text{H}$  NMR (500 MHz,  $\text{CDCl}_3$ , 7.26)  $\delta$  7.62 (d,  $J$  = 8.4 Hz, 2H), 6.66 (d,  $J$  = 8.4 Hz, 2H), 3.83 (br, s, 2H), 1.32 (s, 12H);  $^{13}\text{C}$  NMR (125 MHz,  $\text{CDCl}_3$ )  $\delta$  149.2, 136.5, 114.0, 83.2, 24.8;  $^{11}\text{B}$  NMR (160 MHz,  $\text{CDCl}_3$ )  $\delta$  30 (br s); HRMS (ESI)  $m/z$  calcd for  $\text{C}_{12}\text{H}_{18}\text{BNO}_2$   $[\text{M} + \text{H}]^+$  220.1511, found 220.1513.

**7-amino-4-methyl-6-(4,4,5,5-tetramethyl-1,3,2-dioxaborolan-2-yl)-2H-chromen-2-one (14)**



The reaction was performed by taking 50 mg of starting 7-amino-4-methylcoumarin (0.285 mmol). The rest of the reaction was performed using 2.85  $\mu$ mol [Ir(OMe)COD]<sub>2</sub> (1.0 mol%), 8.55  $\mu$ mol 4,4'-di-*tert*-butyl-2,2'-bipyridine (3.0 mol%), 2.2 equiv HBPIn. Reddish Brown Solid (68 mg, 80% isolated yield); mp: 200-202 °C; <sup>1</sup>H NMR (500 MHz, CDCl<sub>3</sub>, 7.26)  $\delta$  7.83 (s, 1H), 6.43 (s, 1H), 5.96 (s, 1H), 5.3 (s, 2H), 2.38 (s, 3H), 1.35 (s, 12H); <sup>13</sup>C NMR (125 MHz, CDCl<sub>3</sub>)  $\delta$  161.6, 157.7, 156.7, 153.2, 134.6, 110.9, 109.6, 100.2, 84.0, 24.8, 18.6; <sup>11</sup>B NMR (160 MHz, CDCl<sub>3</sub>)  $\delta$  30 (br s); HRMS (ESI) *m/z* calcd for C<sub>16</sub>H<sub>20</sub>BNO<sub>4</sub> [M + H]<sup>+</sup> 302.1566, found 302.1571.

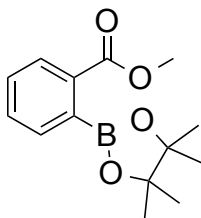
**2-(tert-butylamino)-1-(3-chloro-5-(4,4,5,5-tetramethyl-1,3,2-dioxaborolan-2-yl)phenyl)propan-1-one (15)**



The reaction was performed by taking 100 mg of starting bupropion HCl (0.36 mmol), and adding 3.0 equiv triethylamine, and stirring for two hours in 1 ml THF. The mixture was then filtered and the volatiles removed under reduced pressure to yield the starting bupropion. The rest of the reaction was performed using 3.60  $\mu\text{mol}$   $[\text{Ir}(\text{OMe})\text{COD}]_2$  (1.0 mol%), 10.8  $\mu\text{mol}$  4,4'-di-*tert*-butyl-2,2'-bipyridine (3.0 mol%), 2.2 equiv HBPIn, and 0.75 equiv  $\text{B}_2\text{Pin}_2$ . Orange Yellow Gel (101 mg, 76% isolated yield); Spectra contains minor starting material  $^1\text{H}$  NMR (500 MHz,  $\text{CDCl}_3$ )  $\delta$  8.19 (d,  $J = 1.0$  Hz, 1H), 8.02 (td,  $J = 2.5, 3.9$  Hz, 1H), 7.97 (dd,  $J = 1.0, 2.5$  Hz, 1H), 4.35 (q,  $J = 7.3$ , 1H), 1.35 (s, 12H), 1.27 (d,  $J = 4.2$  Hz, 3H), 1.05 (s, 9H);  $^{13}\text{C}$  NMR (125 MHz,  $\text{CDCl}_3$ )  $\delta$  203.7, 139.2, 136.1, 134.9, 132.1, 130.8, 84.5, 75.0, 52.2, 50.9, 29.6, 24.8, 22.2;  $^{11}\text{B}$  NMR (160 MHz,  $\text{CDCl}_3$ )  $\delta$  30 (br s); HRMS (ESI)  $m/z$  calcd for  $\text{C}_{19}\text{H}_{29}\text{BClNO}_3$   $[\text{M} + \text{H}]^+$  366.2008, found 366.2008. Mixture was racemic.

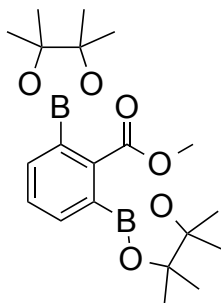
**General Procedure for *ortho*-directed Borylation of Methyl Benzoates.** In a nitrogen filled glovebox, 1.25  $\mu\text{mol}$   $[\text{Ir}(\text{OMe})\text{COD}]_2$  (1.25 mol%) was dissolved in 1 mL THF in a 15 mL pressure tube containing a magnetic stir bar. 1 equiv  $\text{B}_2\text{Pin}_2$  (254 mg), 2.5  $\mu\text{mol}$  (2-(diisopropylsilyl)phenyl)di-*p*-tolylphosphane (2.5 mol%), and 1 mmol methyl benzoate substrate were also added, and the reaction vessel was sealed and heated at 80  $^\circ\text{C}$  for 16h. The reaction mixture was allowed to return to room temperature and the reaction mixture was exposed to air. The volatiles were then removed under reduced pressure and the product was purified by passing it through a short plug of  $\text{SiO}_2$  in MTBE.

**methyl 2-(4,4,5,5-tetramethyl-1,3,2-dioxaborolan-2-yl)benzoate (16)**<sup>1</sup>



The reaction was performed using 2.0 mmol substrate (272 mg), 1.25  $\mu$ mol [Ir(OMe)COD]<sub>2</sub> (1.25 mol%), 0.5 equiv B<sub>2</sub>Pin<sub>2</sub> (254 mg), 2.5  $\mu$ mol (2-(diisopropylsilyl)phenyl)di-*p*-tolylphosphane (2.5 mol%). Obtained via column chromatography; hexanes: EtOAc (9: 1) was a Yellow-Brown Oil (110 mg, 41% yield based on B<sub>2</sub>Pin<sub>2</sub> (81% assay yield by <sup>1</sup>H NMR) and 5% diborylated product); <sup>1</sup>H NMR (500 MHz, CDCl<sub>3</sub>, 7.26)  $\delta$  7.94 (d, *J* = 7.8 Hz, 1H), 7.53-7.48 (m, 2H), 7.42 (dt, *J* = 2.5, 8.4 Hz, 1H), 3.91 (s, 3H), 1.42 (s, 12H).

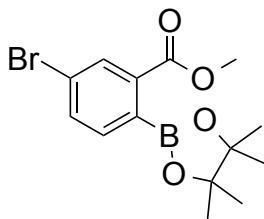
**methyl 2,6-bis(4,4,5,5-tetramethyl-1,3,2-dioxaborolan-2-yl)benzoate (17)**



The reaction was performed using 1.0 mmol substrate (126  $\mu$ l), 2.5  $\mu$ mol  $[\text{Ir}(\text{OMe})\text{COD}]_2$  (2.5 mol%), 2.0 equiv  $\text{B}_2\text{Pin}_2$  (508 mg), 5.0  $\mu$ mol (2-(diisopropylsilyl)phenyl)di-*p*-tolylphosphane (5.0 mol%). Obtained by recrystallization from MeOH/  $\text{H}_2\text{O}$  a White solid (244 mg, 63% isolated yield);  $^1\text{H}$  NMR (500 MHz,  $\text{CDCl}_3$ )  $\delta$  7.70 (d,  $J = 7.4$  Hz, 2H), 7.43 (d,  $J = 7.3$  Hz, 1H), 3.89 (s, 3H), 1.35 (s, 24H);  $^{13}\text{C}$  NMR (125 MHz,  $\text{CDCl}_3$ )  $\delta$  170.6, 141.7, 135.4, 128.9, 84.0, 52.0, 24.8;  $^{11}\text{B}$  NMR (160 MHz,  $\text{CDCl}_3$ )  $\delta$  31 (br s). ; HRMS (ESI)  $m/z$  calcd for  $\text{C}_{20}\text{H}_{31}\text{B}_2\text{O}_6$   $[\text{M} + \text{H}]^+$  389.2307, found 389.2307.

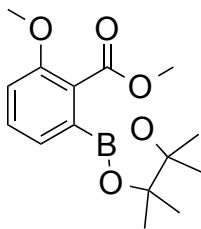


**methyl 5-bromo-2-(4,4,5,5-tetramethyl-1,3,2-dioxaborolan-2-yl)benzoate (18)**



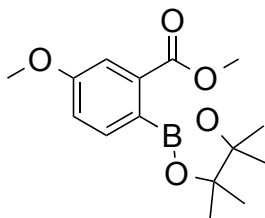
The reaction was performed using 0.5 mmol substrate (107.5 mg), 2.5  $\mu\text{mol}$   $[\text{Ir}(\text{OMe})\text{COD}]_2$  (2.5 mol%), 2.0 equiv  $\text{B}_2\text{Pin}_2$  (254 mg), 5.0  $\mu\text{mol}$  (2-(diisopropylsilyl)phenyl)di-*p*-tolylphosphane (5.0 mol%). Purified by column chromatography; hexanes: EtOAc (9: 1). Obtained Yellow Oil (139 mg, 60% yield (95% assay yield by  $^1\text{H}$  NMR));  $^1\text{H}$  NMR (500 MHz,  $\text{CDCl}_3$ , 7.26)  $\delta$  8.07 (s,  $J = 1.5$  Hz, 1H), 7.64 (dd,  $J = 2.0, 7.8$  Hz, 1H), 7.37 (d,  $J = 7.8$  Hz, 1H), 3.91 (s, 3H), 1.40 (s, 12H);  $^{13}\text{C}$  NMR (125 MHz,  $\text{CDCl}_3$ )  $\delta$  167.1, 135.3, 134.7, 133.7, 131.7, 123.3, 84.2, 52.5, 24.8;  $^{11}\text{B}$  NMR (160 MHz,  $\text{CDCl}_3$ )  $\delta$  31 (br, s); HRMS (ESI)  $m/z$  calcd for  $\text{C}_{14}\text{H}_{18}\text{BBrO}_4$   $[\text{M} + \text{H}]^+$  341.0562, found 341.0575.

**methyl 2-methoxy-6-(4,4,5,5-tetramethyl-1,3,2-dioxaborolan-2-yl)benzoate (19)**



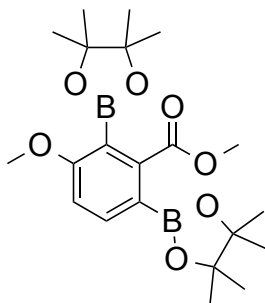
The reaction was performed using 1.0 mmol substrate (166 mg), 1.25  $\mu\text{mol}$   $[\text{Ir}(\text{OMe})\text{COD}]_2$  (1.25 mol%), 1.25 equiv  $\text{B}_2\text{Pin}_2$  (317 mg), 2.5  $\mu\text{mol}$  (2-(diisopropylsilyl)phenyl)di-*p*-tolylphosphane (2.5 mol%). Obtained from recrystallization from MeOH/H<sub>2</sub>O Brown Crystals (240 mg, 82% yield); mp: 84 °C;  $^1\text{H}$  NMR (500 MHz,  $\text{CDCl}_3$ , 7.26)  $\delta$  7.38 (t,  $J$  = 7.3 Hz, 1H), 7.32 (d,  $J$  = 6.4 Hz, 1H), 7.02 (d,  $J$  = 8.3 Hz, 1H), 3.88 (s, 3H), 3.83 (s, 3H), 1.32 (s, 12H);  $^{13}\text{C}$  NMR (125 MHz,  $\text{CDCl}_3$ )  $\delta$  169.1, 156.0, 130.5, 128.1, 126.5, 113.7, 84.0, 55.9, 52.3, 24.8;  $^{11}\text{B}$  NMR (160 MHz,  $\text{CDCl}_3$ )  $\delta$  30 (br, s); HRMS (ESI)  $m/z$  calcd for  $\text{C}_{15}\text{H}_{21}\text{BO}_5$   $[\text{M} + \text{H}]^+$  293.1563, found 293.1574.

**methyl 5-methoxy-2-(4,4,5,5-tetramethyl-1,3,2-dioxaborolan-2-yl)benzoate (20a)<sup>2</sup>**



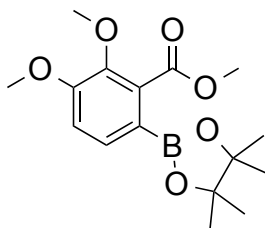
Purified by column chromatography; hexanes: EtOAc (9: 1). Yellow Oil (193 mg, 66% yield) Spectra contains minor amounts of methyl 3-methoxy-2-(4,4,5,5-tetramethyl-1,3,2-dioxaborolan-2-yl)benzoate  $^1\text{H}$  NMR (500 MHz,  $\text{CDCl}_3$ , 7.26)  $\delta$  7.45-7.42 (m, 2H), 7.05 (dd,  $J$  = 2.4, 8.3 Hz, 1H), 3.89 (s, 3H), 3.83 (s, 3H), 1.39 (s, 12H).

**methyl 3-methoxy-2,6-bis(4,4,5,5-tetramethyl-1,3,2-dioxaborolan-2-yl)benzoate (20b)**



Purified by column chromatography; hexanes: EtOAc (9: 1). Yellow Powder (20 mg, 5% yield); mp: 98 °C;  $^1\text{H}$  NMR (500 MHz,  $\text{CDCl}_3$ , 7.26)  $\delta$  7.50 (d,  $J$  = 7.9, Hz, 1H), 6.93 (d,  $J$  = 8.3 Hz, 1H), 3.87 (s, 3H), 3.79 (s, 3H), 1.39 (s, 12H), 1.34 (s, 12H);  $^{13}\text{C}$  NMR (125 MHz,  $\text{CDCl}_3$ )  $\delta$  169.3, 163.6, 139.0, 135.4, 112.3, 83.8, 83.6, 55.6, 52.1, 24.86, 24.81;  $^{11}\text{B}$  NMR (160 MHz,  $\text{CDCl}_3$ )  $\delta$  31 (br, s); HRMS (ESI)  $m/z$  calcd for  $\text{C}_{21}\text{H}_{32}\text{B}_2\text{O}_7$   $[\text{M} + \text{H}]^+$  419.2420, found 419.2434.

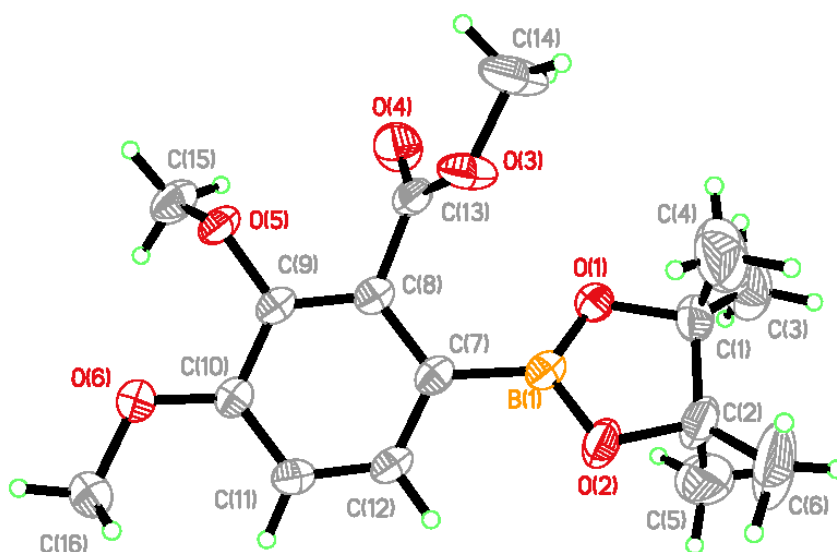
**methyl 2,3-dimethoxy-6-(4,4,5,5-tetramethyl-1,3,2-dioxaborolan-2-yl)benzoate (21)**



Obtained via recrystallization with MeOH/ $\text{H}_2\text{O}$  White crystals (227 mg, 70% yield); mp: 85 °C;  $^1\text{H}$  NMR (500 MHz,  $\text{CDCl}_3$ , 7.26)  $\delta$  7.51 (d,  $J$  = 7.8 Hz, 1H), 6.94 (d,  $J$  = 8.3 Hz, 1H), 3.89 (s, 3H), 3.88 (s, 3H), 3.85 (s, 3H), 1.30 (s, 12H);  $^{13}\text{C}$  NMR (125 MHz,  $\text{CDCl}_3$ )  $\delta$  168.7, 155.0, 145.4, 134.6, 131.8, 112.6, 83.8, 61.6, 55.8, 52.2, 24.8;  $^{11}\text{B}$  NMR (160 MHz,  $\text{CDCl}_3$ )  $\delta$  30 (br, s); HRMS (ESI)  $m/z$  calcd for  $\text{C}_{16}\text{H}_{23}\text{BO}_6$   $[\text{M} + \text{H}]^+$  323.1669, found 323.1677.

**Figure 4.1 methyl 2,3-dimethoxy-6-(4,4,5,5-tetramethyl-1,3,2-dioxaborolan-2-yl)benzoate (21)**

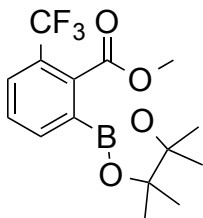
The following are 50% thermal ellipsoidal drawings of the molecule in the asymmetric cell with various amount of labeling.



**Crystal structure determination of methyl 2,3-dimethoxy-6-(4,4,5,5-tetramethyl-1,3,2-dioxaborolan-2-yl)benzoate (21)** **Crystal Data.**  $C_{16}H_{23}O_6B$ ,  $M=322.15$ , monoclinic,  $a = 23.4123(4) \text{ \AA}$ ,  $b = 9.0701(2) \text{ \AA}$ ,  $c = 18.5703(3) \text{ \AA}$ ,  $\beta = 118.6010(10)^\circ$ ,  $V = 3462.24(12) \text{ \AA}^3$ ,  $T = 172.99$ , space group  $C2/c$  (no. 15),  $Z = 8$ ,  $\mu(\text{CuK}\alpha) = 0.767$ , 15915 reflections measured, 3362 unique ( $R_{\text{int}} = 0.0246$ ) which were used in all calculations. The final  $wR_2$  was 0.1943 (all data)

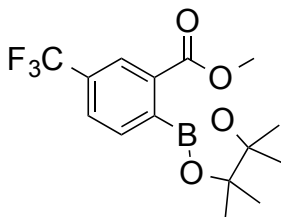
and  $R_1$  was 0.0663 ( $I > 2\sigma(I)$ ).

**methyl 2-(4,4,5,5-tetramethyl-1,3,2-dioxaborolan-2-yl)-6-(trifluoromethyl)benzoate (22)**<sup>2</sup>



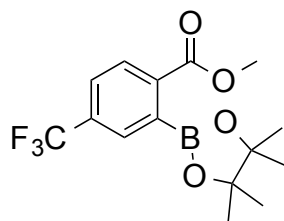
Obtained via recrystallization with MeOH/H<sub>2</sub>O; Black Crystals (270 mg, 82% yield); mp: 60 °C; <sup>1</sup>H NMR (500 MHz, CDCl<sub>3</sub>, 7.27) δ 7.99 (d,  $J$  = 7.9, Hz, 1H), 7.76 (d,  $J$  = 8.3 Hz, 1H), 7.55 (t,  $J$  = 7.8 Hz, 1H), 3.92 (s, 3H), 1.34 (s, 12H).

**methyl 2-(4,4,5,5-tetramethyl-1,3,2-dioxaborolan-2-yl)-5-(trifluoromethyl)benzoate (23)**<sup>2</sup>



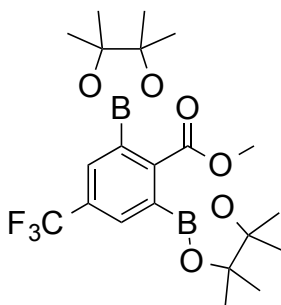
Obtained via recrystallization with MeOH/H<sub>2</sub>O; Brown Powder (266 mg, 81% yield); mp: 55 °C; <sup>1</sup>H NMR (500 MHz, CDCl<sub>3</sub>, 7.27) δ 8.19 (s, 1H), 7.76 (dd,  $J$  = 1.0, 7.8 Hz, 1H), 7.62 (d,  $J$  = 7.8 Hz, 1H), 3.95 (s, 3H), 1.42 (s, 12H).

**methyl 2-(4,4,5,5-tetramethyl-1,3,2-dioxaborolan-2-yl)-4-(trifluoromethyl)benzoate (24a)**



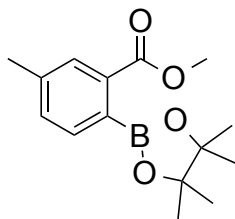
Purified by column chromatography; hexanes: EtOAc (9: 1). Yellow Oil (163 mg, 49% yield);  $^1\text{H}$  NMR (500 MHz,  $\text{CDCl}_3$ , 7.27)  $\delta$  8.04 (d,  $J = 8.3$  Hz, 1H), 7.74 (s, 1H), 7.69 (dd,  $J = 7.8, 0.9$  Hz, 1H), 3.95 (s, 3H), 1.43 (s, 12H);  $^{13}\text{C}$  NMR (125 MHz,  $\text{CDCl}_3$ )  $\delta$  167.4, 136.7, 133.7 ( $J = 32.4$  Hz), 129.1 ( $J = 3.8$ ), 129.0, 126.0 ( $J = 3.8$  Hz), 124.8 ( $J = 272.8$  Hz), 84.5, 52.7, 24.8;  $^{19}\text{F}$  NMR (470 MHz,  $\text{CDCl}_3$ )  $\delta$  -63.0 (s);  $^{11}\text{B}$  NMR (160 MHz,  $\text{CDCl}_3$ )  $\delta$  31 (br, s); HRMS (ESI)  $m/z$  calcd for  $\text{C}_{15}\text{H}_{18}\text{BF}_3\text{O}_4$   $[\text{M} + \text{H}]^+$  331.1331, found 331.1334.

**methyl 2,6-bis(4,4,5,5-tetramethyl-1,3,2-dioxaborolan-2-yl)-4-(trifluoromethyl)benzoate (24b)**



Purified by column chromatography; hexanes: EtOAc (9: 1). Brown Crystals (77 mg, 17% yield); mp: 70-80  $^{\circ}\text{C}$ ;  $^1\text{H}$  NMR (500 MHz,  $\text{CDCl}_3$ , 7.26)  $\delta$  7.93 (s, 2H), 3.89 (s, 3H), 1.34 (s, 12H);  $^{13}\text{C}$  NMR (125 MHz,  $\text{CDCl}_3$ )  $\delta$  169.8, 145.9, 132.6 ( $J = 3.8$  Hz), 130.7 ( $J = 32.4$  Hz), 124.9 ( $J = 272.7$  Hz), 84.5, 52.3, 24.7;  $^{19}\text{F}$  NMR (470 MHz,  $\text{CDCl}_3$ )  $\delta$  -62.8 (s);  $^{11}\text{B}$  NMR (160 MHz,  $\text{CDCl}_3$ )  $\delta$  31 (br, s); HRMS (ESI)  $m/z$  calcd for  $\text{C}_{21}\text{H}_{29}\text{B}_2\text{F}_3\text{O}_6$   $[\text{M} + \text{H}]^+$  457.2188, found 457.2198.

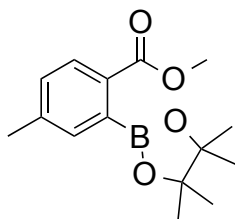
**methyl 5-methyl-2-(4,4,5,5-tetramethyl-1,3,2-dioxaborolan-2-yl)benzoate (25)**<sup>3</sup>



Purified by column chromatography; hexanes: EtOAc (9: 1). Yellow Oil (227 mg, 82% yield);

<sup>1</sup>H NMR (500 MHz, CDCl<sub>3</sub>, 7.27) δ 7.76 (s, 1H), 7.41 (d, *J* = 7.3 Hz, 1H), 7.34 (d, *J* = 7.4 Hz, 1H), 3.91 (d, *J* = 1 Hz, 3H), 2.38 (s, 3H), 1.42 (s, 12H).

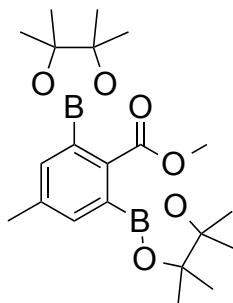
**methyl 4-methyl-2-(4,4,5,5-tetramethyl-1,3,2-dioxaborolan-2-yl)benzoate (26a)**<sup>3</sup>



Product by column chromatography; hexanes: EtOAc (9: 1). White Powder (135 mg, 49% yield);

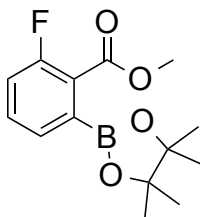
mp: 54 °C; <sup>1</sup>H NMR (500 MHz, CDCl<sub>3</sub>, 7.27) δ 7.85 (d, *J* = 7.8 Hz, 1H), 7.29 (s, 1H), 7.22 (dd, *J* = 1.0, 7.9 Hz, 1H), 3.90 (s, 3H), 2.38 (s, 3H), 1.43 (s, 12H).

**methyl 4-methyl-2,6-bis(4,4,5,5-tetramethyl-1,3,2-dioxaborolan-2-yl)benzoate (26b)**



Purified by column chromatography; hexanes: EtOAc (9: 1) Brown Crystals (54 mg, 13% yield); mp: 158-168 °C;  $^1\text{H}$  NMR (500 MHz,  $\text{CDCl}_3$ , 7.27)  $\delta$  7.45 (s, 1H), 3.87 (s, 3H), 2.35 (s, 3H), 1.36 (s, 12H);  $^{13}\text{C}$  NMR (125 MHz,  $\text{CDCl}_3$ )  $\delta$  170.3, 139.3, 137.7, 135.4, 83.9, 51.9, 116.9;  $^{11}\text{B}$  NMR (160 MHz,  $\text{CDCl}_3$ )  $\delta$  30 (br, s); HRMS (ESI)  $m/z$  calcd for  $\text{C}_{21}\text{H}_{32}\text{B}_2\text{O}_6$   $[\text{M} + \text{H}]^+$  403.2471, found 403.2462.

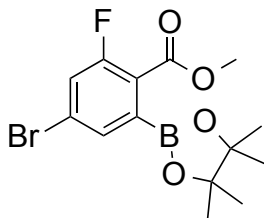
**methyl 2-fluoro-6-(4,4,5,5-tetramethyl-1,3,2-dioxaborolan-2-yl)benzoate (27)**



Purified by column chromatography; hexanes: EtOAc (9: 1). Yellow Oil (281 mg, 84% yield);  $^1\text{H}$  NMR (500 MHz,  $\text{CDCl}_3$ , 7.26)  $\delta$  7.46 (m, 2H), 7.16 (m, 1H), 3.92 (s, 1H), 1.36 (s, 12H);  $^{13}\text{C}$  NMR (125 MHz,  $\text{DMSO-d}_6$ )  $\delta$  166.1, 160.3 ( $J = 251.8$  Hz), 133.2 ( $J = 8.6$  Hz), 130.1 ( $J = 3.8$  Hz), 124.9 ( $J = 13.3$  Hz), 118.8 ( $J = 21.0$  Hz), 84.6, 53.0, 24.9;  $^{19}\text{F}$  NMR 470 MHz,  $\text{CDCl}_3$ )  $\delta$  -115.0 (s);  $^{11}\text{B}$  NMR (160 MHz,  $\text{CDCl}_3$ )  $\delta$  31 (br, s); HRMS (ESI)  $m/z$  calcd for  $\text{C}_{14}\text{H}_{18}\text{BFO}_4$   $[\text{M} + \text{H}]^+$  281.1363, found 281.1371.



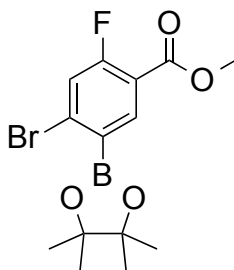
**methyl 4-bromo-2-fluoro-6-(4,4,5,5-tetramethyl-1,3,2-dioxaborolan-2-yl)benzoate (28)**



Purified by column chromatography; hexanes: EtOAc (8.5: 1). Yellow Oil (255 mg, 70% yield);

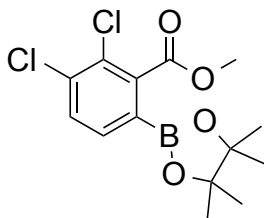
$^1\text{H}$  NMR (500 MHz,  $\text{CDCl}_3$ , 7.28)  $\delta$  7.53 (s, 1H), 7.35 (d,  $J$ = 9.3 Hz, 1H), 3.93 (s,  $J$  = 1.5 Hz, 3H), 1.38 (s,  $J$ =0.9 Hz, 12H);  $^{13}\text{C}$  NMR (125 MHz,  $\text{CDCl}_3$ )  $\delta$  166.2, 160.9 ( $J$ = 261.3), 132.0 ( $J$  = 3.8), 126.1 ( $J$  = 8.6), 122.7 ( $J$  = 12.4), 121.4 ( $J$  = 24.8), 84.6, 52.8, 24.7;  $^{19}\text{F}$  NMR (470 MHz,  $\text{CDCl}_3$ )  $\delta$  -109.7 (s);  $^{11}\text{B}$  NMR (160 MHz,  $\text{CDCl}_3$ )  $\delta$  30 (br, s); HRMS (ESI)  $m/z$  calcd for  $\text{C}_{14}\text{H}_{17}\text{BBrFO}_4$   $[\text{M} + \text{H}]^+$  343.0155, found 343.0150.

**methyl 4-bromo-2-fluoro-5-(4,4,5,5-tetramethyl-1,3,2-dioxaborolan-2-yl)benzoate (29)**



The reaction was performed using 1.0 mmol substrate (233 mg), 1.25  $\mu$ mol  $[\text{Ir}(\text{OMe})\text{COD}]_2$  (1.25 mol%), 1 equiv  $\text{B}_2\text{Pin}_2$  (254 mg), 2.5  $\mu$ mol 4,4-di-tert-butyl bipyridine (2.5 mol%), 1 ml hexanes. Obtained via recrystallization with MeOH/ $\text{H}_2\text{O}$  a Pale White Powder (370 mg, 80% yield) Spectra contains minor amounts of 4-bromo-2-fluoro-3-(4,4,5,5-tetramethyl-1,3,2-dioxaborolan-2-yl)benzoate; mp: 133  $^\circ\text{C}$ ;  $^1\text{H}$  NMR (500 MHz,  $\text{CDCl}_3$ , 7.27)  $\delta$  8.23 (d,  $J$  = 8.3 Hz, 1H), 7.40 (d,  $J$  = 10.3 Hz, 1H), 3.97 (s, 3H), 1.38 (s, 12H) Aromatic couplings are due to H-F couplings;  $^{13}\text{C}$  NMR (125 MHz,  $\text{CDCl}_3$ )  $\delta$  164.2, 163.6 ( $J$  = 268), 140.2 ( $J$  = 1.9 Hz), 133.7 ( $J$  = 9.5 Hz), 121.8 ( $J$  = 24.8 Hz), 117.1 ( $J$  = 8.6 Hz), 84.6, 52.4, 24.8 ( $J$  = 10.5 Hz);  $^{19}\text{F}$  NMR 470 MHz,  $\text{CDCl}_3$ )  $\delta$  -104.6 (s);  $^{11}\text{B}$  NMR (160 MHz,  $\text{CDCl}_3$ )  $\delta$  30 (br, s); HRMS (ESI)  $m/z$  calcd for  $\text{C}_{14}\text{H}_{17}\text{BBrFO}_4$   $[\text{M} + \text{H}]^+$  343.0155, found 343.0160.

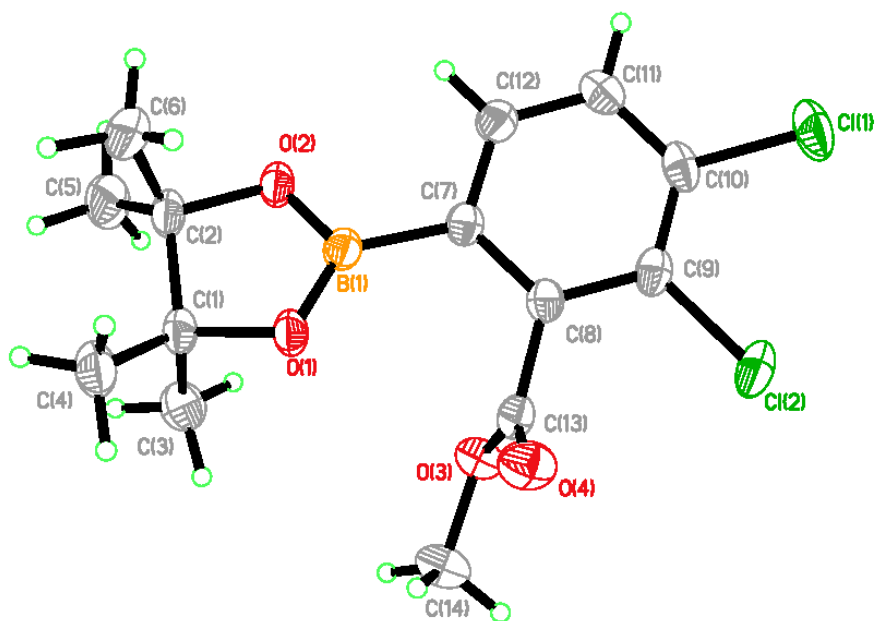
**methyl 2,3-dichloro-6-(4,4,5,5-tetramethyl-1,3,2-dioxaborolan-2-yl)benzoate (30)**



Recrystallized from Pentane Green Crystals (240 mg, 72% yield) Spectra contains minor amounts of unreacted B<sub>2</sub>Pin<sub>2</sub>; mp: 49 °C; <sup>1</sup>H NMR (500 MHz, CDCl<sub>3</sub>) δ 7.64 (d, *J* = 7.8 Hz, 1H), 7.51 (d, *J* = 8.3 Hz, 1H), 3.93 (s, 3H), 1.32 (s, 12H); <sup>13</sup>C NMR (125 MHz, CDCl<sub>3</sub>) δ 167.5, 140.8, 136.0, 134.0, 130.6, 129.0, 84.6, 52.6, 24.7; <sup>11</sup>B NMR (160 MHz, CDCl<sub>3</sub>) δ 30 (br, s); HRMS (ESI) *m/z* calcd for C<sub>14</sub>H<sub>17</sub>BCl<sub>2</sub>O<sub>4</sub> [M + H]<sup>+</sup> 333.0651, found 333.0662.

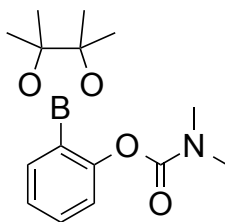
**Figure 4.2** methyl 2,3-dichloro-6-(4,4,5,5-tetramethyl-1,3,2-dioxaborolan-2-yl)benzoate (30)

The following are 50% thermal ellipsoidal drawings of the molecule in the asymmetric cell with various amount of labeling.



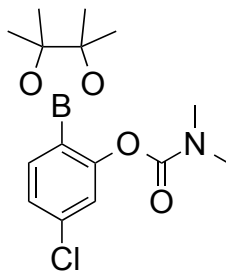
**Crystal Structure Determination of methyl 2,3-dichloro-6-(4,4,5,5-tetramethyl-1,3,2-dioxaborolan-2-yl)benzoate (30).** **Crystal Data.**  $C_{14}H_{17}BCl_2O_4$ ,  $M = 330.99$ , triclinic,  $a = 8.3136(8) \text{ \AA}$ ,  $b = 10.1181(9) \text{ \AA}$ ,  $c = 11.2272(11) \text{ \AA}$ ,  $\alpha = 112.5120(10)^\circ$ ,  $\beta = 92.2620(10)^\circ$ ,  $\gamma = 110.8860(10)^\circ$ ,  $V = 798.00(13) \text{ \AA}^3$ ,  $T = 173.15$ , space group P-1 (no. 2),  $Z = 2$ ,  $\mu(\text{MoK}\alpha) = 0.417$ , 13234 reflections measured, 2930 unique ( $R_{\text{int}} = 0.0266$ ) which were used in all calculations. The final  $wR_2$  was 0.0905 (all data) and  $R_1$  was 0.0337 ( $>2\sigma(I)$ ).

**2-(4,4,5,5-tetramethyl-1,3,2-dioxaborolan-2-yl)phenyl dimethylcarbamate (31)**



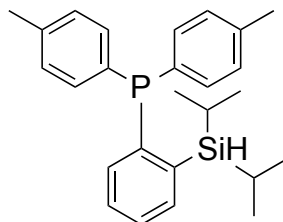
The reaction was performed using 0.5 mmol substrate (82.5 mg), 2.5  $\mu$ mol  $[\text{Ir}(\text{OMe})\text{COD}]_2$  (2.5 mol%), 1 equiv  $\text{B}_2\text{Pin}_2$  (127 mg), 2.5  $\mu$ mol 4,4-di-tert-butyl bipyridine (5.0 mol%), 1.5 ml THF. Purified by column chromatography; hexanes: EtOAc (8.5: 1) using Alizarin as an indicator. Clear Gel (30 mg, 21.5% yield);  $^1\text{H}$  NMR (500 MHz,  $\text{CDCl}_3$ , 7.26)  $\delta$  7.75 (dd,  $J$  = 1.5, 7.3 Hz, 1H), 7.45 (dt,  $J$  = 1.9, 7.8 Hz, 1H), 7.20 (t,  $J$  = 7.4 Hz, 1H), 7.07 (d,  $J$  = 7.8 Hz, 1H), 3.13 (s, 3H), 3.00 (s, 3H) 1.30 (s, 12H);  $^{13}\text{C}$  NMR (125 MHz,  $\text{CDCl}_3$ )  $\delta$  156.3, 155.6, 136.1, 132.2, 124.8, 122.1, 83.4, 36.6, 36.4, 24.9;  $^{11}\text{B}$  NMR (160 MHz,  $\text{CDCl}_3$ )  $\delta$  30 (br, s); HRMS (ESI)  $m/z$  calcd for  $\text{C}_{15}\text{H}_{22}\text{BNO}_4$   $[\text{M} + \text{H}]^+$  292.1723 found 292.1714.

**5-chloro-2-(4,4,5,5-tetramethyl-1,3,2-dioxaborolan-2-yl)phenyl dimethylcarbamate (32)**



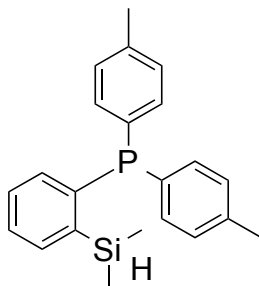
The reaction was performed using 0.5 mmol substrate (99.5 mg), 2.5  $\mu\text{mol}$   $[\text{Ir}(\text{OMe})\text{COD}]_2$  (2.5 mol%), 1 equiv  $\text{B}_2\text{Pin}_2$  (127 mg), 2.5  $\mu\text{mol}$  4,4-di-tert-butyl bipyridine (5.0 mol%), 1.5 ml THF. Purified by column chromatography; hexanes: EtOAc (8.5:1) using Alizarin as an indicator. Clear Gel (26 mg, 12% yield);  $^1\text{H}$  NMR (500 MHz,  $\text{CDCl}_3$ , 7.26)  $\delta$  7.69 (d,  $J = 8.3$  Hz, 1H), 7.18 (dd,  $J = 1.9, 7.8$  Hz, 1H), 7.11 (d,  $J = 1.9$  Hz, 1H), 3.12 (s, 3H), 2.99 (s, 3H), 1.30 (s, 12H);  $^{13}\text{C}$  NMR (125 MHz,  $\text{CDCl}_3$ )  $\delta$  156.8, 155.1, 137.6, 136.9, 125.2, 122.8, 83.6, 36.7, 36.4, 24.9;  $^{11}\text{B}$  NMR (160 MHz,  $\text{CDCl}_3$ )  $\delta$  30 (br, s); HRMS (ESI)  $m/z$  calcd for  $\text{C}_{15}\text{H}_{21}\text{BClNO}_4$   $[\text{M} + \text{H}]^+$  326.1333 found 326.1324.

**(2-(diisopropylsilyl)phenyl)di-*p*-tolylphosphane (SIPBz) (33)**



In a nitrogen filled glove box, 1.0 g (2-bromophenyl)di-*p*-tolylphosphine (2.7 mmol) was dissolved in 2 mL ether and cooled to -30 °C. 2.03 mL of a 1.6 M *n*-BuLi solution was then added drop wise, and the reaction stirred for 30 minutes. Volatiles were removed under reduced pressure, and the leftover material was then dissolved in 2 mL toluene. To the mixture, 0.512 g chlorodiisopropylsilane (3.35 mmol) was then added drop-wise, and the mixture was stirred for 3 hours. The mixture was then filtered, and the precipitate was washed with toluene. Volatiles were removed under reduced pressure to yield a colorless solid white crystals (650 mg, 60% yield); mp: 75 °C; <sup>1</sup>H NMR (500 MHz, C<sub>6</sub>D<sub>6</sub>, 7.14) δ 7.62-7.58 (m, 1H), 7.36-7.33 (m, 1H), 7.31 (d, *J* = 7.8 Hz, 4H), 7.08-7.02 (m, 2H), 6.90 (d, *J* = 7.8 Hz, 4H), 4.57 (m, 1H), 1.98 (s, 6H), 1.47 (m, 2H), 1.17 (d, *J* = 7.3 Hz, 6H), 1.01 (d, *J* = 7.4 Hz, 6H); <sup>13</sup>C NMR (125 MHz, CDCl<sub>3</sub>) δ 144.3 (d, *J* = 10.4 Hz), 143.2, 142.9, 138.1, 136.7 (d, *J* = 15.3 Hz), 134.5 (d, *J* = 10.5 Hz), 134.0, 133.6 (d, *J* = 19.1 Hz), 129.1 (d, *J* = 6.7 Hz), 127.7, 21.2, 19.3 (d, *J* = 10.5 Hz), 12.1 (d, *J* = 6.7 Hz); <sup>31</sup>P NMR (202 MHz, C<sub>6</sub>D<sub>6</sub>) δ -9.82. (s). HRMS (ESI) *m/z* calcd for C<sub>26</sub>H<sub>24</sub>PSi [M + H]<sup>+</sup> 405.2167, found 405.2159.

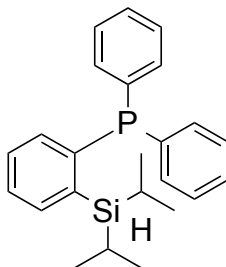
**(2-(dimethylsilyl)phenyl)di-*p*-tolylphosphane (34)**



In a nitrogen filled glove box, 500 mg (2-bromophenyl)di-*p*-tolylphosphine (1.35 mmol) was dissolved in 2 mL ether and cooled to -30 °C. 1.01 mL of a 1.6 M *n*-BuLi solution was then added drop wise, and the reaction stirred for 30 minutes. Volatiles were removed under reduced pressure, and the leftover material was then dissolved in 2 mL toluene. To the mixture, 0.16 g chlorodimethylsilane (1.69 mmol) was then added drop-wise, and the mixture was stirred for 3 hours. The mixture was then filtered, and the precipitate was washed with toluene. Volatiles were removed under reduced pressure to yield a colorless solid (400 mg, 85% yield); mp: 68 °C;  $^1\text{H}$  NMR (500 MHz,  $\text{C}_6\text{D}_6$ , 7.14)  $\delta$  7.61 (d,  $J$  = 6.8 Hz, 1H), 7.37-7.29 (m, 5H), 7.09 (quintet,  $J$  = 7.4, 15.2 Hz, 2H), 6.90 (d,  $J$  = 7.8 Hz, 4H), 5.10-5.06 (m, 1H), 1.99 (s, 6H), 0.42 (d,  $J$  = 3.4 Hz, 6H);  $^{13}\text{C}$  NMR (125 MHz,  $\text{CDCl}_3$ )  $\delta$  145.1, 144.8, 144.0 (d,  $J$  = 10.5 Hz), 138.2, 135.1 (d,  $J$  = 9.3 Hz), 134.3 (d,  $J$  = 9.5 Hz), 133.8, 133.6 (d,  $J$  = 19.1 Hz), 129.4, 129.2 (d,  $J$  = 6.6 Hz), 128.1, 21.3, -2.2 (d,  $J$  = 7.6 Hz);  $^{31}\text{P}$  NMR (202 MHz,  $\text{CDCl}_3$ )  $\delta$  -12.28 (s). HRMS (ESI)  $m/z$  calcd for  $\text{C}_{22}\text{H}_{26}\text{PSi}$   $[\text{M} + \text{H}]^+$  349.1541, found 349.1529.

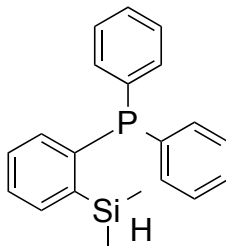


**(2-(diisopropylsilyl)phenyl)diphenylphosphane (35)**



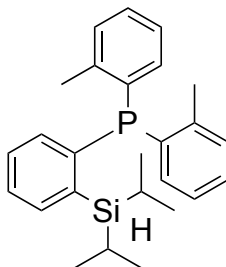
In a nitrogen filled glove box, 500 mg (2-bromophenyl)diphenylphosphane (1.47 mmol) was dissolved in 3.5 mL toluene and cooled to -30 °C. 1.1 mL of a 1.6 M *n*-BuLi solution was then added drop wise, and the reaction stirred for 40 minutes. Volatiles were removed under reduced pressure, and the leftover material was then dissolved in 3.5 mL toluene. To the mixture, 0.277 g chlorodiisopropylsilane (1.83 mmol) was then added drop-wise, and the mixture was stirred for 3 hours. The mixture was then filtered, and the precipitate was washed with toluene. Volatiles were removed under reduced pressure to yield a yellow solid (189 mg, 50% yield); mp: 69 °C;  $^1\text{H}$  NMR (500 MHz,  $\text{C}_6\text{D}_6$ , 7.15)  $\delta$  7.60-7.58 (m, 1H), 7.35 (dt,  $J$  = 1.9, 7.3 Hz, 4H), 7.26 (q,  $J$  = 2.9 Hz, 1H), 7.07-6.97 (m, 8H), 4.57-4.54 (m, 1H), 1.47-1.41 (m, 2H), 1.17 (d,  $J$  = 3.9 Hz, 6H), 0.99 (d,  $J$  = 7.3 Hz, 6H);  $^{13}\text{C}$  NMR (125 MHz,  $\text{CDCl}_3$ )  $\delta$  143.7 (d,  $J$  = 11.5 Hz), 143.4, 143.0, 137.8 (d,  $J$  = 11.5 Hz), 136.8 (d,  $J$  = 15.3 Hz), 134.1, 133.6 (d,  $J$  = 18.1 Hz) 129.2, 128.3 (d,  $J$  = 9.5 Hz), 127.9, 19.3 (d,  $J$  = 5.8 Hz), 12.1 (d,  $J$  = 6.6 Hz);  $^{31}\text{P}$  NMR (202 MHz,  $\text{CDCl}_3$ )  $\delta$  -8.52 (s); HRMS (ESI)  $m/z$  calcd for  $\text{C}_{24}\text{H}_{30}\text{PSi}$   $[\text{M} + \text{H}]^+$  377.1854, found 377.1840.

**(2-(dimethylsilyl)phenyl)diphenylphosphane (36)**



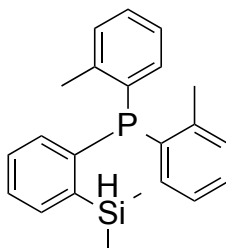
In a nitrogen filled glove box, 500 mg (2-bromophenyl)diphenylphosphane (1.47 mmol) was dissolved in 2 mL toluene and cooled to -30 °C. 1.1 mL of a 1.6 M *n*-BuLi solution was then added drop wise, and the reaction stirred for 40 minutes. Volatiles were removed under reduced pressure, and the leftover material was then dissolved in 2 mL toluene. To the mixture, 0.174 g chlorodimethylsilane (1.85 mmol) was then added drop-wise, and the mixture was stirred for 3 hours. The mixture was then filtered, and the precipitate was washed with toluene. Volatiles were removed under reduced pressure to yield a yellow oil (300 mg, 64% yield);  $^1\text{H}$  NMR (500 MHz,  $\text{C}_6\text{D}_6$ , 7.14)  $\delta$  7.58 (d,  $J$  = 6.9 Hz, 1H), 7.33 (dt,  $J$  = 1.9, 7.8 Hz, 4H), 7.25 (q,  $J$  = 3.9 Hz, 1H), 7.08 (t,  $J$  = 7.4 Hz, 1H), 7.02-6.98 (m, 7H), 5.07 (m, 1H), 0.39 (dd,  $J$  = 1.0, 3.9 Hz);  $^{13}\text{C}$  NMR (125 MHz,  $\text{CDCl}_3$ )  $\delta$  145.3, 145.0, 143.4 (d,  $J$  = 10.4 Hz), 137.6 (d,  $J$  = 10.5 Hz), 135.2 (d,  $J$  = 14.3 Hz), 134.0, 133.8, 133.6 (d,  $J$  = 19.6 Hz), 129.5, 128.4 (m), -2.26 (d,  $J$  = 7.6 Hz);  $^{31}\text{P}$  NMR (202 MHz,  $\text{CDCl}_3$ )  $\delta$  -10.34 (s). HRMS (ESI)  $m/z$  calcd for  $\text{C}_{20}\text{H}_{22}\text{PSi}$   $[\text{M} + \text{H}]^+$  321.1228, found 321.1208.

**(2-(diisopropylsilyl)phenyl)di-*o*-tolylphosphane (37)**



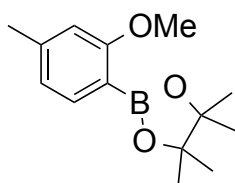
In a nitrogen filled glove box, 250 mg (2-bromophenyl)di-*o*-tolylphosphane (0.679 mmol) was dissolved in 2 mL ether and cooled to -30 °C. 0.505 mL of a 1.6 M *n*-BuLi solution was then added drop wise, and the reaction stirred for 3 hours. Volatiles were removed under reduced pressure, and the leftover material was then dissolved in 3.5 mL toluene. To the mixture, 0.138 g chlorodiisopropylsilane (0.92 mmol) was then added drop-wise, and the mixture was stirred for 3 hours. The mixture was then filtered, and the precipitate was washed with toluene. Volatiles were removed under reduced pressure to yield a yellow solid (200 mg, 73% yield) Spectra contains minor amounts of water; mp: 86 °C; <sup>1</sup>H NMR (500 MHz, CD<sub>2</sub>Cl<sub>2</sub>, 5.32) δ 7.60 (d, *J* = 5.9 Hz, 1H), 7.37 (t, *J* = 7.4 Hz, 1H), 7.29-7.23 (m, 5H), 7.09 (t, *J* = 5.9 Hz, 2H), 6.93 (q, *J* = 3.9 Hz, 1H), 6.71-6.69 (m, 2H), 4.24 (m, 1H), 2.37 (s, 6H), 1.32-1.25 (m, 2H), 1.07 (d, *J* = 7.3 Hz, 6H), 0.86 (d, *J* = 7.4 Hz, 6H); <sup>13</sup>C NMR (125 MHz, CDCl<sub>3</sub>) δ 142.6, 142.37 (d, *J* = 7.6 Hz), 142.31, 136.3 (d, *J* = 3.4 Hz), 133.6 (*J* = 4.7 Hz), 129.9 (d, *J* = 4.8 Hz), 129.2, 128.4, 127.5, 125.9, 21.2 (d, *J* = 10.1 Hz), 19.0, 18.9; <sup>31</sup>P NMR (202 MHz, CDCl<sub>3</sub>) δ -24.85 (s). HRMS (ESI) *m/z* calcd for C<sub>26</sub>H<sub>34</sub>PSi [M + H]<sup>+</sup> 405.2167, found 405.2156.

**(2-(dimethylsilyl)phenyl)di-*o*-tolylphosphane (38)**



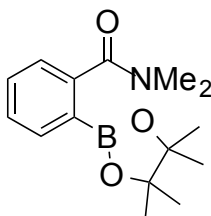
In a nitrogen filled glove box, 125 mg (2-bromophenyl)di-*o*-tolylphosphane (1.47 mmol) was dissolved in 2 mL ether and cooled to -30 °C. 0.26 mL of a 1.6 M *n*-BuLi solution was then added drop wise, and the reaction stirred for 40 minutes. Volatiles were removed under reduced pressure, and the leftover material was then dissolved in 4 mL toluene. To the mixture, 0.04 g chlorodimethylsilane (0.42 mmol) was then added drop-wise, and the mixture was stirred for 3 hours. The mixture was then filtered, and the precipitate was washed with toluene. Volatiles were removed under reduced pressure to yield a whitish yellow solid (110 mg, 92% yield). Spectra contains minor amounts of starting material; mp: 97 °C; <sup>1</sup>H NMR (500 MHz, CD<sub>3</sub>OD, 3.31) δ 7.69 (d, *J* = 5.9 Hz, 1H), 7.39 (t, *J* = 7.3 Hz, 1H) 7.31-7.21 (m, 5H), 7.08 (t, *J* = 6.4 Hz, 2H), 6.91 (q, *J* = 6.4 Hz, 1H), 6.65 (m, 2H), 4.62 (m, 1H), 2.33 (s, 6H), 0.29 (d, *J* = 1 Hz, 6H); <sup>13</sup>C NMR (125 MHz, CDCl<sub>3</sub>) δ 135.5 (d, *J* = 10.5 Hz), 135.4, 135.3, 134.1, 133.1, 130.0 (d, *J* = 4.8 Hz), 129.5, 128.4, 128.22, 125.9, 21.3 (d, *J* = 20.0 Hz), -2.52 (d, *J* = 8.6 Hz); <sup>31</sup>P NMR (202 MHz, C<sub>6</sub>D<sub>6</sub>) δ -24.871 (s). HRMS (ESI) *m/z* calcd for C<sub>22</sub>H<sub>26</sub>PSi [M + H]<sup>+</sup> 349.1541, found 349.1532.

**2-(2-methoxy-4-methylphenyl)-4,4,5,5-tetramethyl-1,3,2-dioxaborolane (39)**<sup>4</sup>

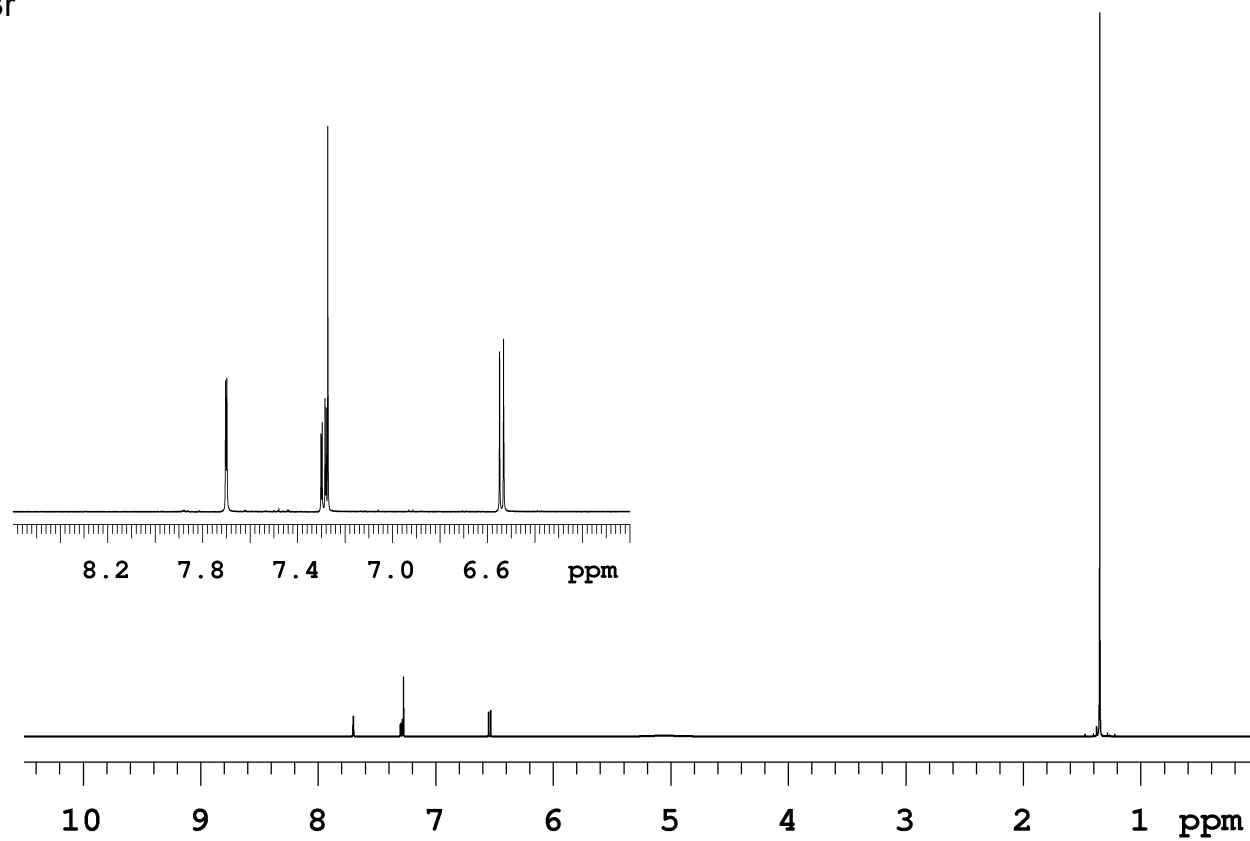


Colorless Solid. mp: 59.5-60 °C; <sup>1</sup>H NMR (500 MHz, CDCl<sub>3</sub>) δ 7.55 (d, 1H, *J* = 7.5 Hz), 6.74 (d, 1H, *J* = 7.3 Hz), 6.65 (s, 1H), 3.80 (s, 3H), 2.33 (s, 3H), 1.32 (s, 12H); <sup>13</sup>C NMR (125 MHz, CDCl<sub>3</sub>) δ 164.3, 142.9, 136.8, 120.9, 111.4, 83.2, 55.7, 24.9, 24.7, 21.9.

***N*-dimethyl-2-(4,4,5,5-tetramethyl-1,3,2-dioxaborolan-2-yl)benzamide (40)**<sup>5</sup>



White Solid. <sup>1</sup>H NMR (500 MHz, CDCl<sub>3</sub>) δ 7.80 (dd, *J* = 7.5, 0.6 Hz, 1H), 7.45 (dt, *J* = 7.5, 1.5 Hz, 1H), 7.37 (dt, *J* = 7.5, 1.5 Hz, 1H), 7.30 (dd, *J* = 7.5, 0.6 Hz, 1H), 2.97 (br, 6H), 1.31 (s, 12H); <sup>13</sup>C NMR (125 MHz, CDCl<sub>3</sub>) δ 172.6, 142.6, 135.0, 131.0, 128.2, 125.5, 83.5, 24.8.

Nc1ccc(Br)cc1BPin

**Figure 5.2.**  $^{13}\text{C}$  NMR (125 MHz,  $\text{CDCl}_3$ ) (1)

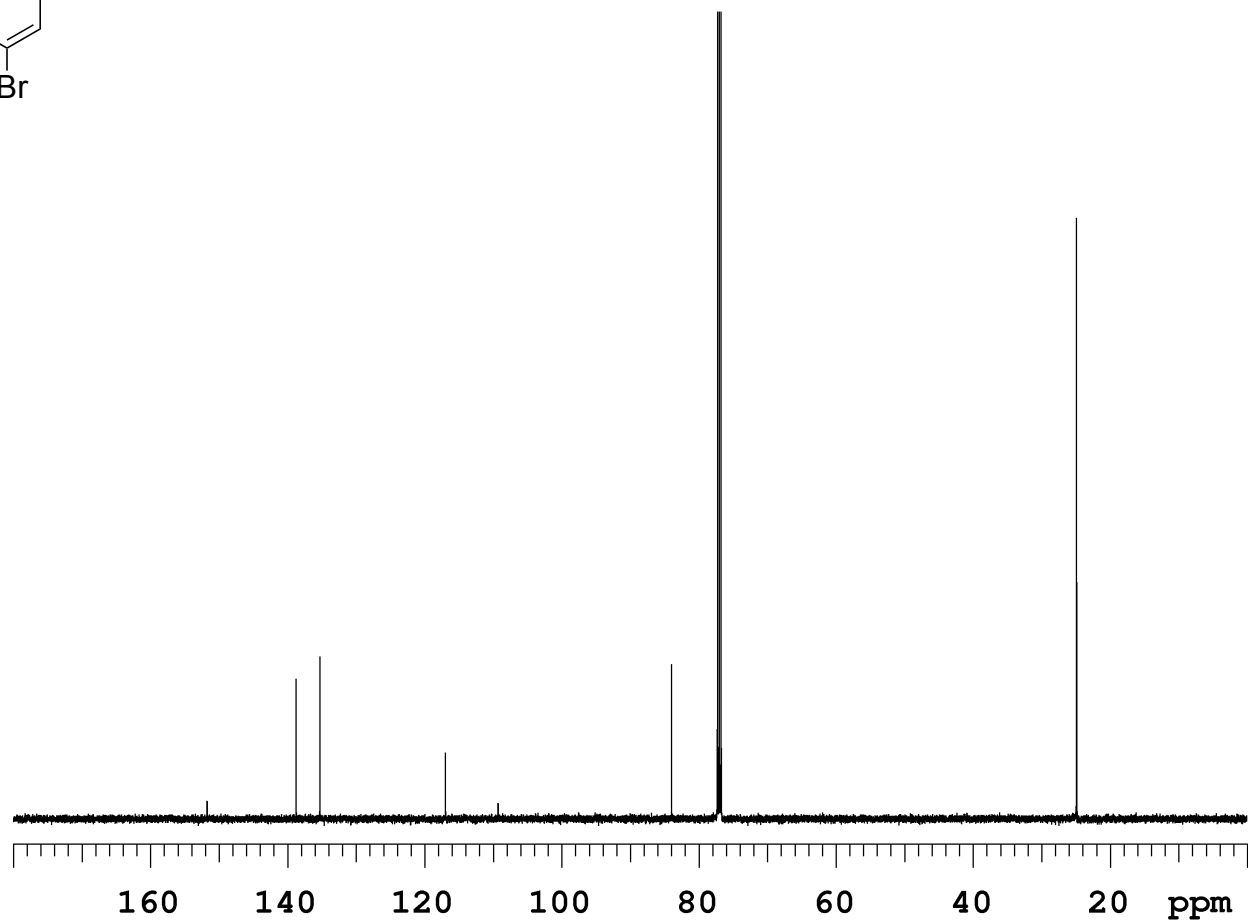
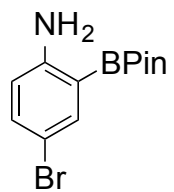


Figure 5.3.  $^1\text{H}$  NMR (500 MHz,  $\text{CDCl}_3$ ) (2)

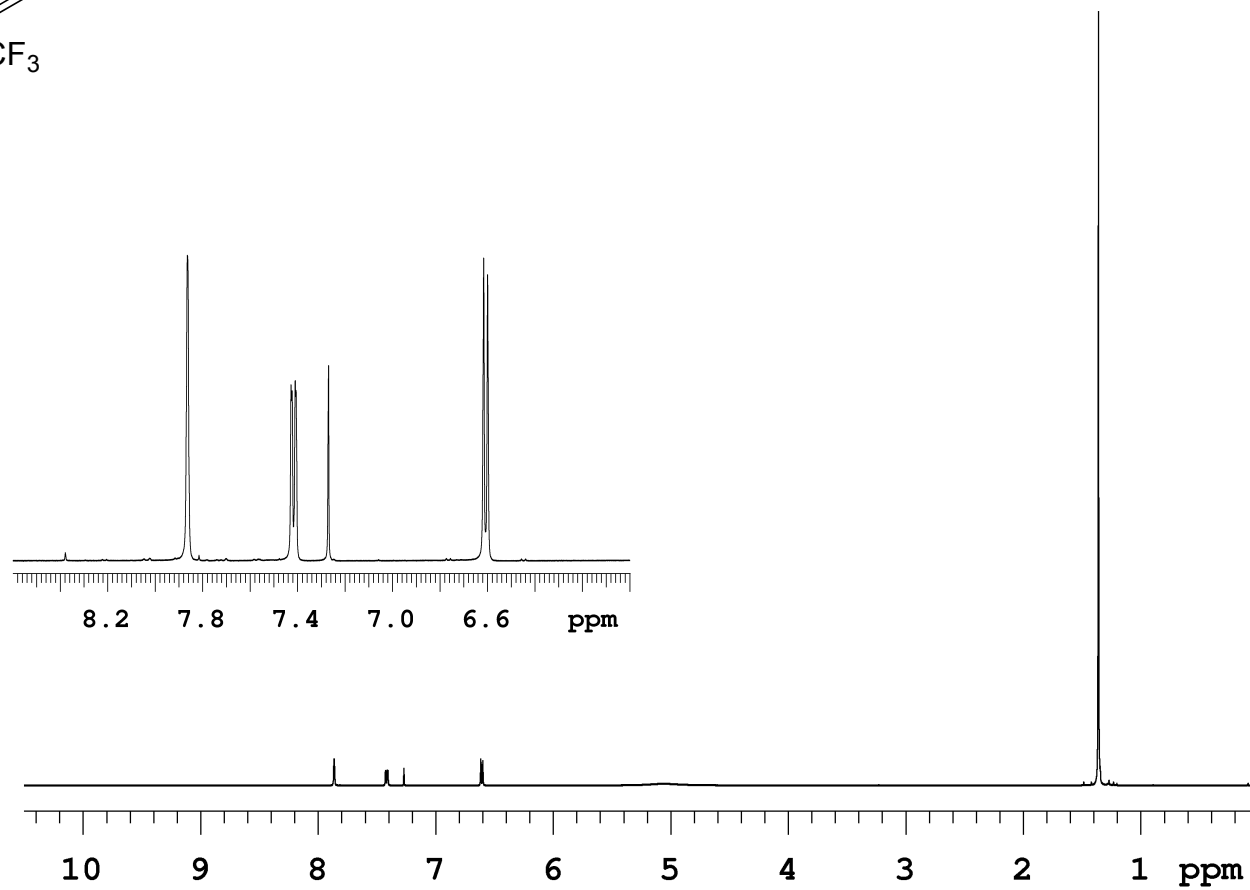
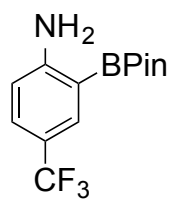




Figure 5.4.  $^{13}\text{C}$  NMR (125 MHz,  $\text{CDCl}_3$ ) (2)

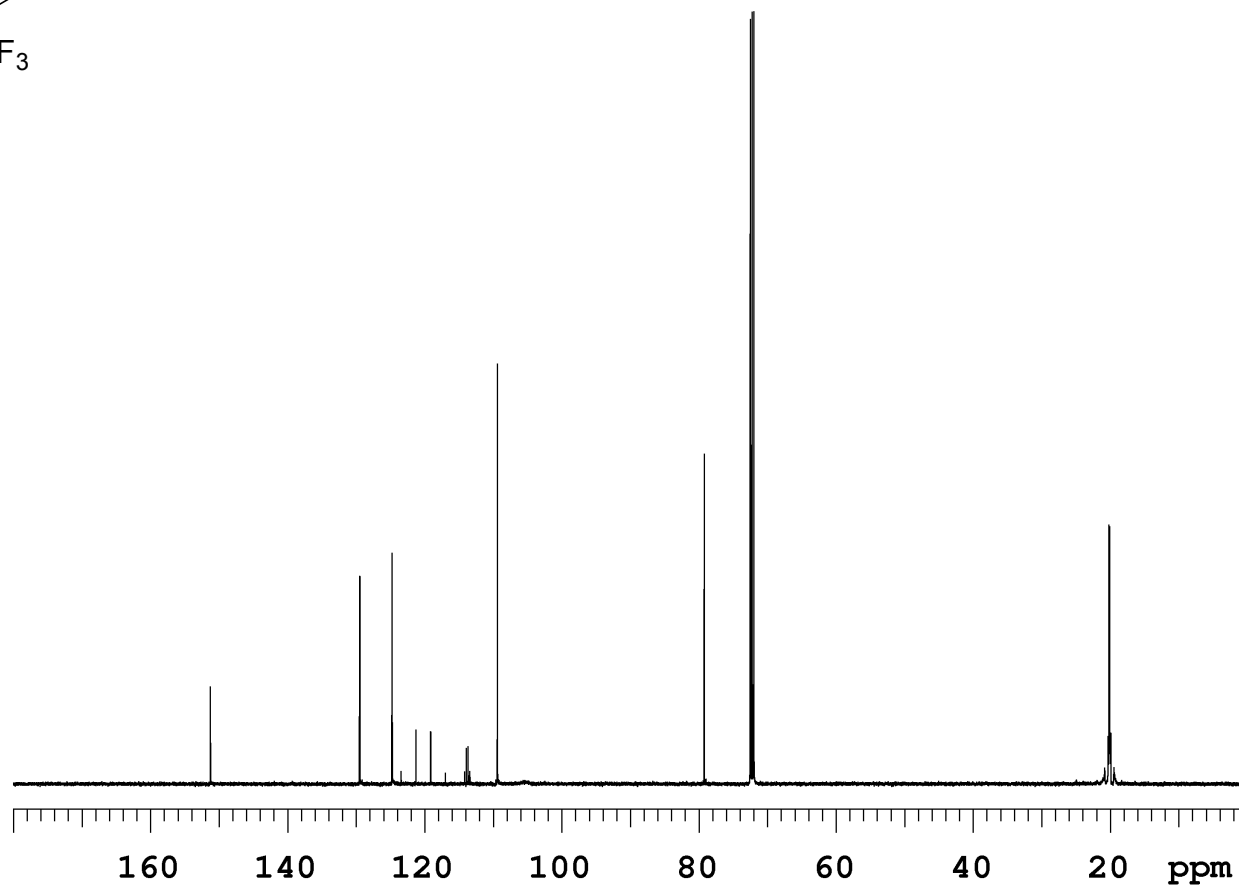
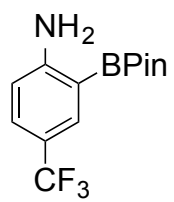


Figure 5.5.  $^1\text{H}$  NMR (500 MHz,  $\text{C}_6\text{D}_6$ ) (3)

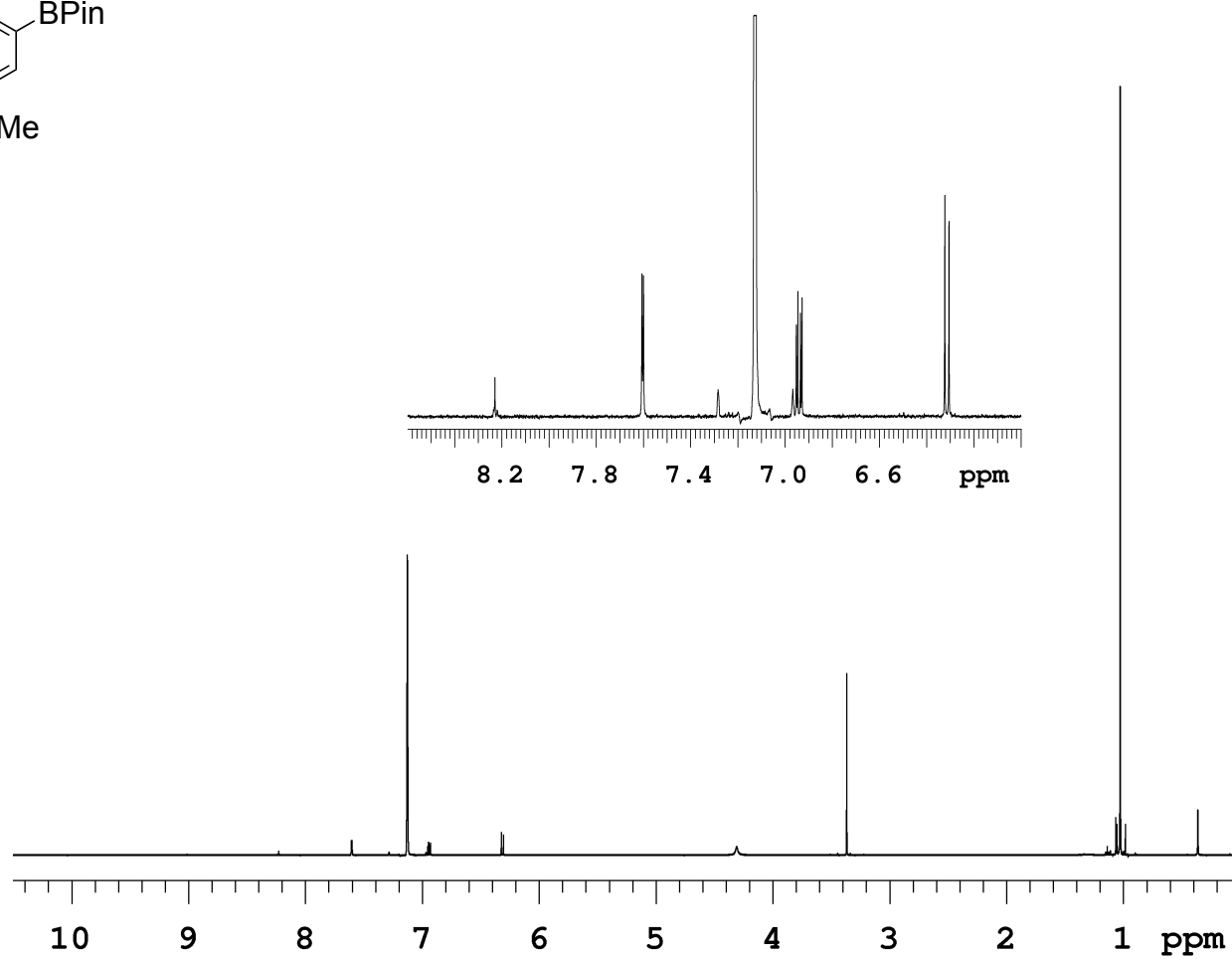
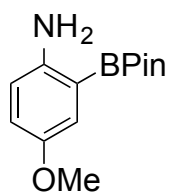


Figure 5.6.  $^{13}\text{C}$  NMR (125 MHz,  $\text{C}_6\text{D}_6$ ) (3)

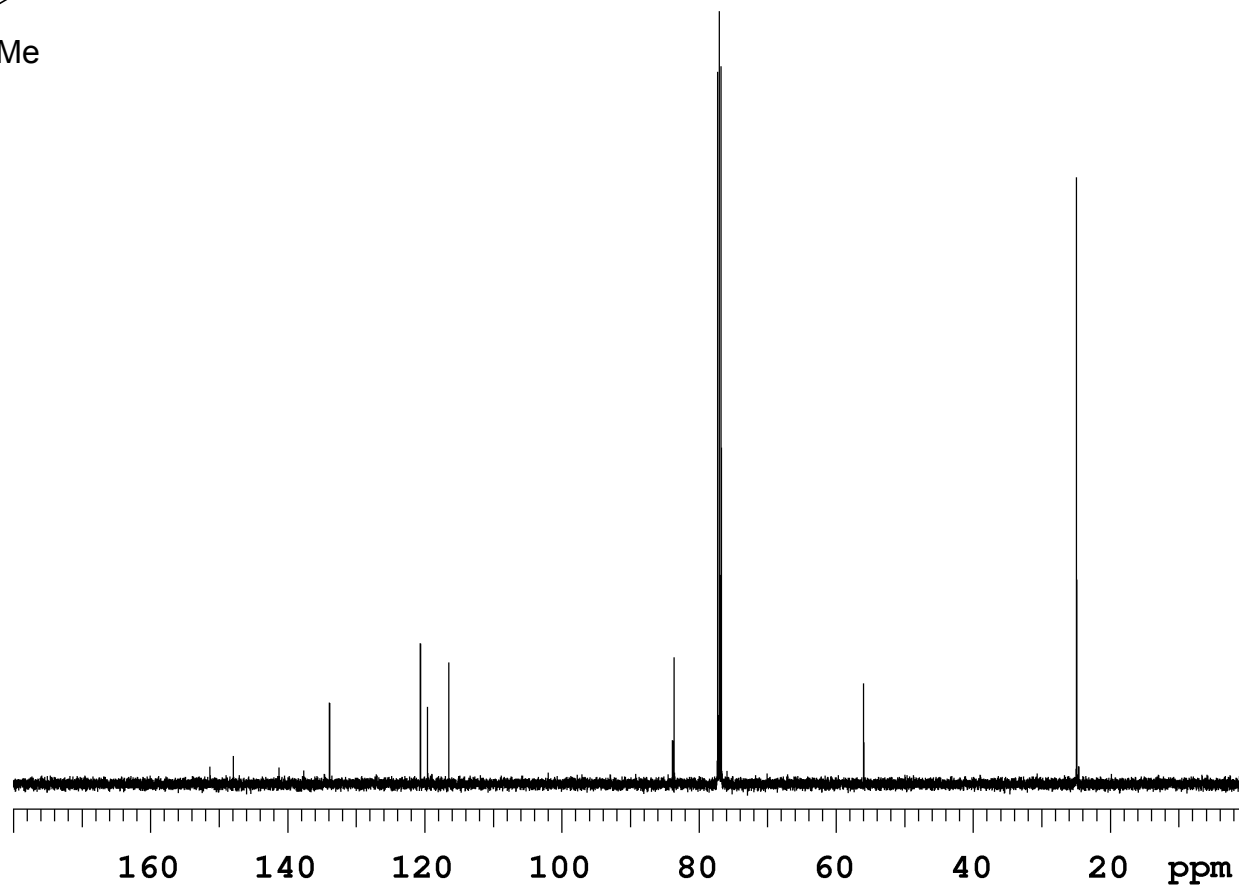
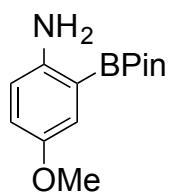


Figure 5.7.  $^1\text{H}$  NMR (500 MHz,  $\text{CDCl}_3$ ) (4)

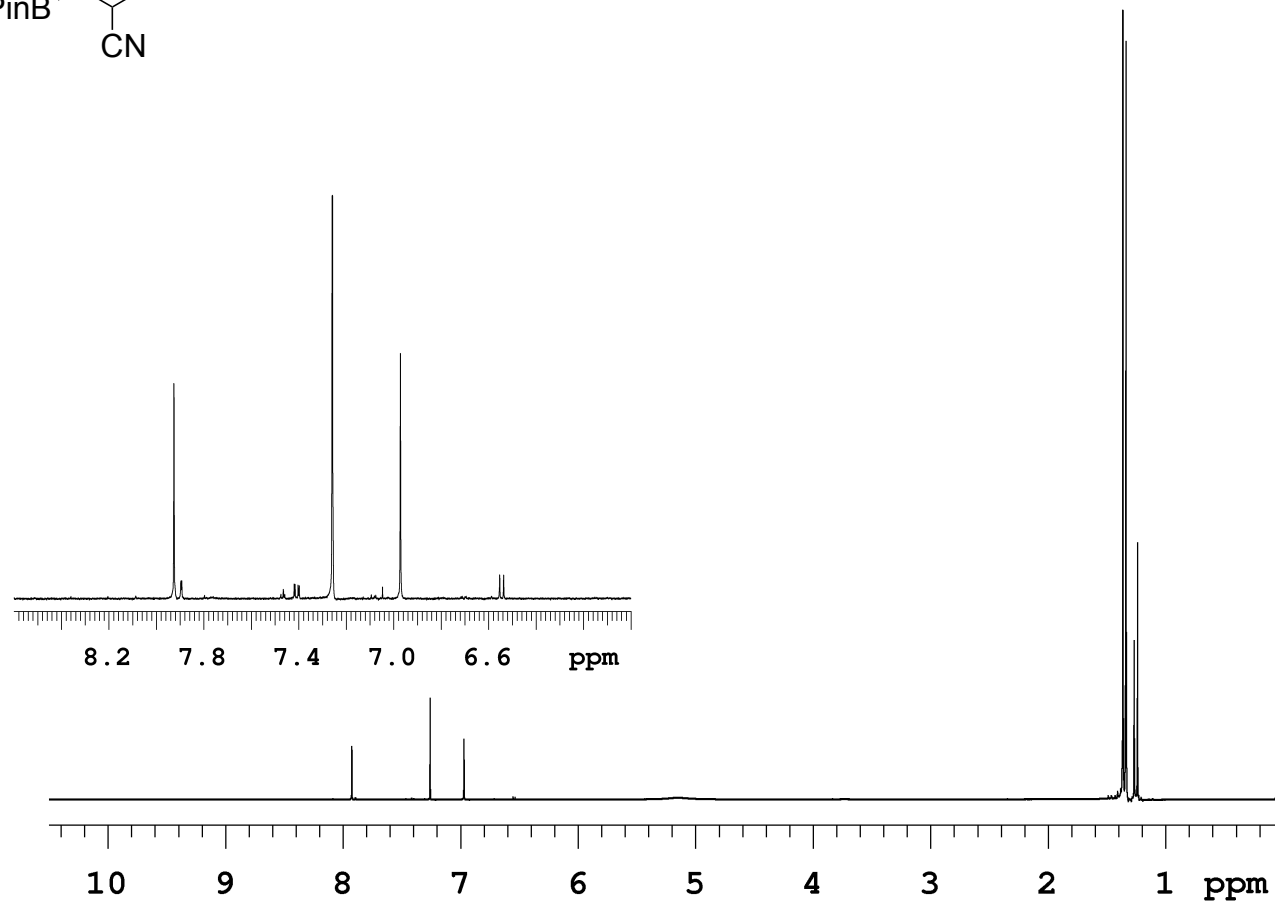
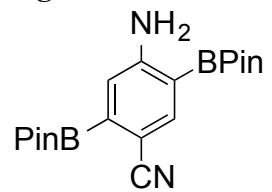


Figure 5.8.  $^{13}\text{C}$  NMR (125 MHz,  $\text{CDCl}_3$ ) (4)

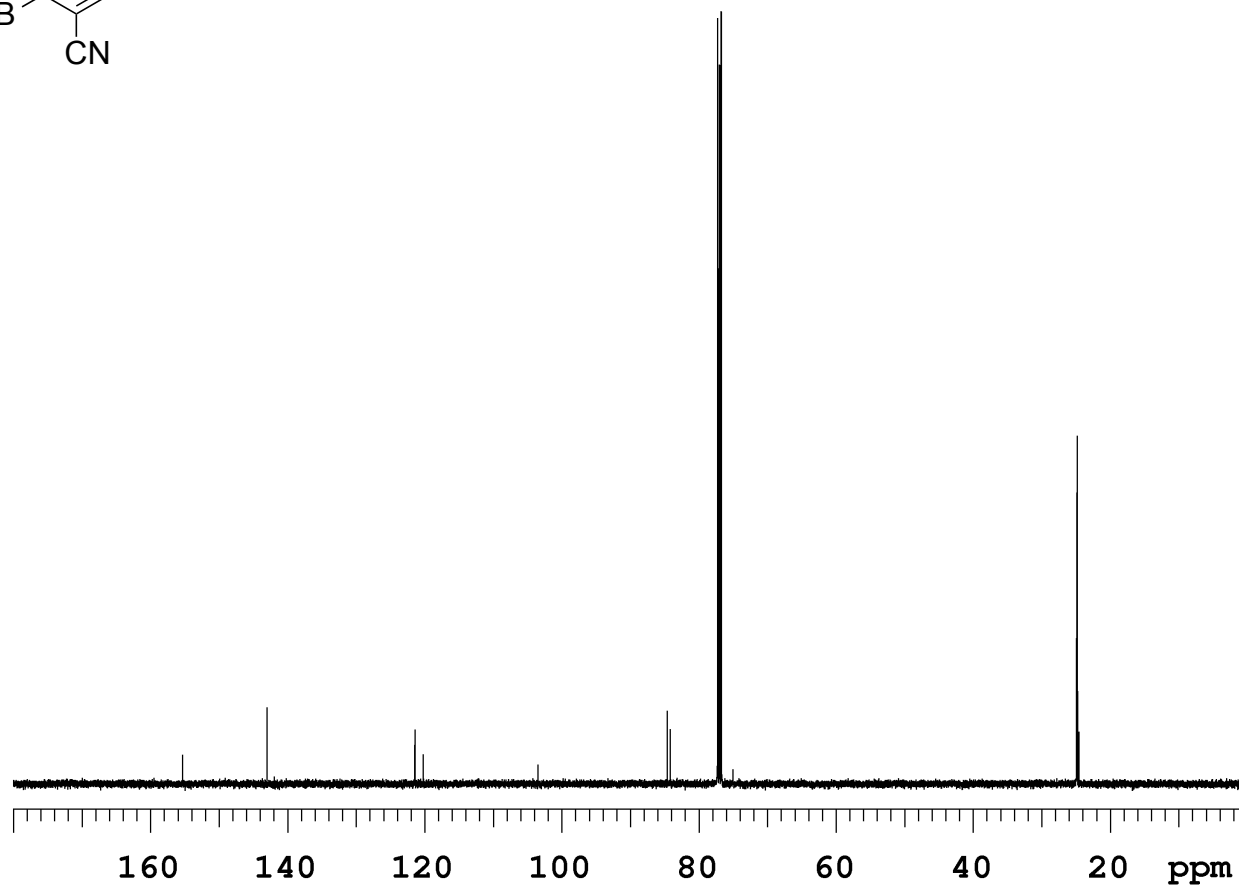
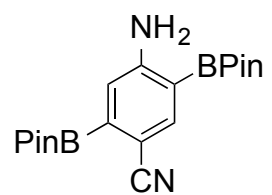


Figure 5.9.  $^1\text{H}$  NMR (500 MHz,  $\text{CDCl}_3$ ) (5)

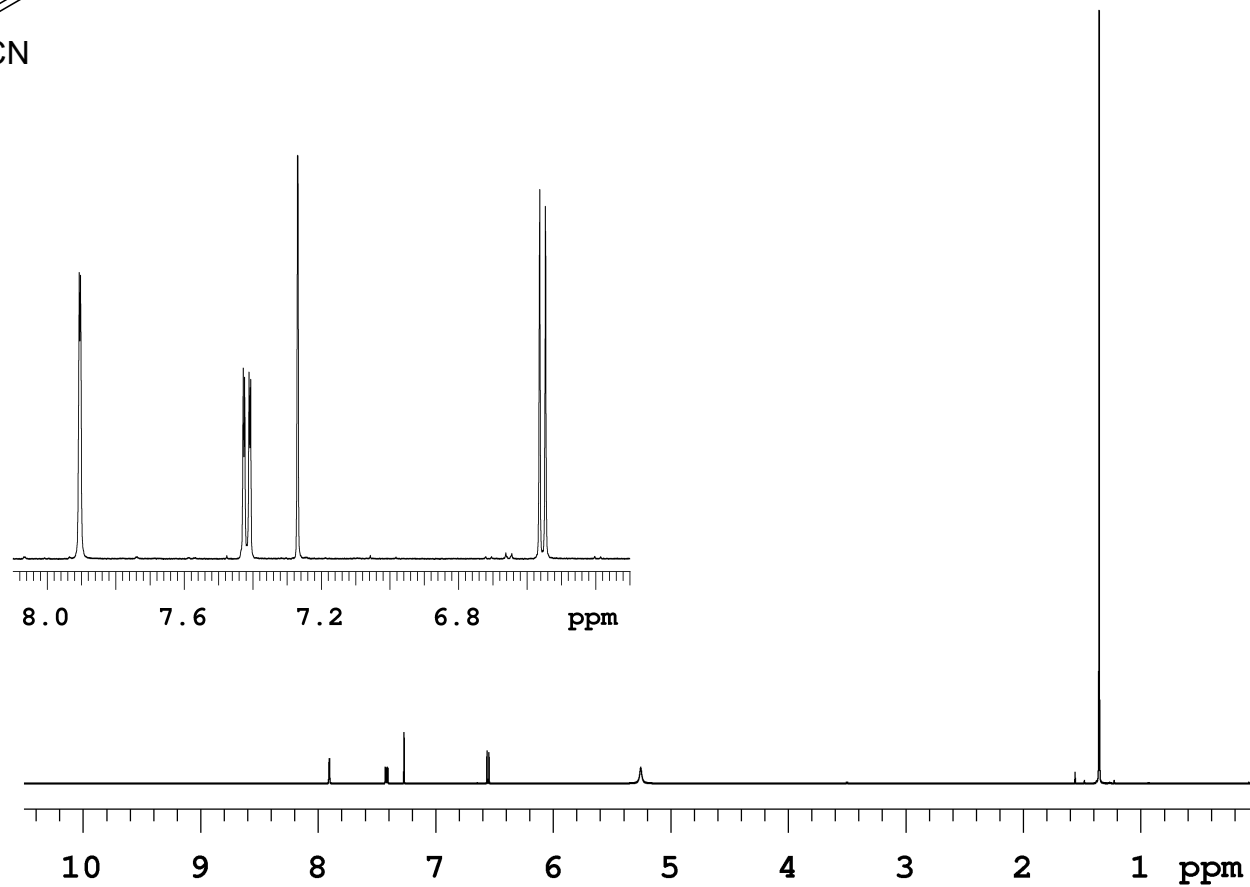
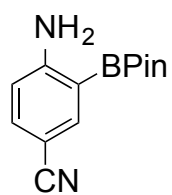


Figure 5.10.  $^{13}\text{C}$  NMR (125 MHz,  $\text{CDCl}_3$ ) (5)

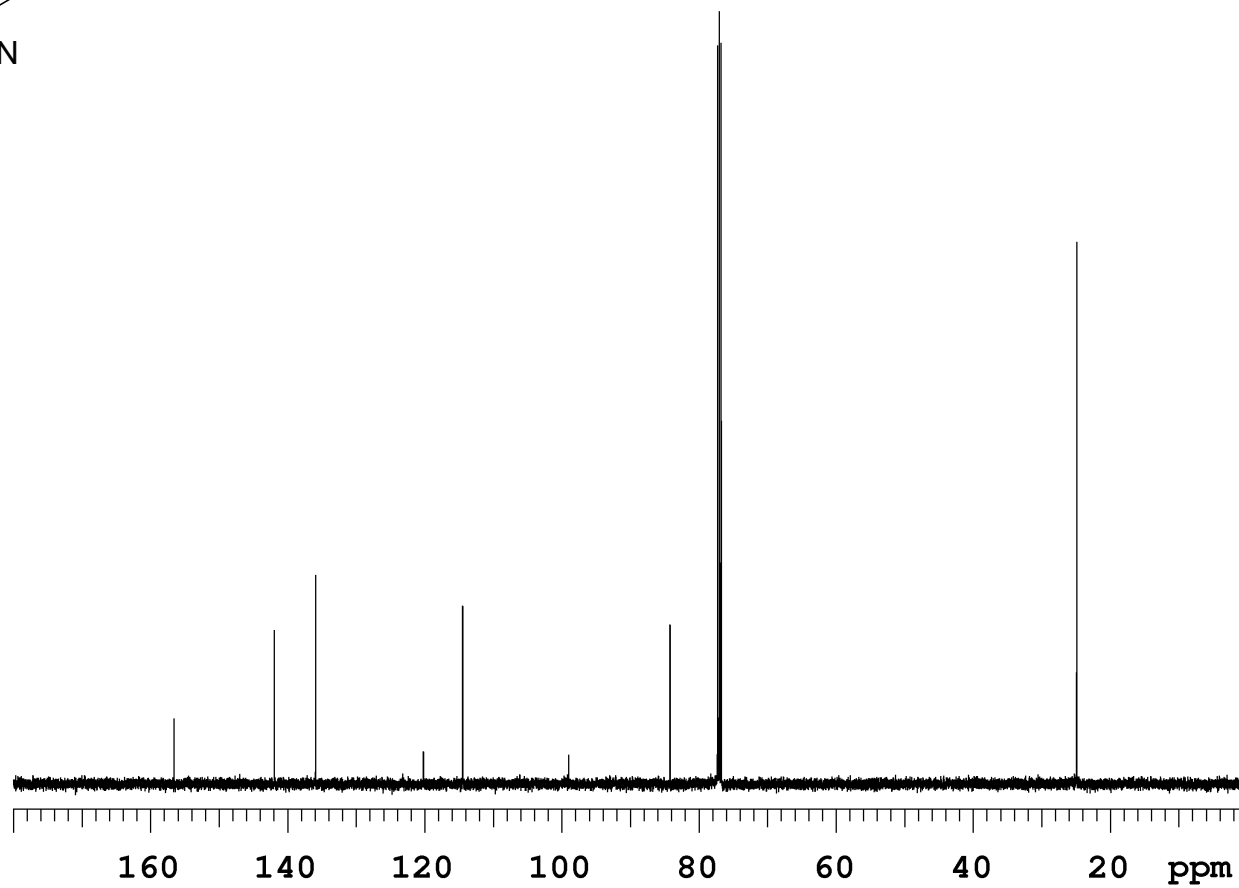
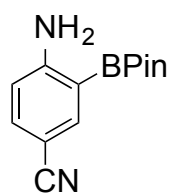


Figure 5.11.  $^1\text{H}$  NMR (500 MHz,  $\text{CDCl}_3$ ) (6a)

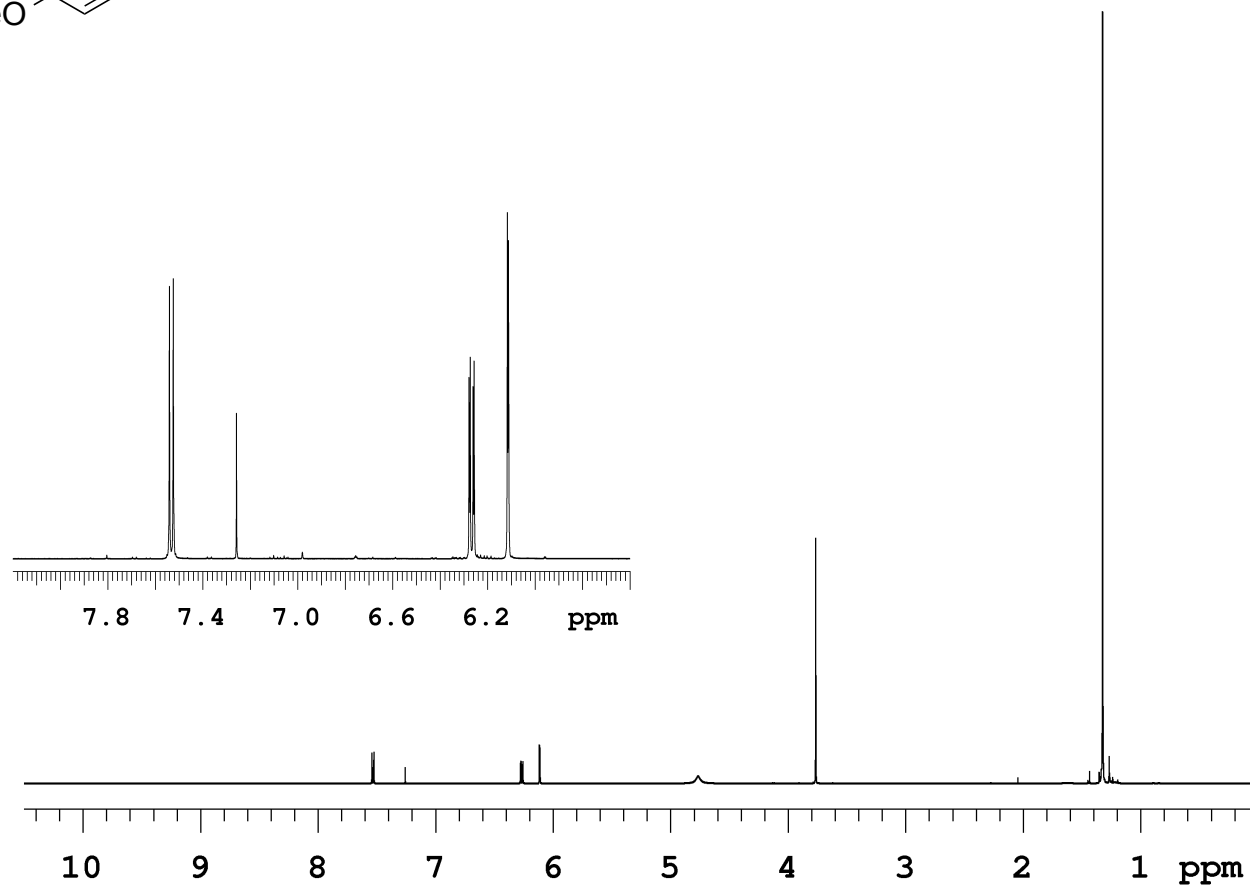
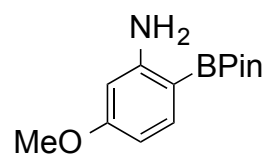




Figure 5.12.  $^{13}\text{C}$  NMR (125 MHz,  $\text{CDCl}_3$ ) (6a)

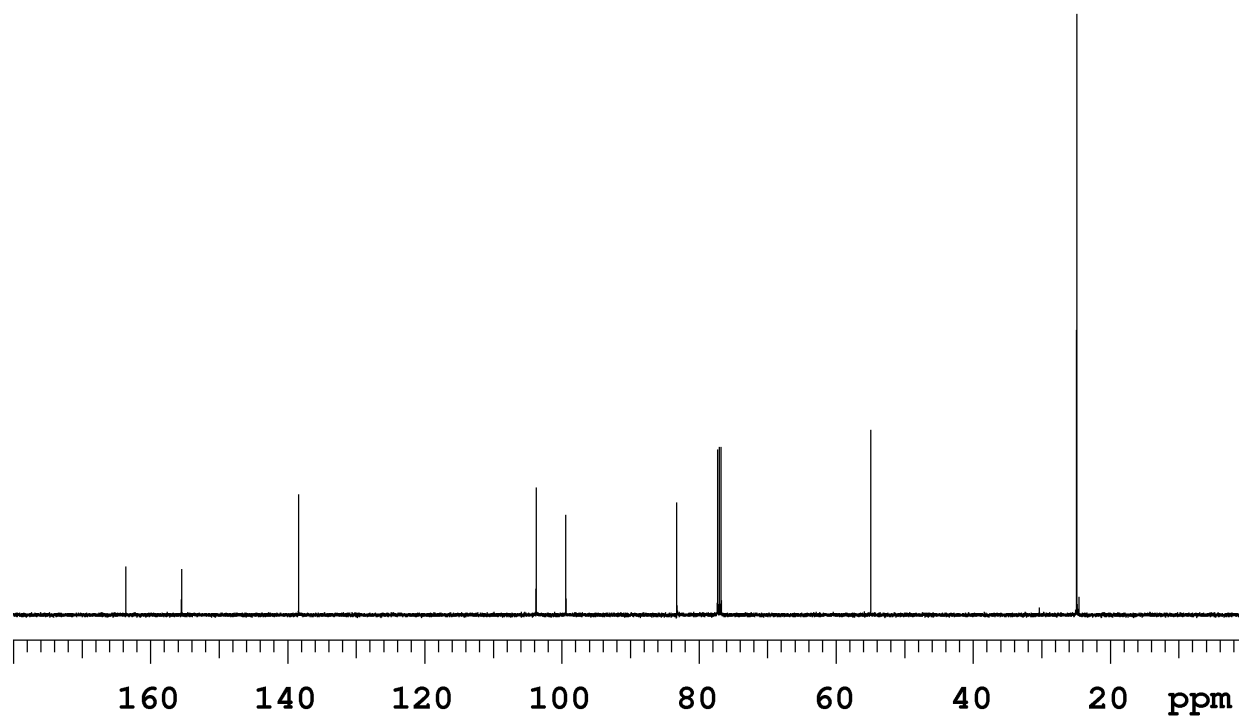
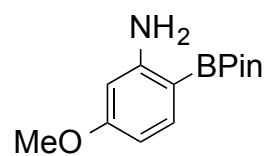


Figure 5.13.  $^1\text{H}$  NMR (500 MHz,  $\text{CD}_3\text{CN}$ ) (6b)

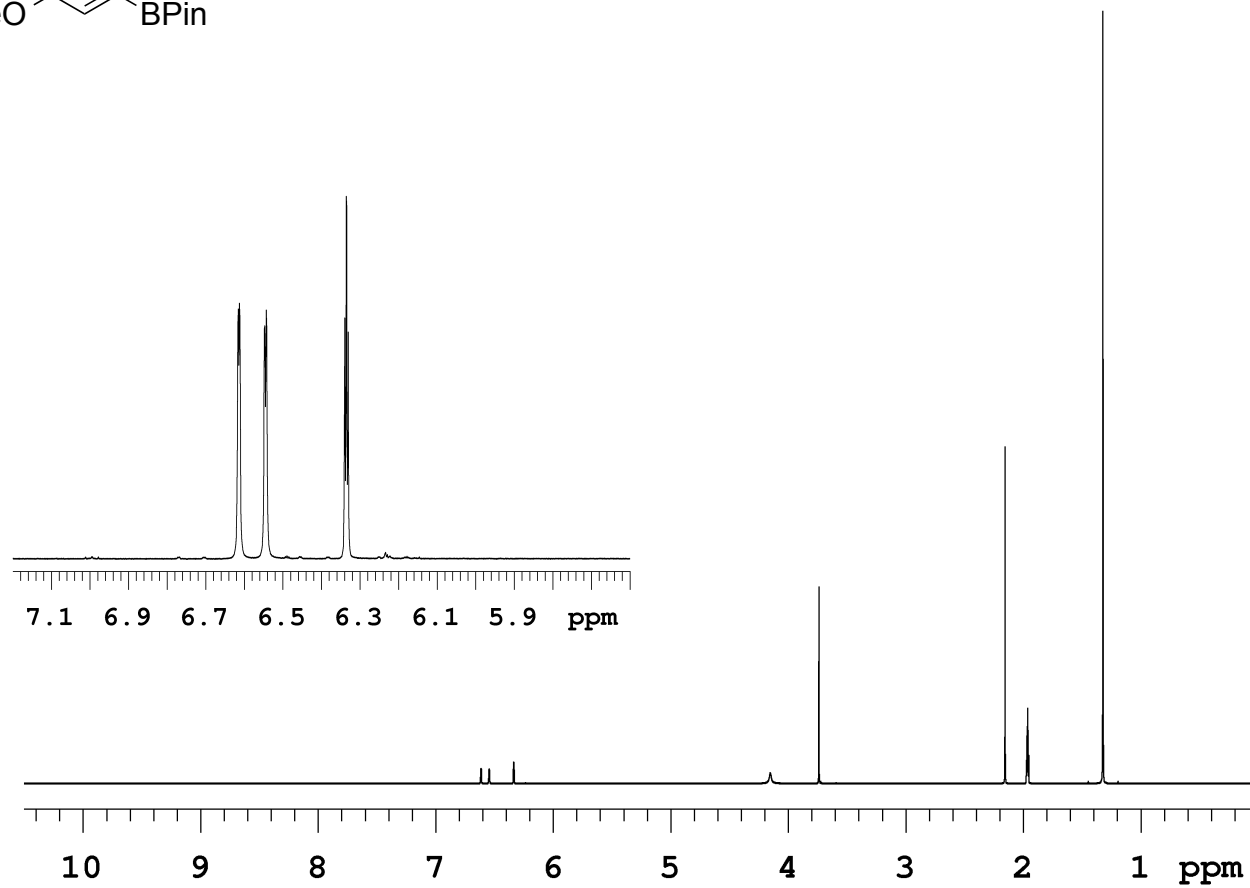
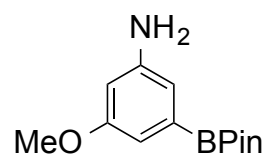


Figure 5.14.  $^{13}\text{C}$  NMR (125 MHz,  $\text{CDCl}_3$ ) (6b)

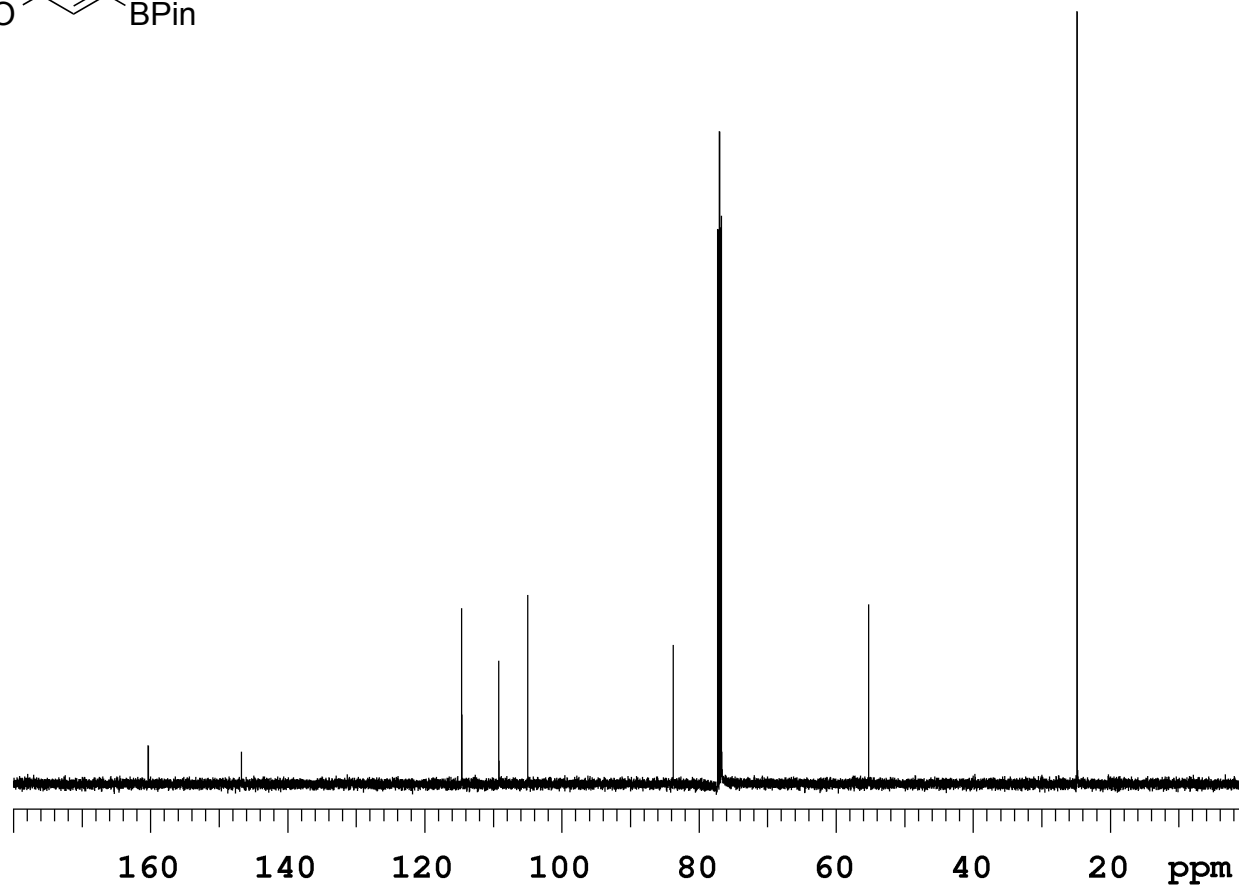
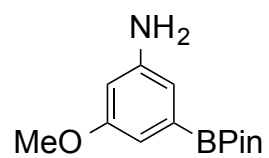


Figure 5.15.  $^1\text{H}$  NMR (500 MHz,  $\text{CDCl}_3$ ) (7)

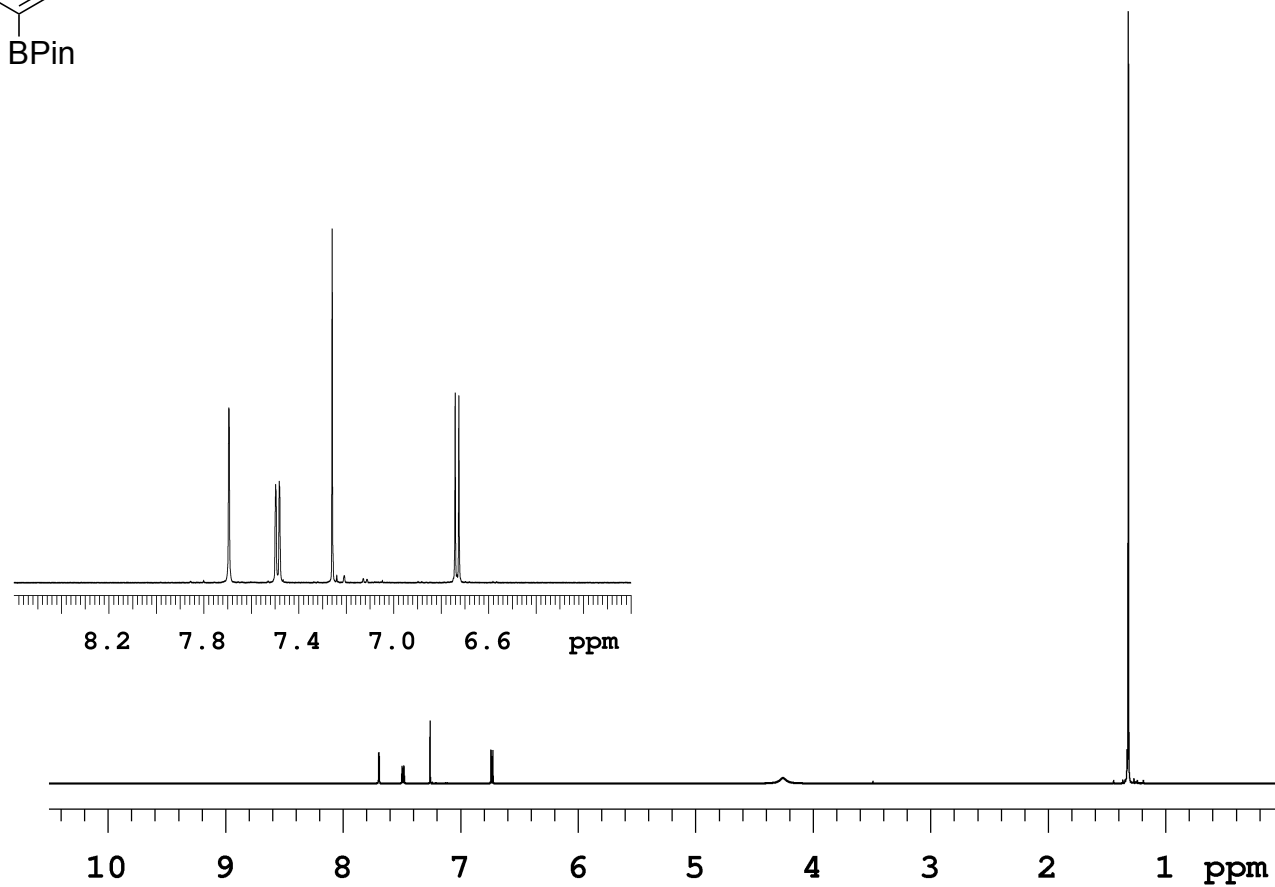
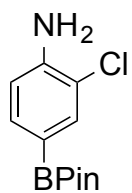


Figure 5.16.  $^{13}\text{C}$  NMR (125 MHz,  $\text{CDCl}_3$ ) (7)

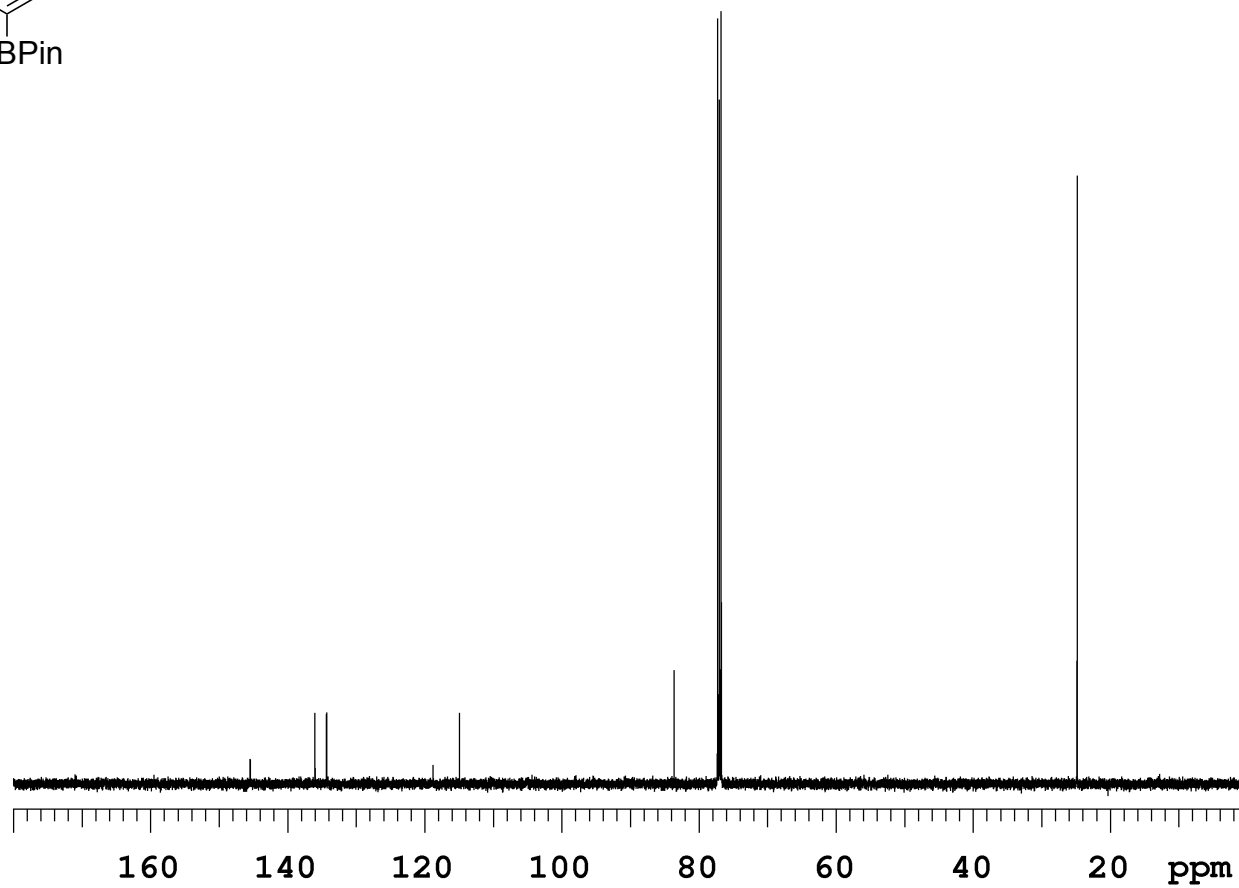


Figure 5.17.  $^1\text{H}$  NMR (500 MHz,  $\text{CDCl}_3$ ) (8)

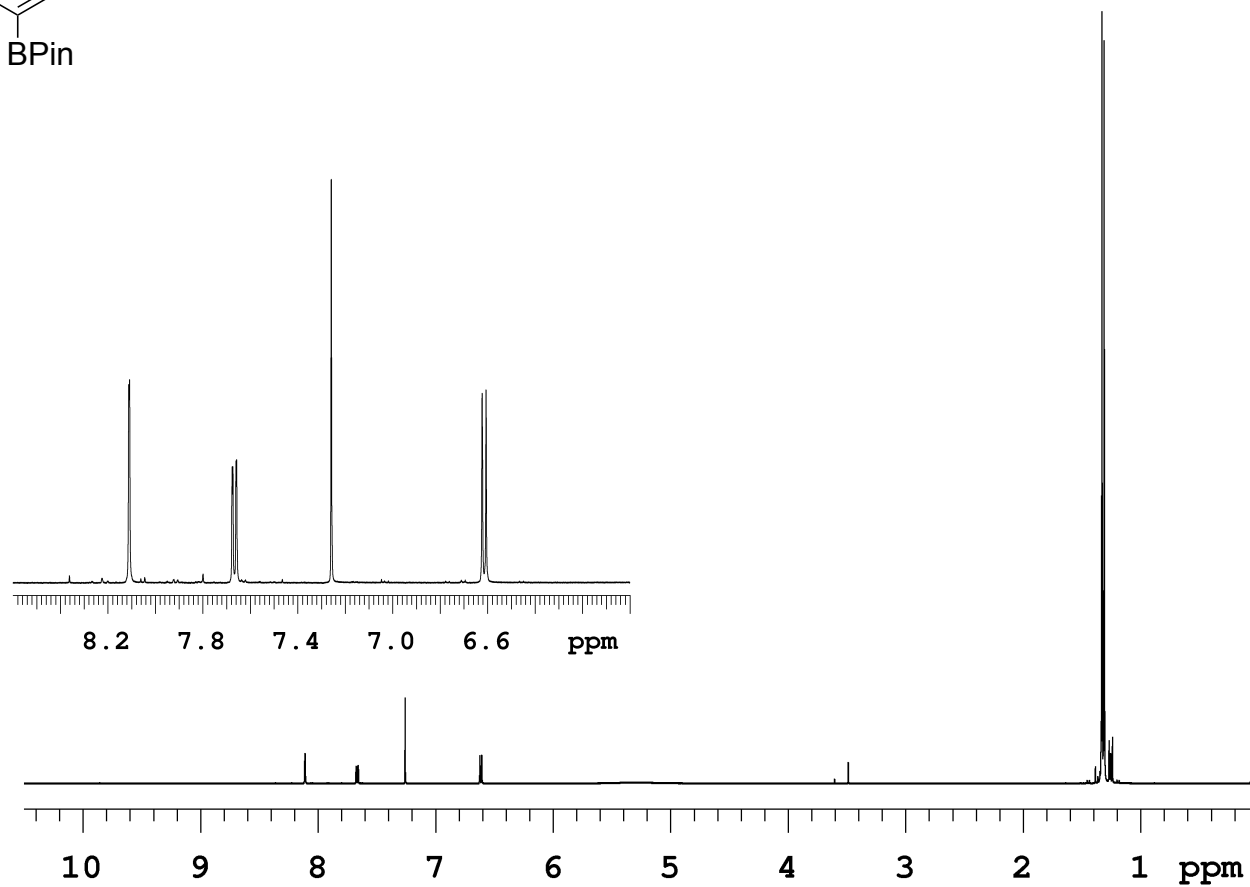
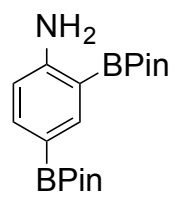


Figure 5.18.  $^{13}\text{C}$  NMR (125 MHz,  $\text{CDCl}_3$ ) (8)

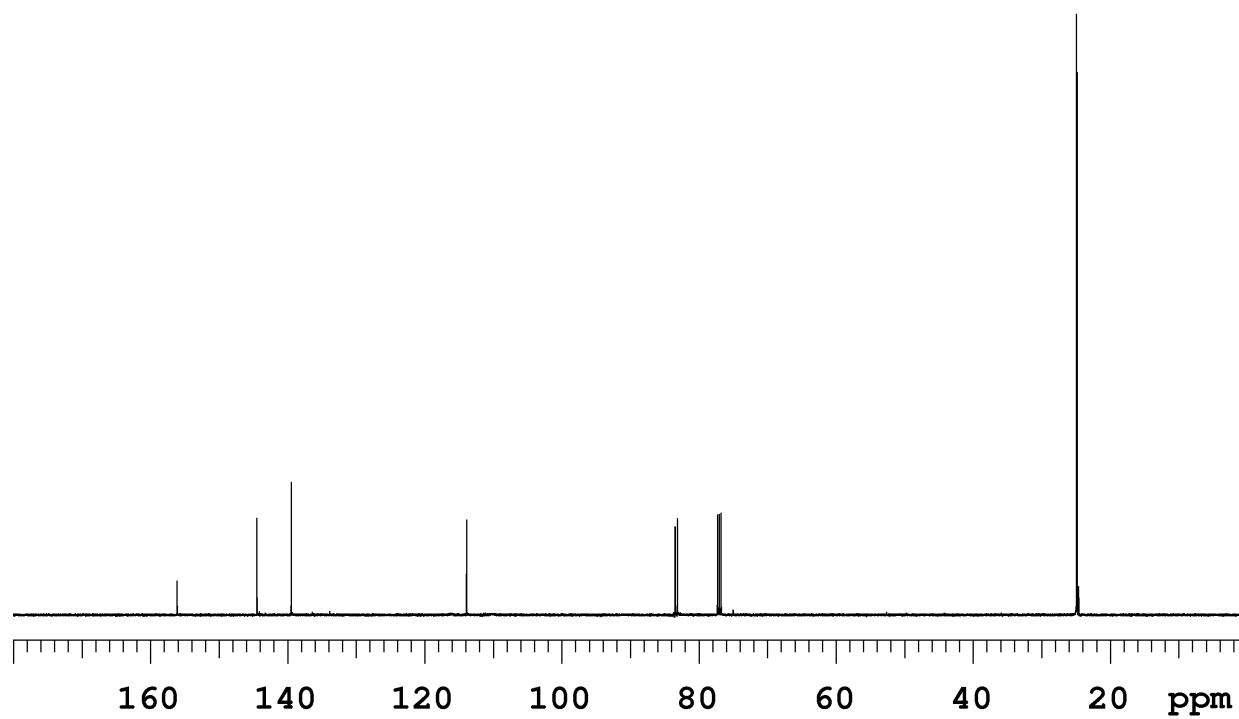
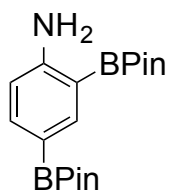


Figure 5.19.  $^1\text{H}$  NMR (500 MHz,  $\text{CDCl}_3$ ) (9)

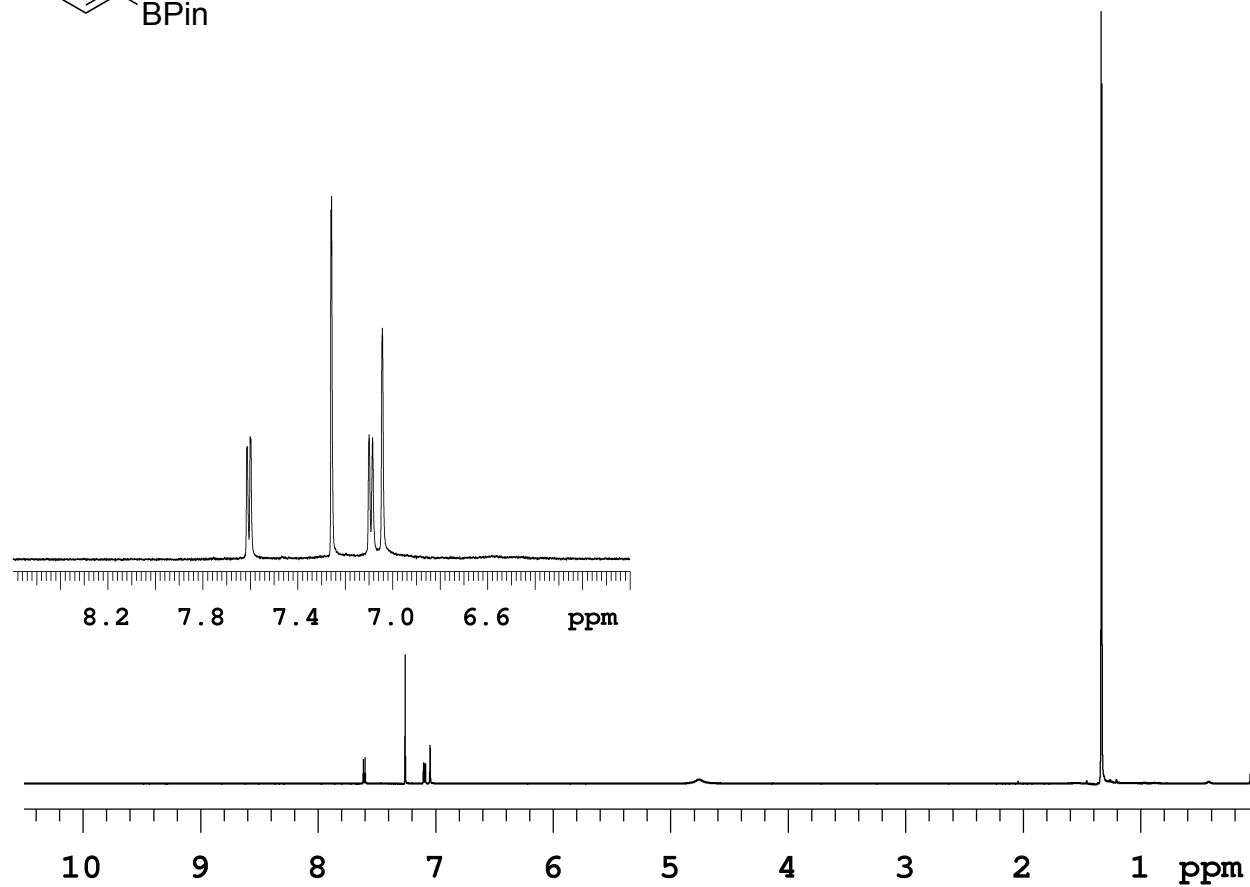
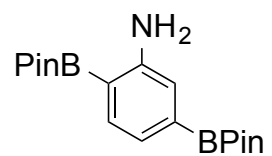




Figure 5.20.  $^{13}\text{C}$  NMR (125 MHz,  $\text{CDCl}_3$ ) (9)

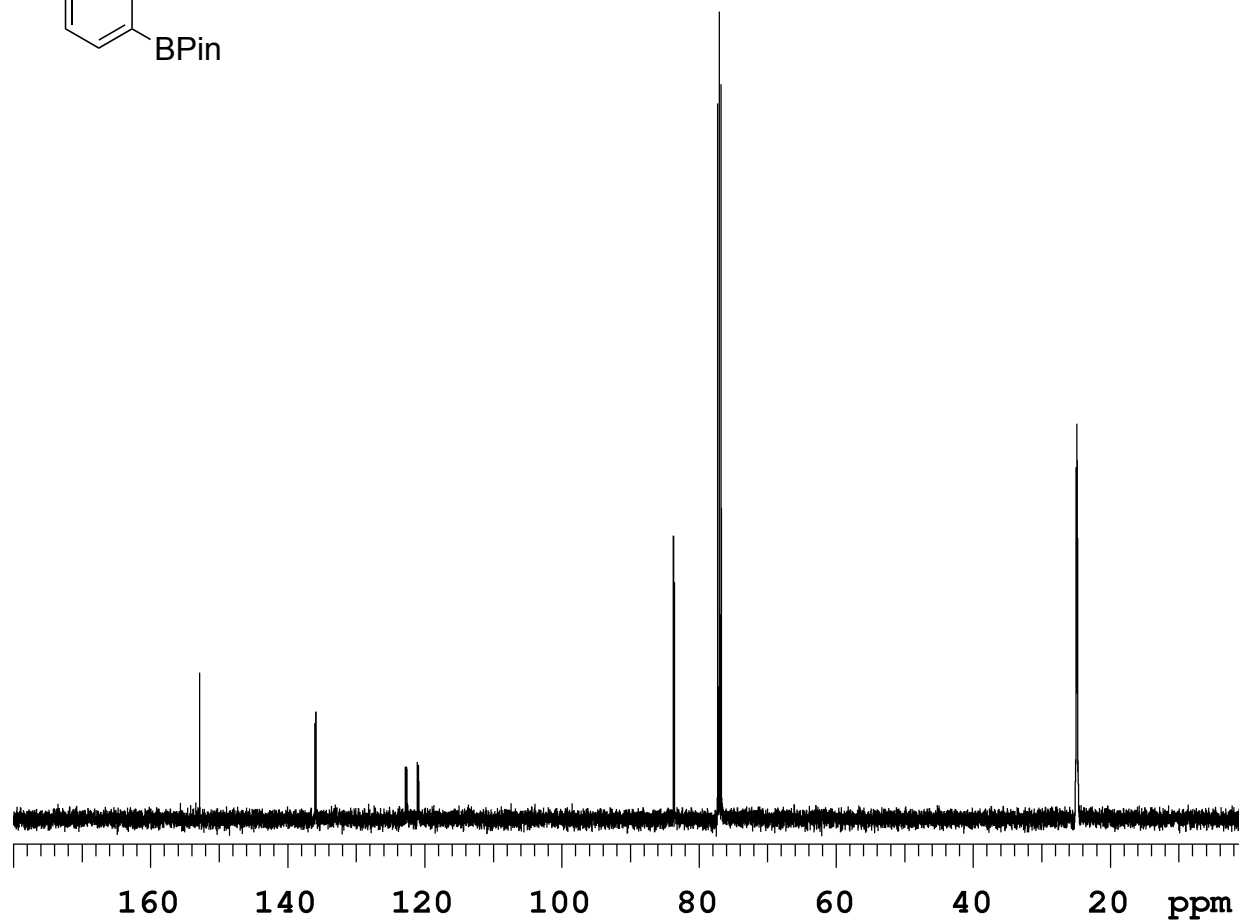
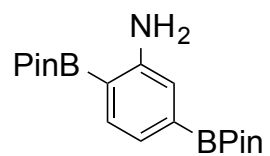


Figure 5.21.  $^1\text{H}$  NMR (500 MHz,  $\text{DMSO-d}_6$ ) (10)

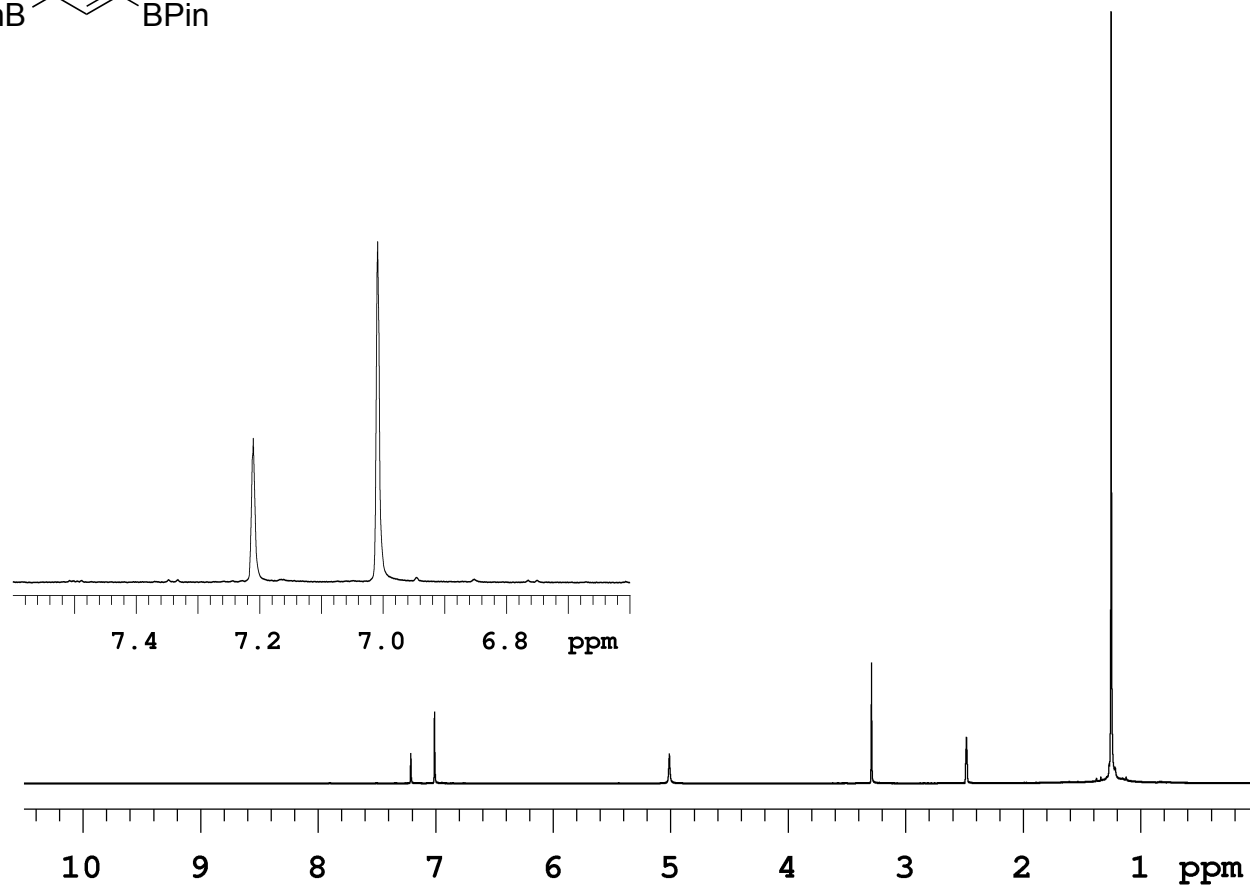
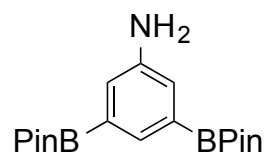


Figure 5.22.  $^{13}\text{C}$  NMR (125 MHz, DMSO- $\text{d}_6$ ) (10)

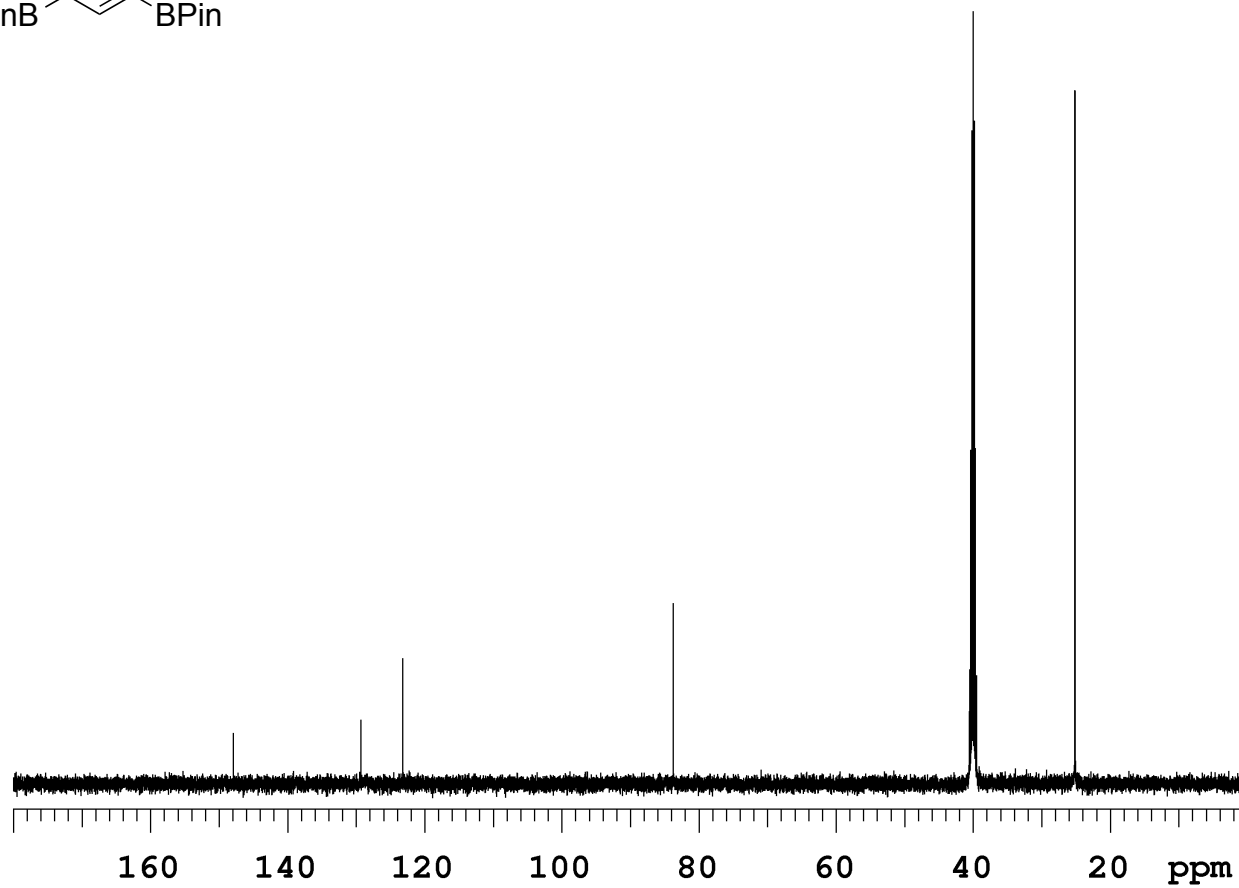
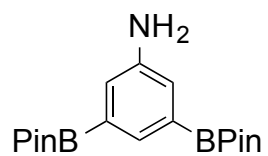


Figure 5.23.  $^1\text{H}$  NMR (500 MHz,  $\text{CDCl}_3$ ) (11)

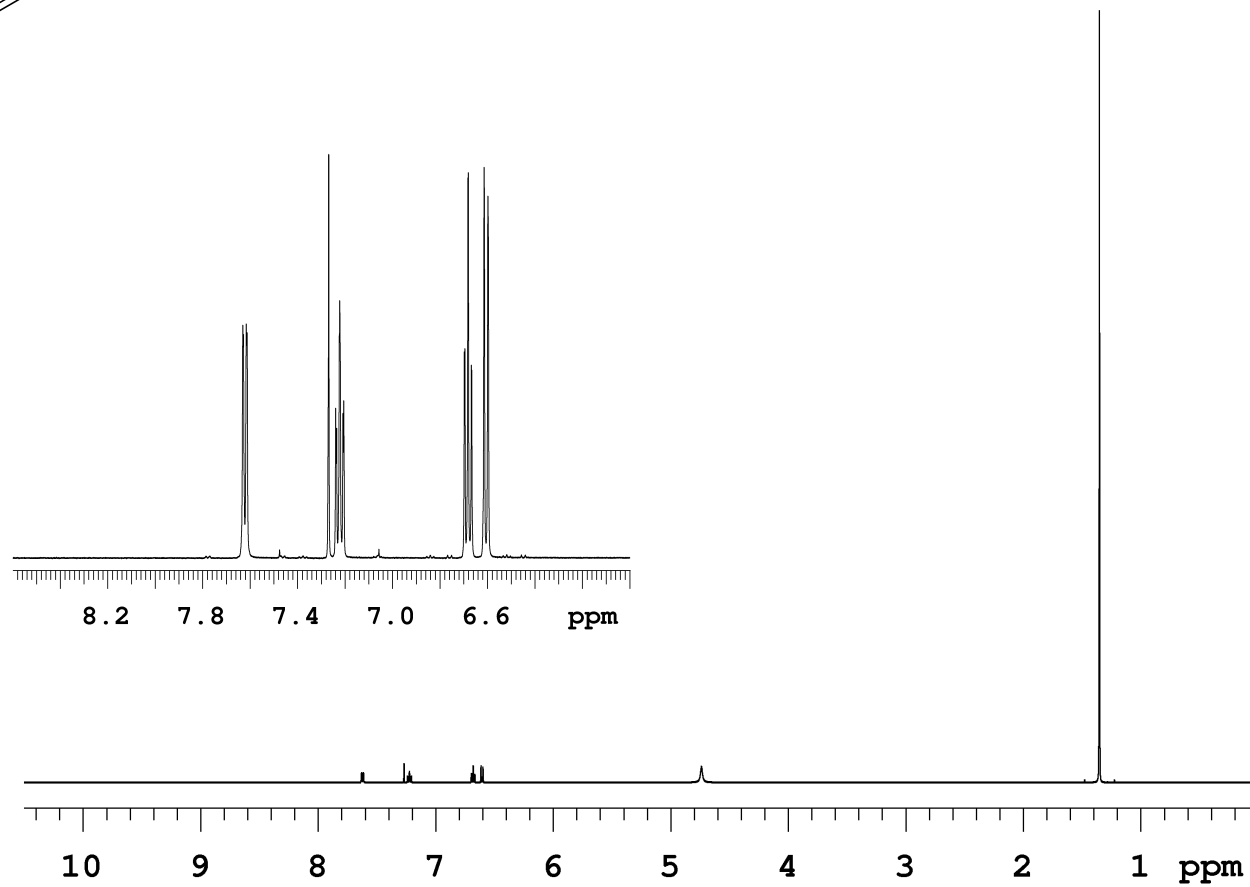
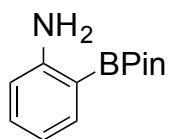


Figure 5.24.  $^{13}\text{C}$  NMR (125 MHz,  $\text{CDCl}_3$ ) (11)

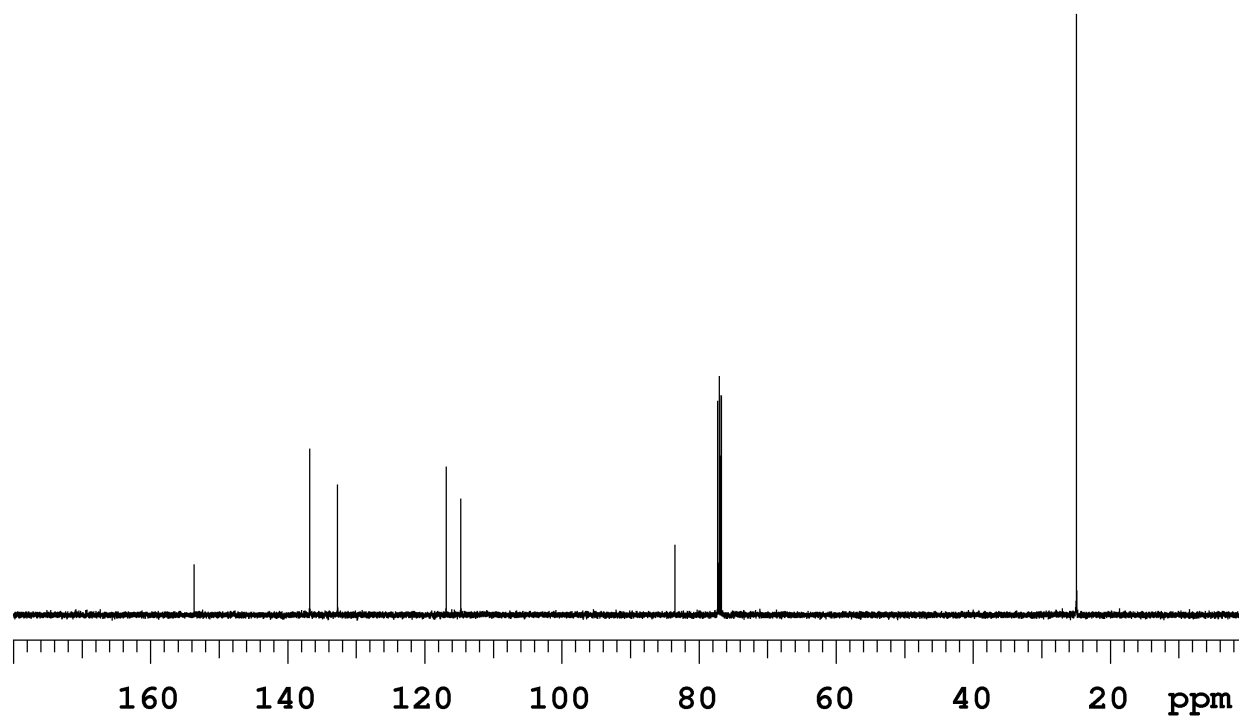
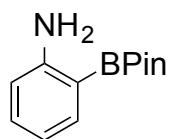


Figure 5.25.  $^1\text{H}$  NMR (500 MHz, DMSO- $\text{d}_6$ ) (12)

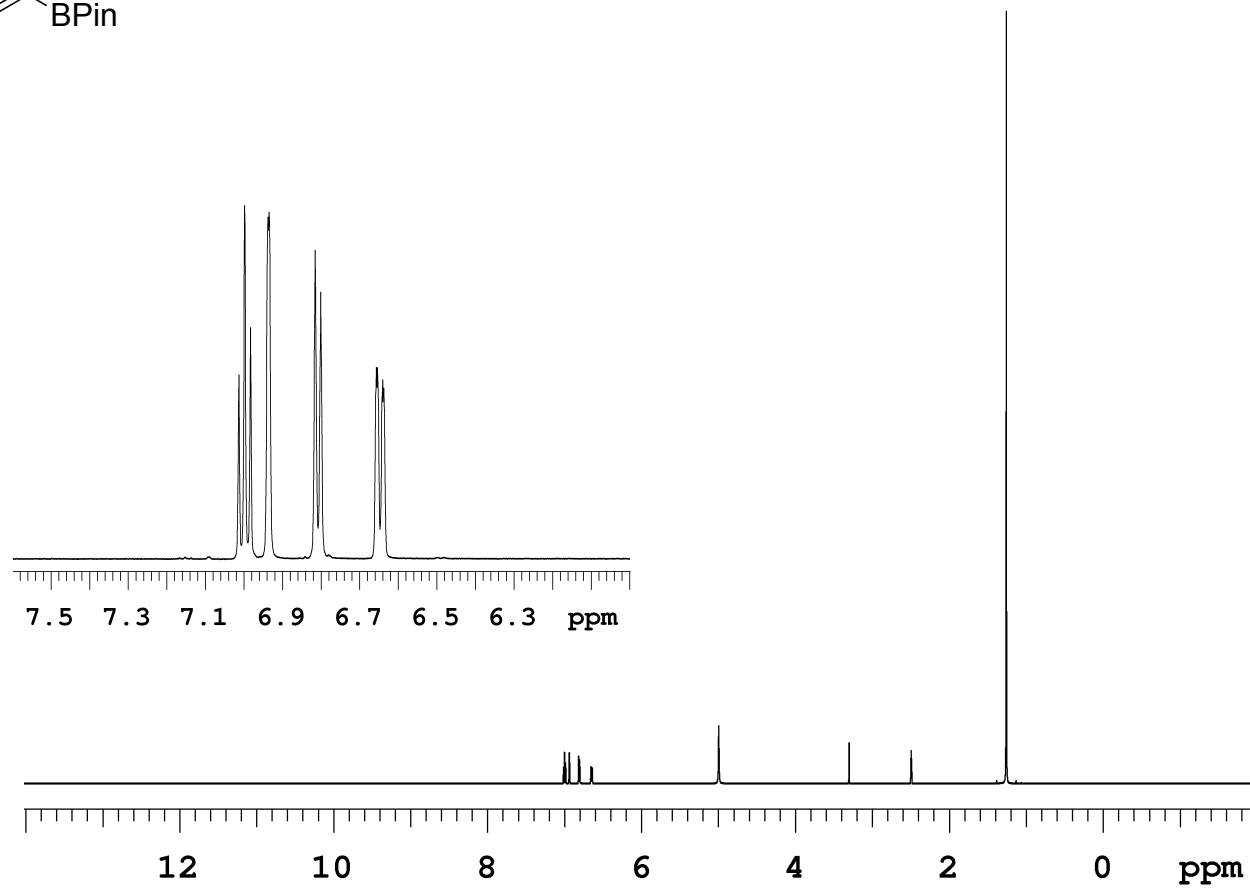
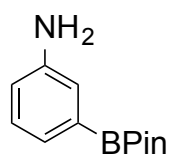


Figure 5.26.  $^{13}\text{C}$  NMR (125 MHz,  $\text{CDCl}_3$ ) (12)

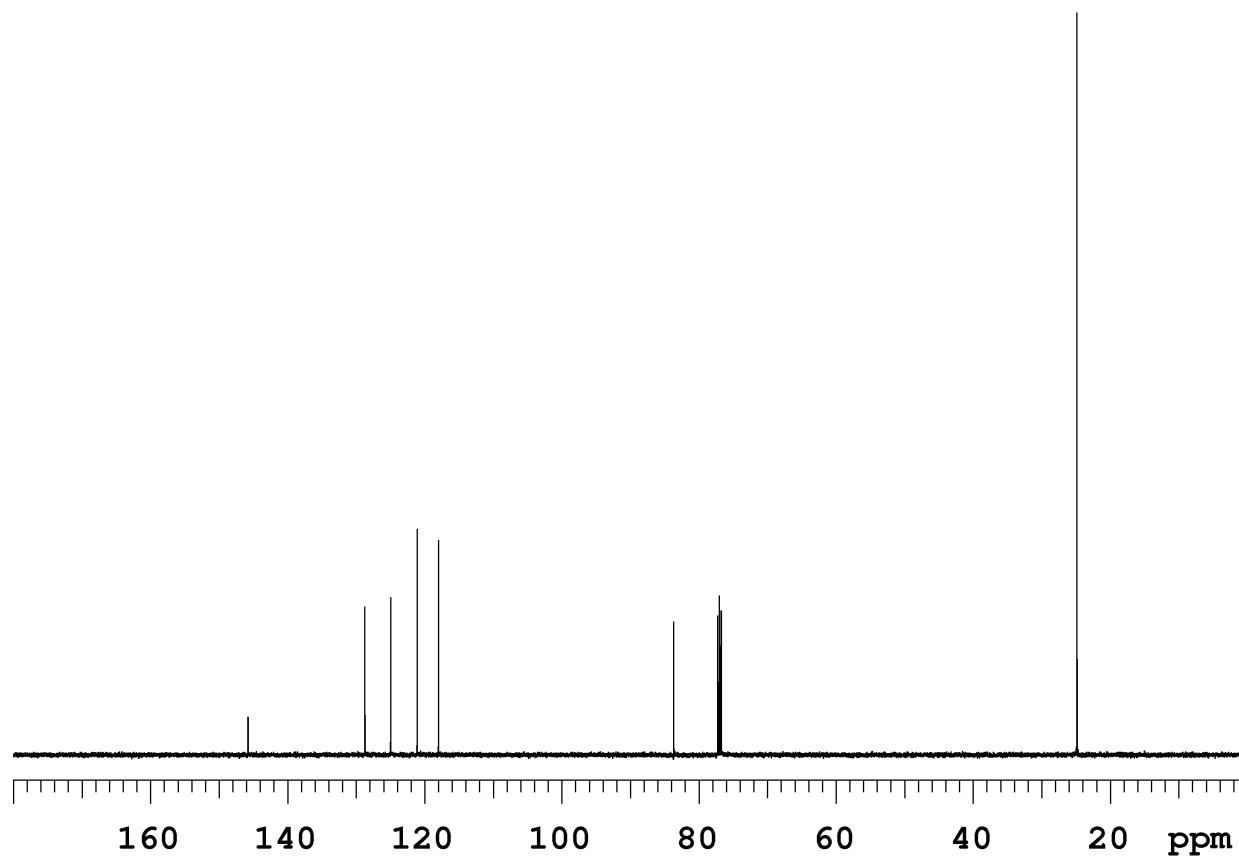
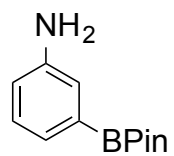


Figure 5.27.  $^1\text{H}$  NMR (500 MHz,  $\text{CDCl}_3$ ) (13)

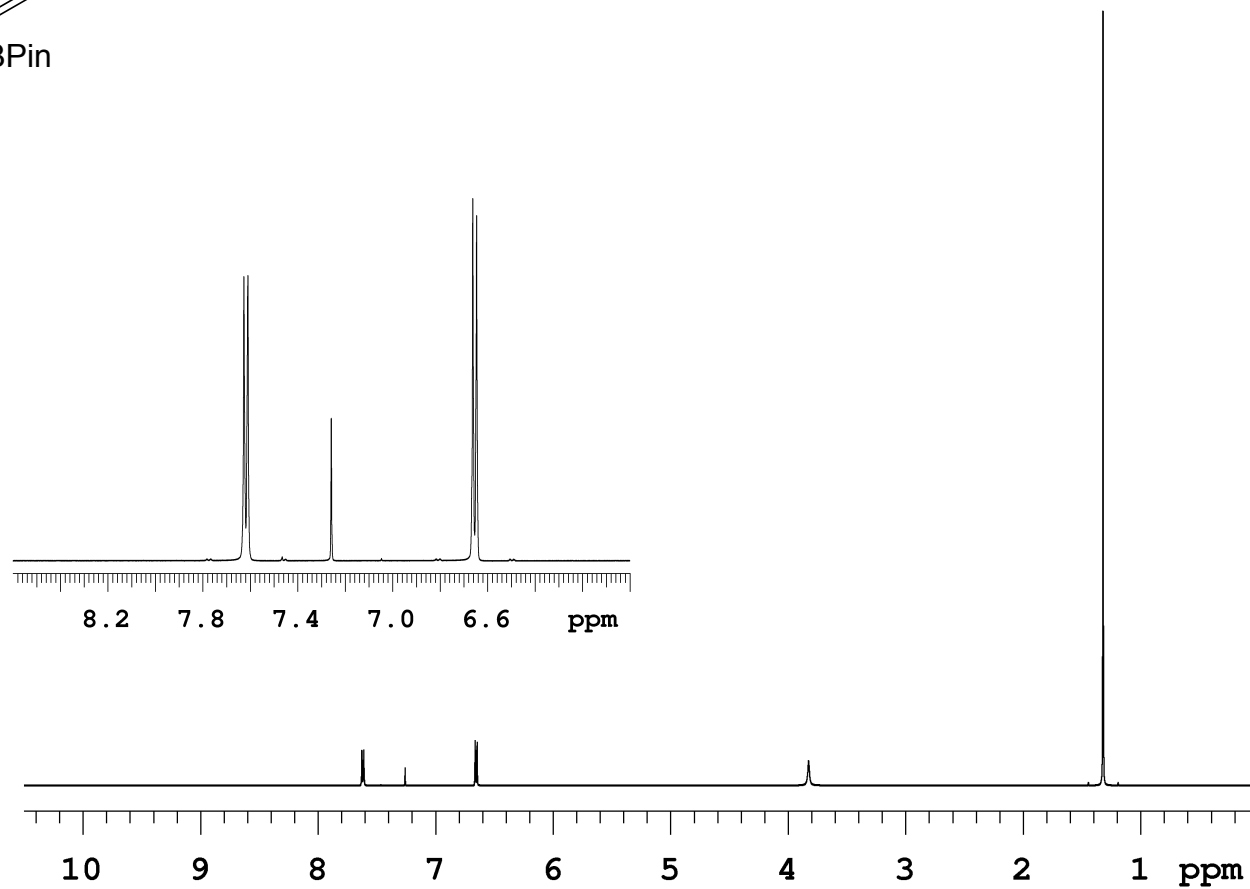
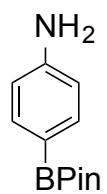




Figure 5.28.  $^{13}\text{C}$  NMR (125 MHz,  $\text{CDCl}_3$ ) (13)

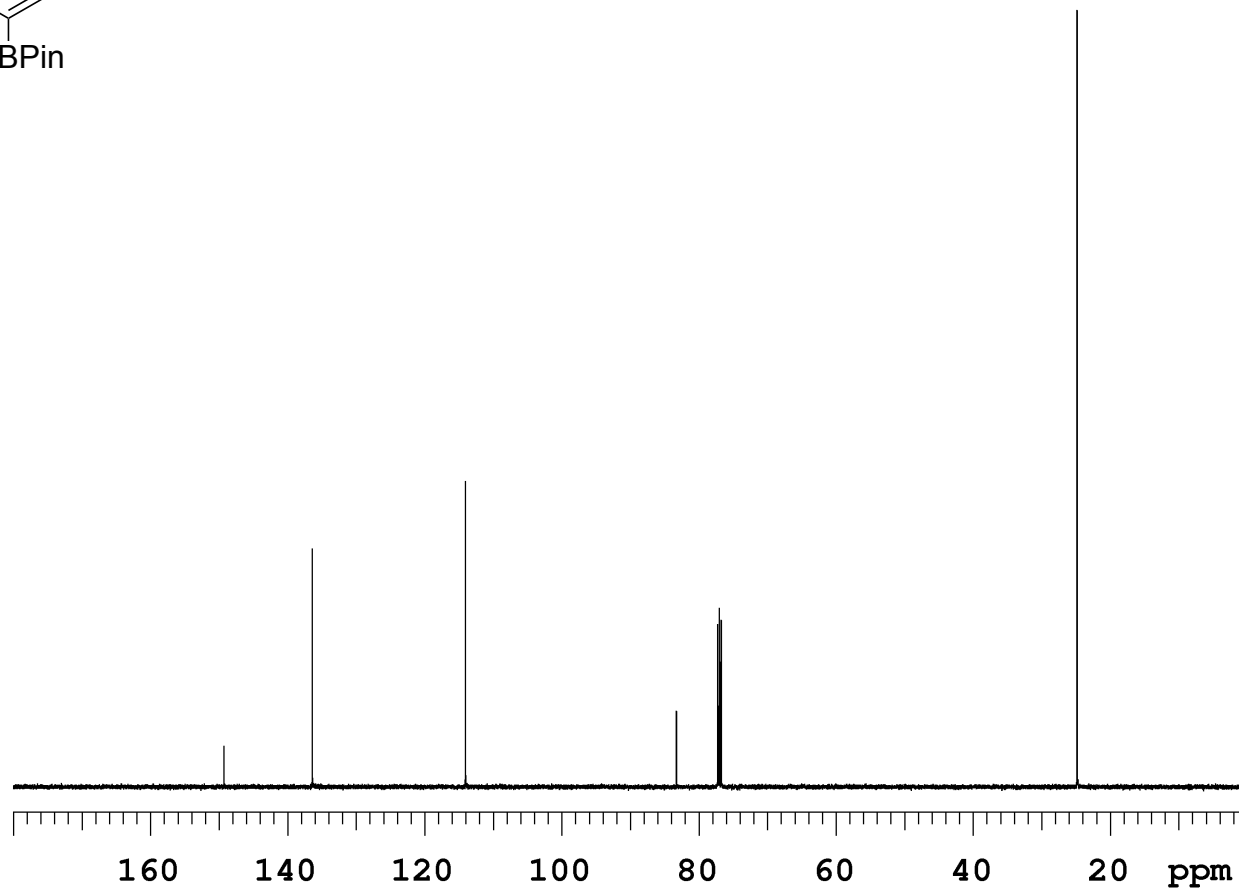
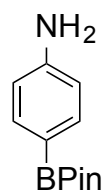


Figure 5.29.  $^1\text{H}$  NMR (500 MHz,  $\text{CDCl}_3$ ) (14)

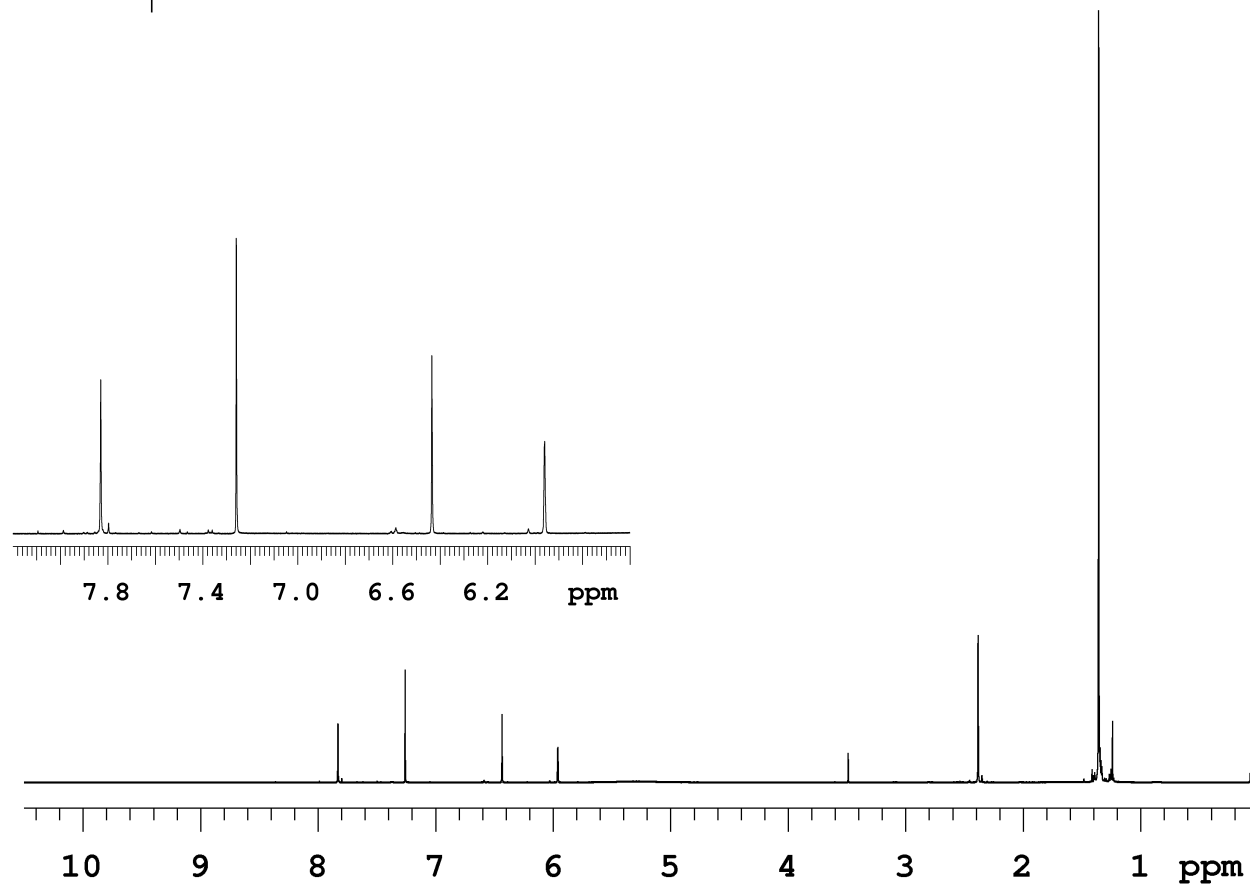
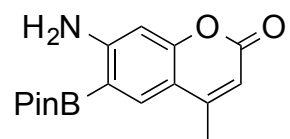


Figure 5.30.  $^{13}\text{C}$  NMR (125 MHz,  $\text{CDCl}_3$ ) (14)

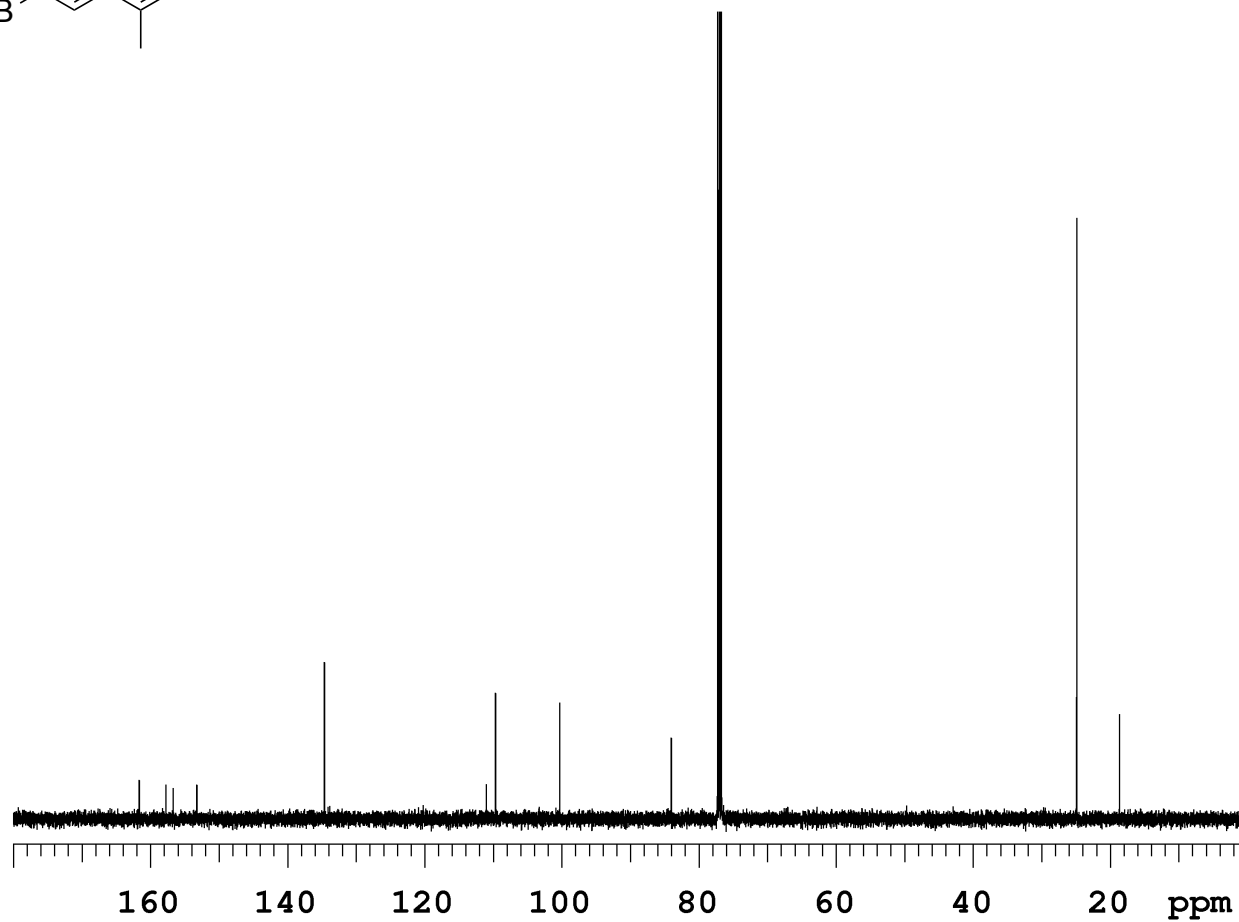
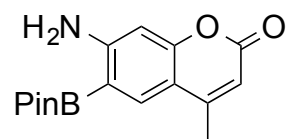


Figure 5.31.  $^1\text{H}$  NMR (500 MHz,  $\text{CDCl}_3$ ) (15)

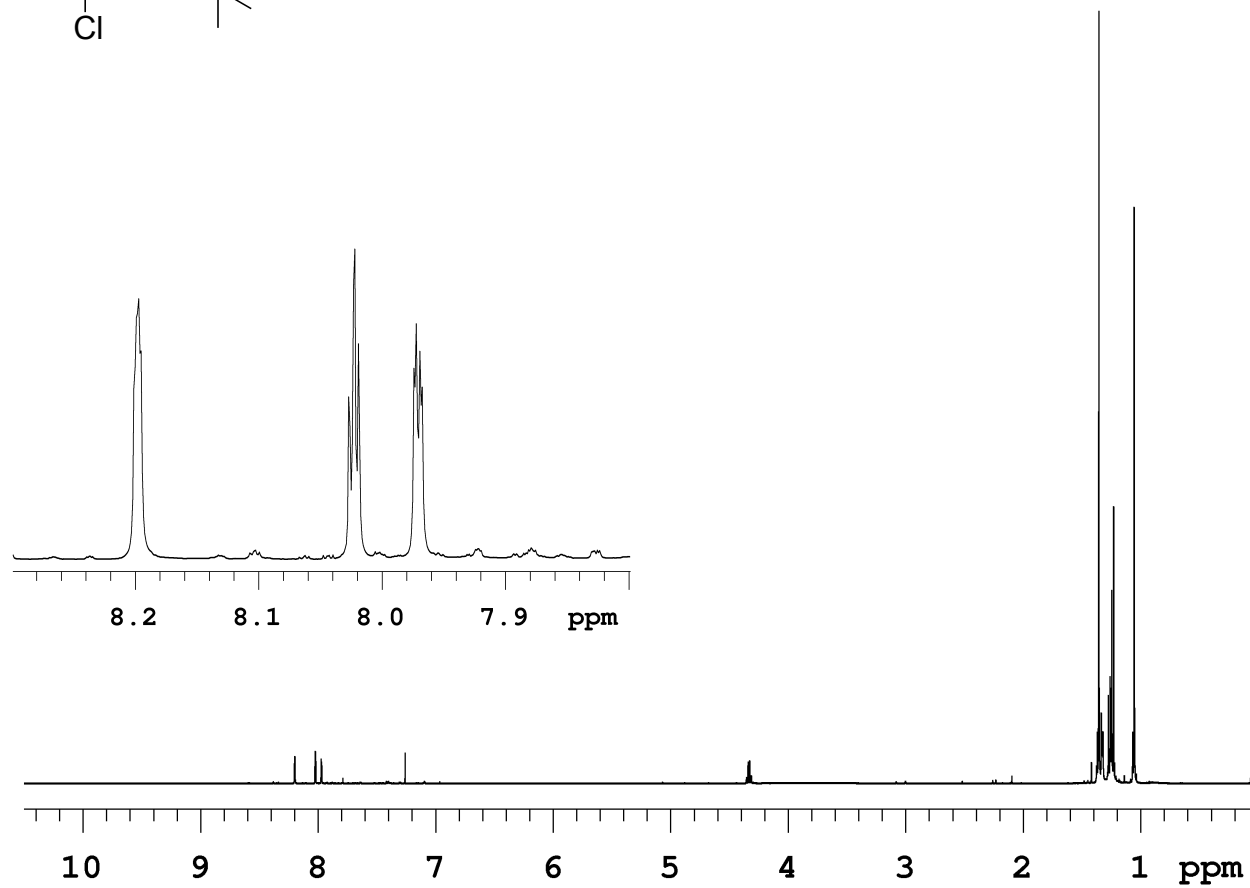
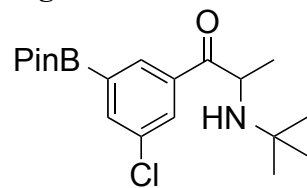


Figure 5.32.  $^{13}\text{C}$  NMR (125 MHz,  $\text{CDCl}_3$ ) (15)

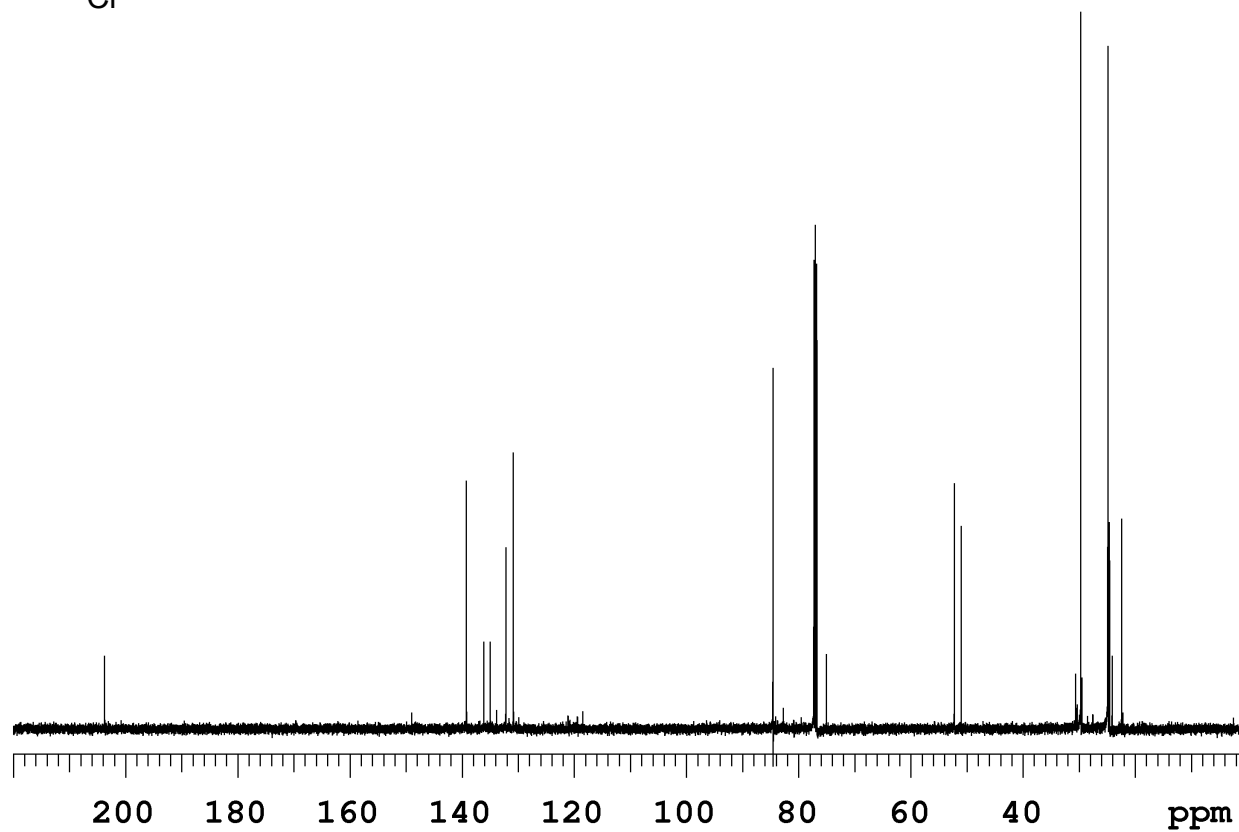
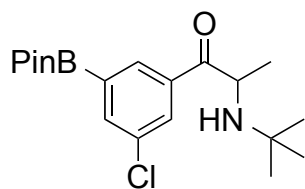


Figure 5.33.  $^1\text{H}$  NMR (500 MHz,  $\text{CDCl}_3$ ) (16)

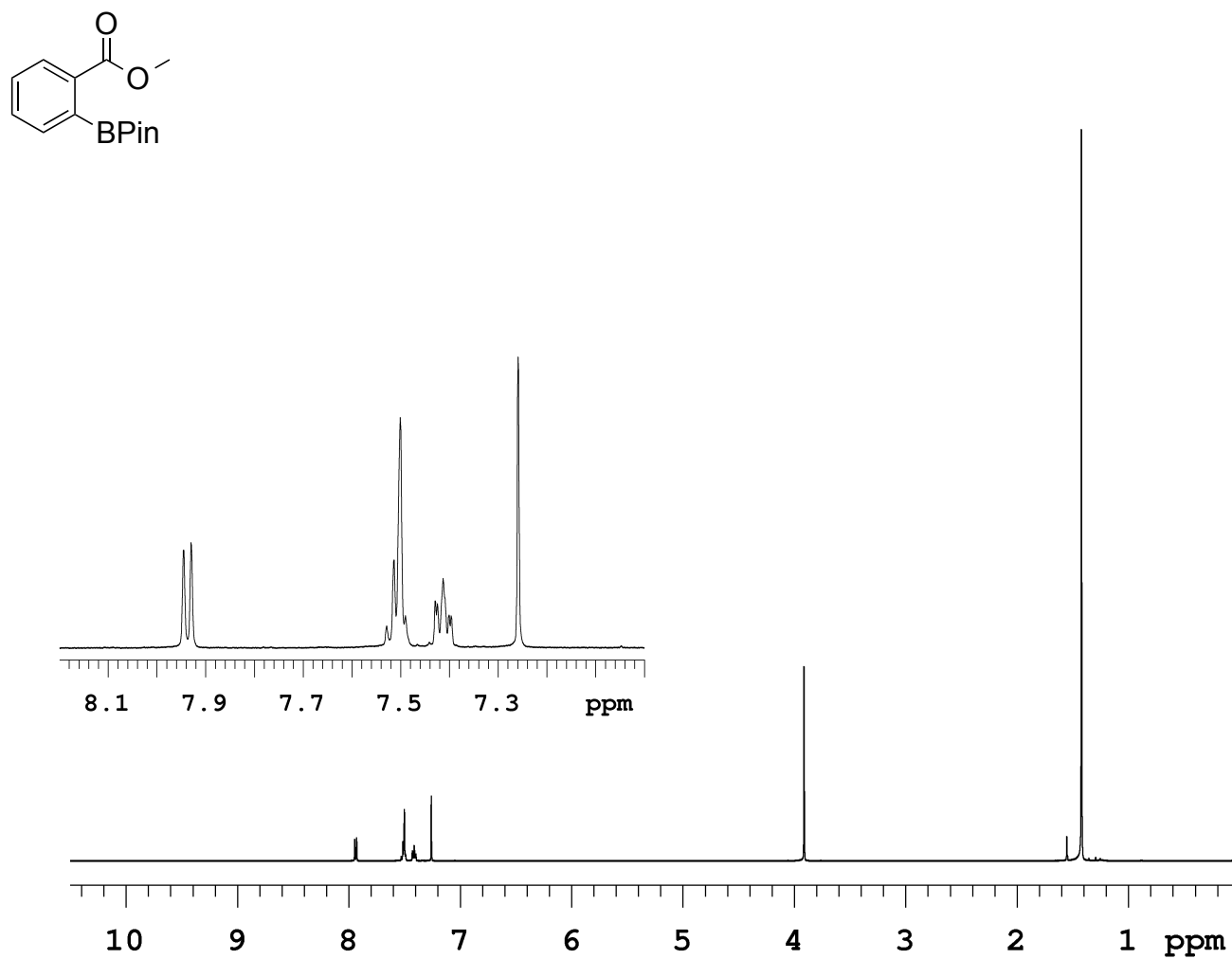


Figure 5.34.  $^{13}\text{C}$  NMR (125 MHz,  $\text{CDCl}_3$ ) (16)

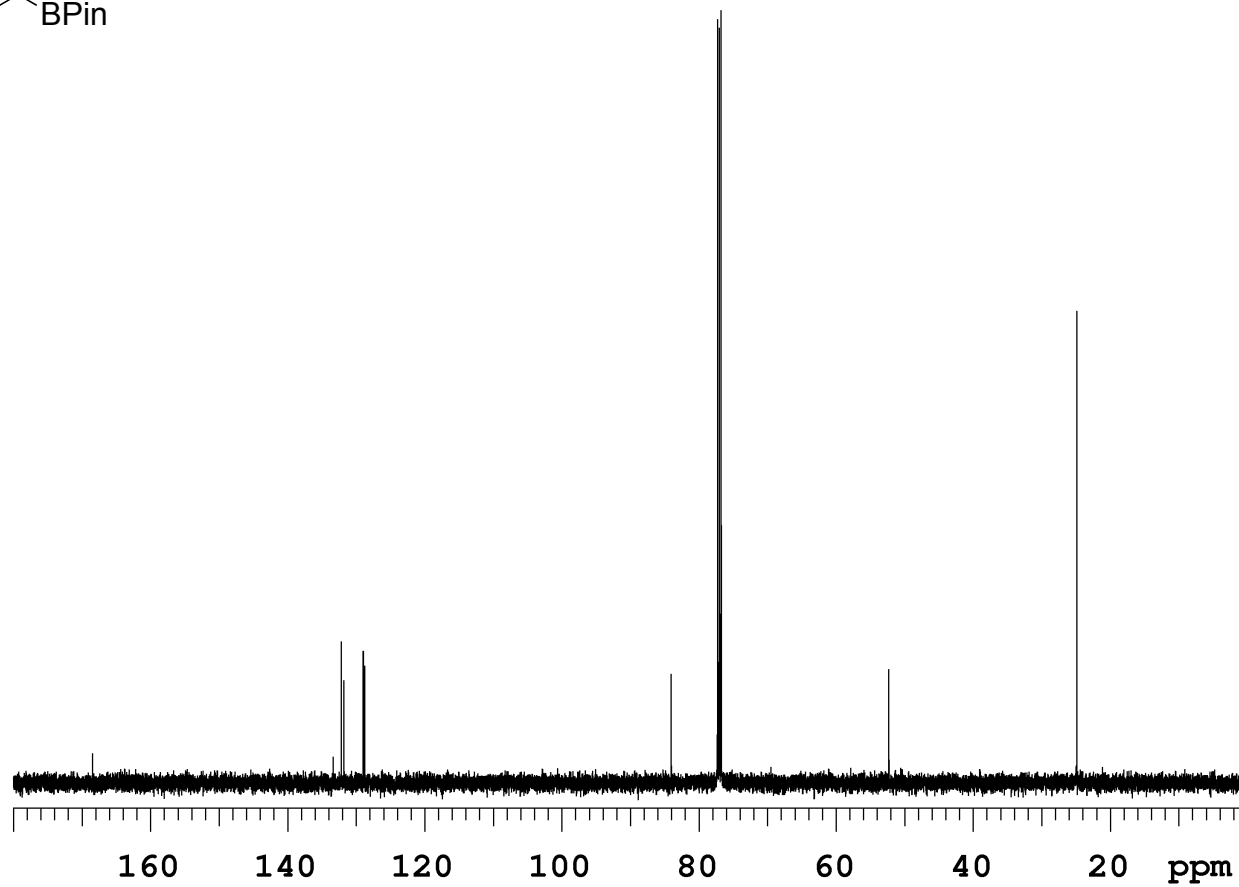
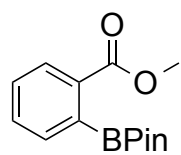


Figure 5.34.  $^1\text{H}$  NMR (500 MHz,  $\text{CDCl}_3$ ) (17)

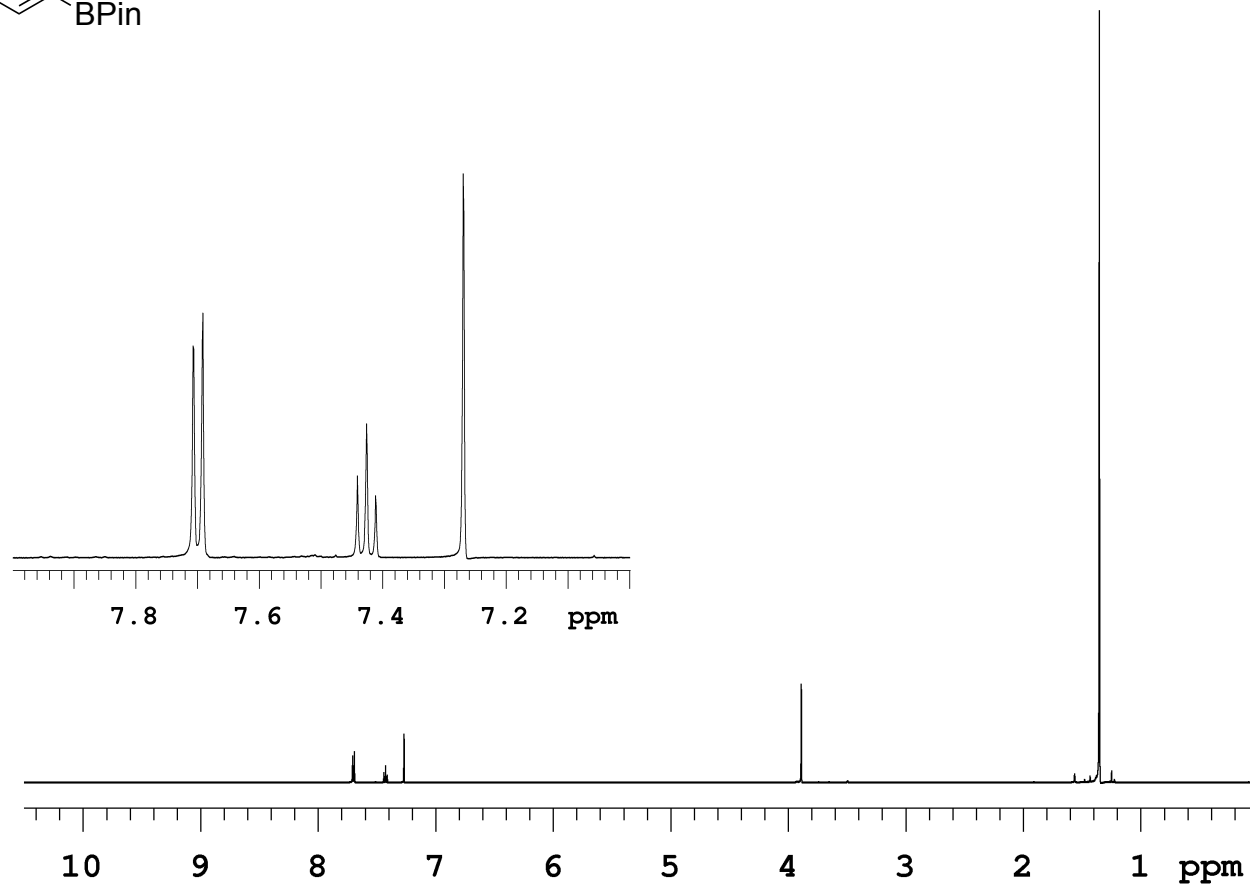
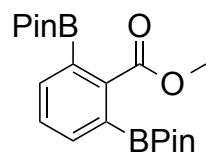




Figure 5.35.  $^{13}\text{C}$  NMR (125 MHz,  $\text{CDCl}_3$ ) (17)

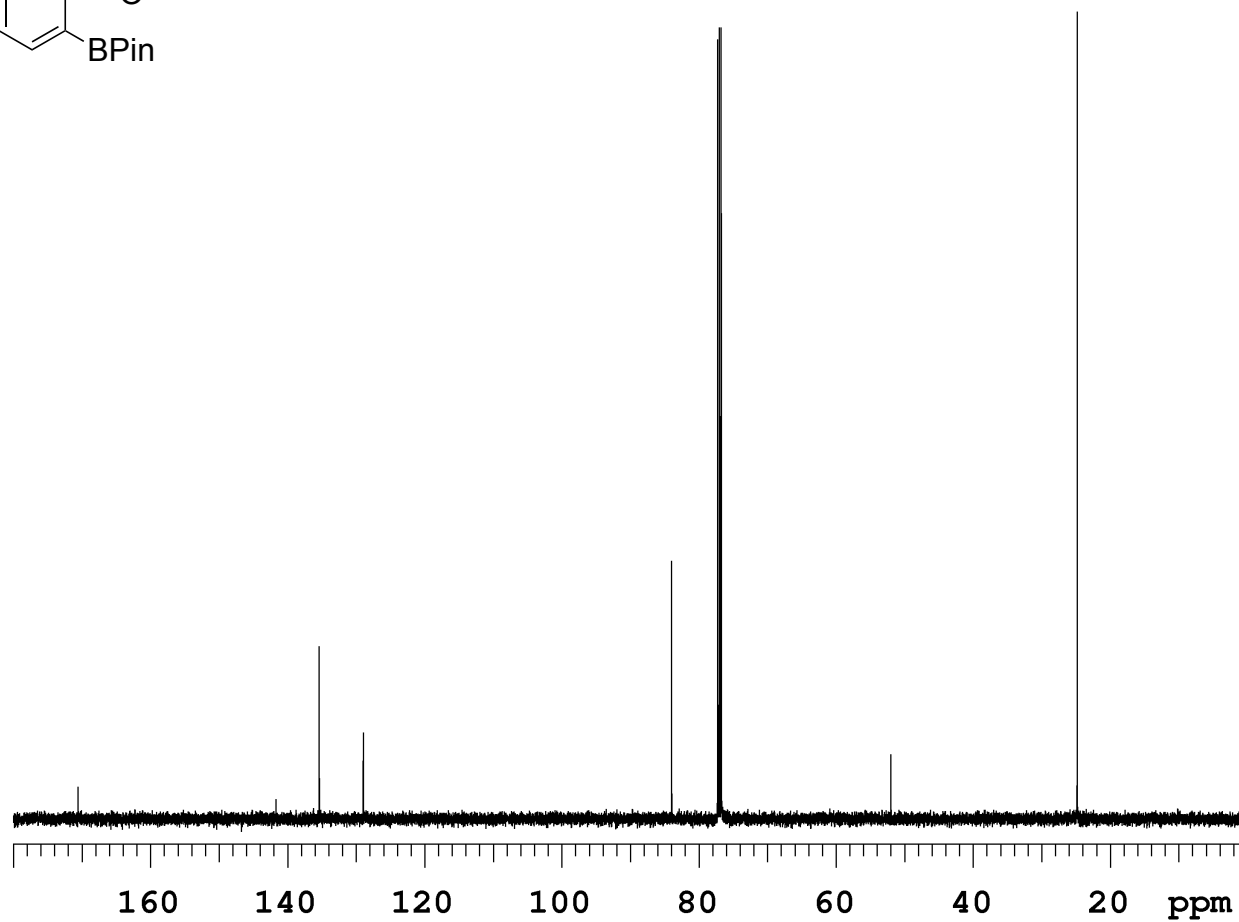
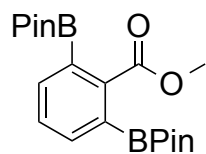


Figure 5.36.  $^1\text{H}$  NMR (500 MHz,  $\text{CDCl}_3$ ) (18)

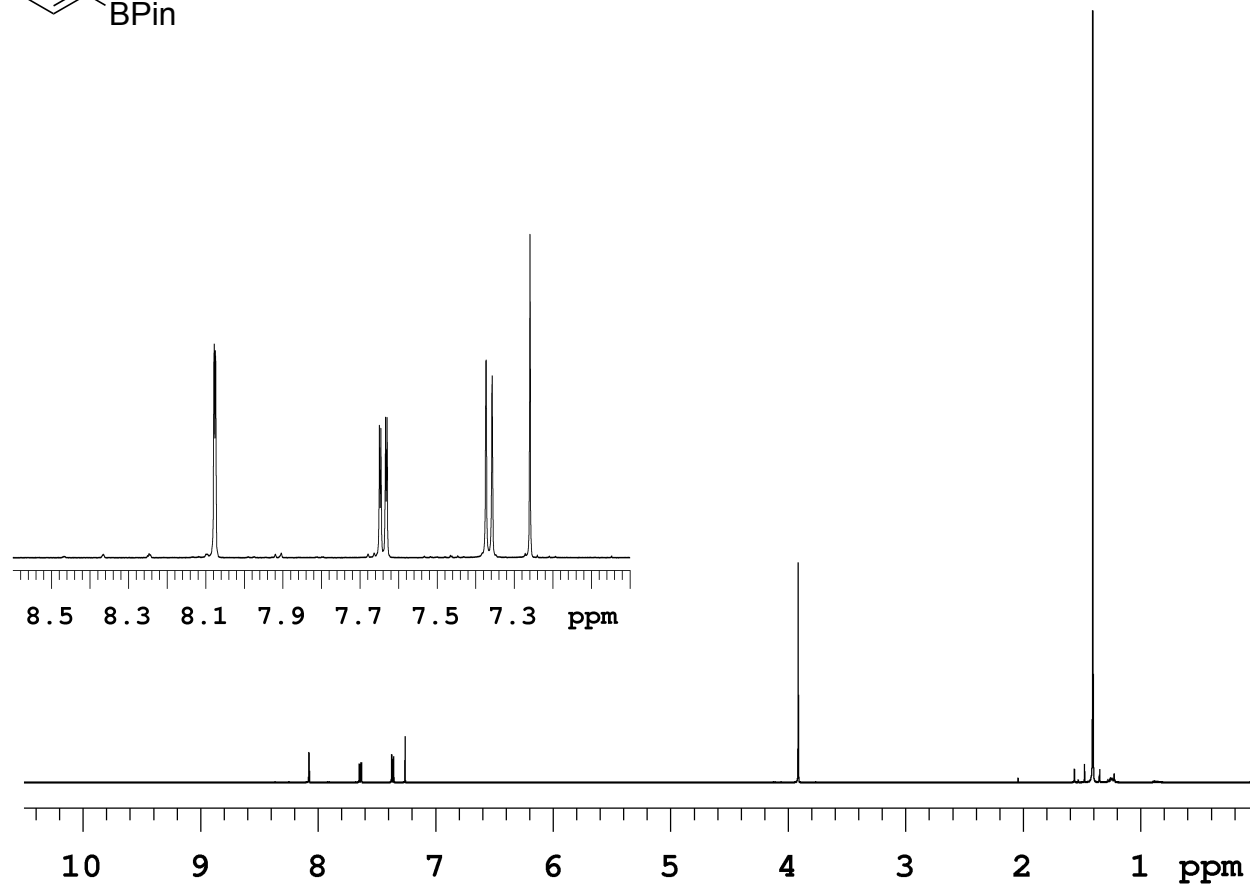
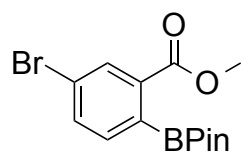


Figure 5.37.  $^{13}\text{C}$  NMR (125 MHz,  $\text{CDCl}_3$ ) (18)

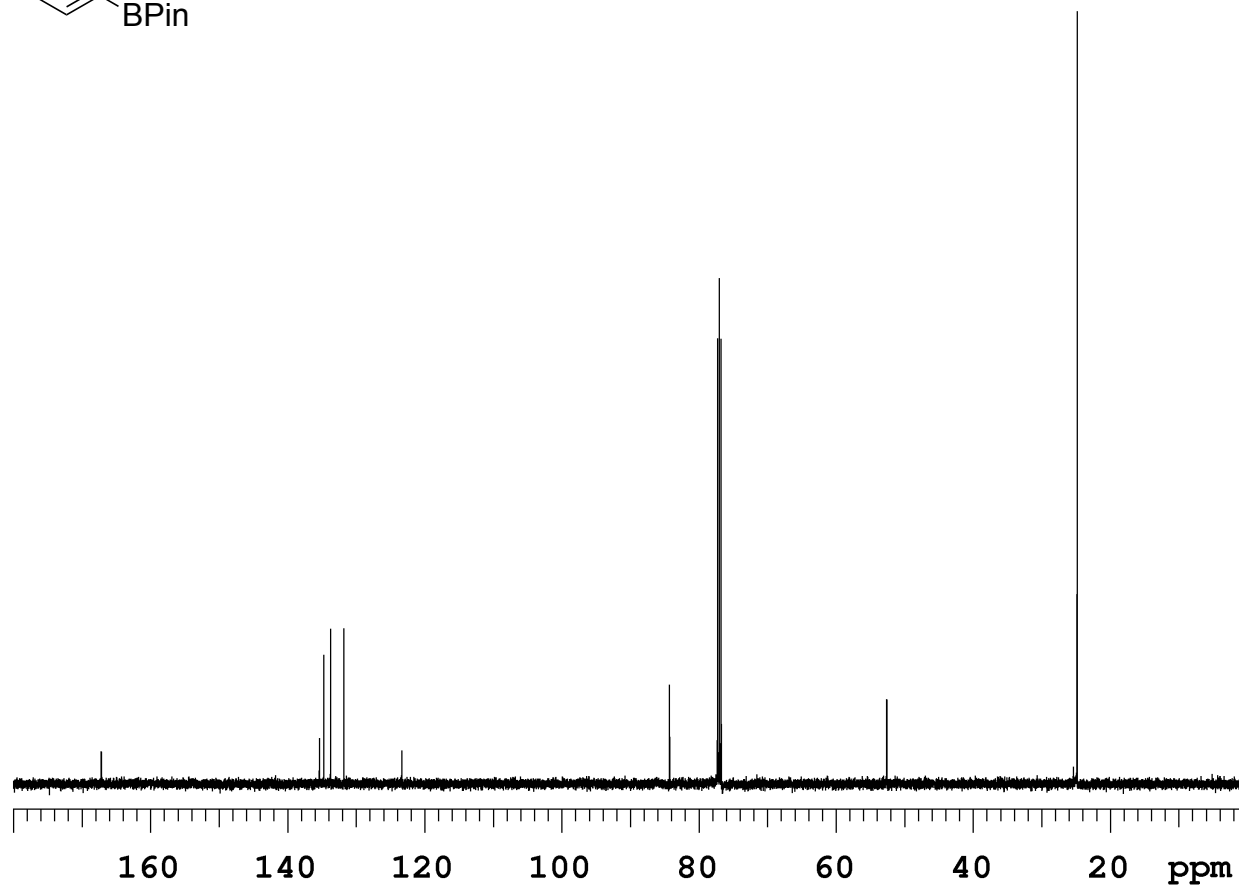
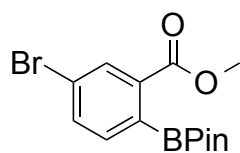


Figure 5.38.  $^1\text{H}$  NMR (500 MHz,  $\text{CDCl}_3$ ) (19)

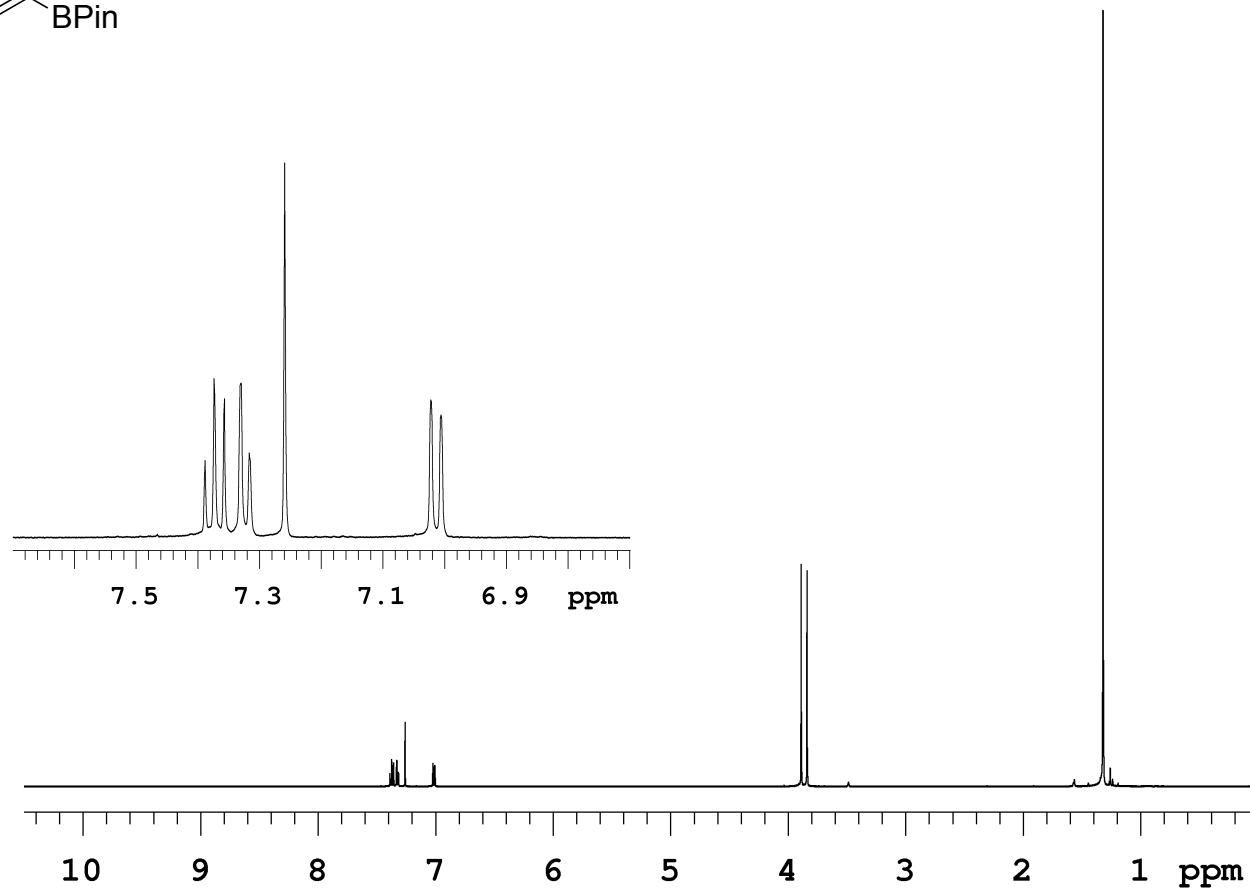
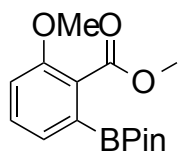


Figure 5.39.  $^{13}\text{C}$  NMR (125 MHz,  $\text{CDCl}_3$ ) (19)

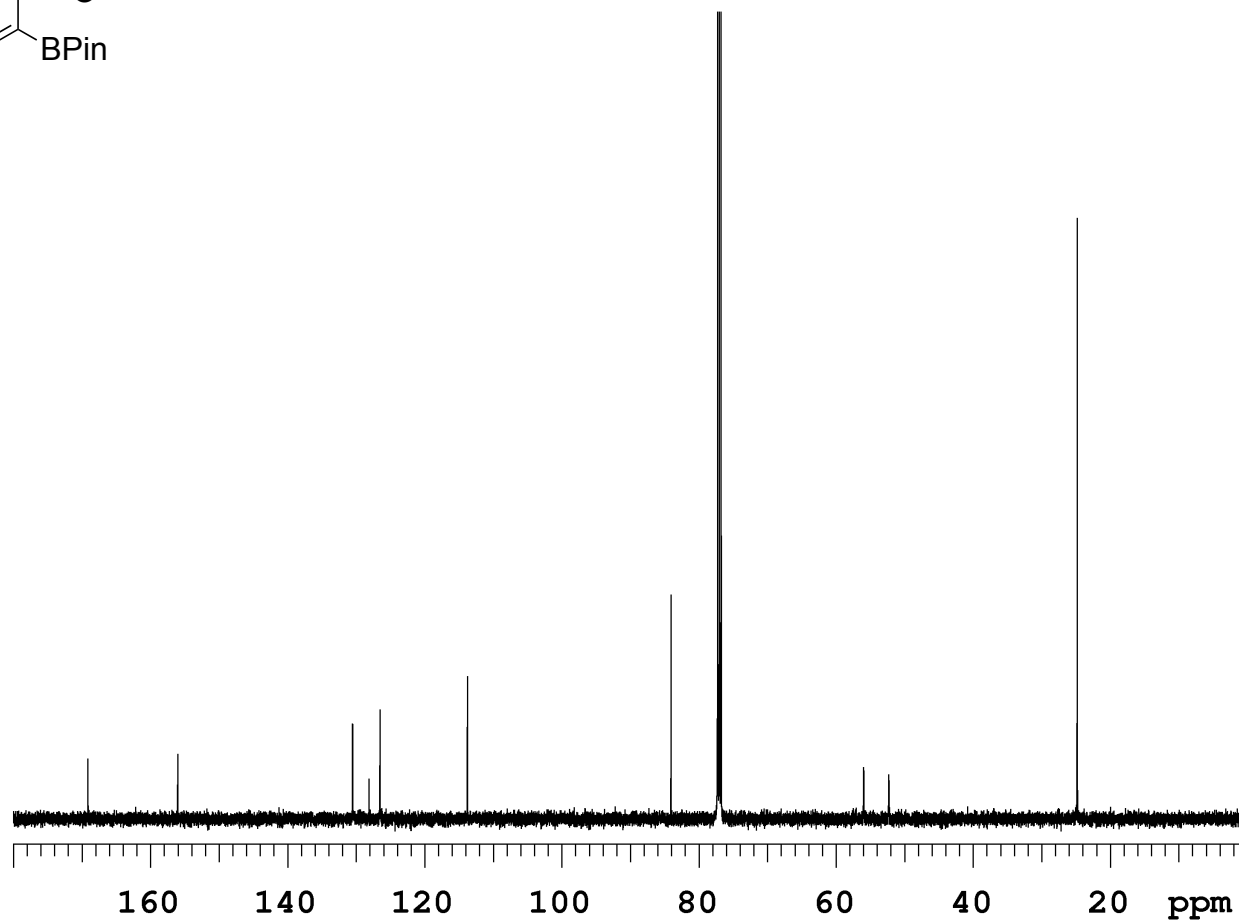
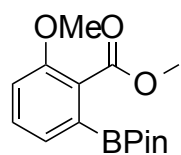


Figure 5.40.  $^1\text{H}$  NMR (500 MHz,  $\text{CDCl}_3$ ) (20a)

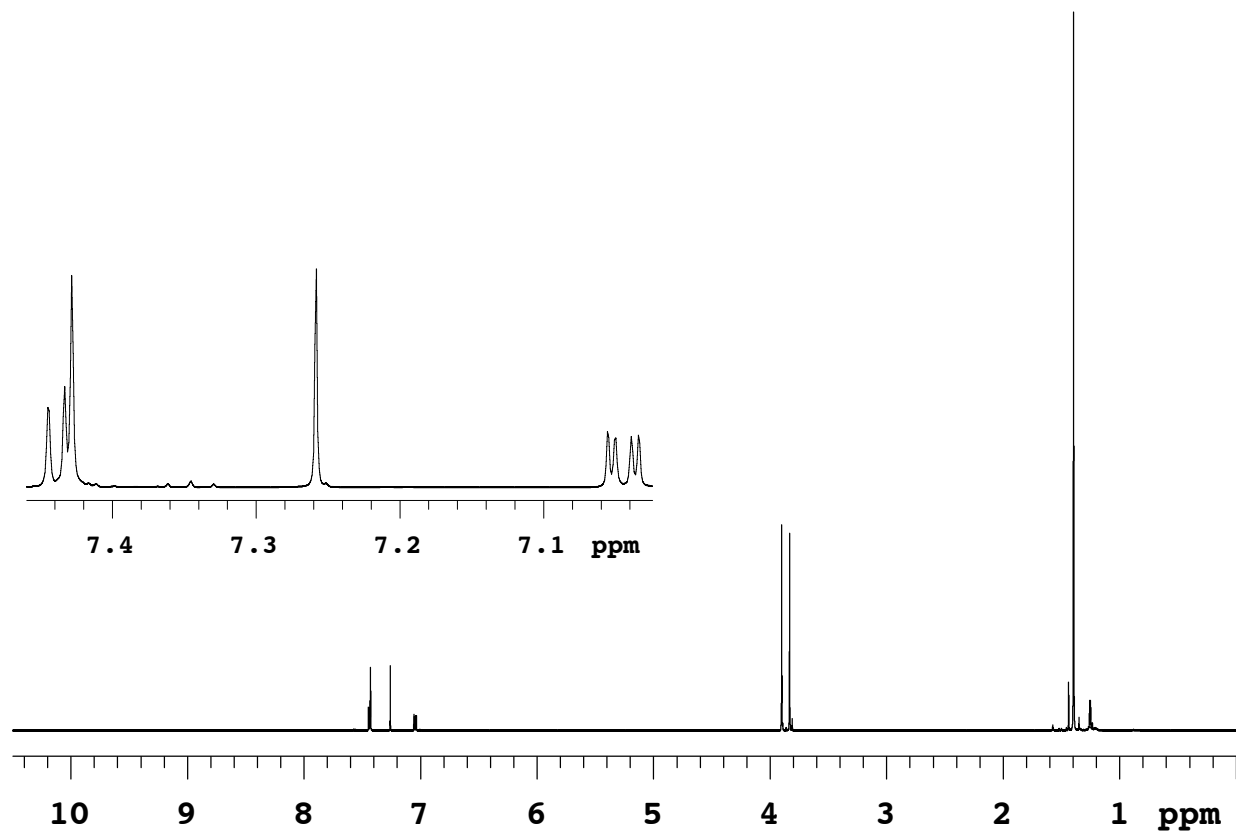
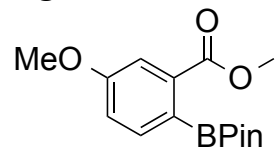


Figure 5.41.  $^{13}\text{C}$  NMR (125 MHz,  $\text{CDCl}_3$ ) (20a)

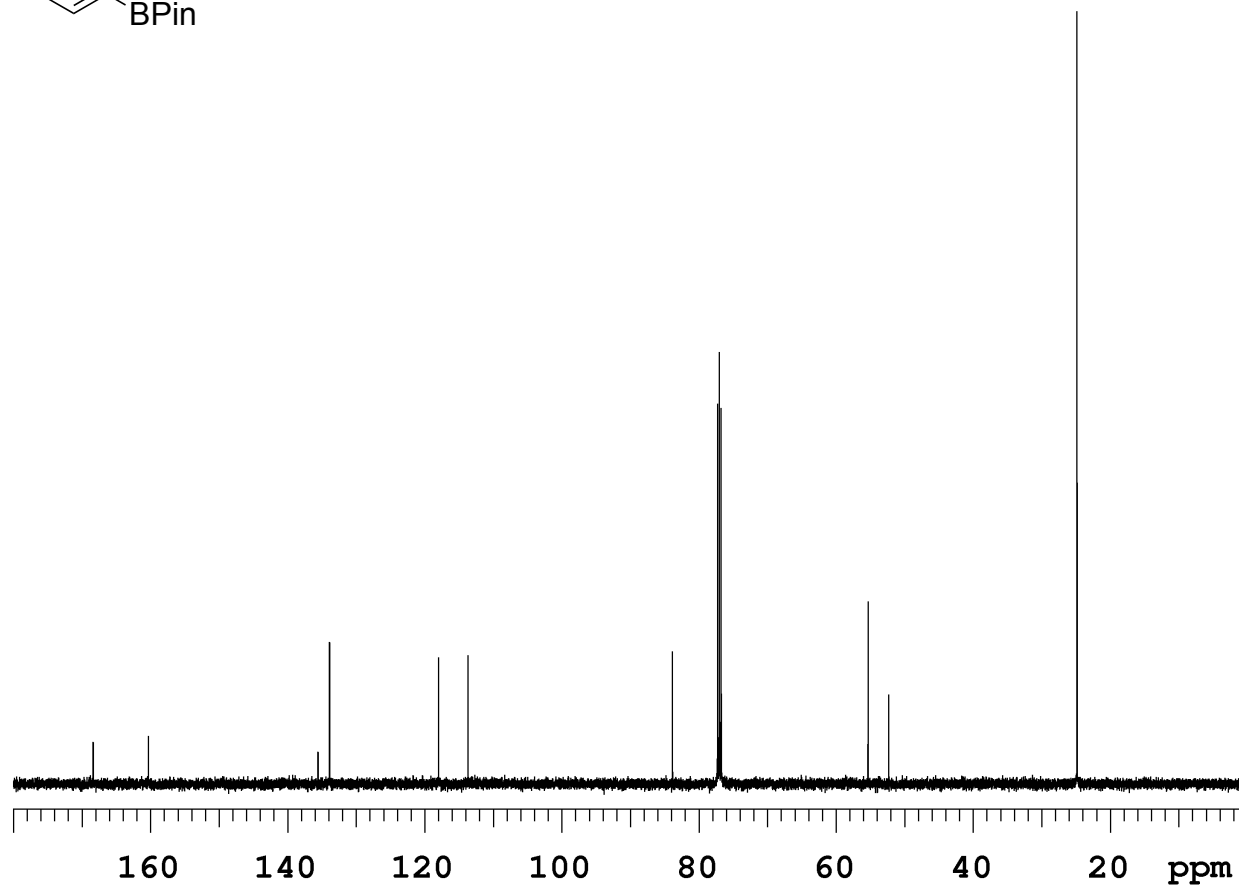
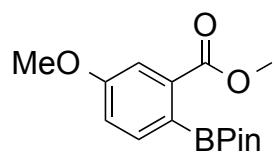


Figure 5.42.  $^1\text{H}$  NMR (500 MHz,  $\text{CDCl}_3$ ) (20b)

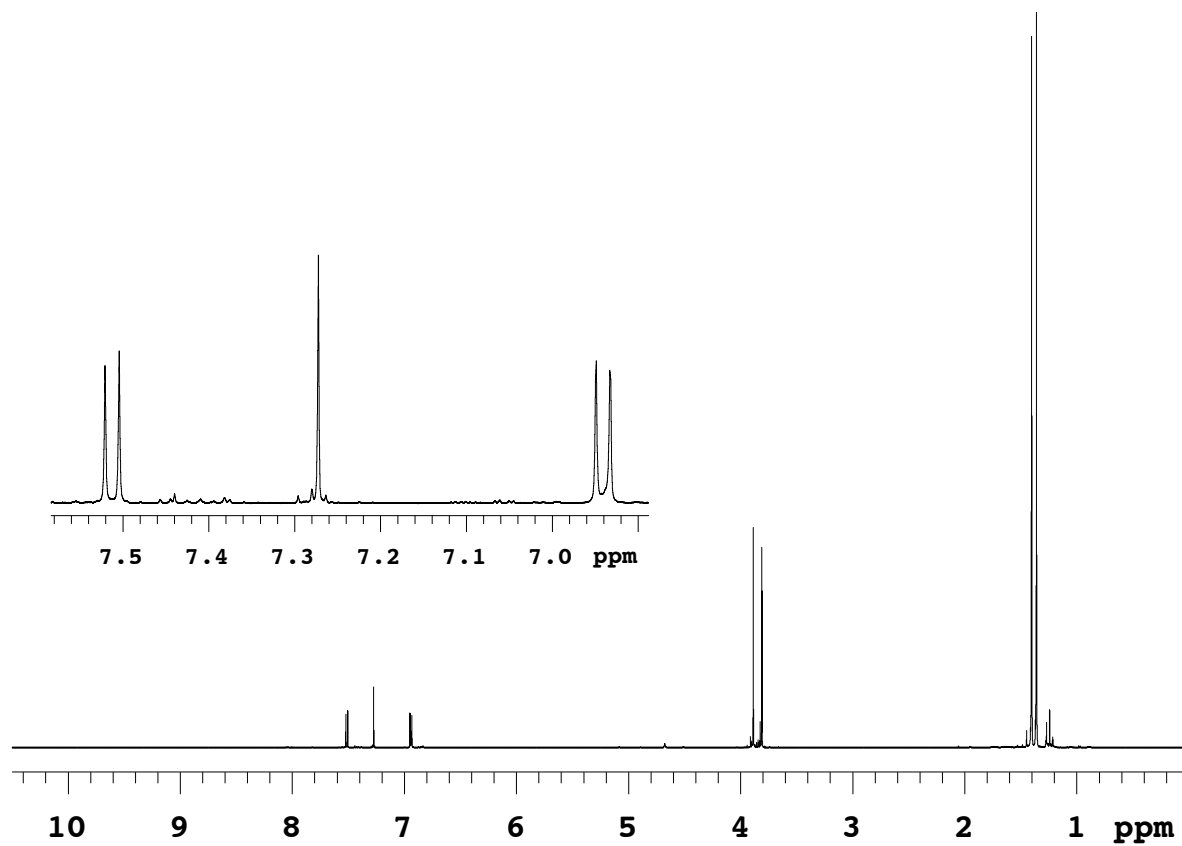
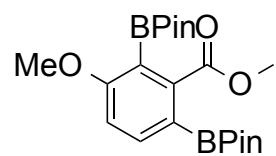




Figure 5.43.  $^{13}\text{C}$  NMR (125 MHz,  $\text{CDCl}_3$ ) (20b)

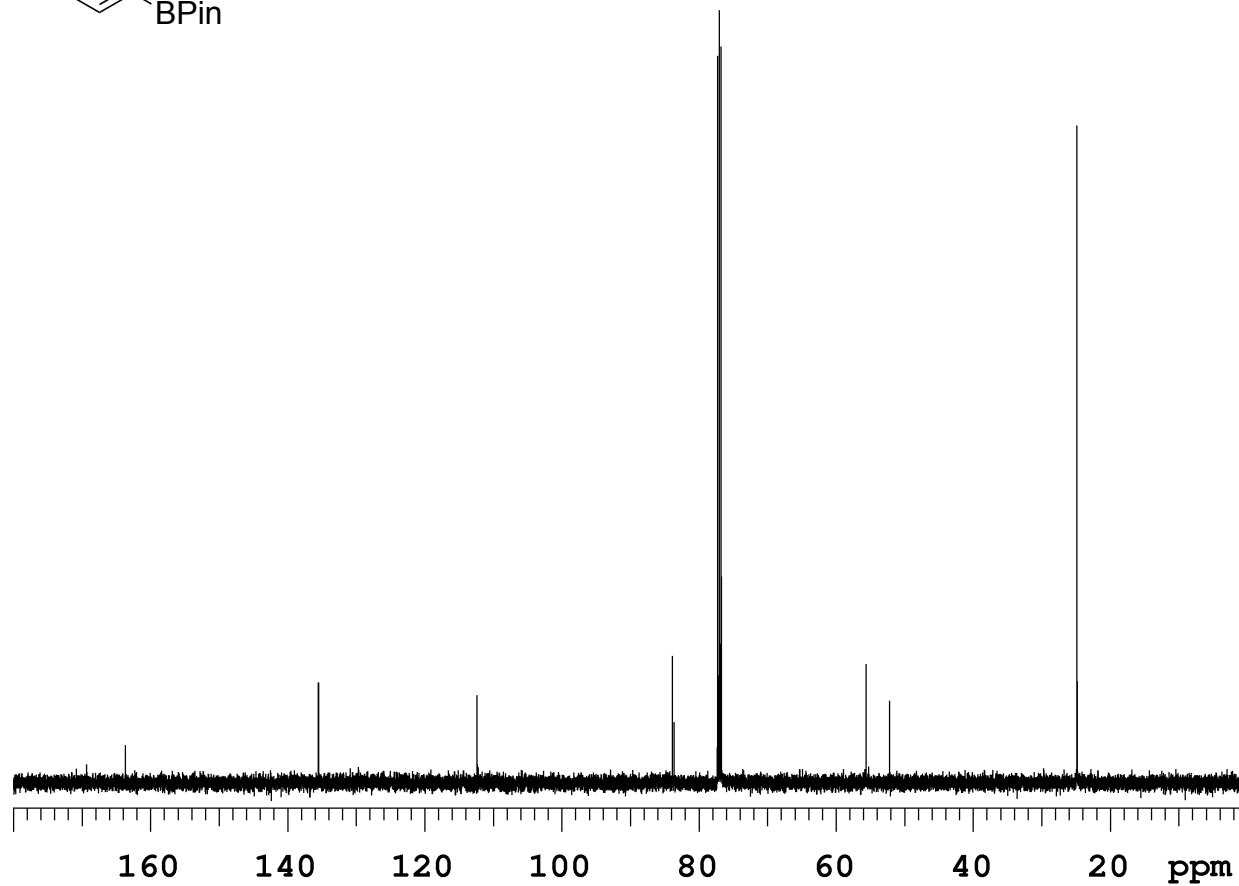
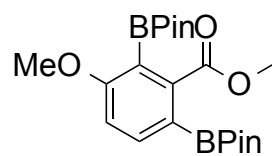


Figure 5.44.  $^1\text{H}$  NMR (500 MHz,  $\text{CDCl}_3$ ) (21)

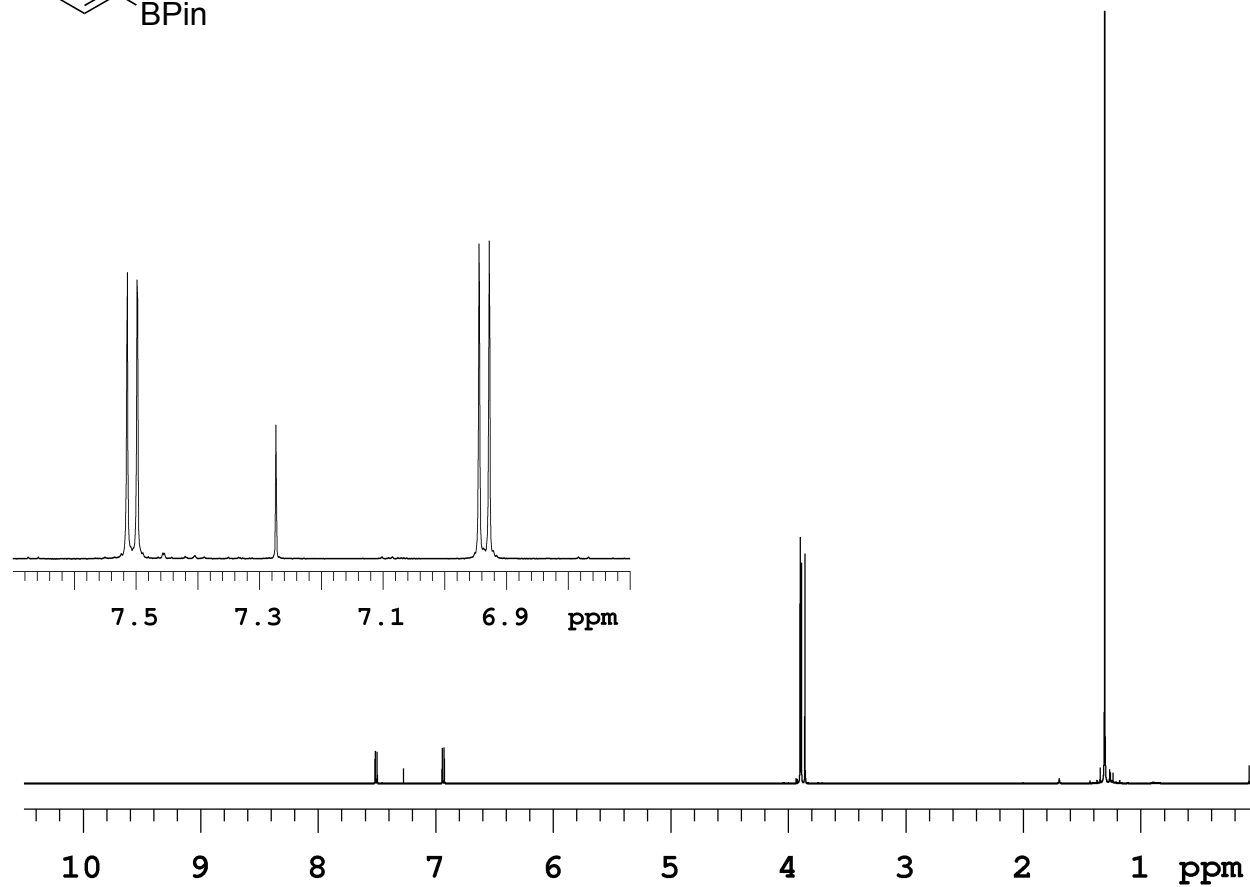
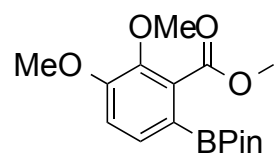


Figure 5.45.  $^{13}\text{C}$  NMR (125 MHz,  $\text{CDCl}_3$ ) (21)

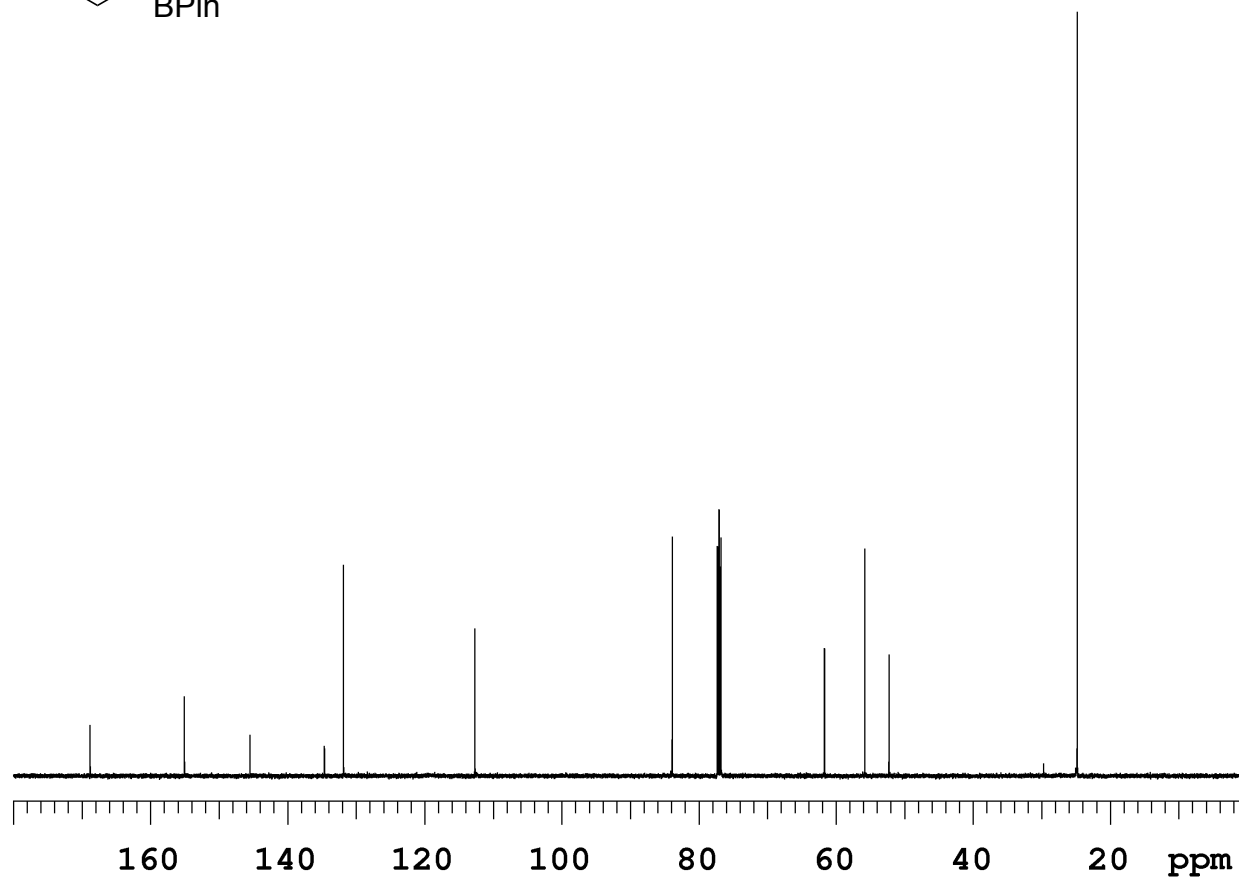
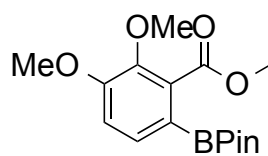
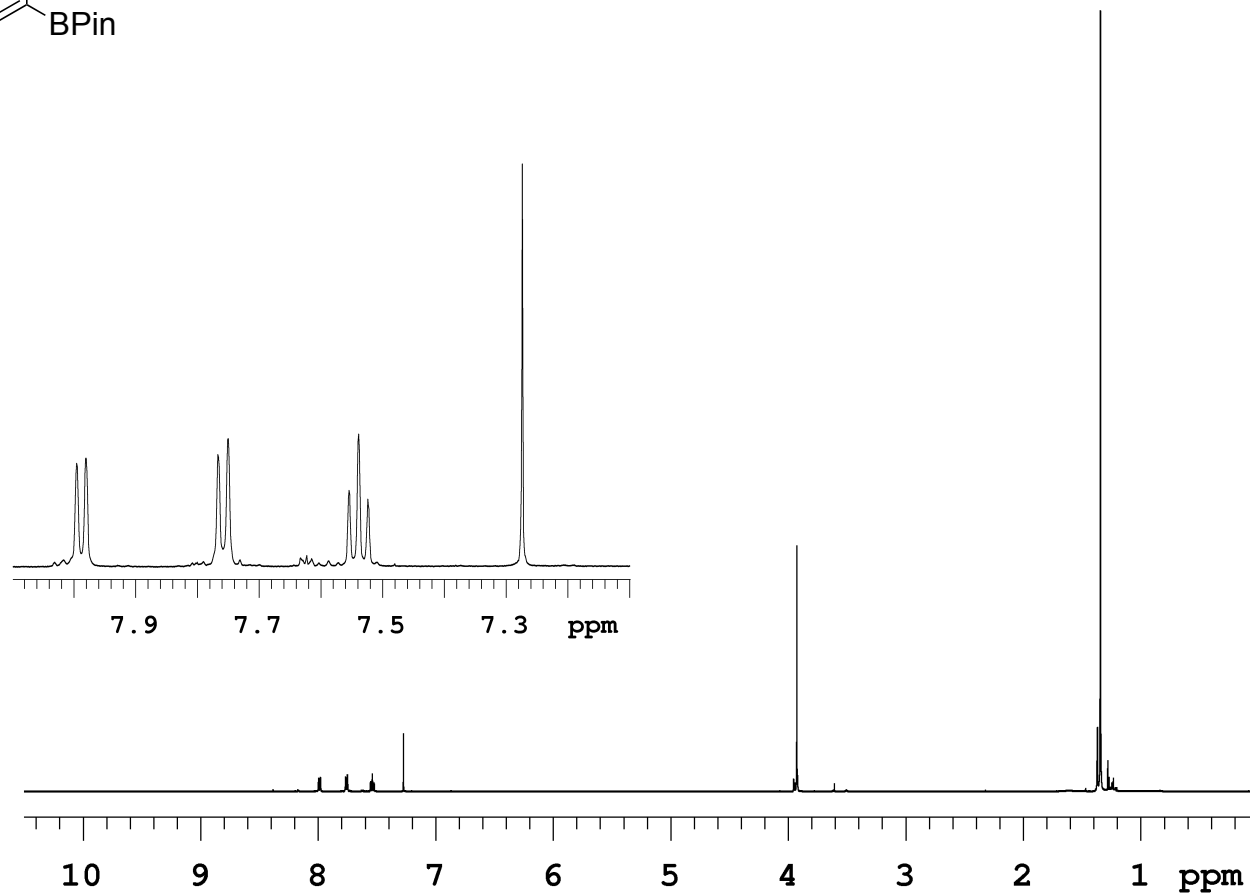
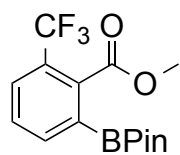


Figure 5.46.  $^1\text{H}$  NMR (500 MHz,  $\text{CDCl}_3$ ) (22)



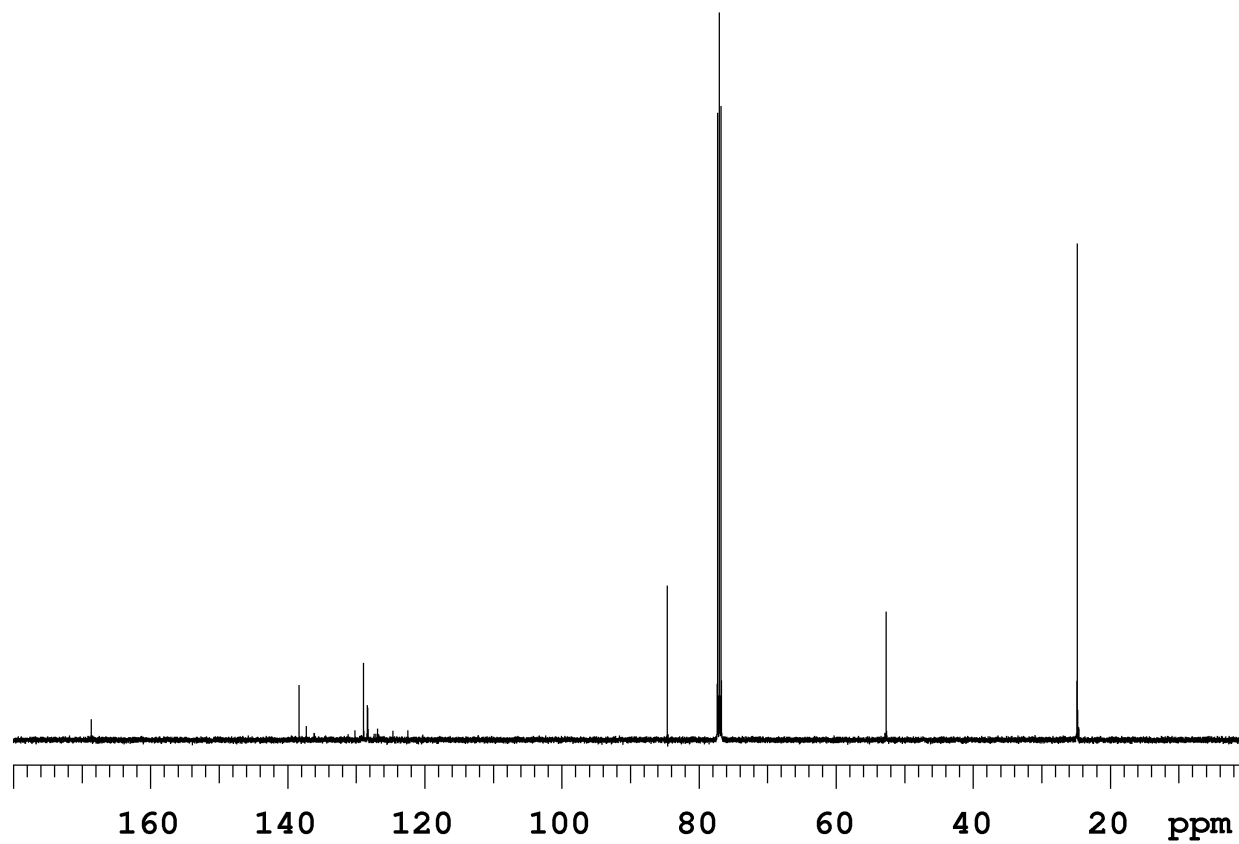



Figure 5.48.  $^1\text{H}$  NMR (500 MHz,  $\text{CDCl}_3$ ) (23)

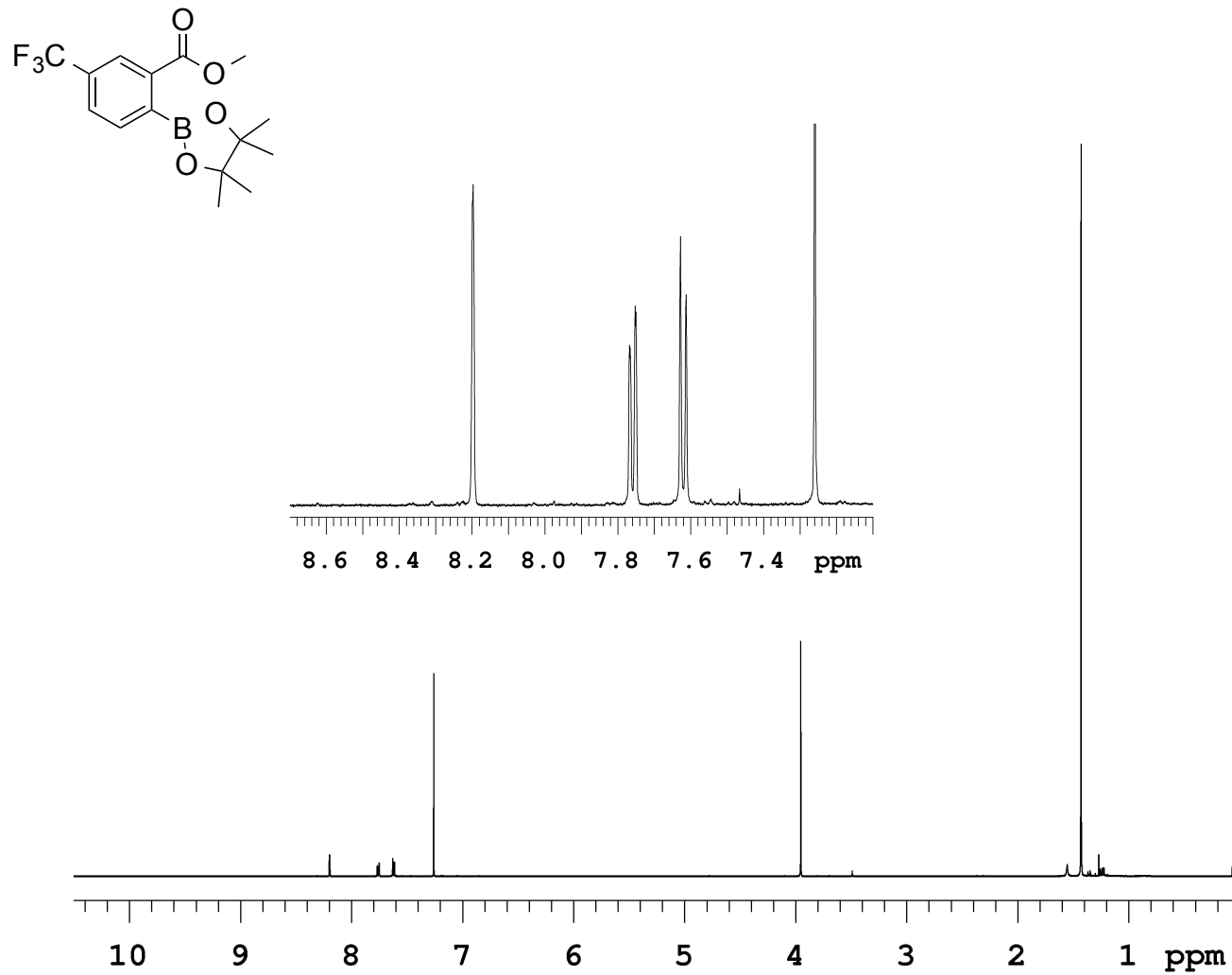


Figure 5.49.  $^{13}\text{C}$  NMR (125 MHz,  $\text{CDCl}_3$ ) (23)

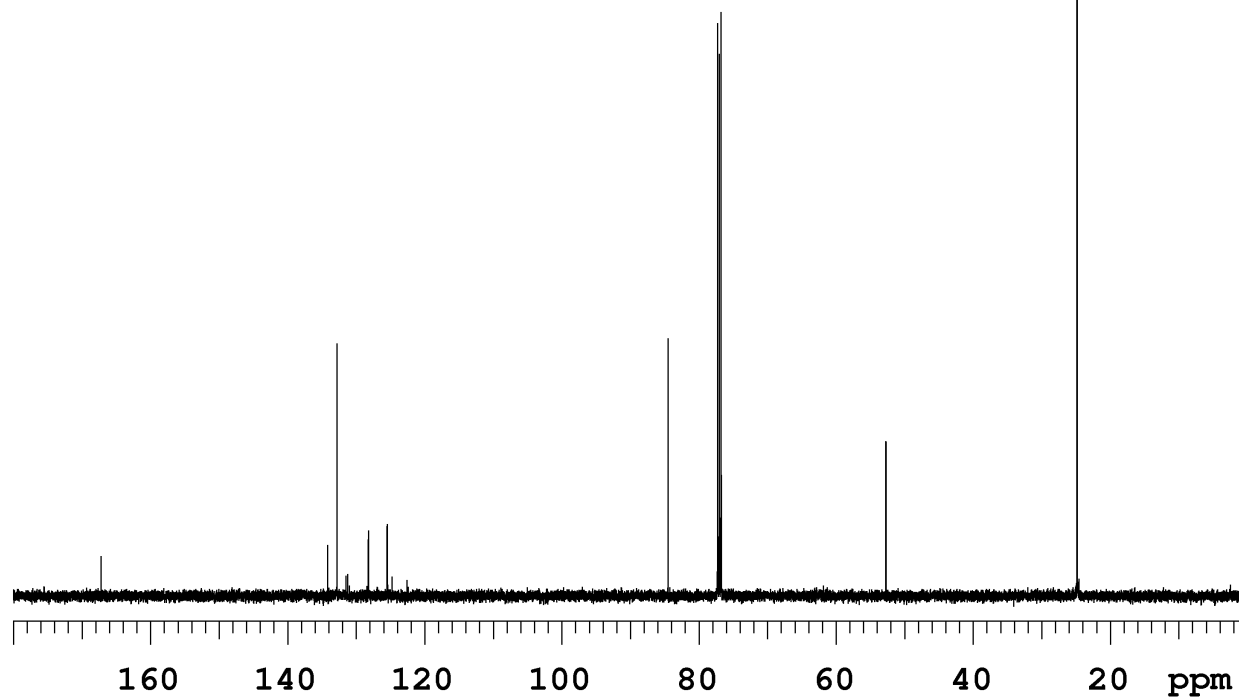
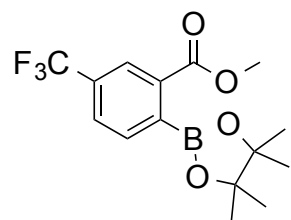


Figure 5.50.  $^1\text{H}$  NMR (500 MHz,  $\text{CDCl}_3$ ) (24a)

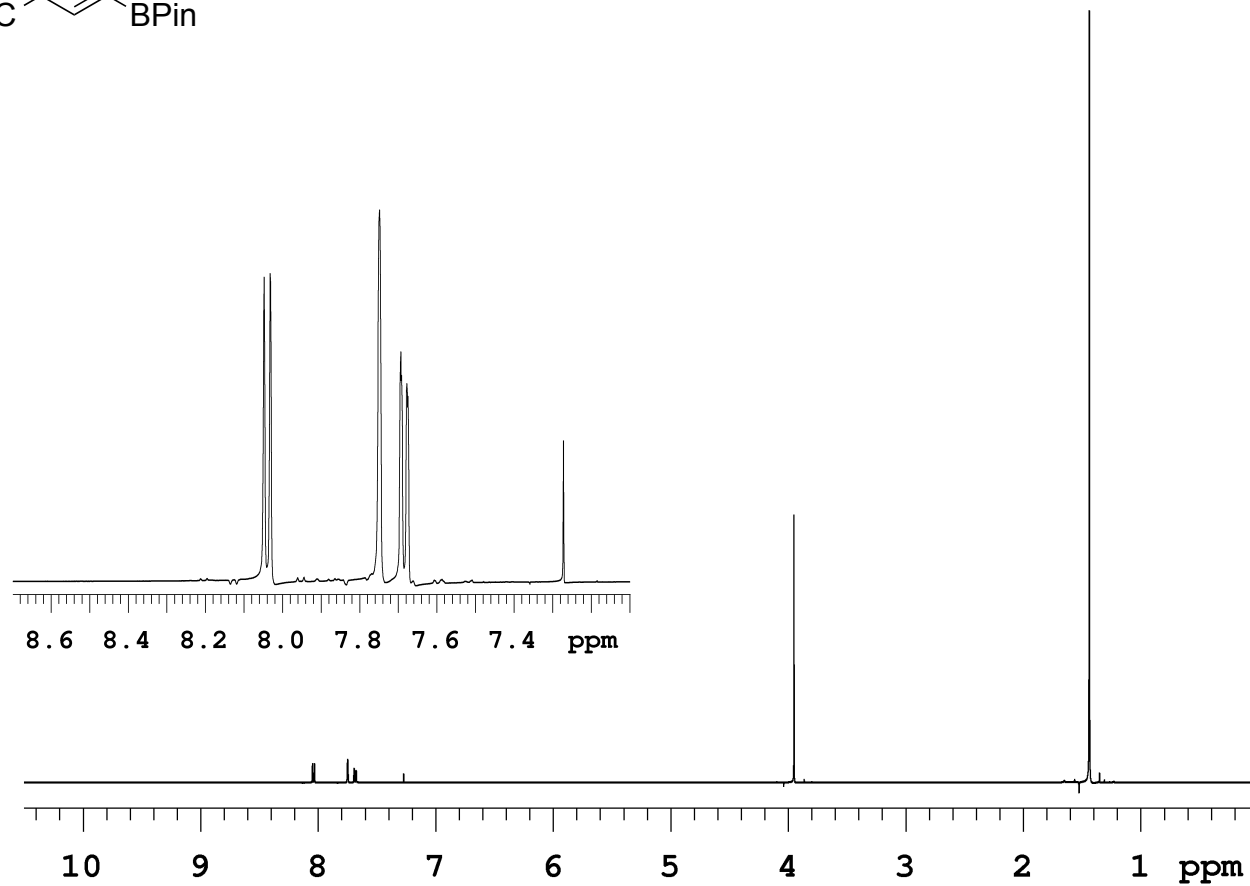
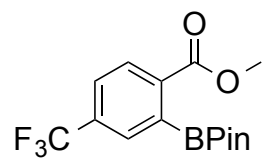




Figure 5.51.  $^{13}\text{C}$  NMR (125 MHz,  $\text{CDCl}_3$ ) (24a)

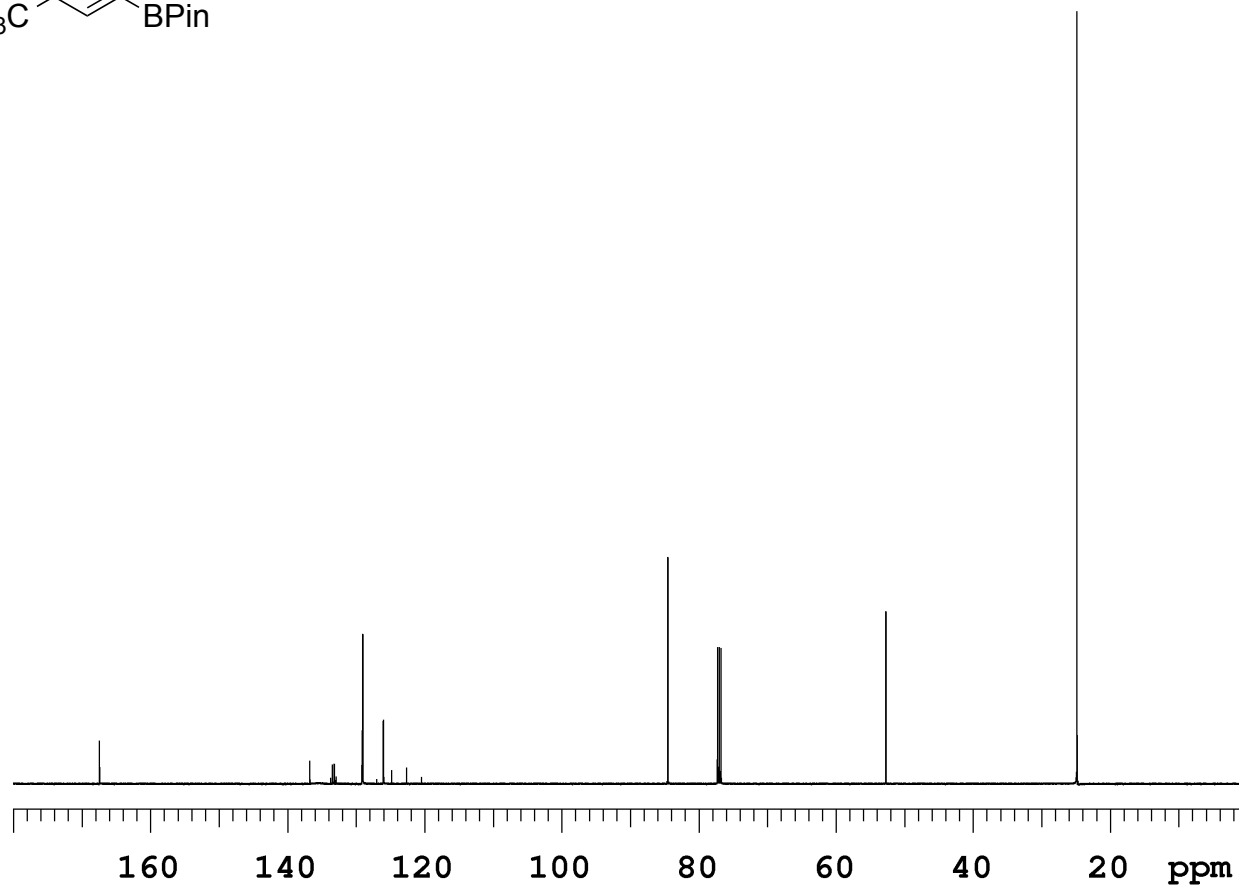
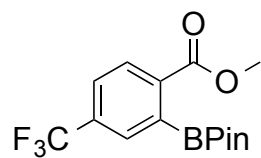


Figure 5.52.  $^1\text{H}$  NMR (500 MHz,  $\text{CDCl}_3$ ) (24b)

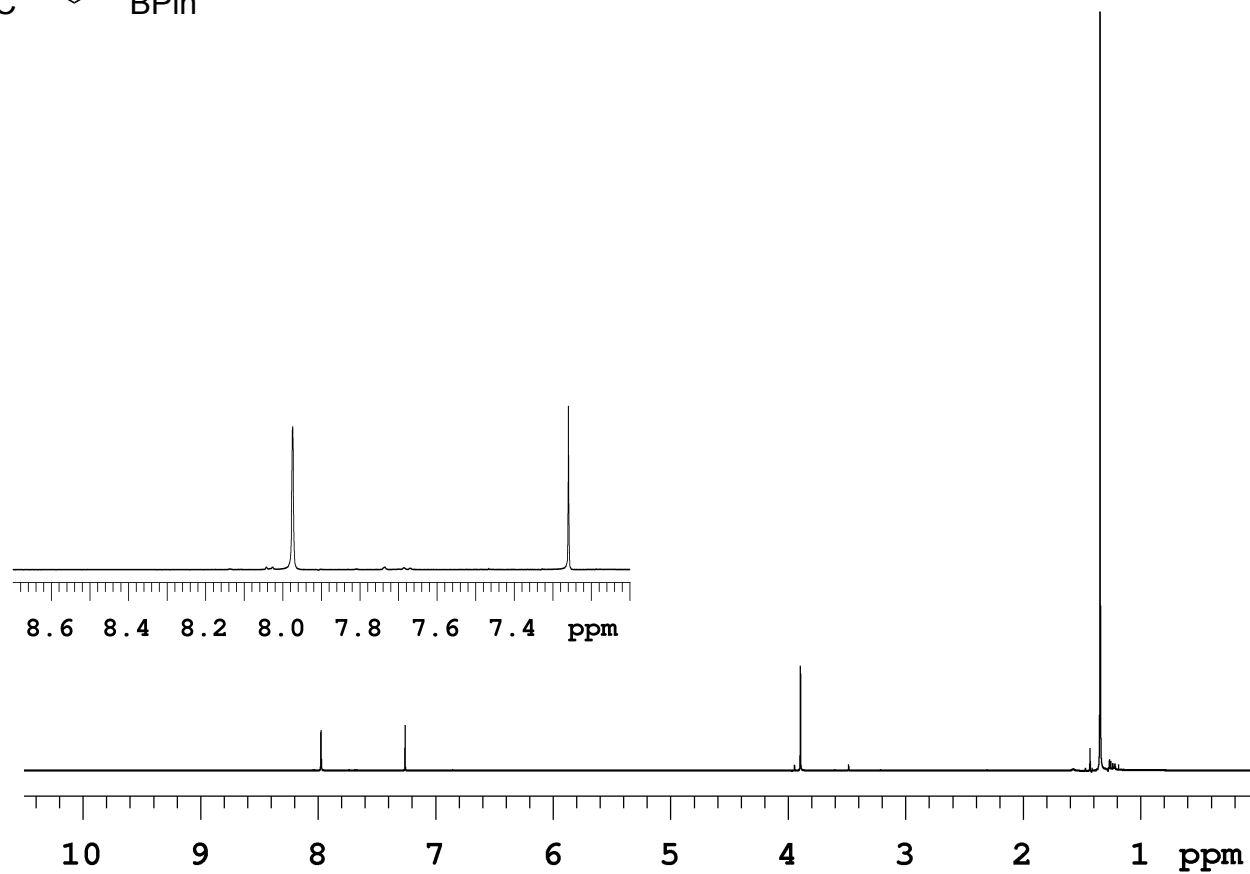
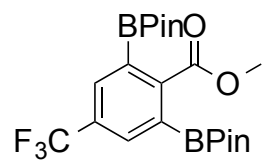


Figure 5.53.  $^{13}\text{C}$  NMR (125 MHz,  $\text{CDCl}_3$ ) (24b)

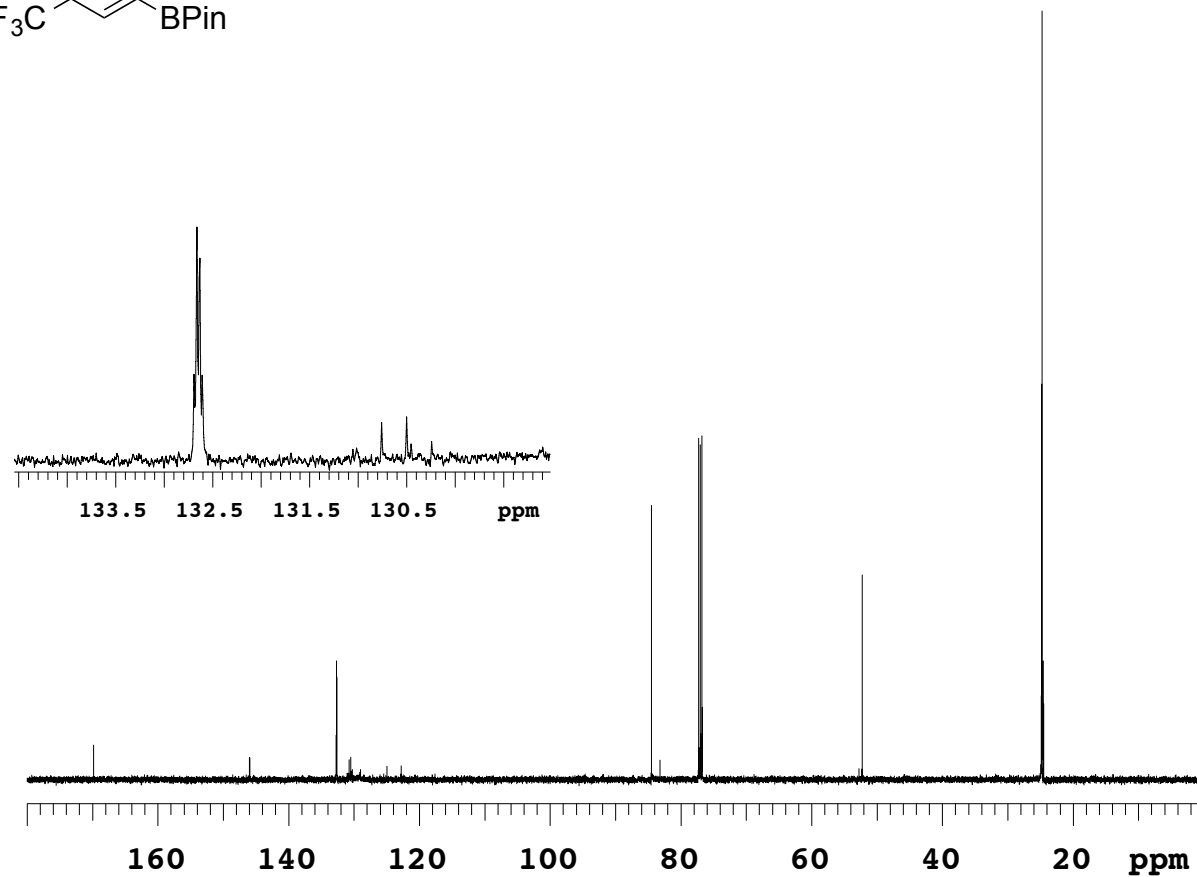
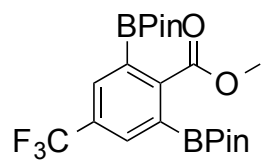


Figure 5.54.  $^1\text{H}$  NMR (500 MHz,  $\text{CDCl}_3$ ) (25)

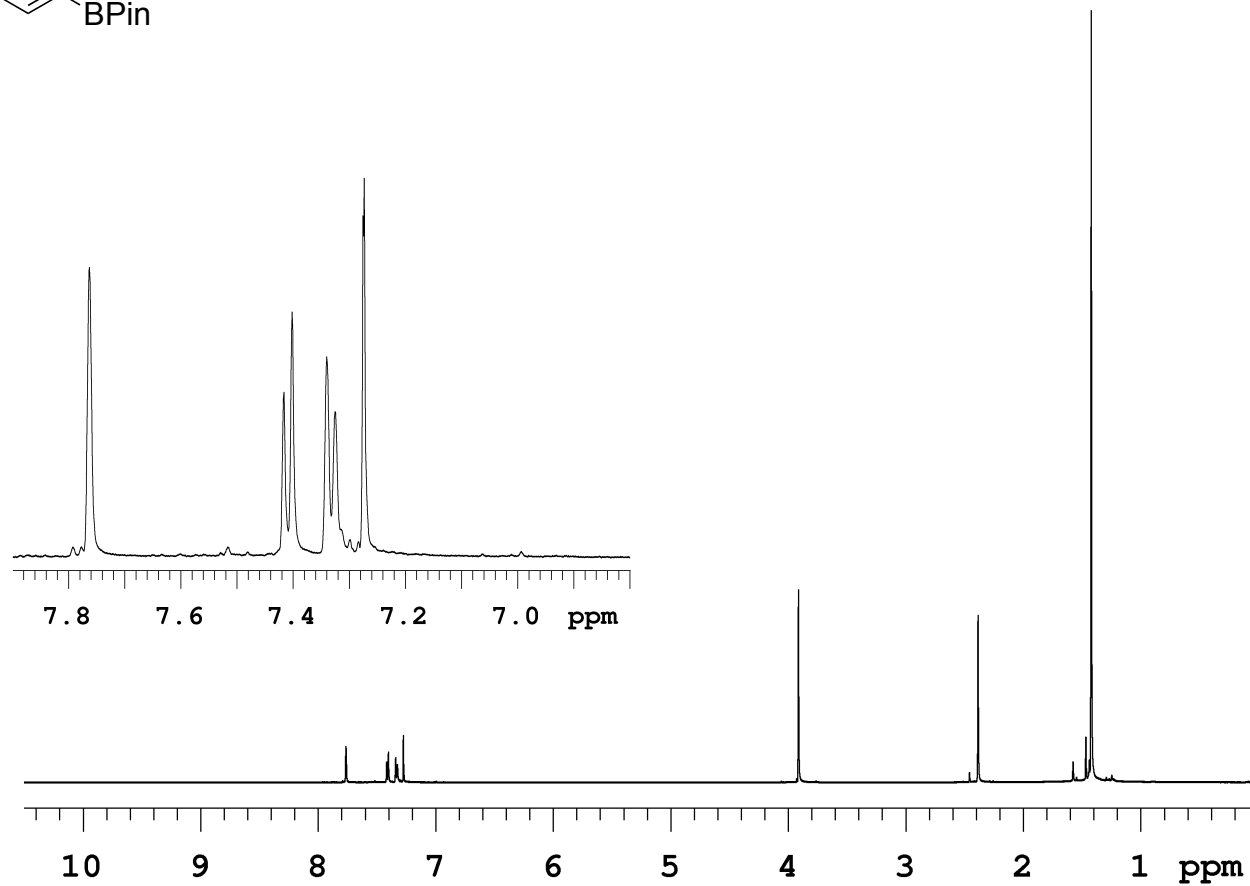
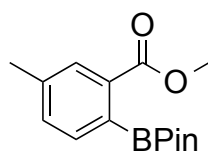


Figure 5.55.  $^{13}\text{C}$  NMR (125 MHz,  $\text{CDCl}_3$ ) (25)

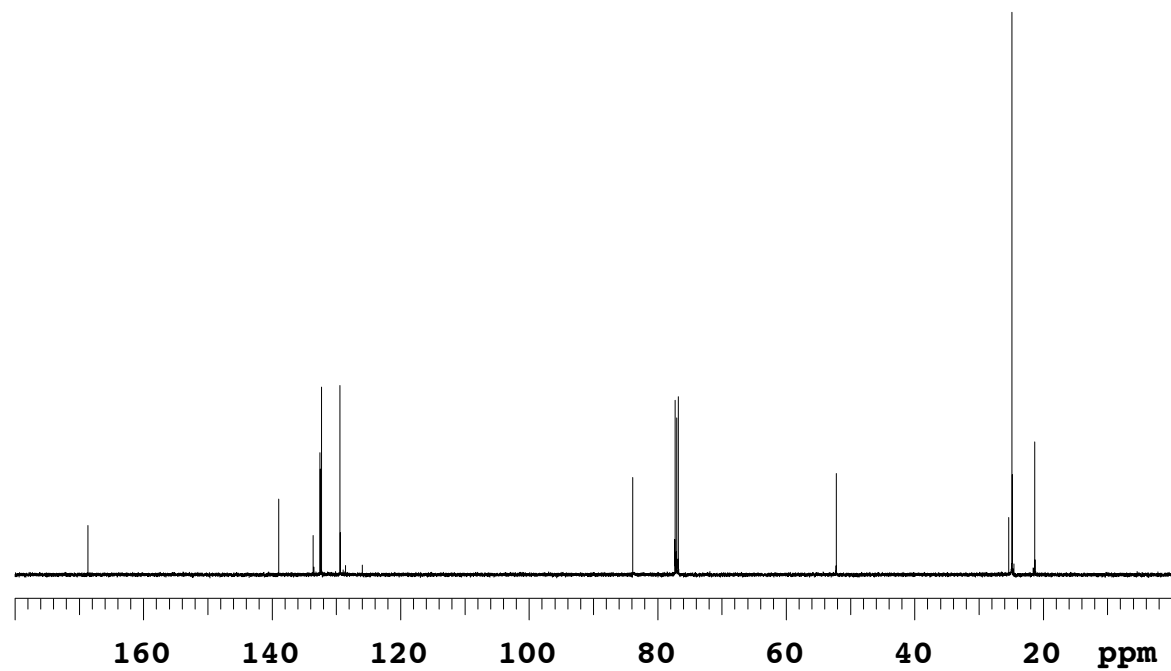
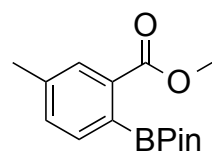


Figure 5.56.  $^1\text{H}$  NMR (500 MHz,  $\text{CDCl}_3$ ) (26a)

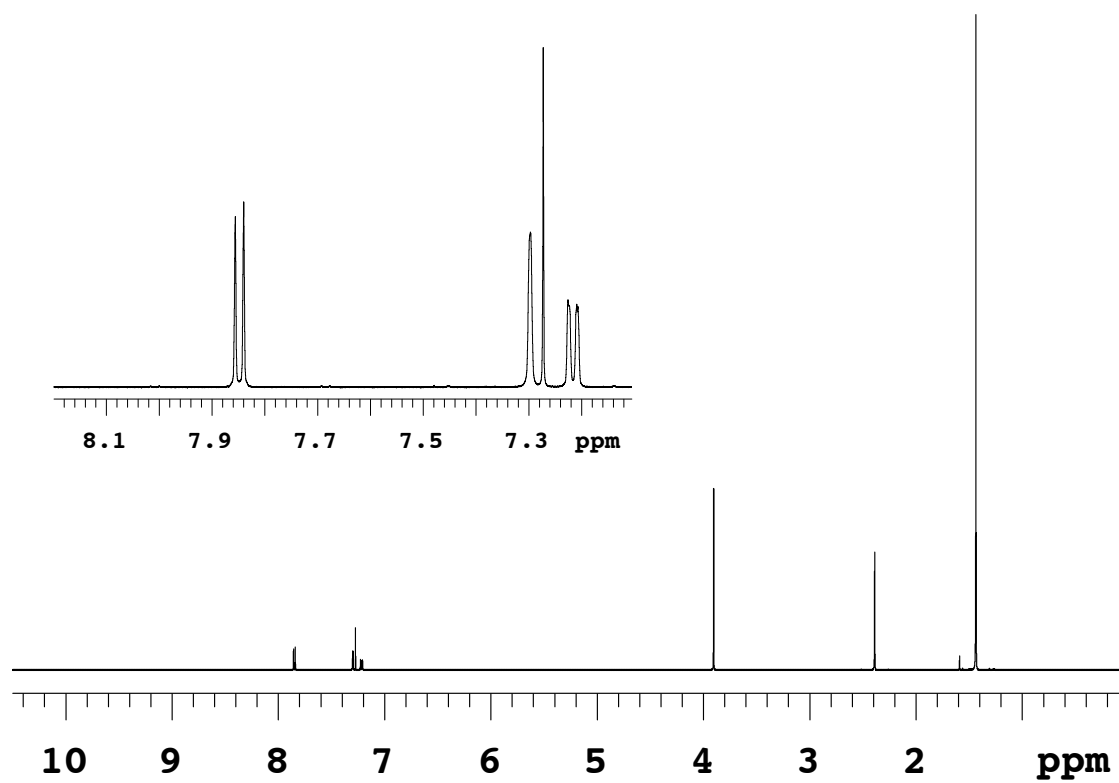
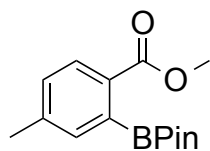


Figure 5.57.  $^{13}\text{C}$  NMR (125 MHz,  $\text{CDCl}_3$ ) (26a)

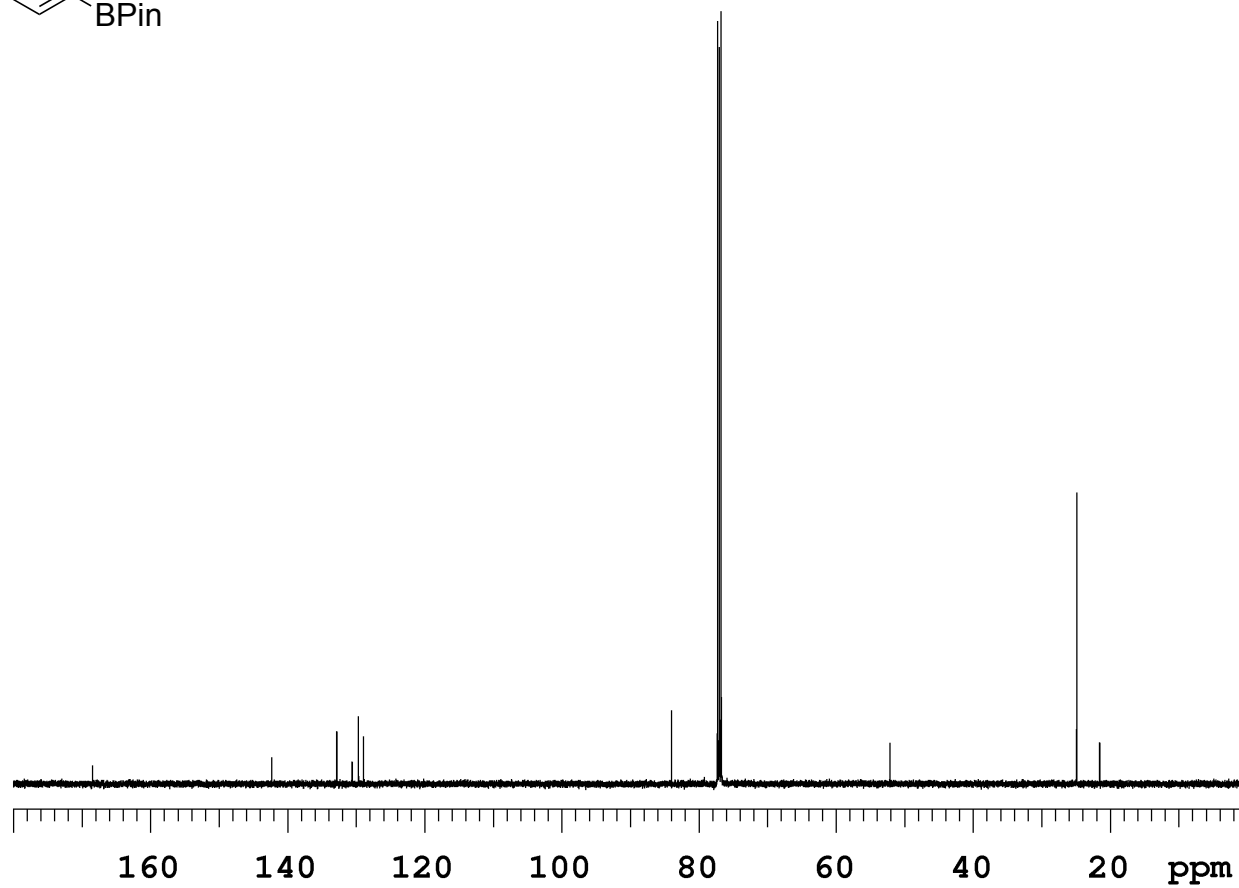
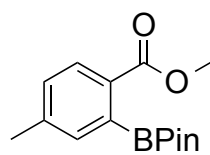


Figure 5.58.  $^1\text{H}$  NMR (500 MHz,  $\text{CDCl}_3$ ) (26b)

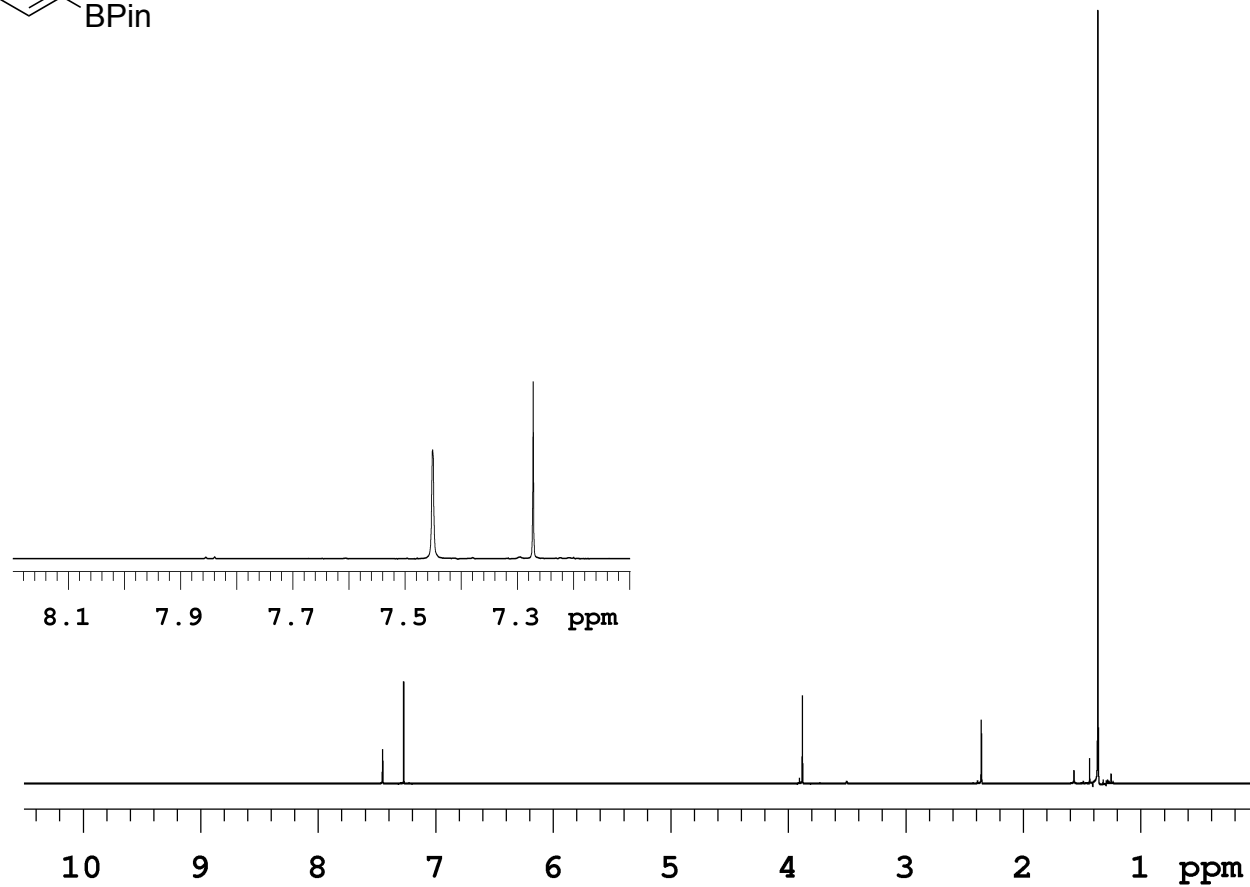
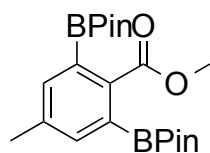




Figure 5.59.  $^{13}\text{C}$  NMR (125 MHz,  $\text{CDCl}_3$ ) (26b)

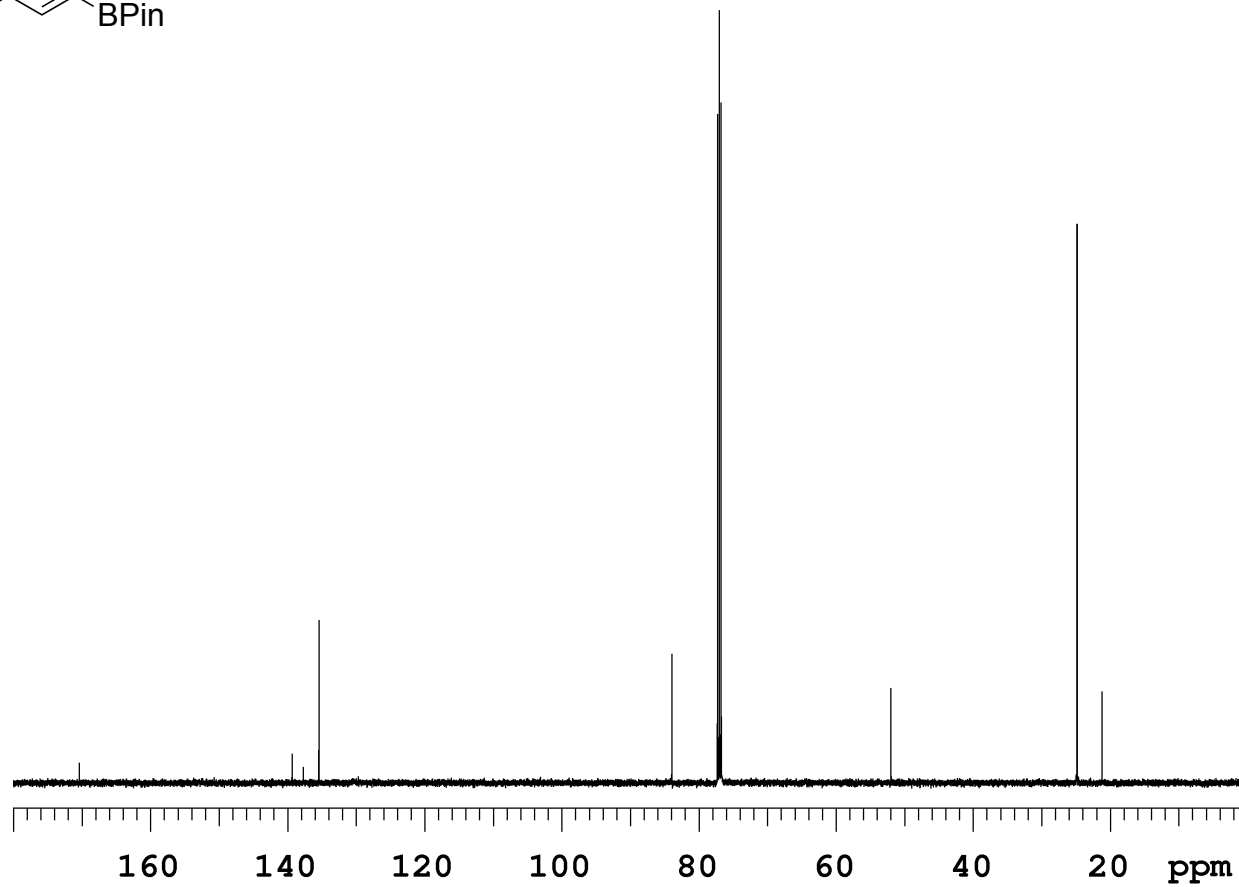
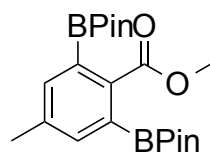


Figure 5.60.  $^1\text{H}$  NMR (500 MHz,  $\text{CDCl}_3$ ) (27)

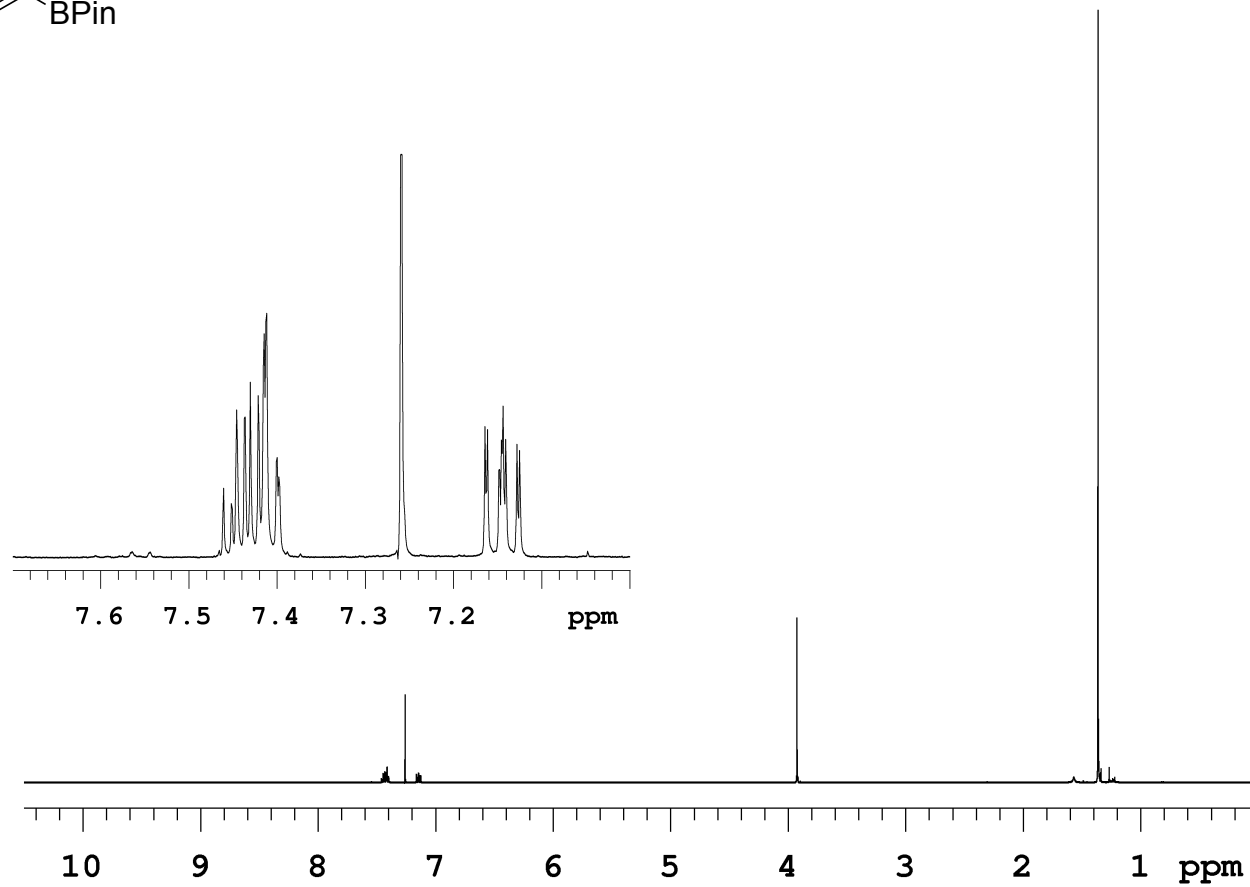
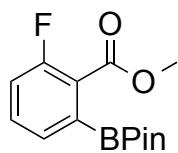


Figure 5.61.  $^{13}\text{C}$  NMR (125 MHz, DMSO- $d_6$ ) (27)

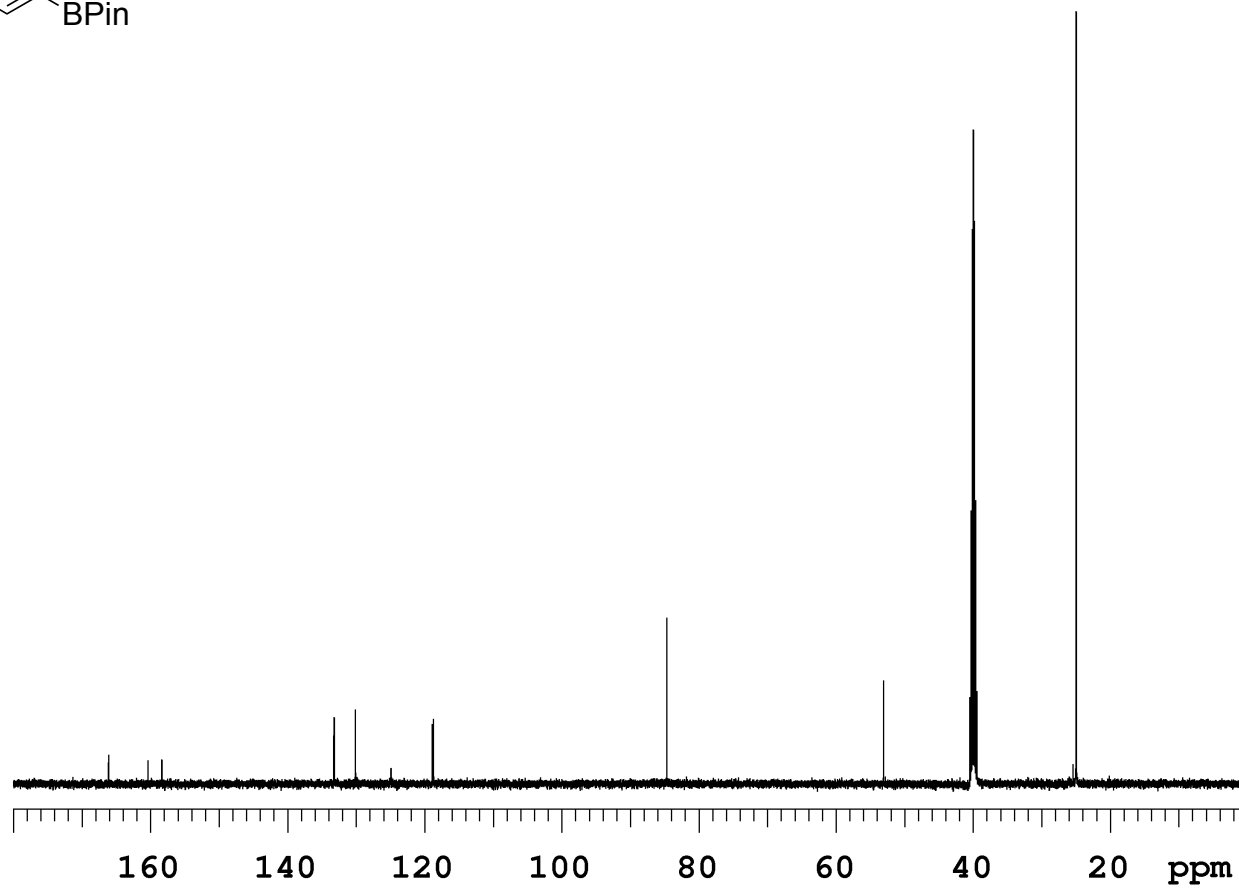
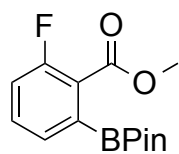


Figure 5.62.  $^1\text{H}$  NMR (500 MHz,  $\text{CDCl}_3$ ) (28)

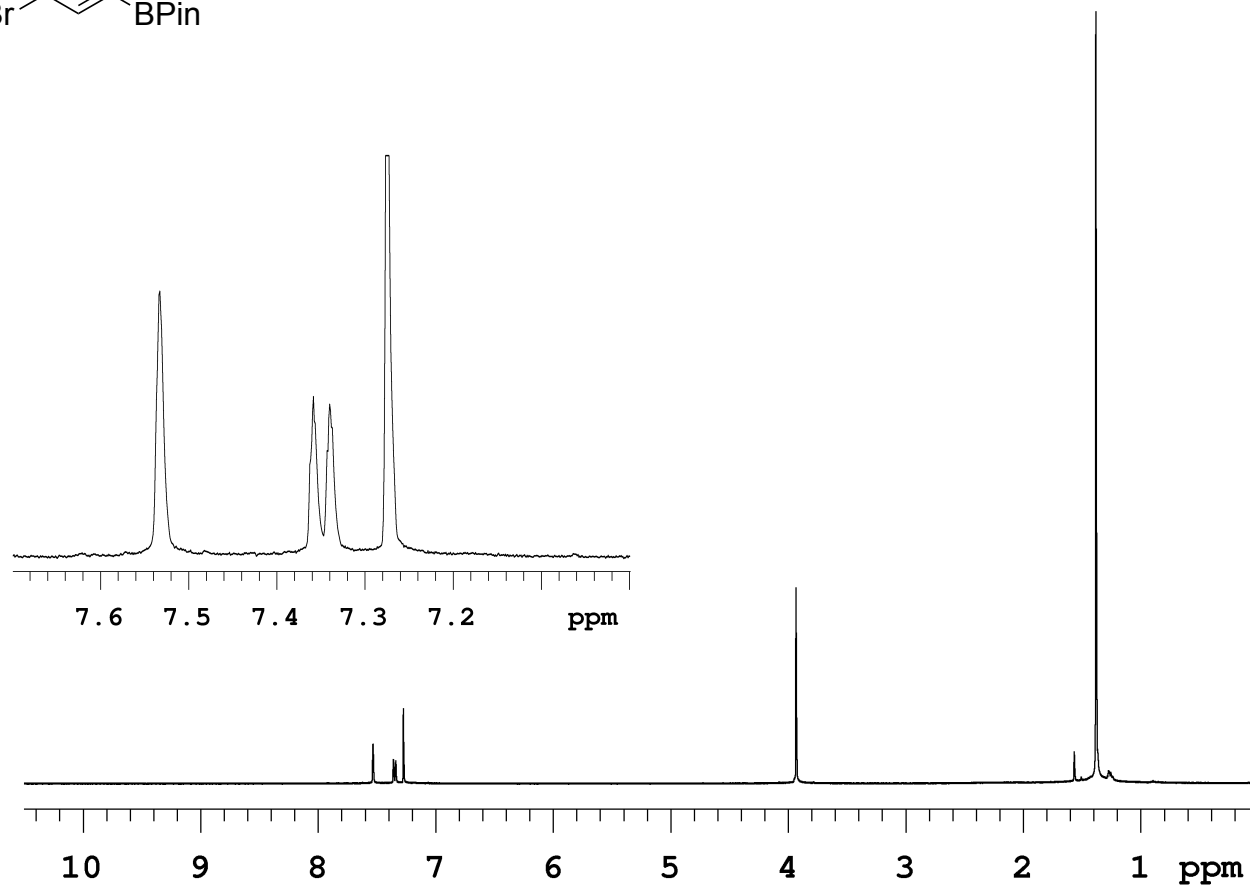
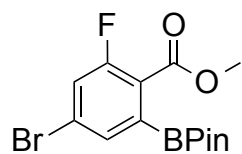


Figure 5.63.  $^{13}\text{C}$  NMR (125 MHz,  $\text{CDCl}_3$ ) (28)

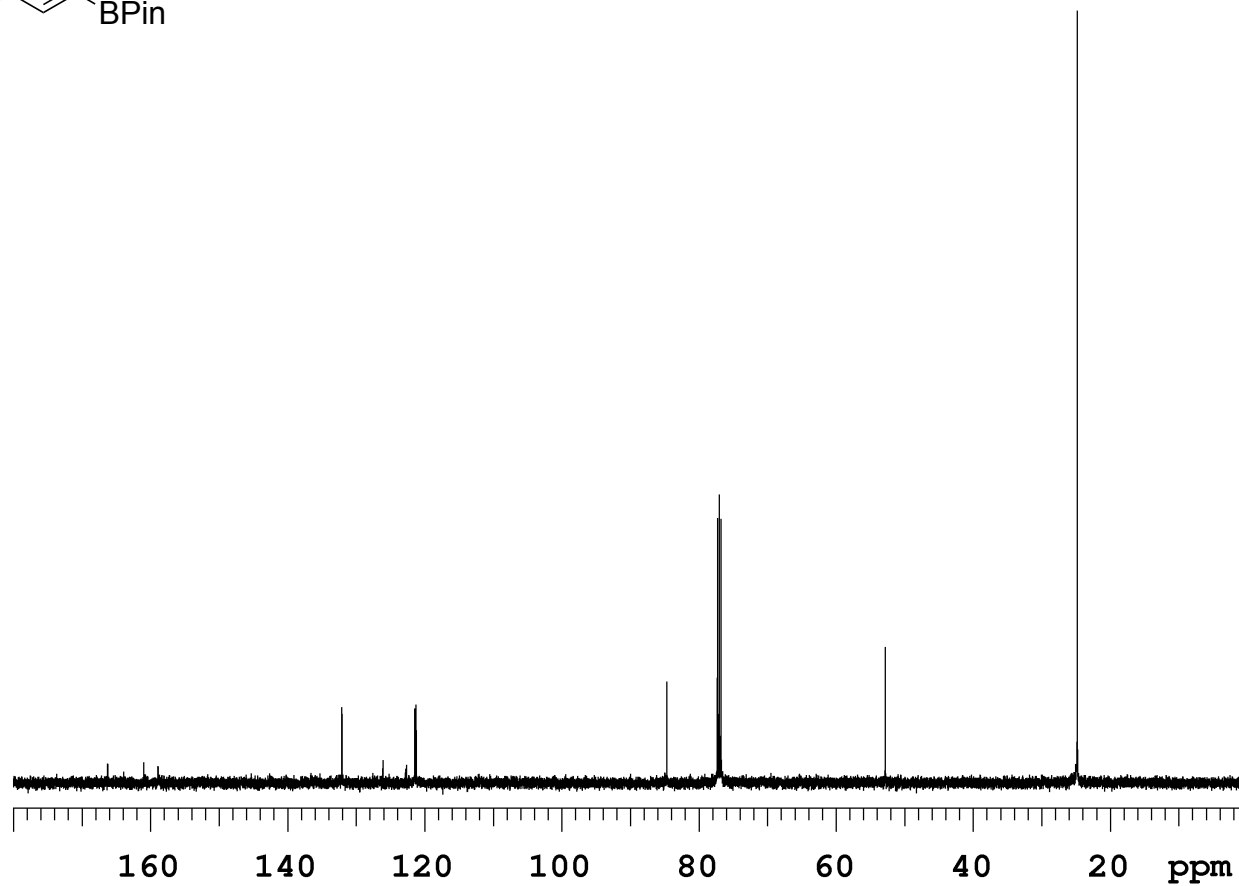
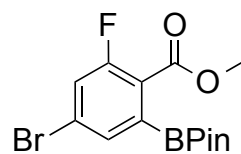


Figure 5.64.  $^1\text{H}$  NMR (500 MHz,  $\text{CDCl}_3$ ) (29)

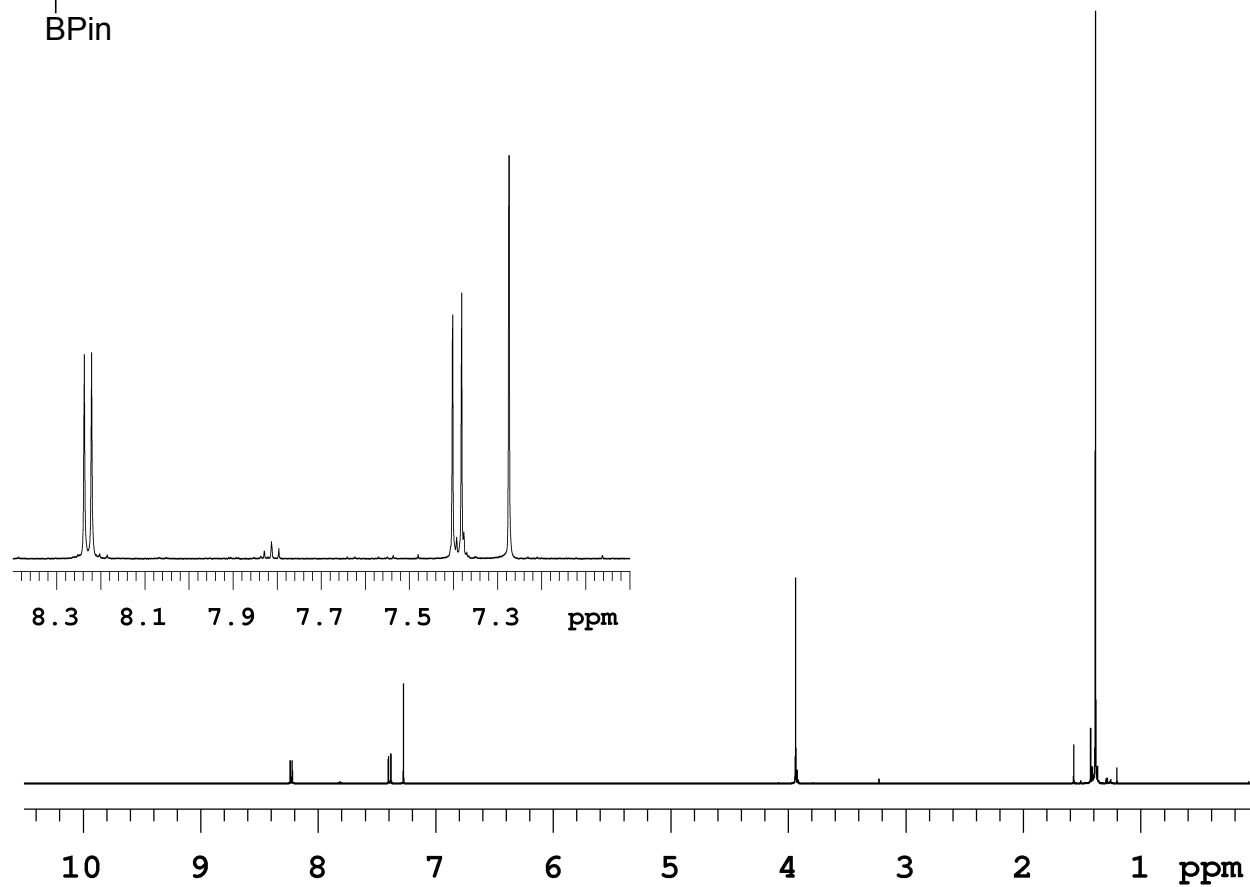
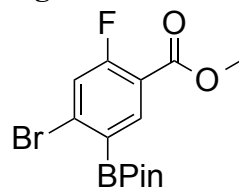


Figure 5.65.  $^{13}\text{C}$  NMR (125 MHz,  $\text{CDCl}_3$ ) (28)

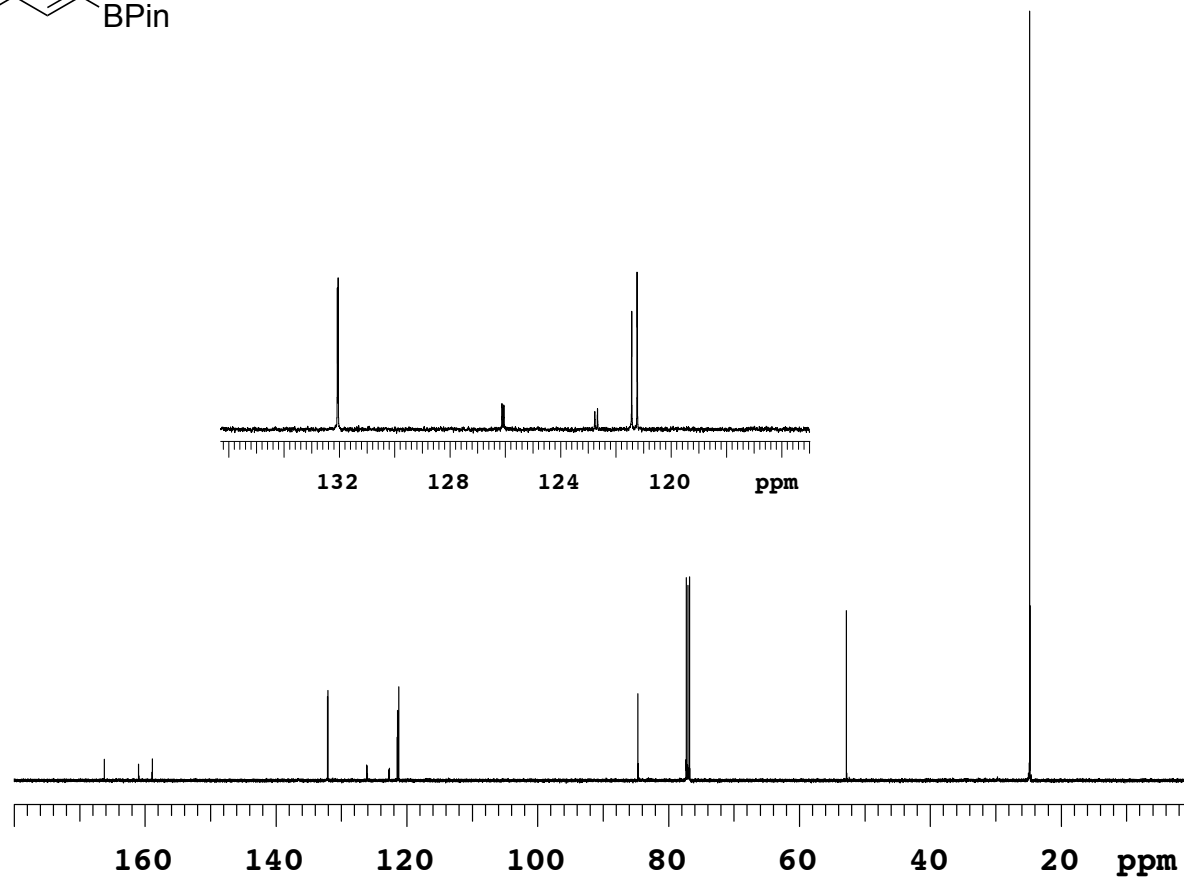
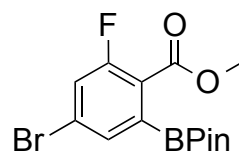


Figure 5.66.  $^1\text{H}$  NMR (500 MHz,  $\text{CDCl}_3$ ) (30)

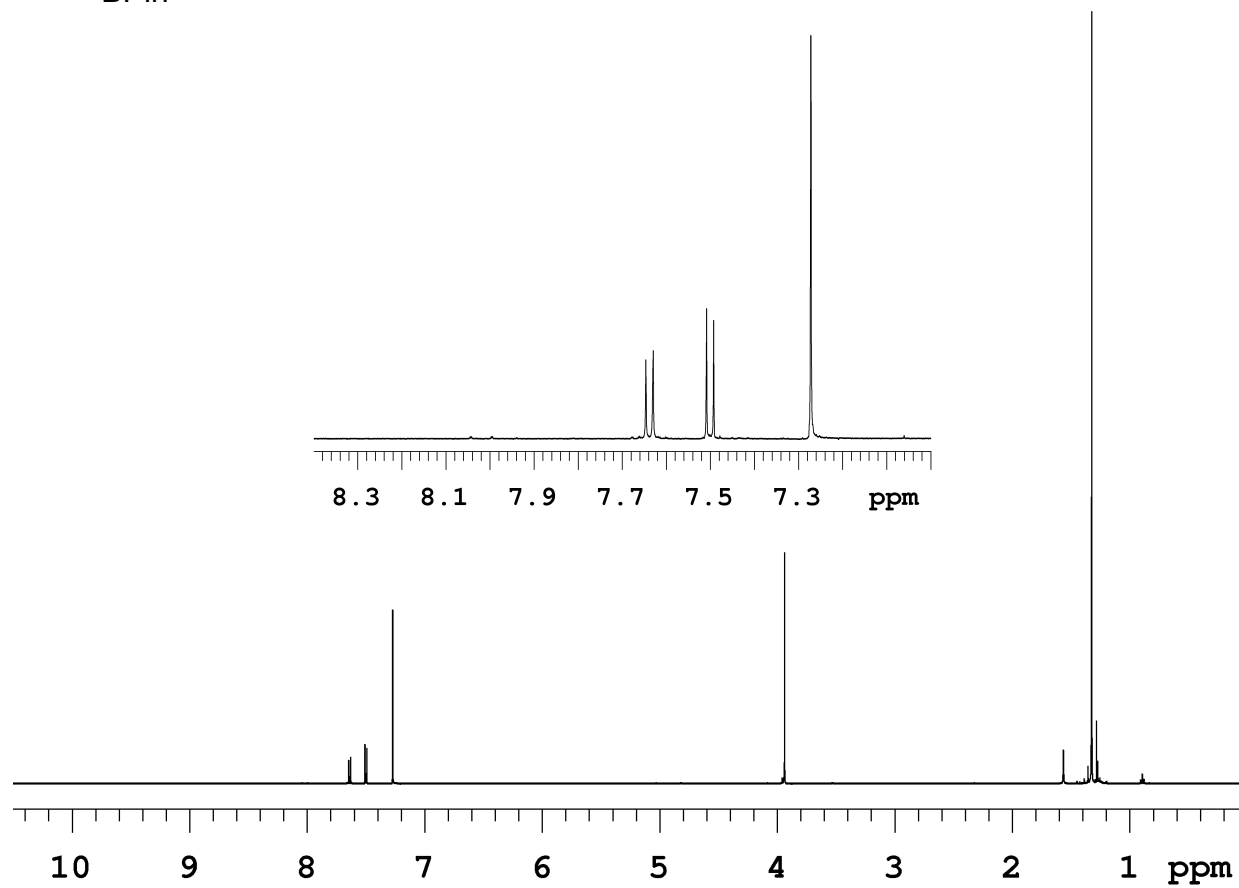
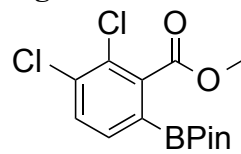




Figure 5.67.  $^{13}\text{C}$  NMR (125 MHz,  $\text{CDCl}_3$ ) (30)

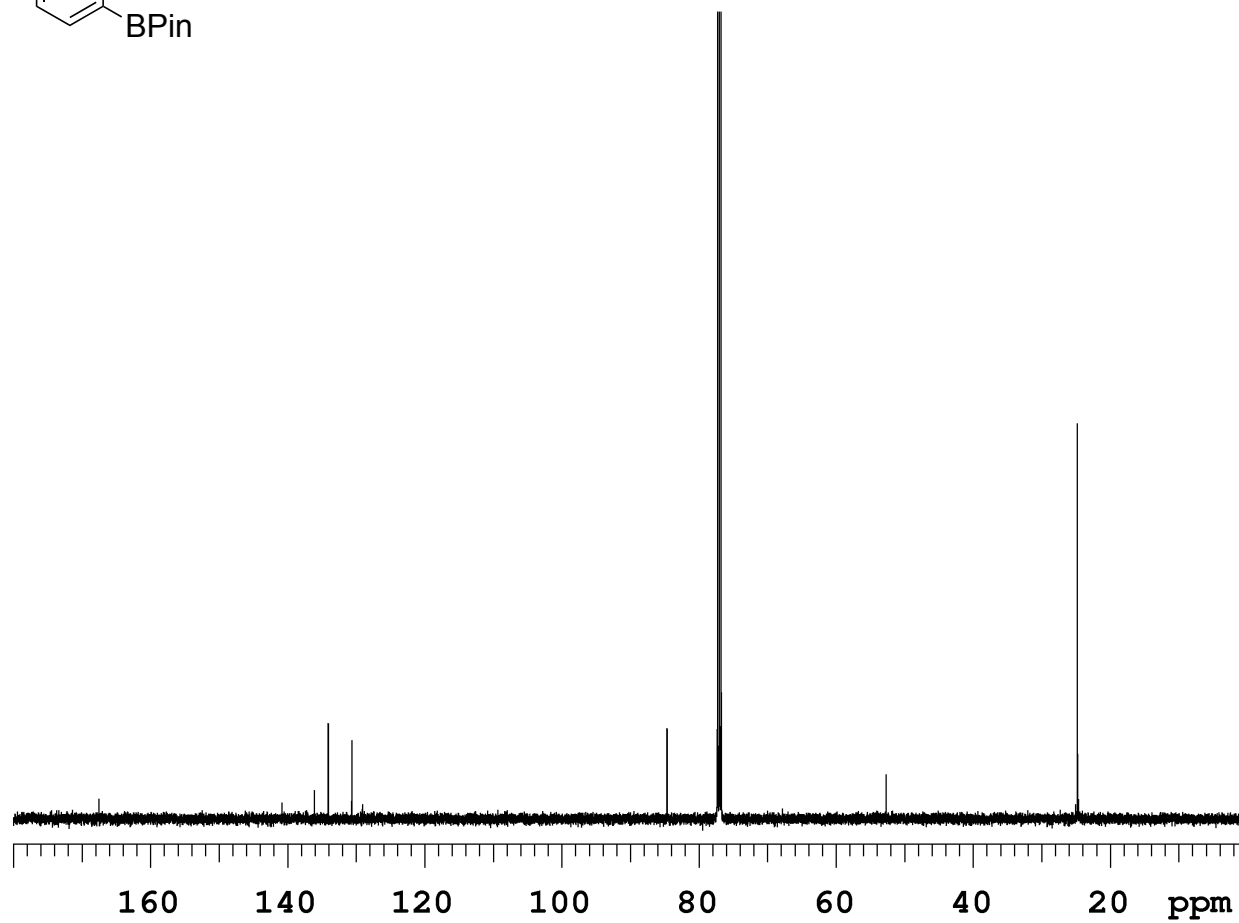
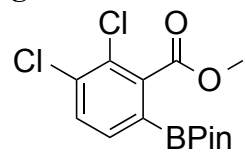


Figure 5.68.  $^1\text{H}$  NMR (500 MHz,  $\text{CDCl}_3$ ) (31)

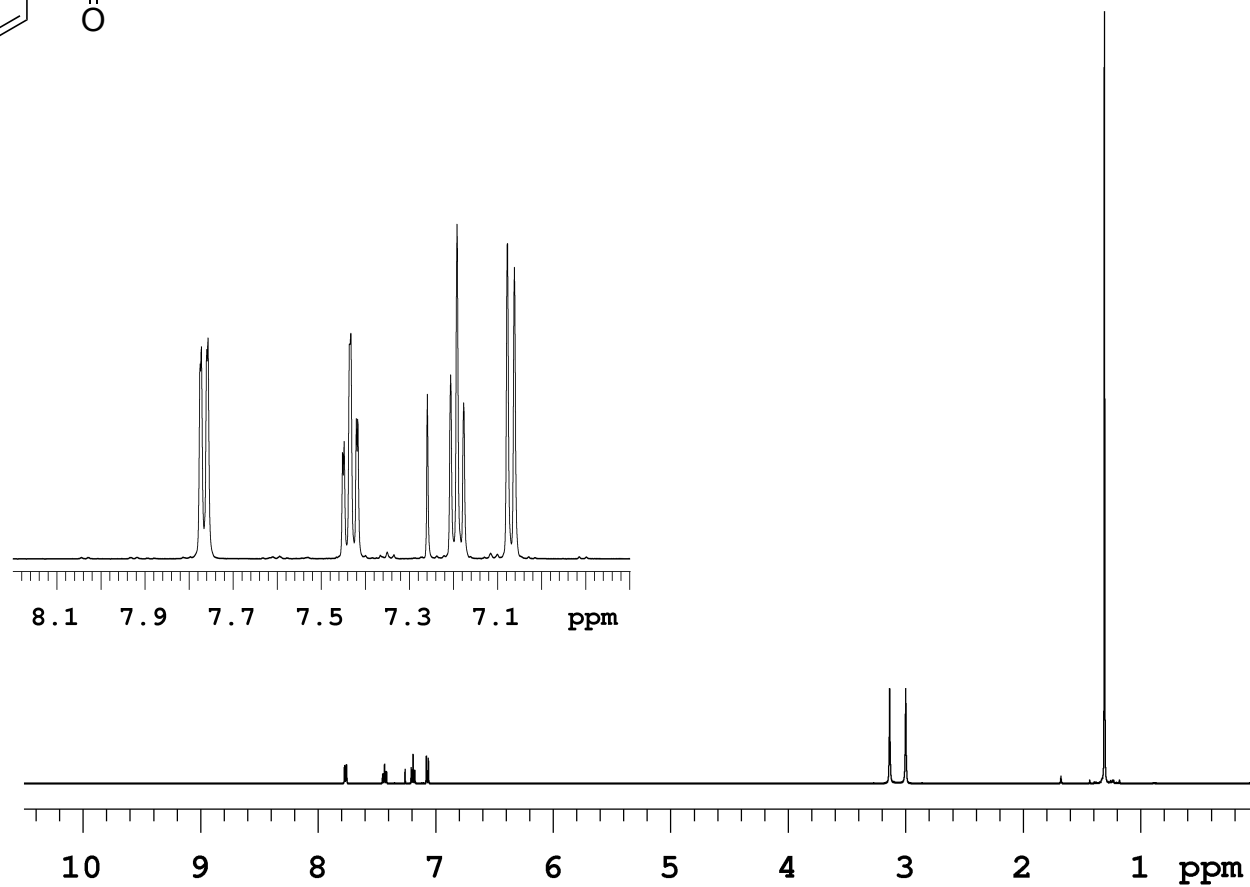
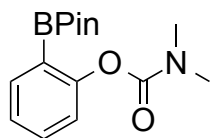


Figure 5.69.  $^{13}\text{C}$  NMR (125 MHz,  $\text{CDCl}_3$ ) (32)

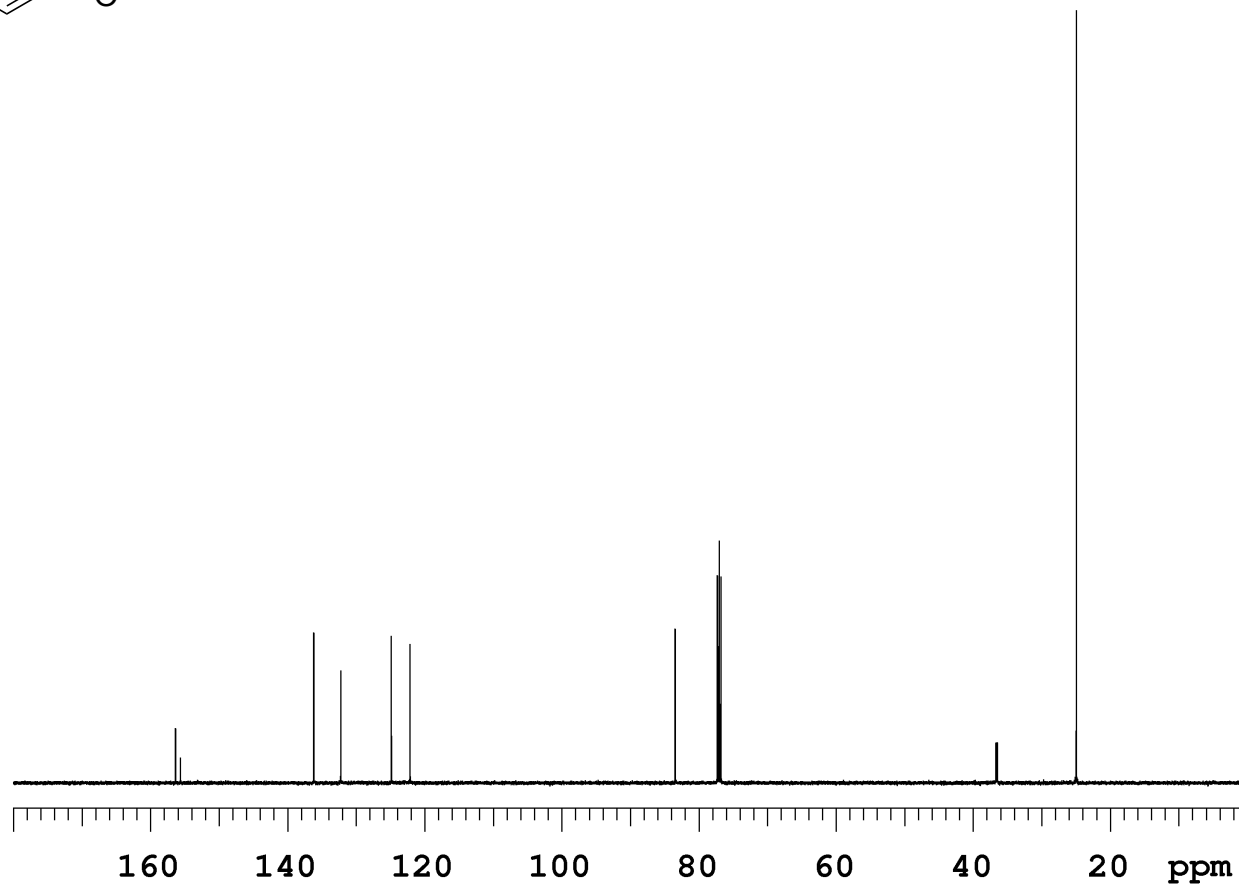
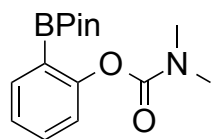


Figure 5.70.  $^1\text{H}$  NMR (500 MHz,  $\text{CDCl}_3$ ) (32)

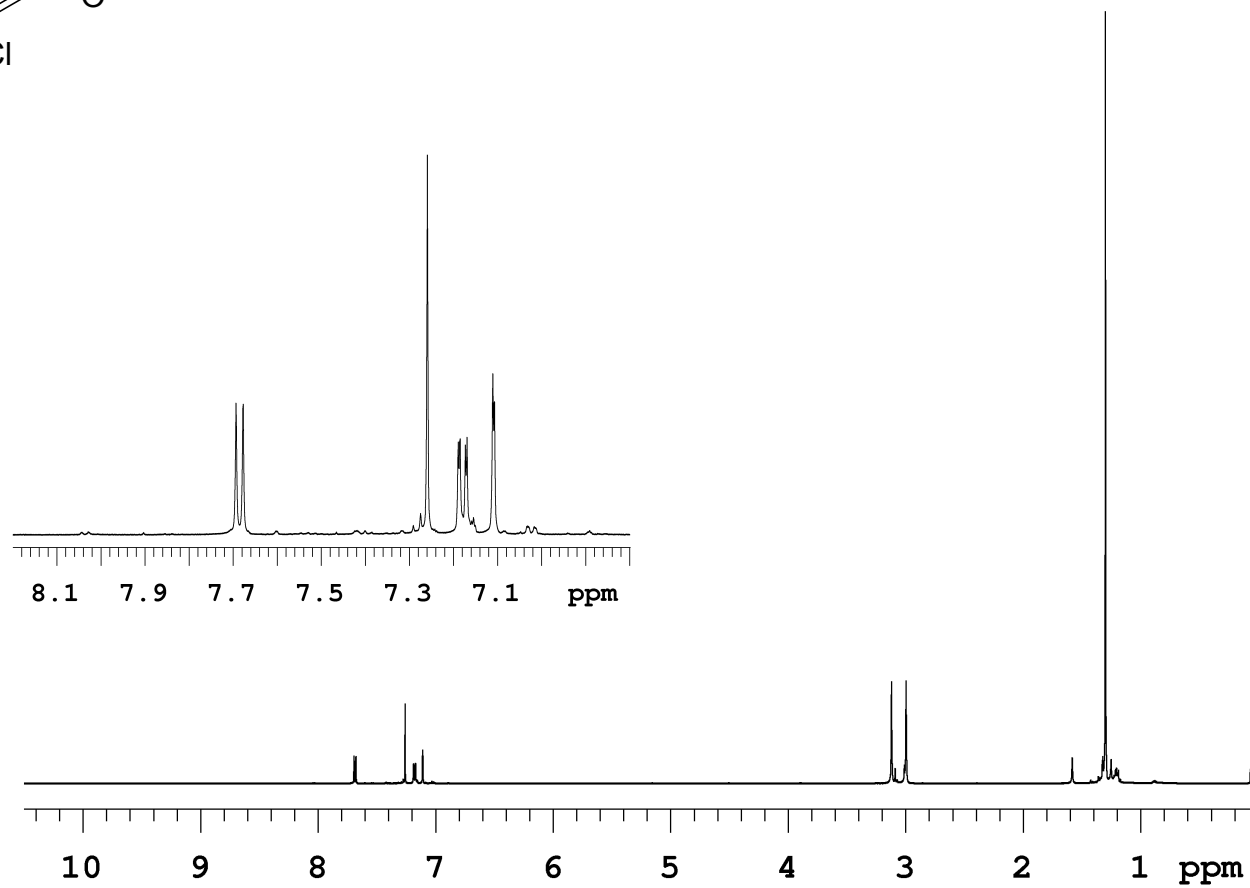
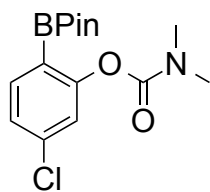


Figure 5.71.  $^1\text{H}$  NMR (500 MHz,  $\text{C}_6\text{D}_6$ ) (33)

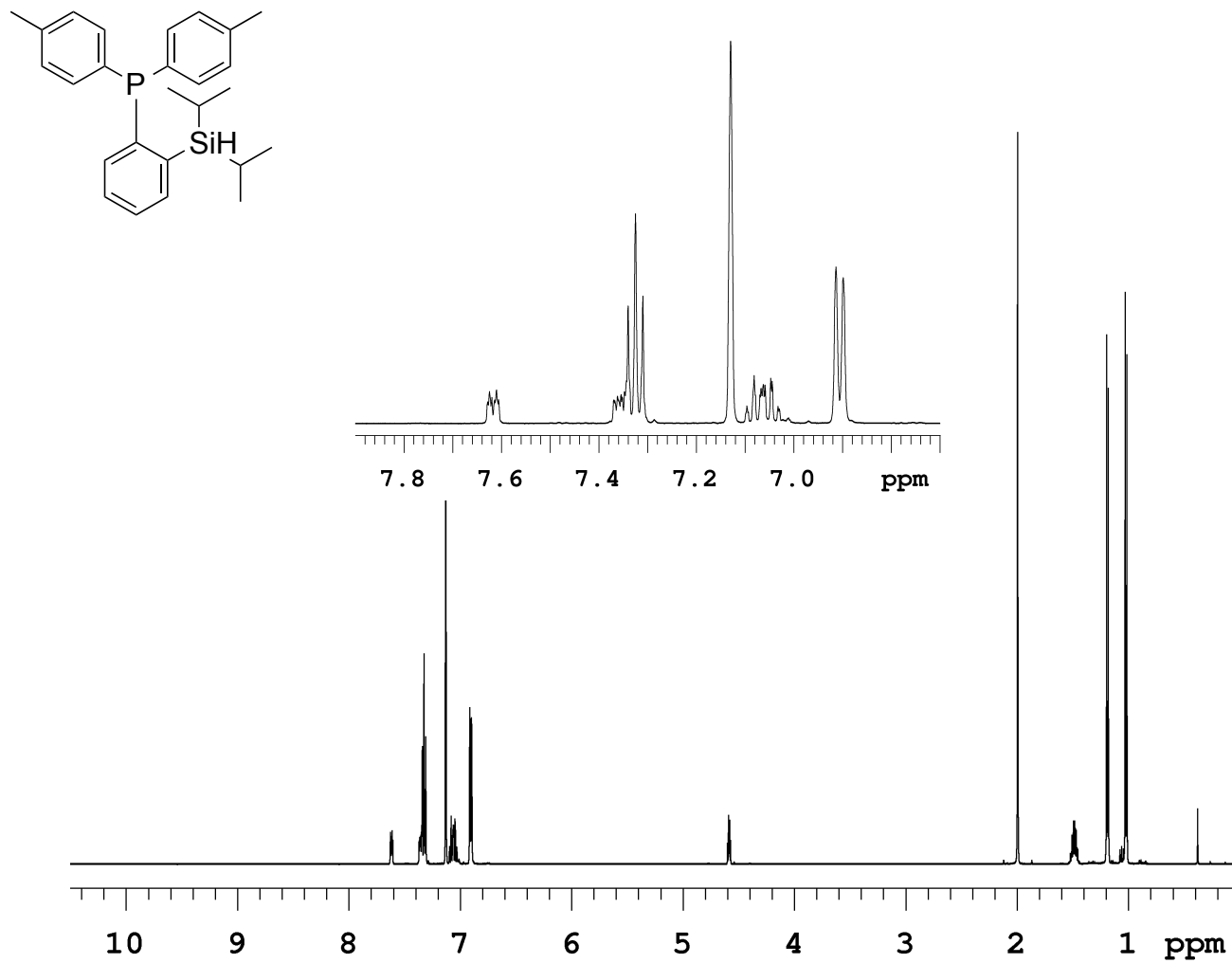


Figure 5.72.  $^{13}\text{C}$  NMR (125 MHz,  $\text{CDCl}_3$ ) (33)

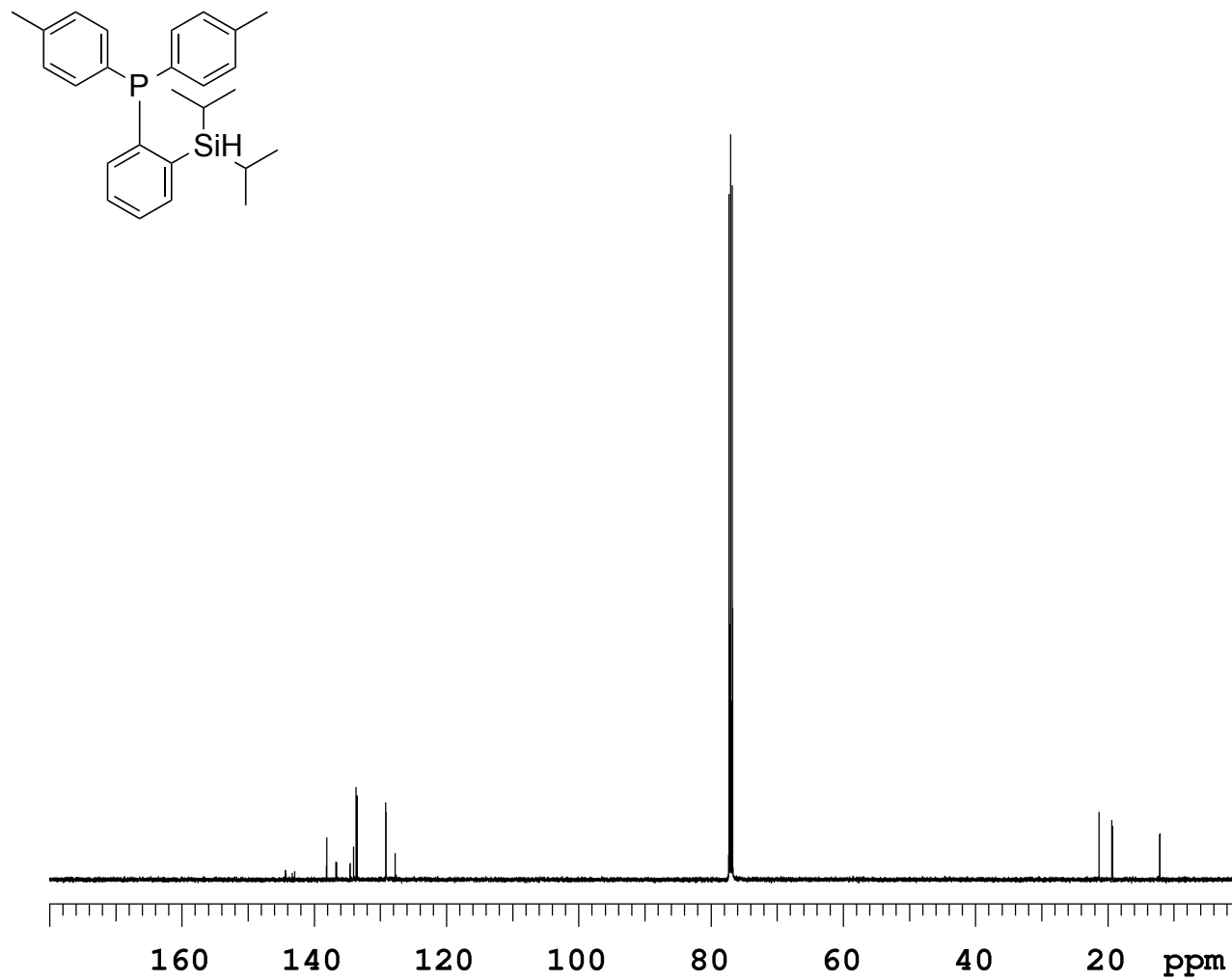


Figure 5.73.  $^1\text{H}$  NMR (500 MHz,  $\text{C}_6\text{D}_6$ ) (34)

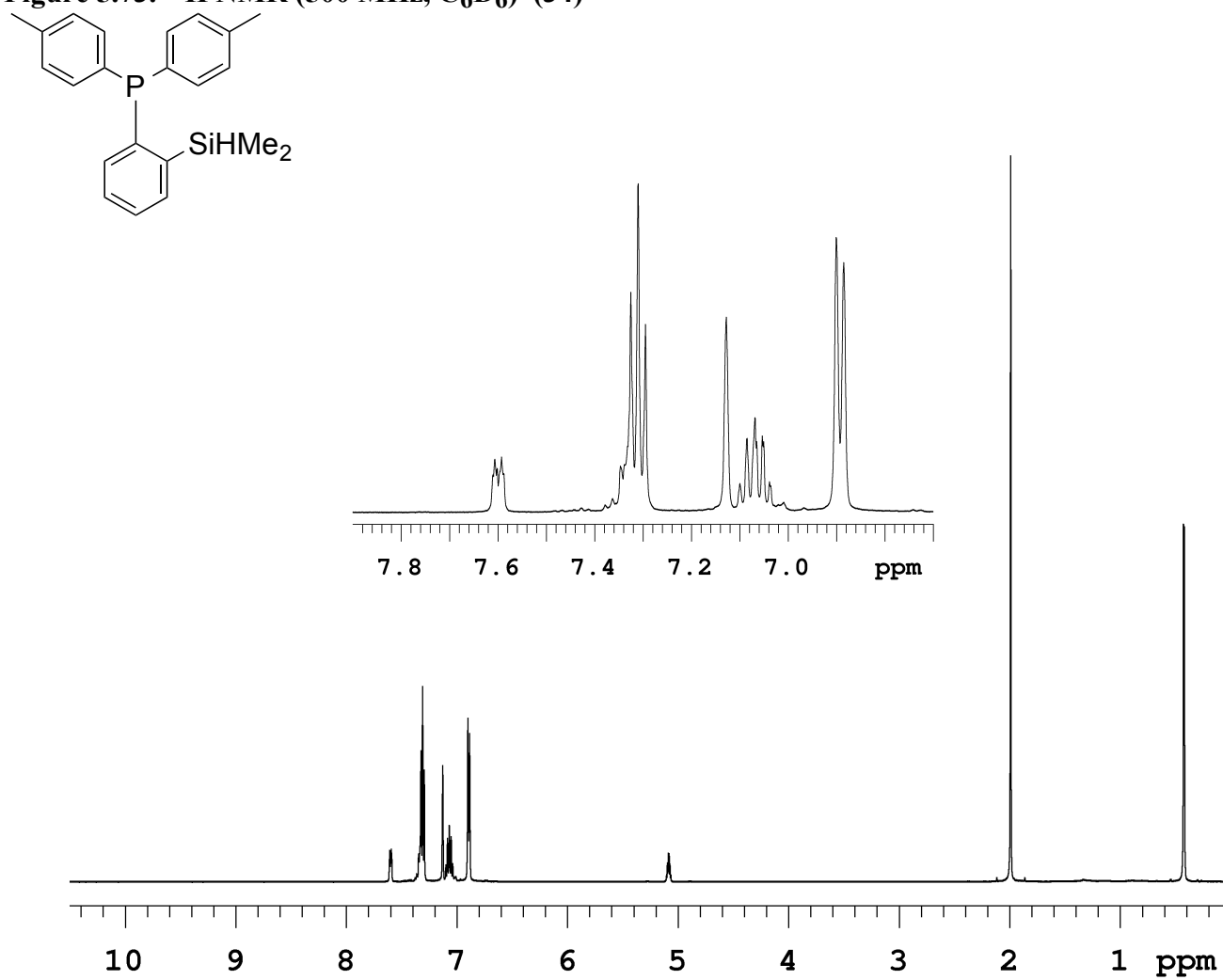


Figure 5.74.  $^{13}\text{C}$  NMR (125 MHz,  $\text{CDCl}_3$ ) (34)

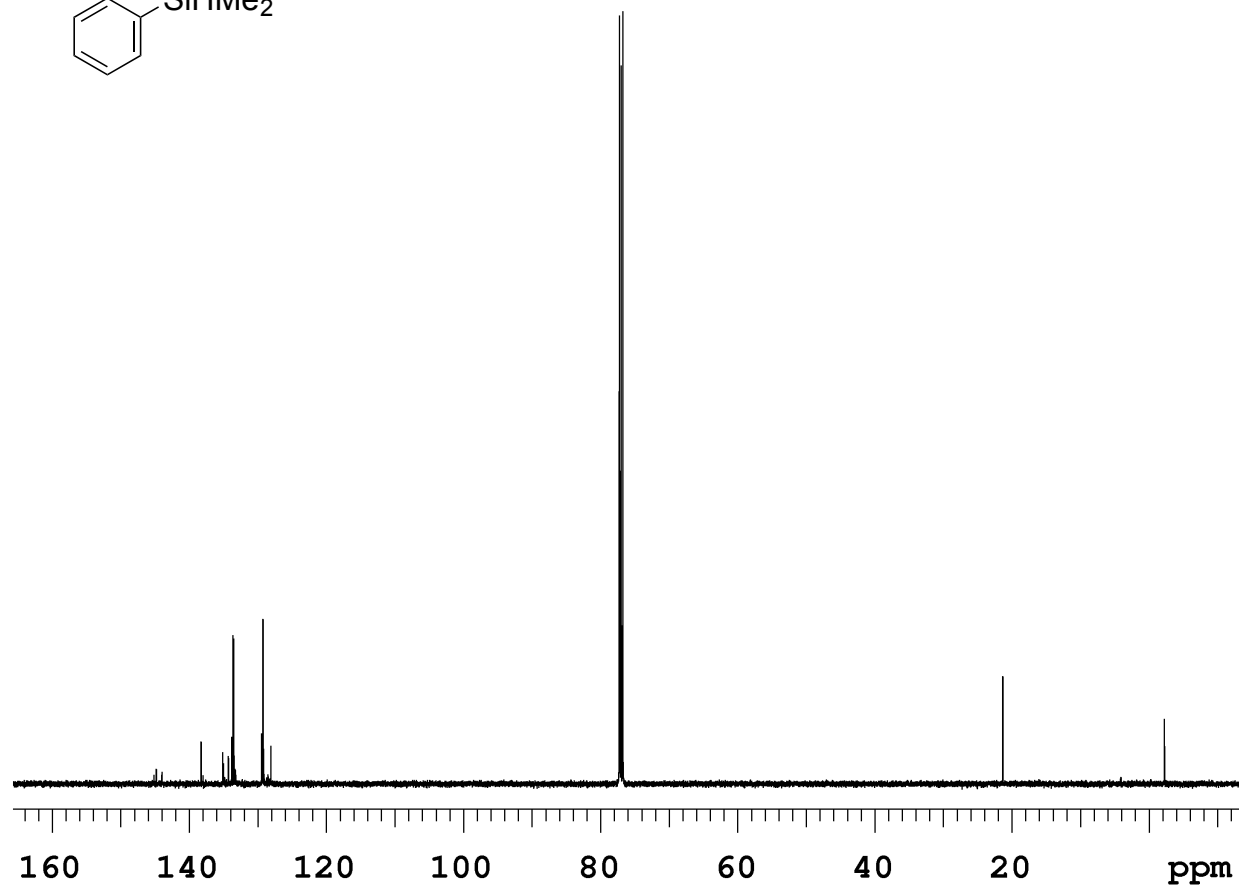
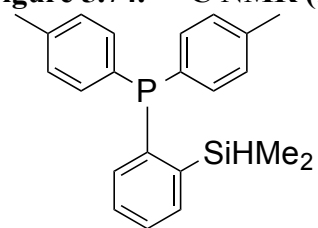




Figure 5.75.  $^1\text{H}$  NMR (500 MHz,  $\text{C}_6\text{D}_6$ ) (35)

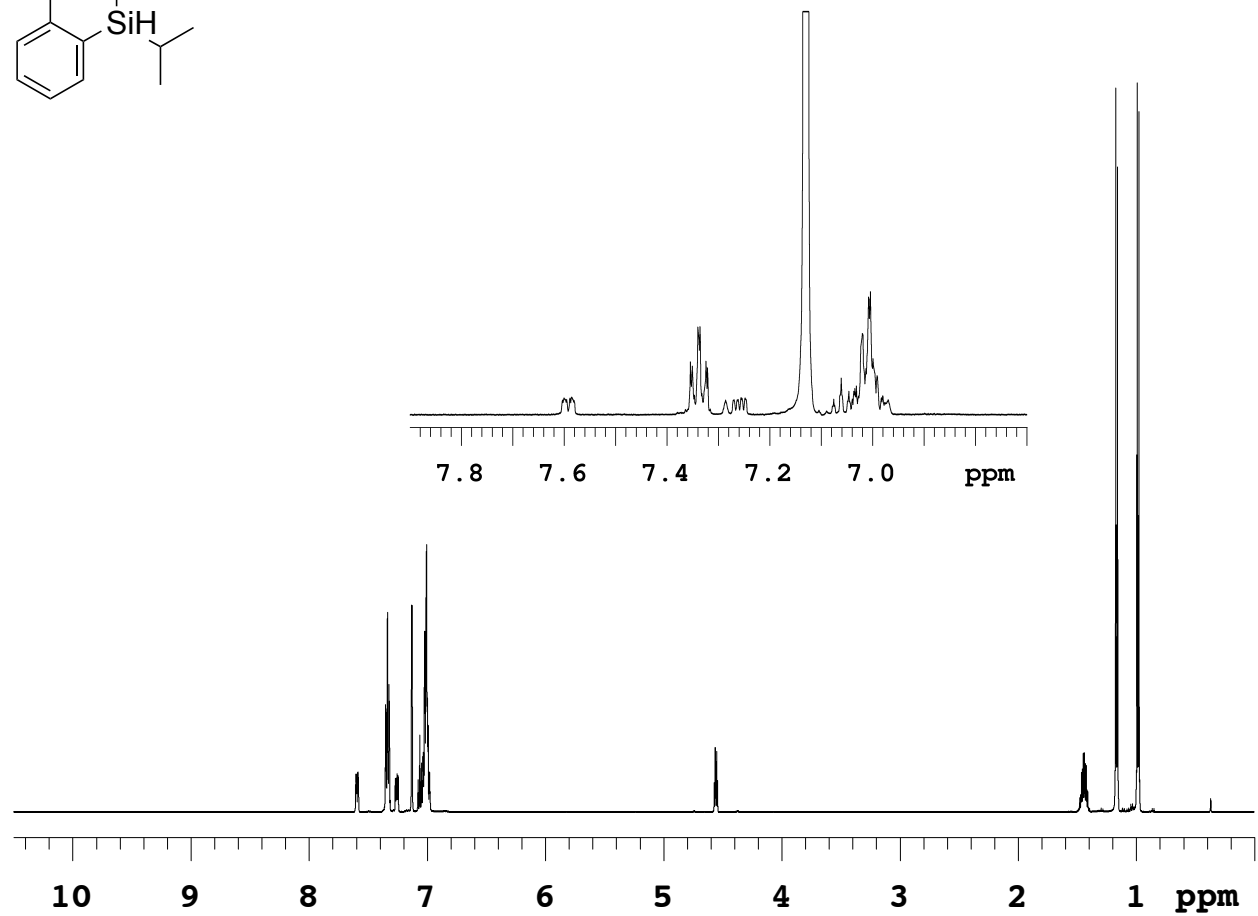
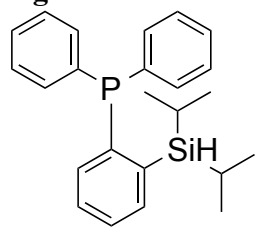




Figure 5.77.  $^1\text{H}$  NMR (500 MHz,  $\text{C}_6\text{D}_6$ ) (36)

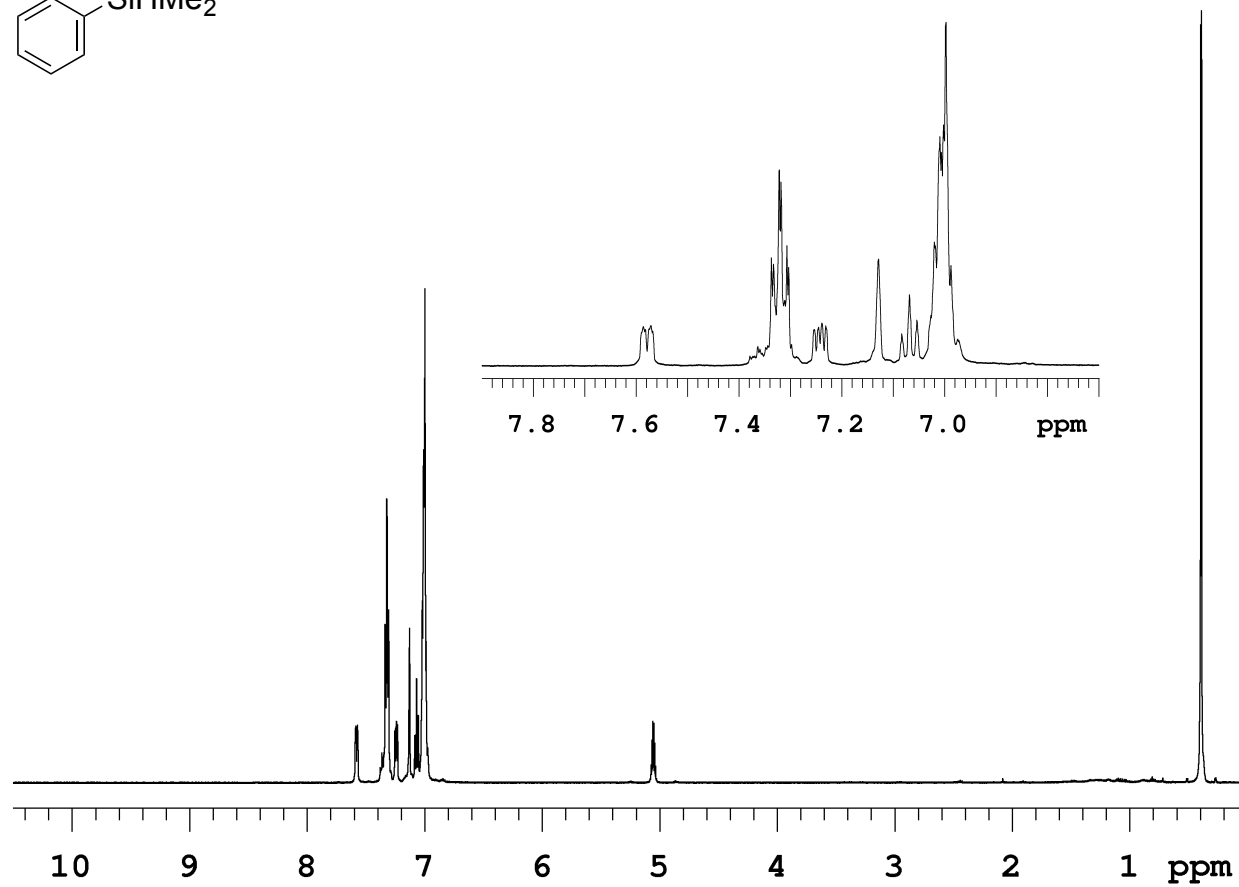
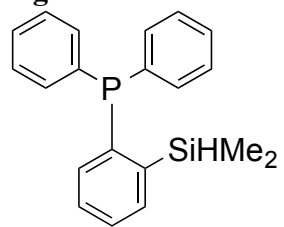


Figure 5.78.  $^{13}\text{C}$  NMR (125 MHz,  $\text{CDCl}_3$ ) (36)

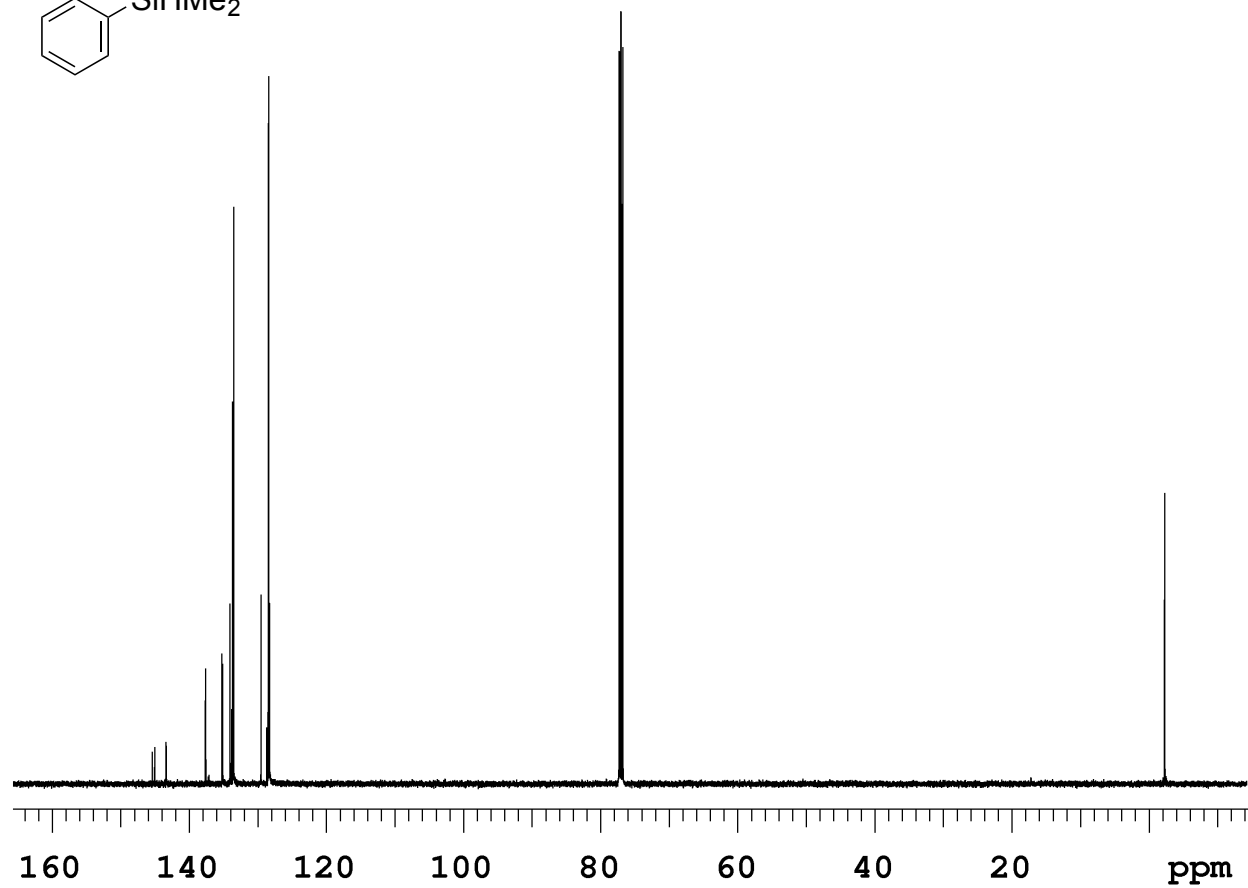
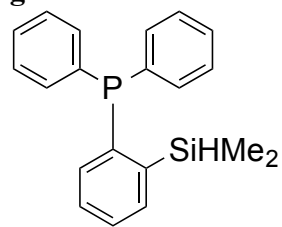


Figure 5.79.  $^1\text{H}$  NMR (500 MHz,  $\text{CD}_2\text{Cl}_2$ ) (37)

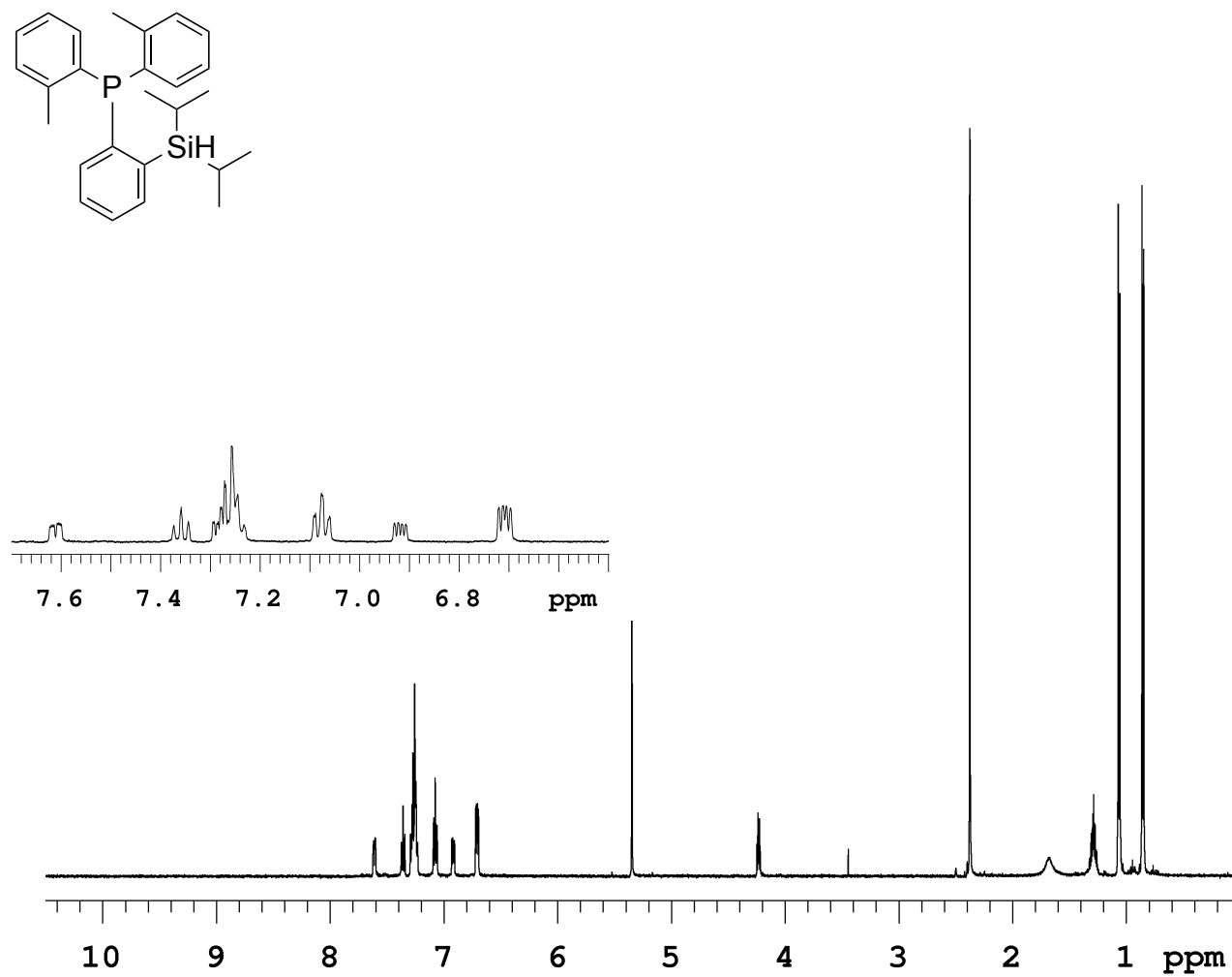


Figure 5.80.  $^{13}\text{C}$  NMR (125 MHz,  $\text{CDCl}_3$ ) (37)

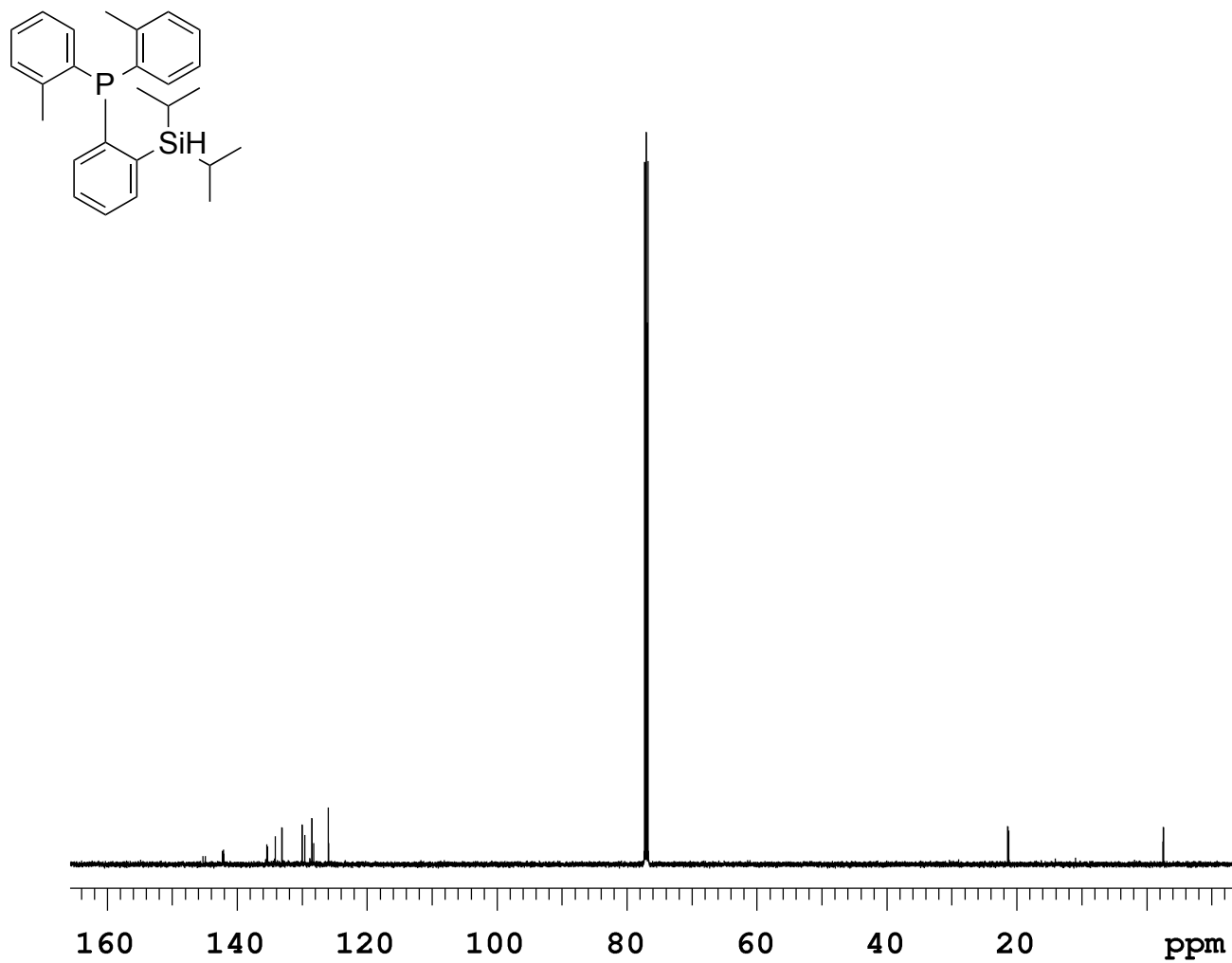


Figure 5.81.  $^1\text{H}$  NMR (500 MHz,  $\text{CD}_3\text{OD}$ ) (38)

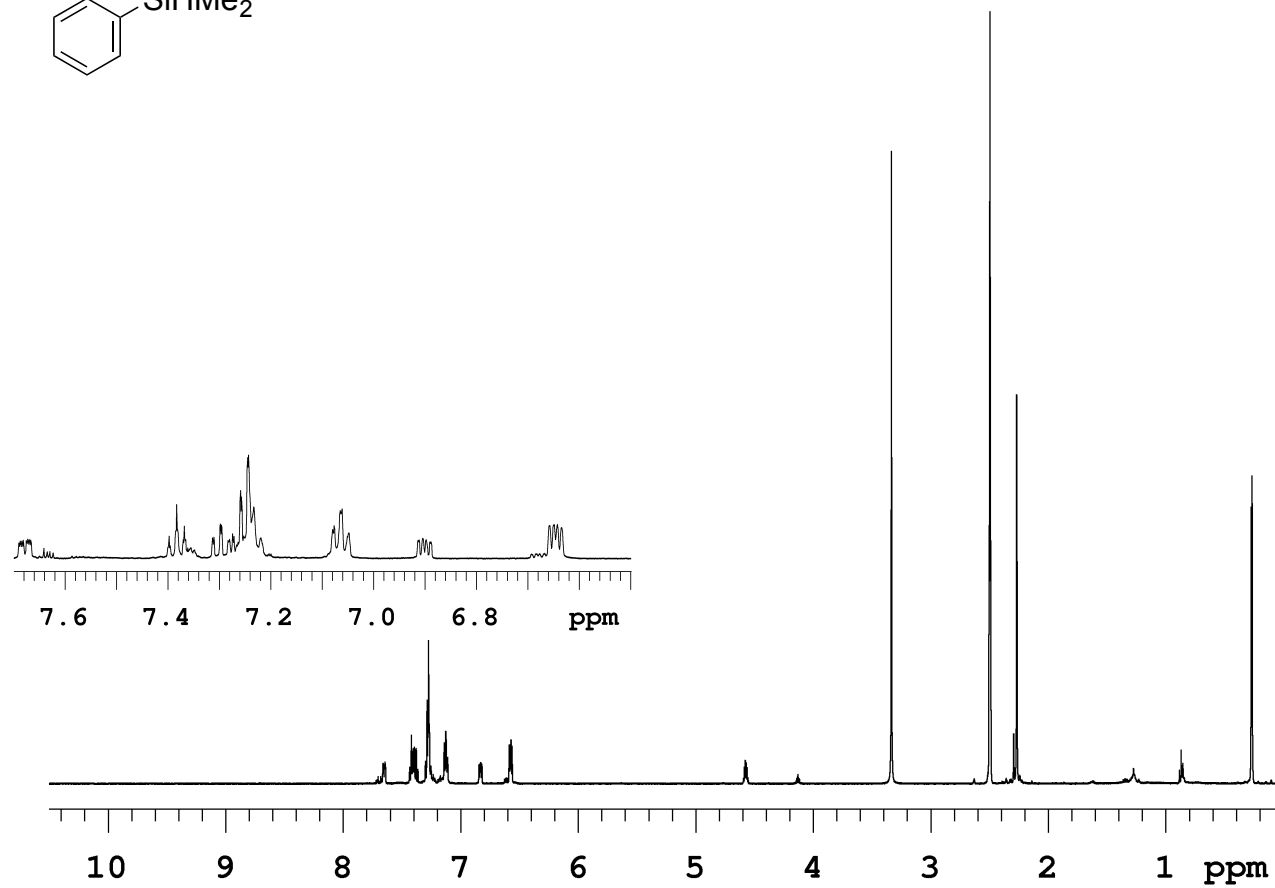
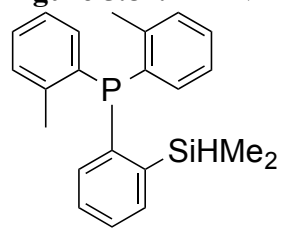
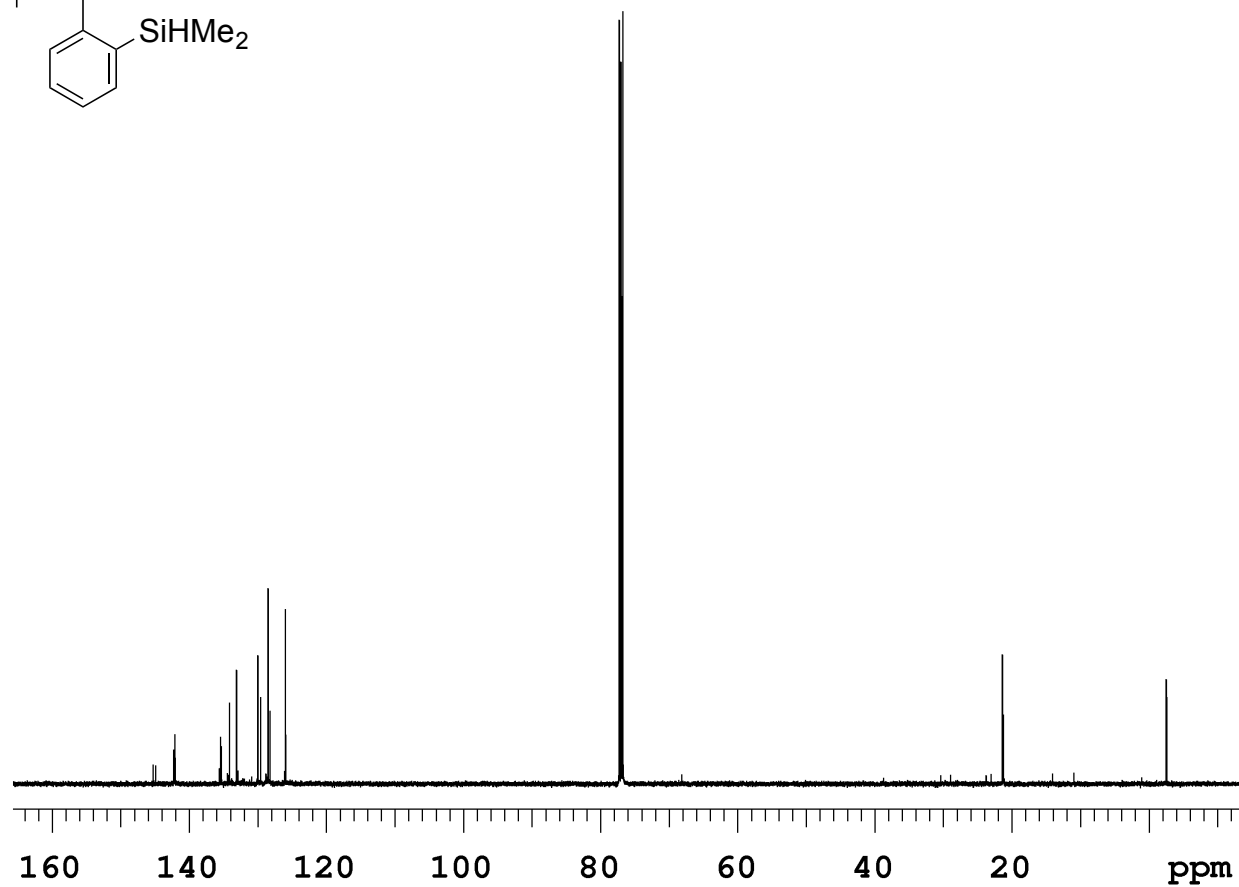
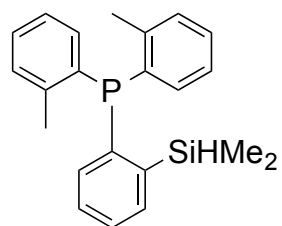


Figure 5.82.  $^{13}\text{C}$  NMR (125 MHz,  $\text{CDCl}_3$ ) (38)





## REFERENCES

## REFERENCES

- 1) Wolan, A.; Zaidlewicz, M. *Org. Biomol. Chem.* **2003**, *1*, 3274
- 2) Kawamorita, S.; Ohmiya, H.; Hara, K.; Fukuoka, A.; Sawamura, M. *J. Am. Chem. Soc.* **2009**, *131*, 5058
- 3) Ishiyama, T.; Isou, H.; Kikuchi, T.; Miyaura, N. *Chem. Commun.* **2010**, *46*, 159.
- 4) Iwashita, M.; Fuji, S.; Hirano, T.; Kagechika, H. *Tetrahedron.* **2011**, *67*, 6073
- 5) Kawamorita, S.; Ohimya, H.; Hara, K.; Fukuoka, A.; Sawamura, M. *J. Am. Chem. Soc.* **2009**, *131*, 5058.